AD-740 111

UNCLASSIFIED

Security Classification

DOCUMENT CONTROL DATA - R & D

(Security classification of title, body of abstract and indexing annotation must be entered when the overall report is classified)

1. ORIGINATING ACTIVITY (Corporate author)	2a. REPORT SECURITY CLASSIFICATION
Aero Materials Department Naval Air Material Center Warminster, Pennsylvania 18974	2b. GROUP

3. REPORT TITLE

Hydrogen Stress Cracking of High Strength Steels

4. DESCRIPTIVE NOTES (Type of report and, inclusive dates)

Final Report

5. AUTHOR(S) (First name, middle initial, last name)

Walter Beck
Edward J. Jankowsky
Philip Fischer

6. REPORT DATE	7a. TOTAL NO. OF PAGES	7b. NO. OF REFS
23 December 1971	224	433

8a. CONTRACT OR GRANT NO.	9a. ORIGINATOR'S REPORT NUMBER(S)
b. PROJECT NO. Task Area Number ZR0011-01-01	NADC-MA-7140
c. Work Unit Number AM-5-02	9b. OTHER REPORT NO(S) (Any other numbers that may be assigned this report) NONE
d.	

10. DISTRIBUTION STATEMENT

11. SUPPLEMENTARY NOTES	12. SPONSORING MILITARY ACTIVITY
Details of illustrations in this document may be better studied on microfiche	Naval Air Systems Command Department of the Navy Washington, D.C. 20360

13. ABSTRACT

This report deals with hydrogen induced embrittlement and stress cracking of high strength steel parts. Selected mechanical methods involving the different types of test specimens for the measurement of hydrogen embrittlement or delayed failure, and relevant methods for the quantitative determination of hydrogen extracted from embrittlement susceptible specimens are presented. Embrittlement resulting from pickling and chemical milling are considered. In addition, case studies of failures are included dealing with electroplated steel aircraft components, weldments, the petroleum industry, parts installed in boilers, pressurized water reactors, pressurized hydrogenation units, and parts cathodically protected. Different techniques for restoring ductility or preventing delayed failure are also included.

A new thermodynamic approach to the interpretation of the hydrogen embrittlement phenomenon is offered and a number of variables which control the generation or minimization of hydrogen embrittlement is analyzed and discussed in the light of electrochemical kinetics.

DD FORM 1 NOV 68 1473 (PAGE 1)

S/N 0101-807-6811

UNCLASSIFIED

Security Classification

A-31408

14. KEY WORDS	LINK A		LINK B		LINK C	
	ROLE	WT	ROLE	WT	ROLE	WT
Hydrogen embrittlement						
Hydrogen stress cracking						
Embrittlement test methods						
High strength steels						
Methods for determination of hydrogen						
Mechanisms (hydrogen embrittlement)						

HYDROGEN STRESS CRACKING
OF
HIGH STRENGTH STEELS

Report No. NADC-MA-7140 23 December 1971

HYDROGEN STRESS CRACKING OF HIGH STRENGTH STEELS

Task Area No. ZR011-01-01
Work Unit No. AM-5-02

This report deals with hydrogen induced embrittlement and stress cracking of high strength steel parts. Selected mechanical methods involving the different types of test specimens for the measurement of hydrogen embrittlement or delayed failure, and relevant methods for the quantitative determination of hydrogen extracted from embrittlement susceptible specimens are presented. Embrittlement resulting from pickling and chemical milling are considered. In addition, case studies of failures are included dealing with electroplated steel aircraft components, weldments, the petroleum industry, parts installed in boilers, pressurized water reactors, pressurized hydrogenation units, and parts cathodically protected. Different techniques for restoring ductility or preventing delayed failure are also included.

A new thermodynamic approach to the interpretation of the hydrogen embrittlement phenomenon is offered and a number of variables which control the generation or minimization of hydrogen embrittlement is analyzed and discussed in the light of electrochemical kinetics.

Reported by: W. Beck
W. BECK,
Electrochemical Research Branch

E. J. Jankowsky
E. J. JANKOWSKY
Chemical Metallurgy Branch

P. Fischer
P. FISCHER
Chemical Metallurgy Branch

Approved by: F. S. Williams
F. S. WILLIAMS, Superintendent
Metallurgical Division

J. H. Bowen
J. H. BOWEN, Acting Director
Aero Materials Department

PREFACE

About 15 years have elapsed since the senior author of this report was privileged to coauthor with George Sachs a monograph on hydrogen stress cracking and hydrogen embrittlement of low alloy aircraft steels, heat treated to high strength levels. At the time of this publication, these phenomena became a matter of serious concern because of the increasing frequency of brittle failures under service conditions, for example, chromium plated landing gears, cadmium plated steel fasteners and weaponry. More recent observations enhanced this concern alarmingly because they indicated that hydrogen induced stress cracking was not limited to electroplated steel parts alone. Hydrogen induced failures were reported for parts chemically milled, pickled, or exposed to paint removers. Hydrogen cracking is a very real danger where hydrogen is used as a liquid fuel in rocket engines for spacecraft and long range missiles.

Embrittlement has been also detected on parts installed in boilers, pressurized water reactors, high pressure hydrogenation units and parts cathodically protected. It would obviously be an oversight not to allude to the desperate fight of the petroleum industry against sulfide corrosion hydrogen stress cracking and the numerous embrittlement problems experienced by the welding engineer.

It was discovered recently that numerous cases of embrittlement, which had been considered to be stress corrosion cracking, were in fact hydrogen stress cracking.

The aforementioned topics are discussed comprehensively. In addition, other subjects, relevant to hydrogen failures are included, e.g., a summary of the methods of mechanical testing, crack propagation measurements, and the determination of hydrogen in steel. Case studies are reviewed in which hydrogen embrittlement is involved in fatigue. The differentiation between stress corrosion cracking and hydrogen stress cracking, and the effect of microstructure and composition of steels are also included.

The timely nature of the scope of this report is illustrated by the fact that hundreds of pertinent papers are published throughout the world every year. Many of them include rather diversified subjects, associated with hydrogen failures, and the engineer who urgently needs quick information about the diagnosis and mitigation of hydrogen failures, or special topics in this domain, finds his task very difficult or impossible. In order to improve this unfortunate situation, the above mentioned topics have been categorized and presented in a clear, simple and understandable form.

A thermodynamic approach was found most appropriate for interpreting consistently a number of phenomena of hydrogen embrittlement and hydrogen stress cracking. In addition, a number of variables which control hydrogen embrittlement generation and its minimization was analyzed. The electrochemical approach was found to be most suitable for this purpose.

This report when regarded in the broader aspects of modern chemical metallurgy, strikingly reflects the complexity of this subject.

ACKNOWLEDGEMENTS

The authors express their sincere appreciation to Mr. Samuel Goldberg, Naval Air Systems Command, J. Hartley Bowen, Jr., Technical Director of the Aeronautical Materials Department, Naval Air Development Center and Mr. F. S. Williams, Superintendent of the Metallurgical Division for their untiring encouragement and support which made possible the completion of this work. Special acknowledgement is given to Dr. J. O'M Bockris, University of Pennsylvania Electrochemistry Laboratory, for elucidative discussions of electrochemical problems associated with hydrogen embrittlement and Commander Robert L. Abbott, USN, former director of the department for his inspiration.

TABLE OF CONTENTS

TABLE OF CONTENTS (Continued)

TABLE OF CONTENTS (Continued)

TABLE OF CONTENTS (Continued)

TABLE OF CONTENTS (Continued)

TABLE OF CONTENTS (Continued)

TABLE OF CONTENTS (Continued)

CHAPTER 1

MECHANICAL TESTING FOR HYDROGEN EMBRITTLEMENT AND HYDROGEN STRESS CRACKING

Hydrogen adversely affects ductility. Therefore, all tests which are used for the determination of this mechanical property, such as bend tests, reduction in area or torsion tests are suitable for measuring hydrogen embrittlement. However, two interrelated phenomena, hydrogen embrittlement and hydrogen stress cracking (delayed failure) have to be distinguished. Embrittlement is a prerequisite for hydrogen stress cracking (an irreversible phenomenon), while hydrogen embrittlement on the other hand is a reversible phenomenon, because an embrittled material can be made ductile by thermal treatment. Since these two interrelated phenomena are used interchangeably, efforts are made in this book wherever possible to emphasize the above stated differences.

A discussion of mechanical tests will be given under two groupings, dynamic and static tests. In addition, the following important parameters will be considered in context with these tests: the effects of loading rate, temperature, notch acuity, grain orientation, specimen size and strength level.

1.1 DYNAMIC TESTS

1.1.1 SLENDER COLUMN BEND TESTS

Bend tests have been used extensively for measuring ductility changes. In these tests a wide variety of specimens have been employed. A thin strip, bent as a column was suggested by Beck in collaboration with Sachs[1]. They recommended a thin strip with a large slenderness ratio bent as a column in a universal testing machine. This test permits accurate measurements in the ductility of a steel over a wide range of embrittlement, as well as continuous straining at a nearly constant rate. The specimen is also inexpensive, a prerequisite when large numbers are required because of scatter in the test data. The specimen is shown in Fig. 1.1.

The fixture used for the tests is shown schematically in Fig. 1.2.

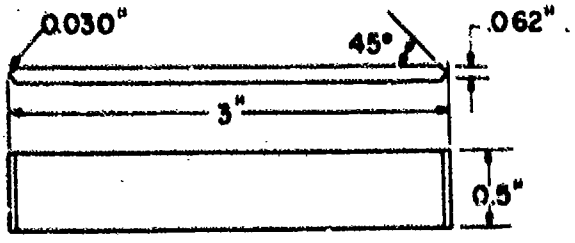

Fig. 1.1 – Columnar bend test specimen (slenderness ratio about 0.175)

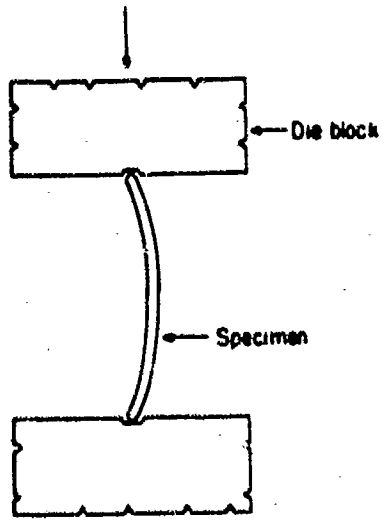

Fig. 1.2 – Bend test set-up for slender column specimen using universal testing machine and two die blocks.

The maximum load, the fracture load, and the decrease in distance between the die blocks of the bending fixture are measured. Maximum elongation of the outside fiber may be computed from the radius of curvature of the maximum bend.

The presence of hydrogen has practically no effect on the stress-strain relationship of a high strength steel, but only determines the termination of the stress-strain curve or the fracture point. The actual strain of the outside fiber can be determined from the decrease in column height. The curve of strain versus column height is essentially linear. The total decrease in column height at fracture is a good measure of the ductility of the specimen, as it is easily convertible into percent elongation at fracture and is more sensitive to hydrogen embrittlement than the fracture load.

In performing hydrogen embrittlement tests of the type described above, consideration must be given to the effect of the rate of straining on the measured ductility loss. This effect will be discussed in detail later.

1.1.2 HALF-RING BEND TEST

The half-ring bend specimen can be employed to good advantage[2, 3], in cases where the test material is only available in the form of tubing. A semi-circular specimen is used in a slow rate compression bend test performed in a universal testing machine. The total cross head travel from the free height along the open diameter to the height at fracture is called "deflection". This value, a measure of the ductility of the steel, is compared with the fracture deflection of an unembrittled ring and may be expressed in percent reduction in deflection.

Half cylinders with an outside diameter of 2 in., a width of 1-1/4 in., and a wall thickness of 1/8 in. have been used frequently. However, sensitivity of the specimens is increased considerably by using narrower half-rings (7/16 in.).

Fig. 1.3 depicts the superior sensitivity of fracture deflection as compared with fracture load to measure ductility. Half-ring speciments were embrittled by electroplating[4].

1.1.3 ZAPFFE'S BEND TEST

Zapffe[5] designed and used a bend test machine for hydrogen embrittlement measurements on steel wires with tensile strengths exceeding 200 ksi. The device is shown in Fig. 1.4 and a review of the test is given by Beck and Sachs[6].

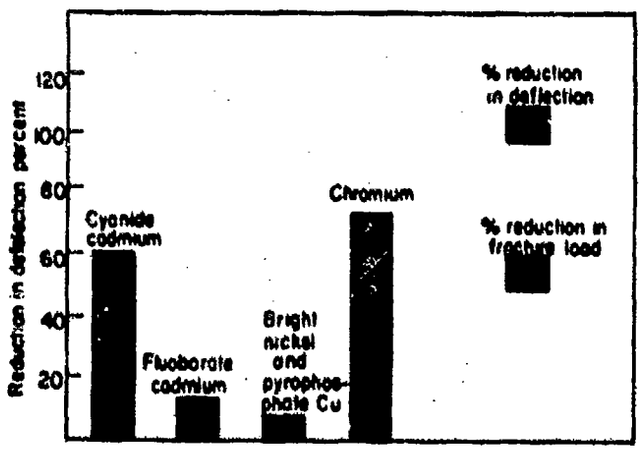

Fig. 1.3 – Comparison of the sensitivities of reduction in deflection with reduction in fracture load measurements on plated half-ring specimens.

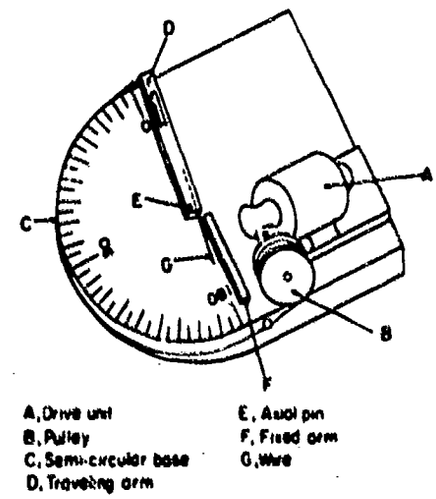

Fig. 1.4 – Constant-rate bend test device for measuring hydrogen embrittlement in steel wire

In this set-up, one arm is fixed while the other can rotate eccentrically about a pivot pin near its end and is motor driven to travel at a constant speed by a wire attached to a pulley and to the traveling arm. This device permits bending of the wire test specimen (held in the rotating arm) over a radius of 1/16 in. at a constant rate of bending of 270^{o} per minute, or 4.5^{o} per second. The angle at the moment of breakage is taken as a measure of hydrogen embrittlement[7].

Chilton[8] modified the set-up and used it for embrittlement measurements on medium strength steel ribbons. Two synchronous motors with speeds of 75 and 30 rps were connected through a worm gear to a moving arm. The angular velocity was generally 2^{o} per second. The specimen was clamped to the moving arm which was welded to a 1/16 in. radius pin. The unclamped end of the specimen was held against a stationary arm tipped with tungsten carbide. As the arm turned, the specimen was bent around the moving pin, and the angle at fracture was measured by a protractor.

1.1.4 MISCELLANEOUS BEND TESTS

Other less precise bend tests are used for a quick evaluation of embrittlement. A common one is the repeated bend test in which a wire or thin strip test specimen is bent back and forth over a radius until it breaks. The number of bends required, which may be markedly affected by absorbed hydrogen if the rate of bending is slow, is a measure of ductility[9,10].

In other tests, a strip, rod, or bar is slowly bent around a mandril and the angle of bend at which fracture takes place is measured. A bending rate of 4^{o} per second is considered suitable.

Another test variation is the vise test used for flat spring steel stock[6]. It is a free end loaded bend test which can be performed at a variety of fixed bending speeds. In this test, the specimen is placed end-wise in a vise and by slowly closing the vise the specimen bends or progressively buckles. The change in the vise opening or the decrease in cord length of the test specimen at fracture may be taken as a measure of hydrogen embrittlement. The vise may also be operated either by hand or by a mechanical drive. The test is then comparable to the slender column bend test previously described. The specimen may be smooth or may contain a shallow notch at the point of maximum bending. It should be stressed that as long as the material is deformed elastically, the test is a constant strain rate test. At the start of plastic deformation, this test becomes one of constant speed produced by the closure of the support jaws. Other dynamic embrittlement tests are described by Sachs and Beck[11].

The above descriptions clearly indicate that bend tests have the advantages of being simple, inexpensive, and fast. However, there are a number of disadvantages. Comparison of the results obtained by various investigators is rather difficult, due to the fact that the results depend on variables such as specimen shape and size, rate of bending, and nature of the bending fixture. Also, it should be emphasized that there is often poor agreement of hydrogen embrittlement, when determined by dynamic bend tests and sustained load tests, which are considered to be more sensitive. (Sustained load tests will be described later.)

The bend angle in the Zapffe machine is not due solely to hydrogen embrittlement, but, in the case of plated specimens, may also be affected by the plating itself. For example, soft electrodeposits, such as cadmium, may act as solid lubricants and lubricate the wire or strip passing over the pin.

It is to be emphasized that dynamic bend tests give qualitative, but not quantitative information about hydrogen embrittlement. Therefore, they should be used for rapid screening rather than as the basis for final judgments.

1.1.5 TENSILE DUCTILITY

The standard tension test gives yield strength, tensile strength, elongation and reduction in area of a specimen. It has been shown that the reduction in area reflects considerable variations in embrittlement, while tensile and yield strength do not. Actually, the tensile strength of a cylindrical section has been found to be clearly affected by hydrogen only in instances of extreme embrittlement. This lack in sensitivity is explained by the fact that even large differences in the ductility of materials do not affect their tensile strengths. This applies particularly to high

strength steels. Fig. 1.5 indicates clearly the aforementioned differences in sensitivity and shows that there is a slight effect on tensile strength only in cases where the values for the reduction in area are extremely low[12].

Elongation is also not a proper measure of ductility, since it depends in a complex manner upon other characteristics of the material[13]. However, it may be a usable indicator of embrittlement depending upon the particular steel and the magnitude of the embrittlement. If a tensile test is performed on standard longitudinal tensile specimens (0.505 in. dia., 2 in. gage length, Federal Test Method 151), it is recommended[13] that a strain rate to yield of 0.005 in./in./min., and a rate of cross head travel from yield to ultimate of 0.15 to 0.20 in./min or less, be maintained.

There is generally better agreement between the results of slow rate reduction in area tests and sustained load tests that those obtained with bend tests.

1.1.6 TORSION AND TORQUE TESTS

Chilton[14] designed a torsion test machine and measured the angle of twist when the specimen failed. In his set-up, two chucks are installed in a lathe bed. An electric motor geared down to 1.3°/sec turns one chuck. The other chuck grips the specimen to prevent slippage and allows movement only along the axis of the specimen. The number of degrees of revolution made by the specimen at failure is measured by a counter attached to the motor.

1.2 STATIC TESTS

1.2.1 CLASSICAL SUSTAINED LOAD DELAYED FAILURE TESTS

Suspending a fixed tensile load on a notched specimen and recording the time to fracture represents a very sensitive and reliable test for detecting and quantitatively evaluating hydrogen embrittlement. In the majority of cases, these tests are conducted in a dead weight lever arm (constant load) stress rupture machine equipped with an electric timer which is automatically arrested at the moment of specimen failure. The evaluation of hydrogen embrittlement is then based on a delayed failure diagram in which applied nominal stress versus time to failure is plotted.

According to Troiano[15], the nature of delayed failure can be appropriately described by four parameters, as illustrated in Fig. 1.6.

- The upper critical stress corresponds to the fracture stress in an ordinary notched tensile specimen.
- The lower critical stress is the applied stress below which delayed failure will not occur. (This stress is often incorrecly called the "static fatigue limit" an analogy to the endurance limit in fatigue.)
- The incubation period is the time required for formation of the first crack.
- The fracture time is the time to specimen failure. In an intermediate stress range, this includes a period of relatively slow crack growth.

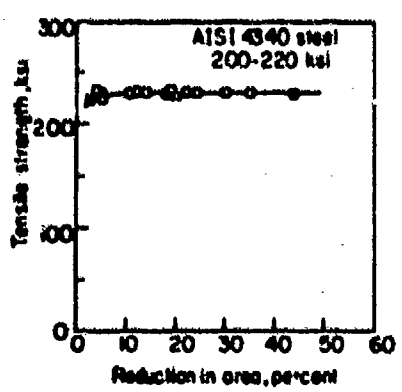

Fig. 1.5 – Relationship between reduction in area and tensile strength of specimens hydrogen embrittled to varying extents.

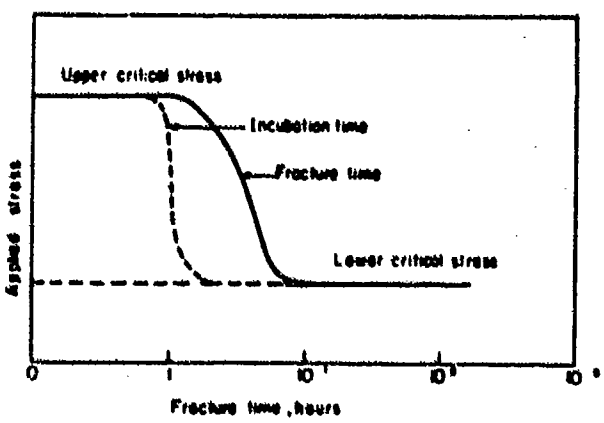

Fig. 1.6 – Schematic representation of delayed failure characteristics of a hydrogenated high strength steel.

Lower critical stresses can be expressed in terms of percentages of the notched tensile strength of the unembrittled specimens to characterize the susceptibility to delayed failure of a high strength steel embrittled by hydrogen.

One of the variables which adversely affects the results of sustained load delayed failure measurements is bending of the test specimen. It has been emphasized in ASTM Standard E-8-65T, issued in 1951 and revised in 1965[16], that departure from conditions of concentric loading introduces bending stresses which are not included in the usual stress computations. Thus, depending on the bending moment, the "true" tensile stress may exceed the calculated stress appreciably. Bending stresses may be reduced to negligibly low values by using appropriate alignment fixtures to ensure concentric loading (axial tensile stress). A simple set-up is recommended in the ASTM Standards. For specimens with threaded ends, the gripping devices should be attached to the heads of the testing machine through properly lubricated spherically seated bearings, and the distance between these ball bearings should be as great as feasible. It is, therefore, suggested that specimens with a long gage length be used. Additional details are given in Fig. 1.7.

A more refined device, using the Sachs precision alignment fixture, is partially described and recommended in a special ASTM committee report issued in 1962[17]. This fixture shown in Figure 1.8 may be used for either button head or threaded specimens.

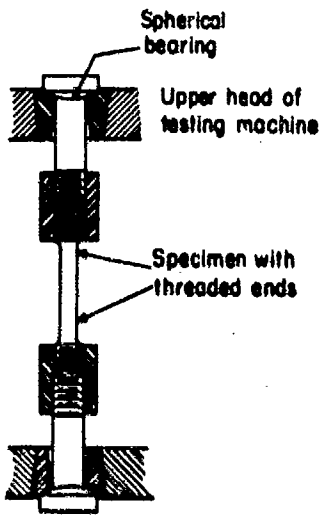

Fig. 1.7 – Gripping device for threaded-end specimens.

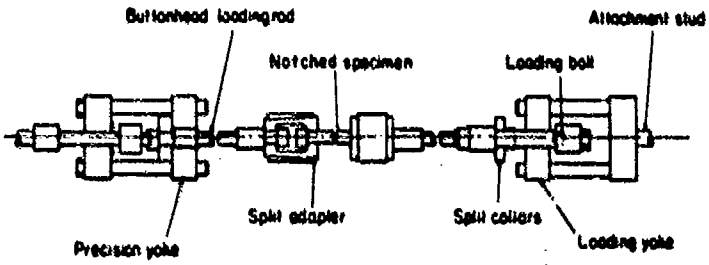

Fig. 1.8 – The Sachs precision alignment fixture.

This device has been described thoroughly by M.H. Jones and B.F. Brown, Jr.[18] who emphasized that the load should be applied through the two balls accurately positioned in line with the axes of the loading rods. The specimen is attached to the loading rods by means of a precision fastening device. The magnitude of the eccentricity depends on the magnitude of tolerances permitted in machining the fixture and the specimen. Thus, the alignment is built into the fixture and specimen assembly. Any factors tending to produce eccentricity external to the assembly are compensated for by low friction loading through the balls. The loading balls are retained in recessed seats in the precision yokes, an arrangement that prevents damage to the seats when the specimen breaks and insures that the balls do not shift their position relative to the loading rod holes. The load is applied to the ball by means of a yoke containing a precise ball seat. The yoke is attached to the machine head by a threaded stud. The ball seat is lubricated with molybdenum disulfide. High temperature alloy button head loading rods are fastened in the precision loading yokes by means of surface ground split collars. The button head specimen is attached to these rods and loaded by precision machined split adapters.

Tolerances stated in the above cited ASTM report are that the centerline of the specimen hole in the yoke must pass through the ball center within 0.0005 in. and all loading surfaces must be square with the loading axis. The total clearance between the specimen, the split collars, and the corresponding hole in the yoke should not exceed 0.0005 in.

A large amount of work with button head specimens indicates that they are very satisfactory when properly machined. With very hard material, it may be desirable to use threaded specimens in place of button headed ones. The same precision yoke can be used. A specially machined nut bears on the shoulders of the collars and transmits the load to the specimen. This nut should be a close fit with the specimen and its loading face should be machined square with the thread axis.

A typical notched tension specimen, recommended by Lockheed Aircraft, which is described in Ref.[13] and copied by numerous investigators for sustained load tests, is shown in Fig. 1.9[13].

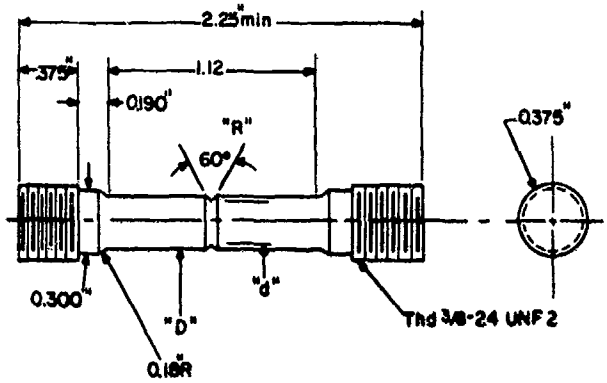

Major dia. "D" 0.2500 ± 0.0001" Minor dia. "d" 0.1768 ± 0.0001" Notch radius "R" 0.0060 ± 0.0010"

Fig. 1.9 -- Standard notched tensile specimen configuration. (Direction of grain, longitudinal).

It is a general practice to load the first specimen to 75 percent of the notch tensile strength and then progressively lower the load on each succeeding specimen. The marked scatter in these measurements makes it desirable to break a great number of bars and, if necessary, to statistically evaluate the data.

1.2.2 SIMPLIFIED SUSTAINED LOAD TESTS

A number of investigators have simplified the classical stress rupture machine. For example, Boeing Aircraft eliminated the bulky dead weight lever arm by replacing it with a loading nut[19]. The load is applied simply by turning the nut which is assembled on top of a supporting frame which is part of the static tension jig. Additional details are given in Fig. 1.10.

Load is measured by means of strain gages placed on the ring type dynamometer. This set-up is also used for embrittlement testing in vapor atmospheres[20]. The specimen is attached to the frame with a split bushing and connected to the dynamometer bar with a split nut. Concentric loading is accomplished by the installment of two ball joints which assure a self aligning system, and by careful alignment of the top and bottom holes of the supporting frame.

In another device, very similar to the Boeing fixture, load is applied by turning a large loading nut. Stress measurements are made by strain gages attached to a reduced section of the loading screw, and the load is transmitted to the test specimen through an elastic ring. Springs are installed to reduce the effect of relaxation of the specimen or apparatus. As can be seen from Fig. 1.11, the assembly contains an electrolytic cell which can be used for continuous hydrogen charging of the steel while under load.

The use of spring loaded specimens for tests under sustained load is demonstrated in Fig. 1.12. This type of apparatus has been used for studying the embrittling effect of high pressure hydrogen gas[21]. It contains an exposure cell in which hydrogen pressures up to 10 ksi or more can be maintained. The tensile load is applied by compressing heavy duty springs, and is generally determined by measuring the distance between the plates, and converting it to stress through previously determined curves of stress versus spring deflection. Temperature can be controlled by enclosing the test cell in an electrically heated jacket The tensile loads have to be corrected by the load on the notched cross section exerted by unbalanced gas pressure on the notched faces.

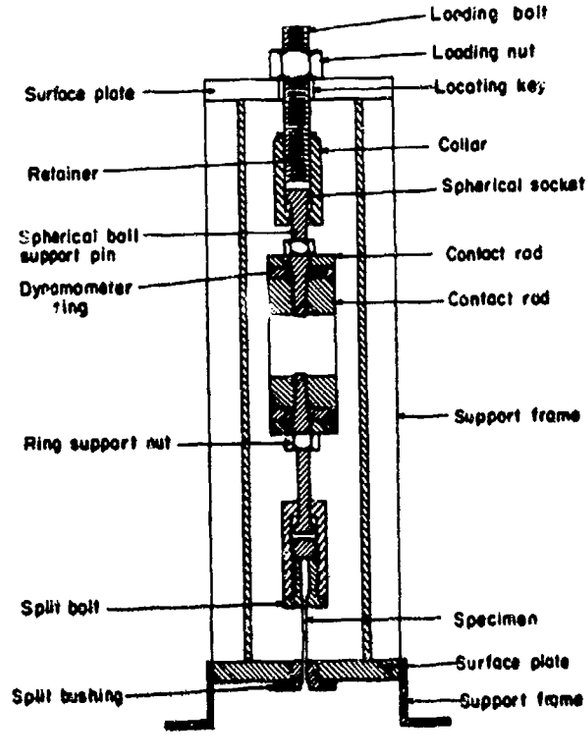

Fig. 1.10 – Cutaway view of static tension jig showing loading nut and bolt. To prevent eccentric loading of the specimens, all flat loading surfaces were faced-off normal to the channel supports within ± 1°, all holes were line drilled on center-line within ±0.01 in. and perpendicular to the surface plates within ± 1°.

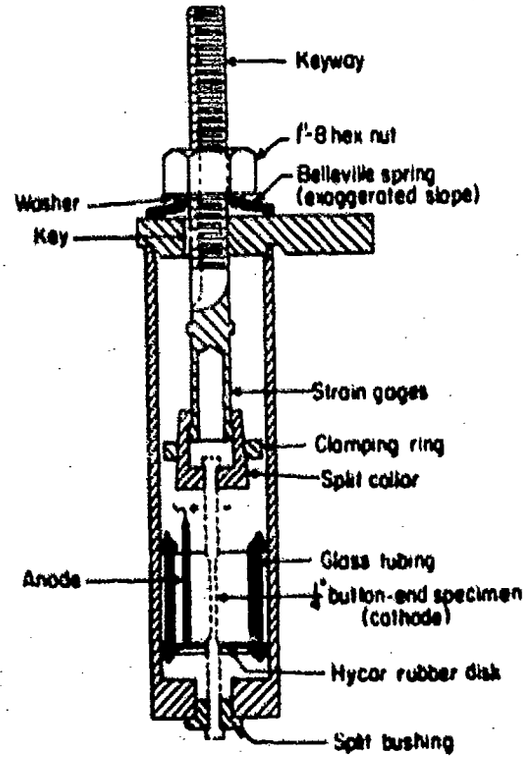

Fig. 1.11 – Static-loading device for testing 1/4 in. button head specimens. An electrolytic cell is incorporated for charging specimens with hydrogen while under stress.

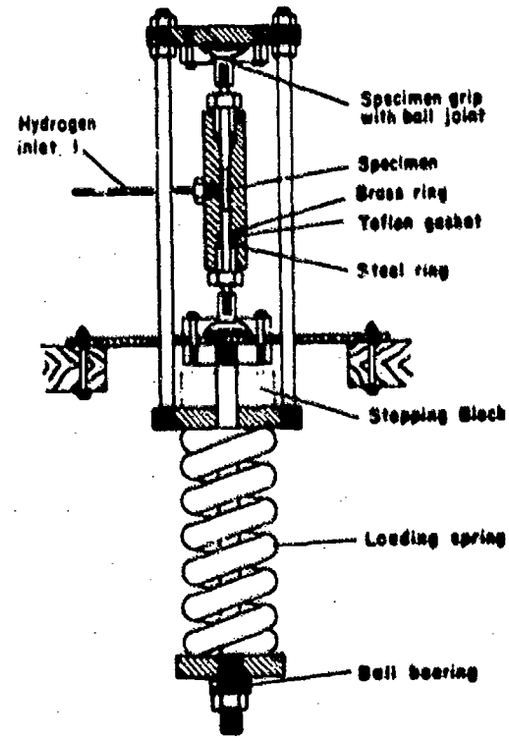

Fig. 1.12 – spring loaded device for sustained load testing in gaseous environments.

Another modification of the sustained load test represents a marked simplification of the classical set-up. This method, which was first used for hydrogen embrittlement testing by Raring and Rinebolt[22], also eliminates the stress rupture machine. This device, shown in Fig. 1.13a, has been used to advantage by numerous investigators.

The stressing ring is steel, generally heat treated to R_c 43. According to the designers, the specimen and specimen holders have to be aligned on an accurately determined diameter. Contact between the loading bolts and the outside of the ring should be made through mild steel bolsters to provide uniform load distribution. The large bottom nut is cut with a micrometer thread about 1-1/2 in. long to provide thread strength. The specimen is loaded by tightening the bottom nut until the diameter of the ring corresponds to the desired load. Raring and Rinebolt succeeded in preventing introduction of torque into the specimen during loading, by securing the stressing ring to a surface plate to which shackles are fastened that restrain the grips. The details are shown in Fig. 1.13b. Considerable elastic energy is stored in the ring while under load. The sudden release of energy when failure occurs displaces the tightening nut which activates a mechanism connected to a microswitch (Fig. 1.13c). An electric timer controlled by the switch records the time to fracture.

It has been established that the load remains essentially constant during the test period. On loaded specimens, the diameter of ring corresponds to the prevailing load. This is obtained from the load versus diameter calibration curve for the ring, which is determined by comparing the diameter with that of a standard proving ring loaded in a tensile machine. Care should be taken in machining both the stressing ring and individual specimens to minimize non-axial loading.

A sustained load test suggested for bolts is the torque bolt test[23]. The test device consists of a fixture in which a bolt is loaded to a fixed torque. The head is cocked at a slight angle by means of a tapered washer. Friction is minimized by using light machine oil between the bolt and the washer. The shank of the bolt is subjected to both tension and bending under load. These conditions, which simulate mismatched loading in service, result in delayed failures under the heads of the bolts and in the threads. As a rule, the device consists of a hardened steel block through which holes have been drilled to accommodate the bolts. Time to fracture is recorded. Failure time at constant torque has been found to vary markedly with variables that are known to affect hydrogen embrittlement. A simple torque testing fixture is shown in Fig. 1.14. More complex fixtures based on the same principle have been described by Sachs and Beck[24].

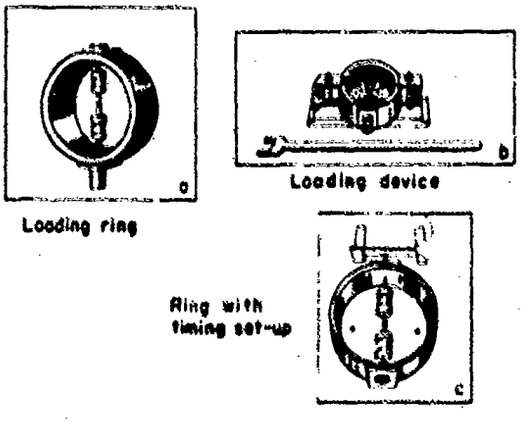

Fig. 1.13 – Modified sustained loading apparatus.

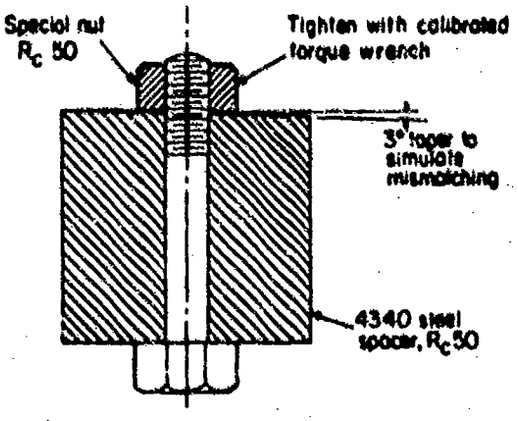

Fig. 1.14 – Simple fixture for sustained-load torque tests on steel bolts.

1.2.3 STATIC BEND TESTS

A simple test has been suggested in which a number of relatively thick specimens are bent as beams to various angles in a bending fixture. The levels of the outer fiber stresses can be varied in a wide range by setting the specimens to a calculated deflection with the aid of a depth micrometer. Time to failure is recorded as a function of applied stress and degree of hydrogen embrittlement. Notched as well as unnotched specimens can be exposed[13].

Another simple test was suggested by Allread and Robinson[25]. These investigators tested horizontally oriented cylindrical notched tension specimens supported in a recess at one end and slipped into the extension of a lever arm to which a dead weight was applied at the other end. Load was adjusted by sliding the weight hanger on the arm to provide the desired bending moment on the specimen. They suggested the use of a fixture with six suspensions for simultaneous testing at different stress levels, enabling a rather rapid estimate of the lower critical stress.

1.2.4 STRESSED RING TESTS

Douglas Aircraft has recommended the use of a statically loaded test ring with the load applied through a spacer,[26] as depicted in Fig. 1.15. The ring specimens are normally taken from steel tubing, while the stressing bars are usually machined from rectangular bar stock. Rings are distorted by a vise with rubber padded jaws to allow the insertion of the stressing bar. In this manner, one obtains a load which is maintained until the ring breaks. One attractive feature of this specimen, in addition to its simplicity, is that it can be plated or pickled under stress.

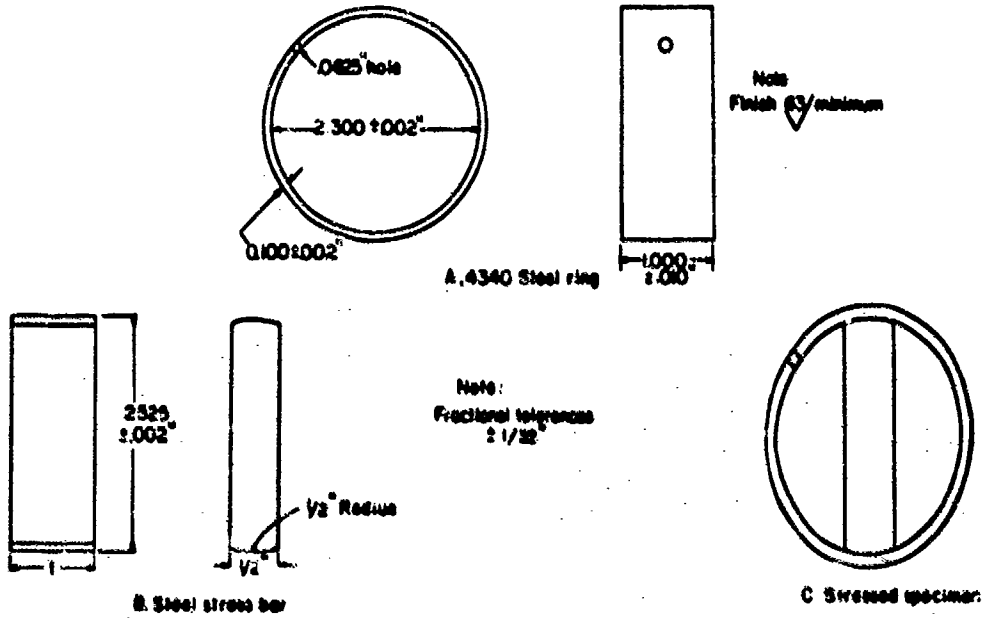

Fig. 1.15 – Special ring test specimen and stress bar (Douglas Aircraft).

A more refined ring specimen, called the notched C-ring, was designed by Williams, Beck, and Jankowsky[2,27-31]. It can be used to advantage under conditions in which stress rupture machines and other methods requiring bulky equipment are not applicable. This procedure has the unique feature of being remote indicating. Strain changes can be recorded simultaneously on numerous specimens exposed at different locations.

One important part of the device consists of a calibrated loading bolt. The notched C-ring specimens, henceforth called "rings", consist of 1-1/4 in. sections cut from 2.0 in. diameter, 1/8 in. wall steel tubing. Notches are cut by careful grinding after heat treatment. Specimen dimensions are given in Fig. 1.16.

The rings are stressed by tightening a nut on the loading bolt. In the majority of the experiments, a 1/4-28 AISI 2330 steel bolt was used, with two SR-4 type AD-7 strain gages attached. To increase the strain, the cross sectional area of the bolt was reduced by drilling a 0.224 in. hole in its center.

A limited number of measurements were made with a bolt of improved design (Fig. 1.16) which consisted of a 1/4-28 bolt of 2024 aluminum alloy with its diameter reduced to 0.177 in. over a 1 in. length. A single strain gage was inserted in a 1/16 in. hole drilled 1-1/2 in. deep in the center of the bolt. Identical results were obtained with both types of bolts. The advantages of the internally instrumented bolt are: (1) the strain gage is protected against damage; (2) the bolt can be readily reused; and (3) errors from bending are compensated for as effectively as using two gages on opposite sides.

The strain gages attached to the steel bolt form two arms of a bridge circuit. The other arms consist of two strain gages attached to a similar unstrained bolt for temperature compensation. A schematic diagram of the electrical wiring is shown in Fig. 1.17.

The unbalance in the bridge circuit resulting from strain in the bolt was recorded by a galvanometer-type oscillograph. The deflections were calibrated in terms of bolt stress. An unnotched C-ring, 0.075 in. wall thickness with a strain gage having a 1/8 in. active length mounted at the center of its outside (tension) surface, was loaded in compression in a universal testing machine, and the strains produced for various loads were recorded. The stresses corresponding to each of these strains were then calculated. Fig. 1-18 is a plot of these values.

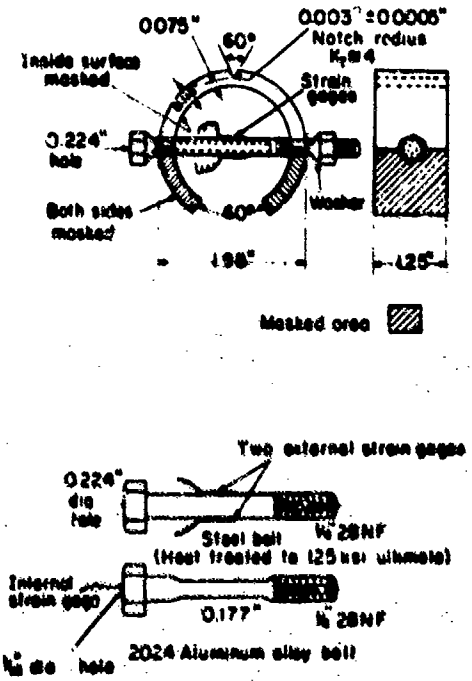

Fig. 1.16 – Notched C-ring and two types of instrumented loading bolts.

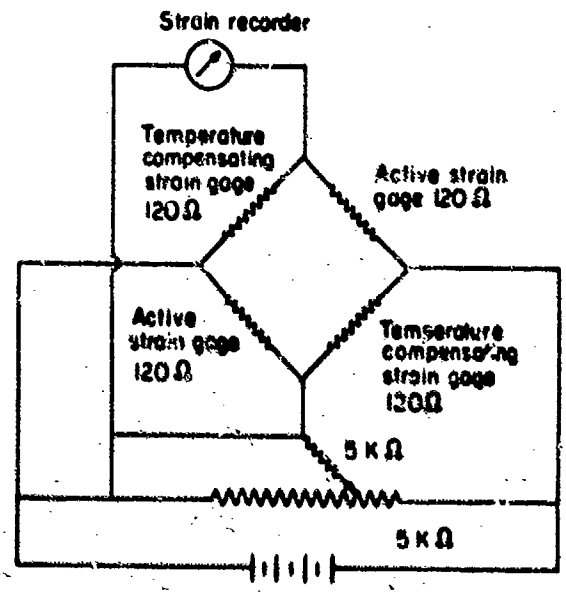

Fig. 1.17 – Strain gage wiring diagram.

The load required to produce a given nominal stress in a notched ring is the same as that required to produce a surface stress of the same magnitude in an unnotched ring, provided the section moduli are the same. For rings of equal diameter, this means that the thickness of the unnotched ring must be the same as the thickness beneath the root of the notch in the notched ring. It is then possible to relate directly the maximum surface stresses obtained from loads on an unnotched ring to nominal notched ring stresses resulting from restraining bolt loads, and thus to bolt stresses (Fig. 1.19).

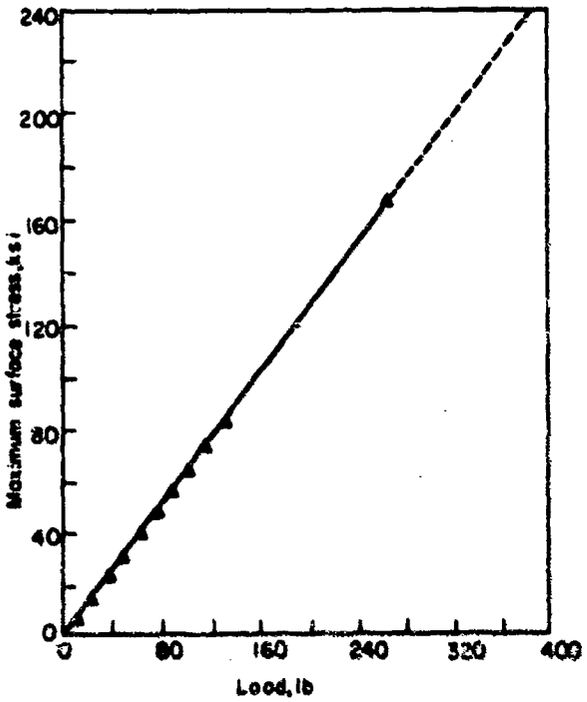

Fig. 1.18 – Ring stress versus applied load (unnotched C-ring, 0.075 in. wall thickness).

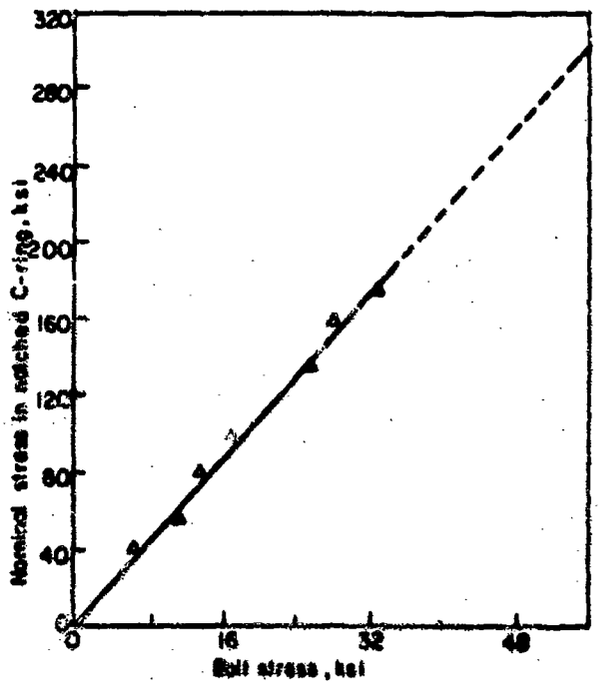

Fig. 1.19 – Plot of nominal stress in notched C-ring versus bolt stress.

To permit a convenient calculation of nominal stresses for specimens differing only by the depth of the notch and the thickness of the ring, a "corrected" value for the moment arm, was obtained by substituting the stresses calculated from the measured strains and the corresponding applied load, P, required to produce these stresses by the formula,

$$S = \frac{6PV}{bd^2} \quad \text{or} \quad V = \frac{Sbd^2}{6P} \tag{1.1}$$

where:

S = the maximum nominal stress parallel to the longitudinal axis of the beam at the root of the notch, calculated from measured strains,

P = the applied load,

V = the moment arm "corrected" for specimen curvature,

d = the thickness of the cross section at the root of the notch, and,

b = the section width.

The nominal stresses in the ring produced by various loads computed from Equation (1.1), were then plotted versus the corresponding bolt stresses. The linear nature of this plot is illustrated in Fig. 1.19 and bolt stresses determined from the oscillogram were converted to nominal stress in the ring using this diagram.

Some special specimens, designed for determining hydrogen induced cracking are described in the chapters dealing with hydrogen induced and controlled crack propagation, hydrogen embrittlement in aqueous environments, and hydrogen embrittlement in steel weldments.

1.3 IMPORTANT PARAMETERS TO BE CONSIDERED IN HYDROGEN EMBRITTLEMENT TESTS

1.3.1 LOADING RATE

Some striking examples of the effect of loading rate on hydrogen embrittlement measurements were presented by Beck et al[32]. In general, ductility increases with increasing rate of bending for all the indicated current densities (Fig. 1.20) and charging times (Fig. 1.21).

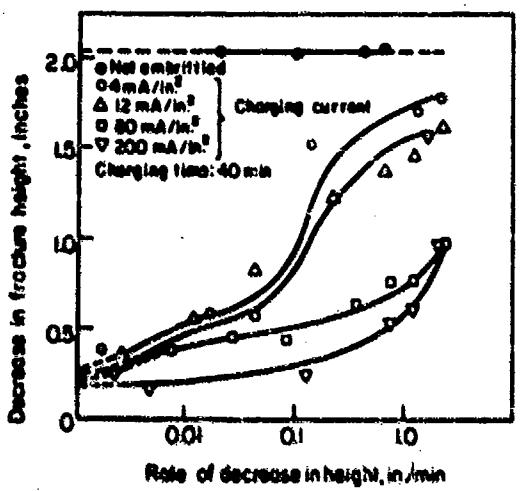

Fig. 1.20 – Effect of bending rate (rate of decrease in height) on ductility (decrease in fracture height of columnar specimen) of SAE 1050 (R_C 48) spring steel. Hydrogen Charged in 10% NaOH.

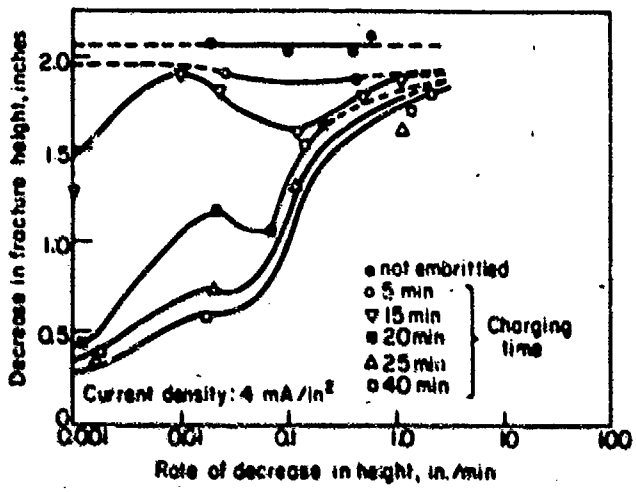

Fig. 1.21 – Effect of bending rate (rate of decrease in height) on ductility (decrease in fracture height of columnar specimen) for different charging times (SAE 1050 steel R_C 48).

This effect is also seen in Fig. 1.22, where higher strain rate tests show very little embrittlement.

On the basis of the effect illustrated above, it is understandable why high strain rate tests, such as impact tests, are insensitive to hydrogen embrittlement, whereas the sustained load test with zero strain rate represents the most sensitive test. The strain rate effect also explains why hydrogen embrittlement has been called low strain rate embrittlement by several investigators.

Many more examples dealing with the strain rate effect are reported by Elsea[33].

1.3.2 TEMPERATURE

It has been established that there is comparatively little occurrence of hydrogen embrittlement at relatively low and high temperatures. However, there is a high occurrence in an intermediate range of temperatures including room temperature. The reason for this phenomenon is the low diffusion rate of hydrogen at low temperatures and its high rate of out-diffusion at elevated temperatures. The following two figures strikingly illustrate these facts[15].

Fig. 1.23 shows the effect of test temperature on time to fracture of notched, hydrogen charged specimens, and a linear dependency of the logarithm of fracture time on test temperature, indicating reasonably linear Arrhenius plots.

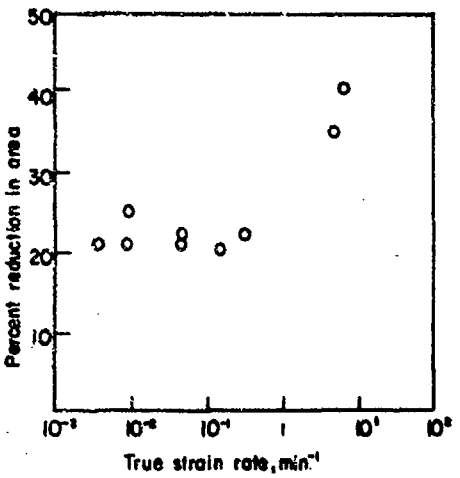

Fig. 1.22 – Relationship between reduction in area and true strain rate for high strength steel test bars containing more than 6 ppm of hydrogen (Vacuum extracted at 1000 C).

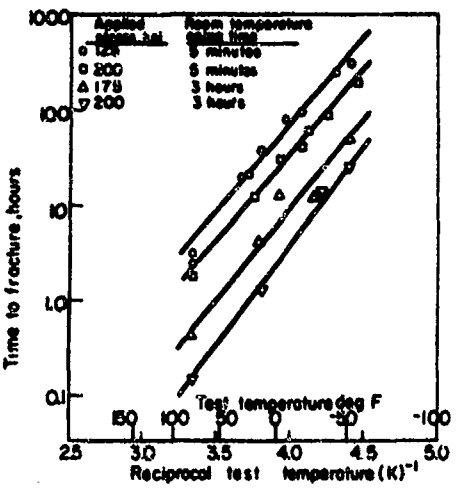

Fig. 1.23 – Fracture time versus test temperature for sharp notched specimens for different aging times and applied stresses. AISI 4340 steel (230 ksi) charged for 5 min at 20 mA/in^2 in 4% H_2SO_4.

Accelerated hydrogen diffusivity as reflected in the lessening of the reduction in bend deflection[34] with rising temperature of the test solution, is depicted in Fig. 1.24. Thus, at higher solution temperatures, the quantity of absorbed hydrogen drops and ductility is recovered accordingly.

1.3.3 NOTCH ACUITY

A review of the comprehensive work done in this field at Case Institute of Technology, and by Sachs and collaborators has been made by Elsea et al[33]. Results typical of hydrogen embrittlement were obtained by Sachs[35] on high strength AISI 4340 steel, and vanadium modified 4340 steel, bright cadmium plated to standard procedures. These studies deal with the fracture strength at 100 hours of sustained loading. The fracture strength decreased sharply (from 275 to 100 ksi as K_t was increased from 1 to 5. Increasing K_t up to about 11 did not accomplish a further decrease in fracture strength below that determined at $K_t = 5$.

Johnson[36] has recently presented some results on the effect of notch root radius on delayed fracture of cadmium plated high strength (260-280 ksi) AISI 4340 steel. The marked increase in failure time at the lower critical stress with increasing notch root radius from 0.0001 to 0.025 in. is illustrated in Fig. 1.25

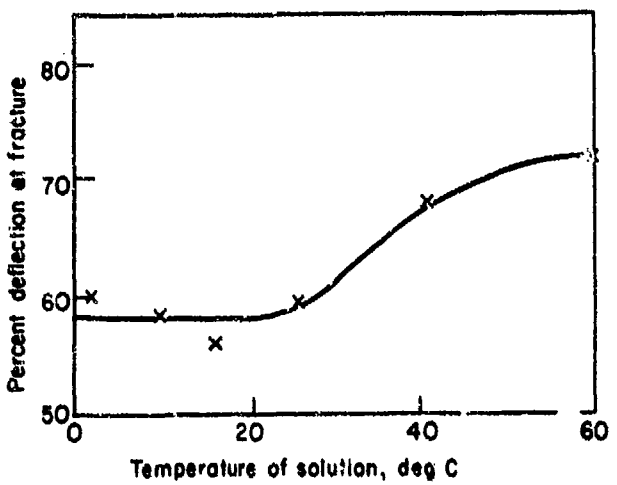

Fig. 1.24 – Effect of hydrogen charging solution temperature on fracture deflection of AISI 4340 steel charged for 30 min at 10 mA/cm^2 in a 0.01M NaOH + 0.02 M NaCN solution.

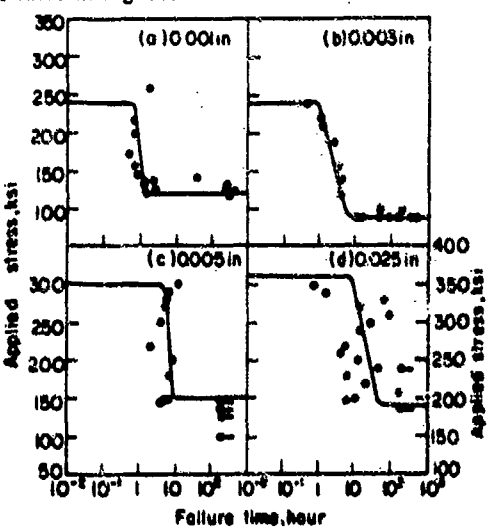

Fig. 1.25 – Delayed failure curves for specimens of various notch root radii Cd plated (0.0005 in.) AISI 4340 steel 260-280 ksi strength level.

Fig. 1.26 depicts the dependency of notch tensile strength (NTS) and failure time on notch radius[37]. Increase of the radius from less than 0.001 to about 0.003 in. brings about a rapid rise in notch tensile strength and failure time. Further increase of the notch radius has a relatively small effect.

1.3.4 GRAIN ORIENTATION

Very little work has been done in this domain. Some recently published studies by Hughes et al.[38] are reproduced in Fig. 1.27.

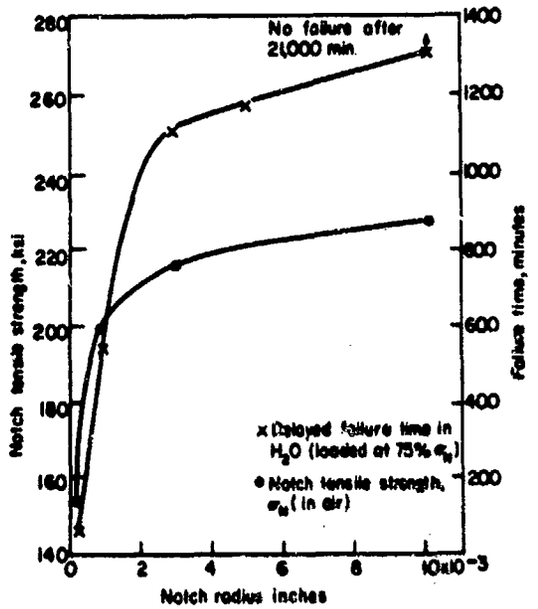

Fig. 1.26 – Effect of notch radius on notch tensile strength and delayed failure characteristics of 300M steel, 220 ksi strength level at 68 F.

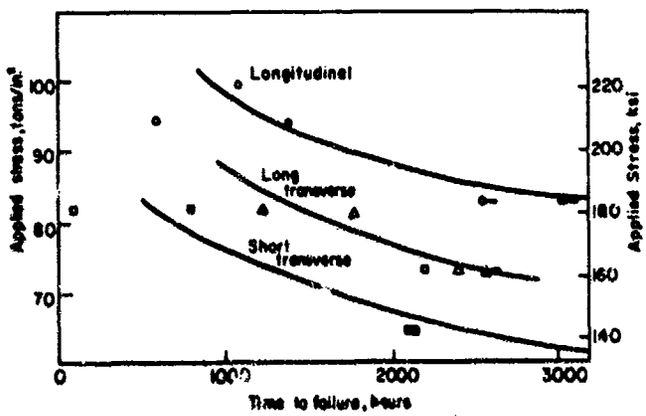

Fig. 1.27 – Comparison of susceptibility to cracking for three grain directions of the unnotched 107 tons/in² (257 ksi) steel specimens stressed in 3% NaCl solution.

The measurements were performed with low alloy steel. Unnotched specimens were subjected to dead weight loading and exposed to a 3.0% NaCl solution.* Cracking susceptibility, as determined by delayed fracture measurements, was significantly greater in the short transverse than in the longitudinal direction. The results obtained for the long transverse direction show that its susceptibility is between those of the other two grain directions. However, taking into account the differences in the inherent ductilities between the unexposed longitudinal and transverse specimens, respectively, these results do not appear to indicate differences in hydrogen embrittlement susceptibility unequivocally as a result of differences in directionality[39]. Appreciable differences in susceptibility to delayed brittle failure may only reflect the superior mechanical behavior of the unplated longitudinal material, a phenomenon which actually has nothing to do with hydrogen embrittlement.

*Failures in these experiments, probably resulted from stress corrosion cracking. The effects of grain direction is considered the same for both stress corrosion cracking and hydrogen stress cracking for most martensitic steels. These experiments, therefore, serve to illustrate the effect.

1.3.5 SPECIMEN SIZE

Work done in this field is rather limited. Elsea made studies which showed, that the failure time of embrittled smooth specimens increases with increasing size[40]. He later made a detailed report of the effect of specimen size[33].

According to studies performed by Sachs[35], notch strength is raised with increasing section size, and susceptibility to sustained load failures of hydrogen charged specimens decreases accordingly.

Davis and Gray[41] worked with centrally notched, cylindrical, low alloy steel specimens (K_t = 3.2) with an ultimate tensile strength of 269 ksi. The specimens were baked for 24 hours after cadmium plating. The sizes of the sustained load test bars were 1/4 in. and 1 in. diameter, measured on the reduced section. In general, the smaller test pieces were slightly more embrittled than the larger ones.

The effect of section size on the rate of recovery from hydrogen embrittlement is of great interest from a practical standpoint. This problem will be discussed in detail in a later section.

1.3.6 STRENGTH LEVEL

As described in the literature, the resistance of statically loaded, hydrogen containing high strength steel to delayed brittle fracture decreases rapidly with increasing strength level[35] after a limiting value has been exceeded. The practical importance of this phenomenon is vividly illustrated by the fact that the demand for steels of higher and higher strength level for weight saving in the aircraft and missile industry is increasing rapidly.

The following results were taken from other recent publications. Fig. 1.28 illustrates that by increasing the ultimate tensile strength of the material above is limiting value of 88 tons/in^2 (194 ksi) a rather marked reduction in the rupture strength of hydrogen embrittled, unnotched AISI 4340 steel specimens takes place[38]. (Specimens were embrittled in 0.1N hydrochloric acid. Corrosive effect of the acid was disregarded.)

The effect of specimen hardness on delayed brittle failure was investigated by Allread and Robinson[25]. The results, plotted in Fig. 1.29, show distinctly the effect of hardness on the critical stress applied to a notched specimen (0.01 in. root radius) of low alloy steel.

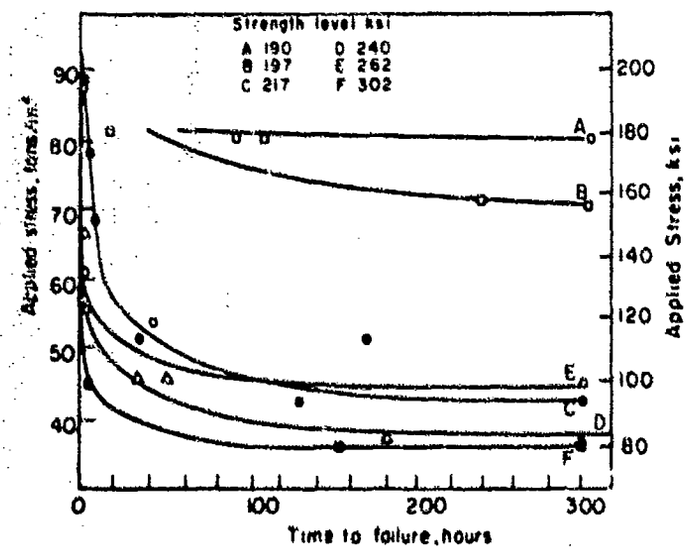

Fig. 1.28 – Effect of strength level and applied stress on time delay to failure of unnotched steel specimens stressed in longitudinal direction in 0.1N HCl solution.

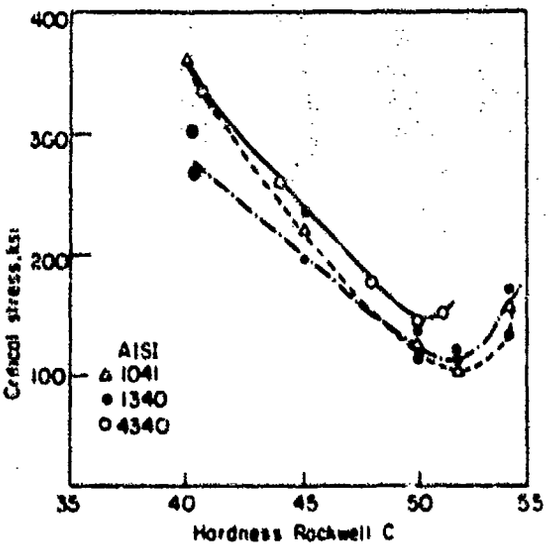

Fig. 1.29 – Effect of hardness on susceptibility to hydrogen cracking for three medium high carbon steels. Notch radius 0.01 in., cyanide cadmium plate 0.0005 in.

Critical stress in Fig. 1.29 is the highest stress the specimen can carry for 24 hours without fracturing. The specimens were plated with cadmium from a cyanide bath preceded by a short time cathodic treatment in dilute sulfuric acid. The curves showed similar trends, a sharply descending branch followed immediately by an ascending branch[35]. The well defined minimum is located at R_C 50.

Another example of the effect of strength level is given in Fig. 1.30, in which the effect is illustrated by means of ductility measurements on half ring bend specimens[42].

It is interesting to note that the loss in ductility was nearly constant at all strength levels, but that this loss amounts to a much lower percentage of the total ductility of materials heat treated to 180 ksi than material at the 260-280 ksi level.

Additional instructive examples dealing with the effect of strength level on susceptibility to delayed failure can be found in the report by Elsea et al.[33].

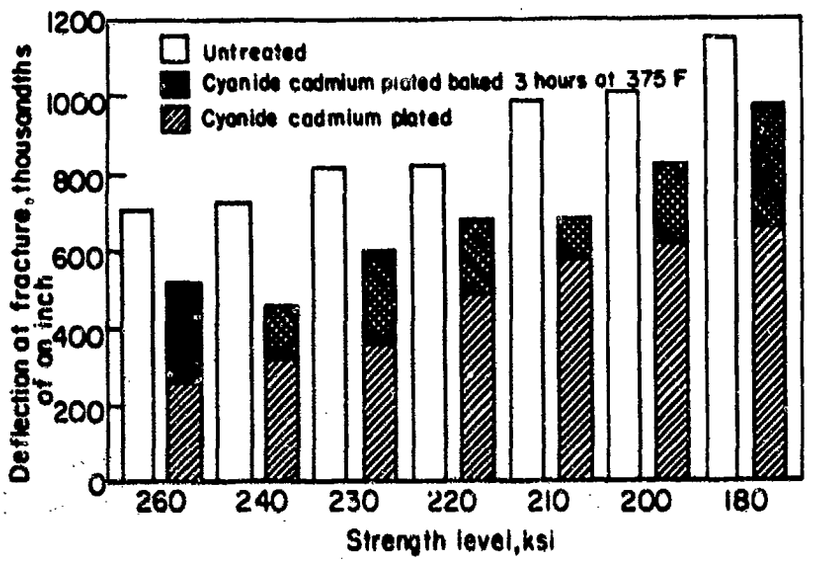

Fig. 1.30 – Effect of various strength levels on fracture deflection for untreated, cyanide cadmium plated and cyanide cadmium plated and baked AISI 4340 steel.

REFERENCES

[1] W. Beck, E.P. Klier, and G. Sachs, "Constant Strain Rate Bend Test on Hydrogen Embrittled High Strength Steels", *Trans. AIME*, **206**, pp. 1263-1268 (1956).

[2] W. Beck and E.J. Jankowsky, "Effects of Plating High Tensile Strength Steels", *Proc. Am. Electroplaters' Soc.*, **44**, pp. 47-52 (1957).

[3] E.W. Dougherty, "Methods for Minimizing Hydrogen Embrittlement in Electroplated High Strength Alloy Steel", *Plating*, **57**, pp. 415-422 (1964).

[4] Ref. [2], p. 50.

[5] C.A. Zapffe and M.E. Haslem, "A Test for Hydrogen Embrittlement and Its Application to 17% Cr-1% C Stainless Steel Wire", *Metals Technol.* (1947).

[6] G. Sachs and W. Beck, "Survey of Low Alloy Aircraft Steels, Heat Treated to High Strength Levels", *WADC Tech. Rept. 53-254, pt, I*, p. 14, Air Force Materials Lab. (WPAFB) Dayton, Ohio (Jun 1954).

[7] G.E. Wood and W.L. Mitchell, "Relieving Hydrogen Embrittlement in Fully Hardened Electroplated Steel", *Metal Progress*, **91** (3), pp. 79-80 (1967).

[8] E. Chilton, "Development of Electroplating Processes to Eliminate Hydrogen Embrittlement in High Strength Steel", *WADC Tech. Rept. 57-514*, p. 6, Air Force Materials Lab (WPAFB) Dayton, Ohio (Jan 1958).

[9] R.L. Mills and F.J. Edeskuty, "Hydrogen Embrittlement of Cold Worked Steels", *Chemical and Engineering Progress*, **52** (11), pp. 477-480 (1956).

[10] D.D. Perlmutter and B.F. Dodge, "Effects of Hydrogen on Properties of Metals", *Ind. Eng. Chem.* **48**, pp. 885-892 (1956).

[11] Ref. [6], p. 46.

[12] B.F. Brown, "Effect of Baking on Delayed Fracture of Electroplated Ultra High Strength Steel", *NRL Report 4839*, p. 5 Naval Research Lab., Washington, D.C. (Oct 1956).

[13] "Methods of Testing for Hydrogen Embrittlement", Final Report on ARTC Project W-95, Rept. No. NOR-59-472, p. 5, Northrop Corp. (Norair Div.), Hawthorne, Calif., (Oct 1959).

[14] Ref. [8], p. 7.

[15] A.R. Troiano, "The Role of Hydrogen and Other Interstitials in the Mechanical Behavior of Metals", *Trans. ASM*, **52**, pp. 54-80 (1960).

[16] *ASTM Standards* Part 30 E8-65T, p. 137 (issued 1951), revised 1965.

[17] "Screening Tests for High Strength Alloys Using Sharply Notched Cylindrical Specimens", Fourth Rept. of a Special ASTM Committee, *Mater. Res. Std.*, **2**, 200 (1962).

[18] M.H. Jones and W.F. Brown, Jr., "An Axial Loading Creep Machine", *ASTM Bulletin No. 211*, p. 55, ASTM, Philadelphia, Pa. (Jan 1956).

[19] W L. Cotton, "Hydrogen Embrittlement of High Strength Steels During Cadmium, Chromium and Electroless Nickel Plating", *Plating*, **47**, pp. 169-175 (1960).

[20] G.L. Hanna and E.A. Steigerwald, "Influence of Environment on Crack Propagation and Delayed Failures in High Strength Steels", Tech. Documentary Rept. No. RTD-TDR-63-4225, p. 12, Air Force Materials Lab (WPAFB) Dayton, Ohio, (Jan 1964).

[21] R.H. Cavett and H.C. van Ness, "Embrittlement of Steel by High Pressure Hydrogen Gas", *Welding, J.*, **42**, Research Suppl., 317 ff (1963).

[22] R.H. Raring and J.A. Rinebold, "A Small and Inexpensive Device for Sustained Loading Testing", *ASTM Bulletin, No. 213*, ASTM, Philadelphia, Pa., (1956).

[23] Ref. [6], p. 12.

[24] Ref. [6], p. 7.

[25] W.O. Allread and G.H. Robinson, "A Simple Test for Hydrogen Embrittlement", *Metal Progress*, **86**(5), pp. 102-106 (1964).

[26] D.J. Cash and W. Scheuerman, "High Strength Steel Can Be Cadmium Plated Without Embrittlement", *ibid.*, **75** (2), p. 93, (1959).

[27] R.L. McGlasson and W.D. Greathouse, "Stress Corrosion Cracking of Oil Country Tubular Goods", *Corrosion*, **15**, p. 437, (1959).

[28] F.S. Williams, W. Beck, and E.J. Jankowsky, "A Notched Ring Specimen for Hydrogen Embrittlement Studies", *Proc. ASTM*, **60**, pp. 1192-1202 (1960).

[29] E.J. Jankowsky, W. Beck, and F.S. Williams, U.S. Patent 3,034,340, (May 15, 1962), "Electrical Crack Measuring Device for Determining Metal Deterioration",

[30] "Evaluation of the Cyanide and Fluoborate Cadmium Plating Baths for Hydrogen Embrittlement under Different Plating Conditions", Report 8901, McDonnell Aircraft Corp., St. Louis, Mo., (July 1962).

[31] "A Comparison of the Cadmium Fluoborate and the Cadmium Cyanide Plating Process and the Degree of Hydrogen Embrittlement Imparted by Each Process to High Tensile Strength Steels", Report 9082, McDonnell Aircraft Corp., St Louis, Mo., (Oct 1962).

[32] W. Beck, E.P. Klier, and G. Sachs, "Constant Strain Rate Bend Tests On Hydrogen Embrittled High Strength Steels", *Trans, AIME*, **206**, p. 1266, (1956).

[33] A.R. Elsea and E.E. Fletcher, "Hydrogen Induced Delayed Brittle Failures of High Strength Steels", *DMIC Rept.* **196**, 102 ff, Battele Memorial Inst., Cblumbus, Ohio, (Jan. 1964).

[34] W. Beck, A.L. Glass, and E. Taylor, "The Role of Absorbed CN-Groups in the Hydrogen Embrittlement of Steel", *J. Electrochem, Soc.*, **112**, pp. 53-59 (1965).

[35] E.P. Klier, B.B. Muvdi, and G. Sachs, "The Response of High Strength Steels in the Range of 180 to 300 ksi to Hydrogen Embrittlement from Cadmium Plating", *Proc. ASTM*, **58**, p. 605, (1958).

[36] B.G. Johnson, "Method of Test for Hydrogen Embrittlement Due to Electrolytic Cadmium Plating", Fourth Pacific Area Meeting of ASTM, Los Angeles (1962), *ASTM STP No. 345*, ASTM, Philadelphia, Pa. (1962).

[37] G.L. Hanna, A.R. Troiano, and E.E. Steigerwald, "A Mechanism for the Embrittlement of High Strength Steels by Aqueous Environments", *Trans. ASM*, **57**, 668 ff (1964).

[38] P.C. Hughes, I.R. Lamborn and B.B. Liebert, "Delayed Fracture of a Low Alloy Steel in Corrosive Environments", *J. Iron Steel Inst.*, **203**, 156 ff (1965).

[39] W. Beck, E.J. Jankowsky, and W.H. Golding, "Fatigue and Delayed Brittle Failure of Vacuum Melted and Cadmium Plated Steel", *Corrosion*, **7**, pp. 709-715 (1967).

[40] E.R. Slaughter, E.E. Fletcher, A.R. Elsea, and S.K. Manning, "An Investigation of the Effects of Hydrogen on the Brittle Failure of High Strength Steels", WADC Tech. Rept. 56-83, Air Force Materials Lab. (WPAFB) Dayton, Ohio, (June 1955).

[41] H.C. Davis and J.A. Gray, "A Study of the Size Effect in the Plating Embrittlement of High Strength Steels", Royal Aircraft Establishment Tech. Rept. No. 66168, Farnborough, England (June 1966).

[42] S. Goldberg, "Corrosion Protection of High Strength Steels", *Symposium About the Load Carrying Applications of High Strength Steels*, DMIC Report No. 210, p. 87, Batelle Memorial Inst., Columbus, Ohio (October 1964).

CHAPTER 2
THE DETERMINATION OF HYDROGEN IN STEEL AND RELATED TOPICS

This chapter is devoted to a description and analysis of some of the methods suggested for the determination of hydrogen in steel and associated problems, such as the storage of hydrogen charged specimens, hydrogen standards, and the correlation of hydrogen content with hydrogen embrittlement.

2.1 METHODS FOR THE DETERMINATION OF HYDROGEN

Commonly used methods of hydrogen analysis are solid state hot vacuum extraction, vacuum fusion, vacuum-tin fusion and thermal conductivity. The first three analytical methods are described thoroughly in the literature[1-3].

2.1.1 HOT VACUUM EXTRACTION

A convenient set-up for hydrogen analysis called the LECO hydrogen analyzer is commercially produced in this country by Laboratory Equipment Corporation in St. Joseph Michigan. In this instrument, the hydrogen is extracted along with carbon monoxide and nitrogen by a combination of heat and vacuum, and the total gas pressure is determined. Hydrogen is converted by copper oxide to water and is absorbed in an anhydrone column. The pressure of the remaining gas mixture is then determined. The difference between the total gas pressure and that produced by the mixture ($CO + N_2$) is the pressure due to hydrogen. This difference is converted to concentration by standard conversion factors.

2.1.2 THERMAL CONDUCTIVITY

Analysis of the evolved gases for hydrogen by means of thermal conductivity has definite advantages as compared with other vacuum extraction methods. The advantages are that it eliminates the often questionable conversion of hydrogen to water vapor in the copper oxide furnace, simplifies the apparatus, and increases the speed of analysis. A properly prepared and weighed specimen can be analyzed in only 10 minutes with an approximate error of ±0.12 ppm of hydrogen. Another thermal conductivity method using a carrier gas (similar to gas chromatography for the analysis of hydrogen in weldments is described in detail in Chapter 8).

Chipman et al.[4] modified the classical vacuum tin fusion technique by replacing the copper oxide furnace, the freeze out traps and the gas circulating components by a conductivity cell, a conductivity measuring bridge, and a mixing chamber. These investigators used a sensing element consisting simply of a platinum wire suspended in the center of the cell. The current needed to maintain the wire at a specified temperature is determined by the rate of heat exchange between the wire and the volume of the surrounding gas. The current is determined by means of a bridge circuit and is a measure of the thermal conductivity of the gas.

The gas extracted from steel is essentially a mixture of hydrogen, nitrogen and carbon monoxide. The hydrogen content normally exceeds that of the other gases by about 50 percent. The thermal conductivities of carbon monoxide and nitrogen are practically identical while that of hydrogen is about seven times greater than that of the other gases. The thermal conductivity of the gaseous mixture (H_2, N_2 and CO), at a known pressure and temperature can then be related directly to the percentage of hydrogen by suitable calibration of the cell. The same principle is used in the catharometer, which is described in the chapter dealing with hydrogen embrittlement in weldments.

2.1.3 ELECTROMETRIC TITRATION

Hydrogen can also be determined by electrometric methods[5]. The hot extracted hydrogen is carried by means of argon gas to a furnace containing hot copper oxide, where it is oxidized to water, which is passed over carbon forming carbon monoxide and oxidized to carbon dioxide. The carbon dioxide is absorbed in an alkaline solution, and the quantity of hydroxide necessary to restore the original pH is determined electrometrically and the quantity of extracted hydrogen calculated. The advantage of this method is its simplicity and speed.

Another technique for the determination of hydrogen based on polarography, was suggested by Franklin and Franklin[6].

2.1.4 THE LAWRENCE HYDROGEN DETECTION GAGE

Another hydrogen determination method using the Lawrence hydrogen detection gage (LHDG) is based on pressure measurements using an ionization gage[7-9]. Current applications are: (1) monitoring hydrogen pick-up by metals during plating or processing procedures used for activating, pickling, cleaning, and paint stripping, (2) determining the permeability of plating to hydrogen, and (3) measuring hydrogen formed by corrosion processes. The instrument is comprised of a probe (a metal vacuum tube), electroplating power sources, electronic controls for the different functional components, integrator, probe clean-up capability, a temperature controlled oven and a recorder. The probe and associated electronics are the heart of the instrument.

The probe or sensing element is used as an ionization gage for measuring hydrogen pressures between 10^{-3} and 10^{-8} torr. The gage contains an electron emitting filament, grids that serve as anodes, and an ionization plate that collects positive ions formed by the bombardment of residual gases by electrons emitted by the filament and collected by the grids. When the electron emission current and the potential of grids and collector-plate are maintained at fixed values, the relationship between pressure and ionization current can be considered sufficiently linear for measurement of hydrogen pressure. Since the only gases which can permeate the steel shell at temperatures below 500 C are hydrogen and its isotopes, the instrument provides a powerful tool for the determination of hydrogen. A block diagram is depicted in Fig. 2.1.

The probe is used as the experimental specimen for each run. For example, if the hydrogen embrittling characteristics of a plating bath are to be evaluated, the probe is plated and the hydrogen generated during the process, which has entered the probe is measured. Calibrations are performed in a NaOH/NaCN solution by cathodically charging the probe with hydrogen.

After hydrogen charging (calibration, plating, etc), the probe is washed, dried, and placed in the LHDG oven at 208 C. The use of a temperature controlled oven is to increase the sensitivity and precision of results. The ionization gage measurement, as noted on the recorder tracing, shows a rapid increase to a hydrogen peak (HP) reading followed by a decrease. This reading is proportional to the hydrogen absorbed by the probe and, therefore, is not equal to the total hydrogen generated. A recorder tracing of a calibration run showing hydrogen peak (pressure in arbitrary units) vs. time is given in Fig. 2.2.

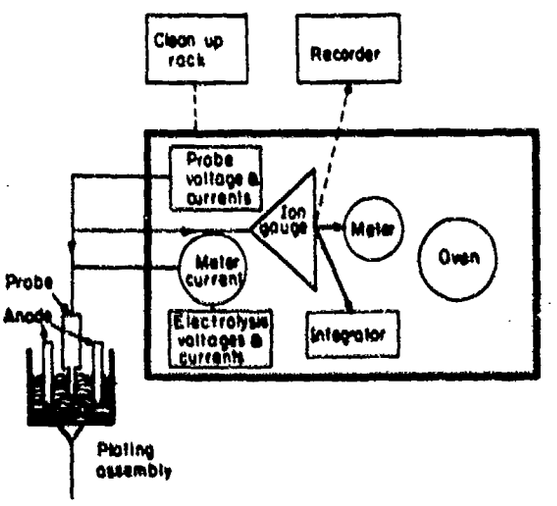

Fig. 2.1 – Block diagram of Lawrence hydrogen detection gage and accessories.

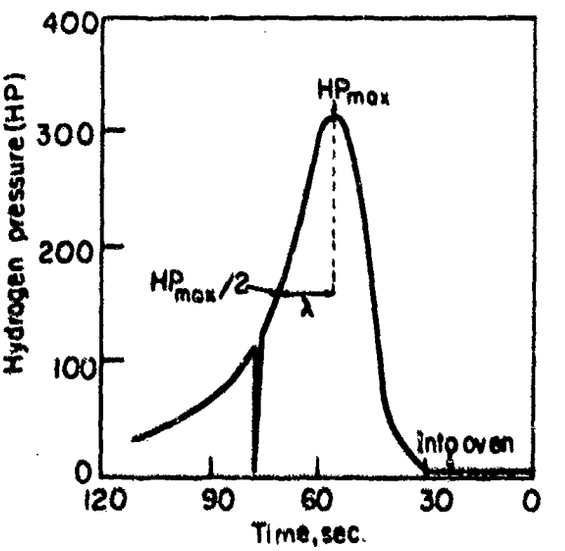

Fig. 2.2 – Typical plot of hydrogen pressure, HP Peak in arbitrary units versus time. The ascending branch indicates hydrogen input while the descending branch shows hydrogen output (out diffusion and gettering effects).

A permeability factor, λ, can be determined from the recorder tracing. This factor for the shell and the plated metal coating is calculated as the half-life of the pressure peak, which is the time interval from $HP_{max}/2$ during the outgassing period.

The effect of the type of cadmium plating and its thickness on HP peak and on the permeability factor[10] is impressively shown in Table 2.1.

TABLE 2.1 – LAWRENCE HYDROGEN DETECTION GAGE MEASUREMENTS FOR DULL (POROUS) AND BRIGHT (DENSE) CADMIUM PLATE

Average Plating Thickness	HP Peak		Permeation Factor	
Mil	Dull	Bright	Dull	Bright
0.045	24	320	46	45
0.110	60	1827	47	68

The hydrogen concentration in the steel wall of the probe as indicated by the HP peak represents a relative value. A definite advantage of the procedure is that it is rather simple and requires a short testing time. A disadvantage is the limited life of the tubes (so far only available in steel). In the current design, a paint coating is used at the probe base, which may interact with agressive materials subjected to hydrogen testing. This interaction may result in paint destruction and even hamper the proper functioning of the probe. Limited data obtained to date indicate that the instrument appears to have good reproducibility and sensitivity. The use of this method for correlating hydrogen content with hydrogen embrittlement is discussed in section 2.2.3.

2.1.5 ELECTROCHEMICAL HYDROGEN PERMEATION

The electrochemical hydrogen permeation method[11], developed some years ago, offers a powerful tool for the exploration of the problem of correlating hydrogen absorption with hydrogen embrittlement. The experimental set-up, used in these permeation studies, consists essentially of two compartments containing the electrolytes which are separated by a thin metal membrane. The hydrogen produced on one side, e.g., by cathodic polarization permeates the membrane and is ionized on the diffusion (anodic) side, by maintaining a constant anodic potential. A schematic is given in Fig. 2.3.

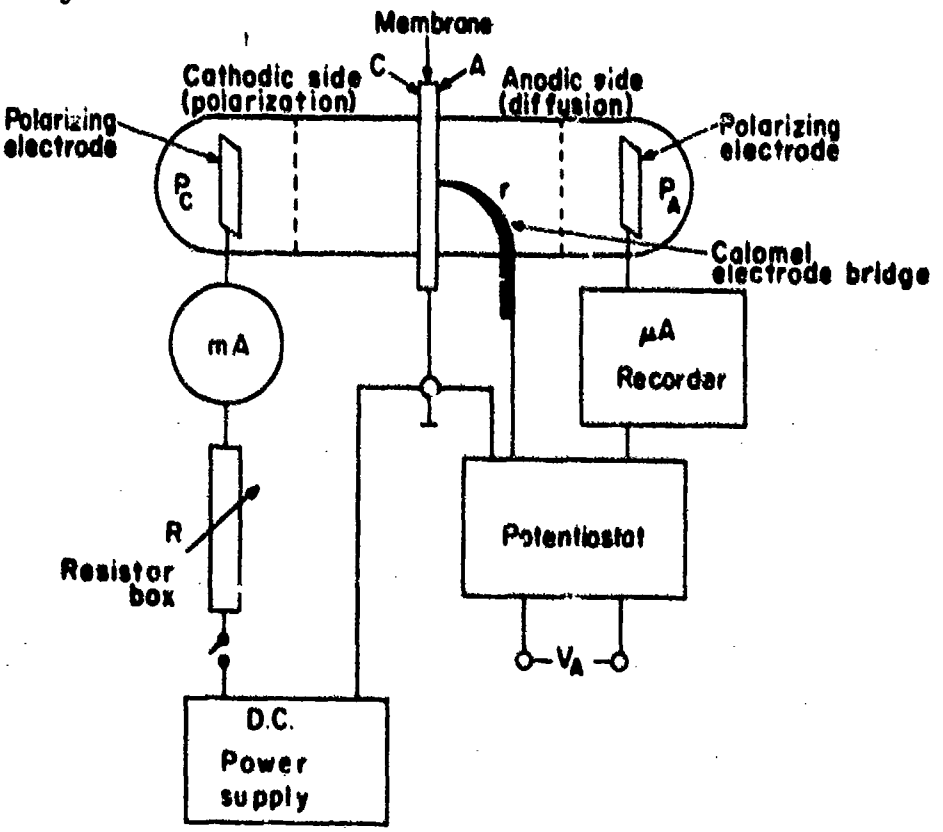

Fig. 2.3 – A schematic of the experimental set-up for measuring hydrogen permeation currents

In this method, the hydrogen concentration on the surface of the polarization side is constantly maintained at a maximum concentration C_O, while on the diffusion side it is maintained at zero concentration, C_L, where L is the membrane thickness.

The permeation method[12] gives essentially two parameters the change in current with time (transient) and the steady state hydrogen permeation current (I_{∞}). The hydrogen diffusion coefficient (D_H) can be calculated from these parameters. The complete hydrogen concentration profile in the membrane can be calculated at any instant after initiation of cathodic polarization by the following equation.

$$C_O - C_L = \frac{J_{\infty} L}{D_H FZ} \qquad (2.1)$$

F = Faraday

Z = number of electrons involved in the reaction

F = Thickness of the membrane, cm

The maximum hydrogen concentration, C_O, as indicated by the above stated boundary conditions can be calculated from the above equation (when $C_L = 0$). The hydrogen profile is obtained from this equation for all conditions where $C_L \neq 0$. Hydrogen can of course also be generated by acid pickling or by contact of the steel with a more anodic metal, conditions which can easily be reproduced in the permeation cell.

These are rather singular cases and it would be of much greater practical importance to obtain the quantity of hydrogen introduced into steel during electroplating, because it is this hydrogen which induces the embrittlement.

2.1.6 LESS COMMON METHODS FOR MEASURING HYDROGEN

A number of investigators determined hydrogen permeation through a thin steel membrance by means of a manometric method. This method suffers from lack of sensitivity and can only be used when the hydrogen concentration in the specimen exceeds 1 ppm. Another drawback will be discussed in a later section. Recently, Troiano et al.[13, 14] determined the rate of hydrogen evolution on the diffusion side of a cathodically charged austenitic stainless steel membrane by this method. The experimental circumstances prevailing in this permeation experiment meet the conditions for hydrogen entry, a prerequisite for hydrogen embrittlement. Hydrogen in charged alpha iron in "true solid solution" was measured by Lord et al.[15] by means of ultrasonic attenuation (1 ppm or less).

2.2 PROBLEMS ASSOCIATED WITH HYDROGEN ANALYSIS

2.2.1 HYDROGEN STANDARDS

In spite of the high sensitivity of most of the analytical procedures just described, appreciable fluctuations in the results of hydrogen determinations due to a lack of reliable standards presented serious problems to investigators. It was not possible to distinguish between analytical and sampling errors in hydrogen analysis, and the possibility of taking full advantage of the results of analytical hydrogen determinations for hydrogen embrittlement studies was seriously hampered. Hydrogen analysis presents a problem unique in the field of metallurgical gas analysis because of the high solubility and diffusivity of hydrogen in steel over a wide range of temperatures. Despite formidable handicaps, reliable steel standards for hydrogen determination were produced recently by the British Welding Research Association, Cambridge[16] and will be of great value in alleviating the problem of unreliable standards.

Steel standards were prepared with precisely known hydrogen contents, using an encapsulation technique. Since the hydrogen content of the capsules remains constant indefinitely at room temperature, and since the hydrogen level is predetermined independently of analytical techniques, the specimen can be used to advantage as standards in hydrogen gas analysis. By heating the container to 650 C, a small but significant proportion will be dissociated and the atomic hydrogen formed will thus be free to diffuse through the steel wall. The outward diffusion will continue as long as a concentration gradient exists throughout the wall thickness. A prerequisite of hydrogen standard design is, therefore, the sealing of a precisely known volume of the gas in an appropriate steel container. The British research group succeeded in solving the problem by: (1) determining precisely the volume of hydrogen gas enclosed in a

cylindrical steel container; (2) sealing the container in such a manner that none of the enclosed gas is lost either before, during, or after the sealing operation. The recepticle consists of a short cylindrical thin walled tube of low carbon mild steel, closed by a spherical ball lid made of 18-8 stainless. The volume of the container and hence of hydrogen is varied by changing the diameter of the cylinder. The capsule is sealed by means of an appropriate resistance welding technique. Welding is completed in 40 to 100 milliseconds, thus reducing the risk of losing gas from the capsule to a minimum.

Coe[17] recently developed another encapsulation technique, which is predominantly used in welding.

2.2.2 SAMPLE STORAGE MINIMIZING HYDROGEN LOSS

It is well known that specimens containing hydrogen, introduced by any type of charging procedure lose hydrogen when stored at room temperature. The rate of hydrogen loss is determined by a number of variables, particularly composition, temperature, storage time, and to a degree, specimen size. For studies involving hydrogen analysis, where as a rule a great number of specimens are charged under the same conditions, the problem of storing the test samples without losing hydrogen becomes crucial. Since the hydrogen diffusion rate is slowed down with decreasing temperatures, it has been suggested that the specimens be stored in an appropriate cooling medium and analyzed as quickly as possible after their removal. Typical results[18] are plotted in Fig. 2.4

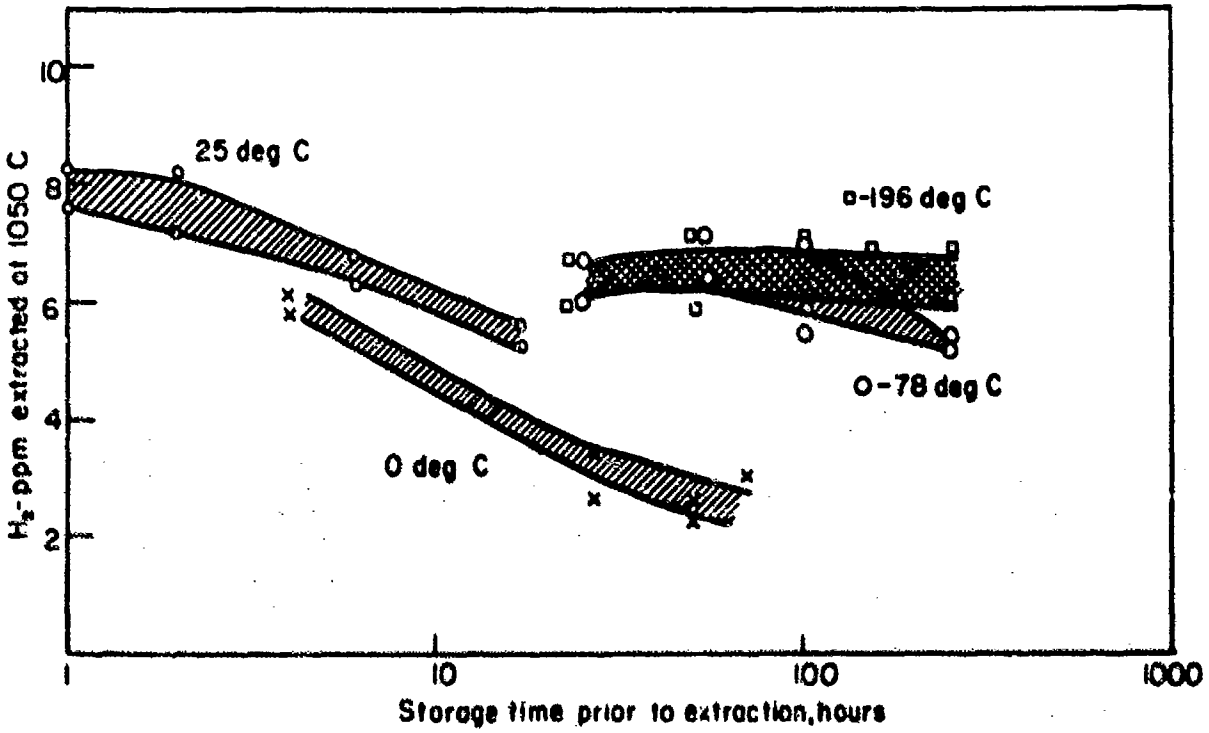

Fig. 2.4 – Effect of storage temperature and time on hydrogen loss of cathodically charged ferritic Armco iron specimens containing about 8 ppm of hydrogen

Figure 2.4 shows that it is not safe to keep the specimens at room temperature, because the hydrogen content gradually decreases. Storage in an ice-water mixture shows some improvement as compared with room temperature storage. The results plotted in the diagram indicate that the specimens cannot be stored even one day at a temperature of 0 deg. C, without losing an appreciable portion of their hydrogen content. Storage in a dry ice-acetone mixture (-78 C) is satisfactory for periods up to 6 days. If samples are to be stored for as long as a week or more, they must be kept in liquid nitrogen (-196 C). The width of the scatter band gives an indication of the reproducibility of this type of measurement.

2.2.3 CORRELATING HYDROGEN CONTENT WITH HYDROGEN EMBRITTLEMENT

Comparatively little work has been done in this domain. Predictions of embrittlement using the Lawrence gage (section 2.1.4) require correlation of the determined HP peak produced by a specific treatment, with any

mechanical embrittlement test on specimens subjected to the same treatment. The effect of this specific treatment on hydrogen embrittlement may then be predicted by HP peak measurements. The Douglas stressed ring test[19, 20] has been used successfully to correlate HP peak measurements with hydrogen embrittlement.

Seabrook et al.[18] correlated reduction in area, determined on cathodically charged SAE 1020 steel specimens, with their hydrogen content obtained by the vacuum-tin fusion method. Results are plotted in Fig. 2.5.

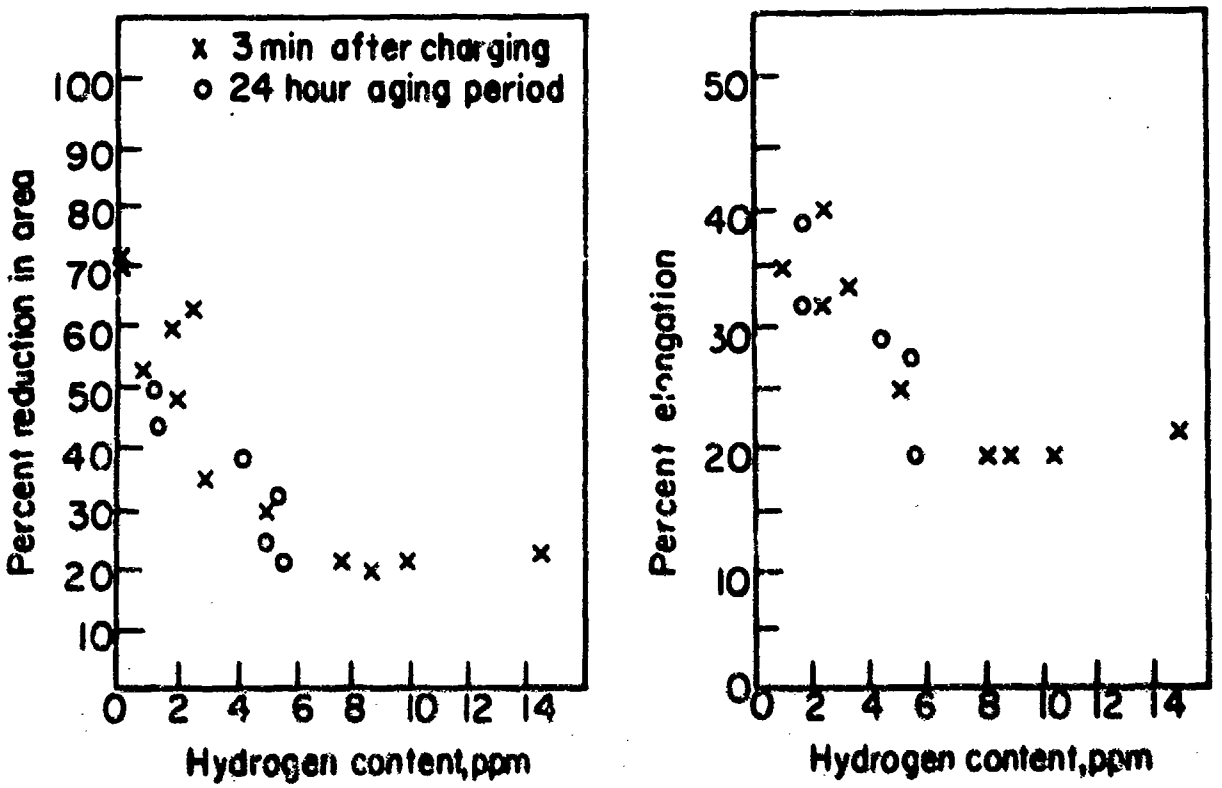

Fig. 2.5 – Effect of varying hydrogen content on the tensile ductility. SAE 1020 steel cathodically charged. Rate of testing, 0.05 in./min. Data are shown for tests performed 3 min. after charging and after 24 hours aging at room temperature.

This plot shows ductility dropping sharply with hydrogen content increasing up to about 6 ppm. These results indicate a definite relationship between embrittlement and quantity of hydrogen charged into the test bar. Aged specimens fit essentially the same curve as that of the unaged bars. So far it is not certain if the above relationship for 1020 steel holds for other steels.

Figure 2.6 is a good example of the effect of the "residual hydrogen" in cast steel on hydrogen embrittlement. The hydrogen quantity retained in the ingot[21] depends on variations in melting technique and hydrogen segregation. The samples were taken from three positions in the ingot. The hydrogen was determined by vacuum extraction at 1050 C and is reported as relative volume, which represents the quantity of hydrogen which, when measured at STP occupies the same space as the quantity of steel analyzed, provided the sample is free of pores.

The relative volume, RV, is 12.72 cm^3 of hydrogen per 100 g of steel. The true breaking stress is defined as the maximum load divided by the final reduced area. This stress may be considered a true measure of ductility and, therefore, the curves show clearly increasing loss in ductility of aged and normalized test bars with increasing hydrogen content. Apparently the trends of the curves are primarily determined by the thermal treatments.

Hobson and Sykes[22] found that large spatial variations in the residual hydrogen content of large forgings increased with decreasing sample size.

The next example is an attempt to correlate the so-called "mobile hydrogen" with the delayed failure behavior of a steel alloy. According to Brittain[23] it is not the total hydrogen obtained at high extraction temperature which causes embrittlement, but rather that portion extracted at a temperature as low as 350 C (the "mobile hydrogen"). The steel was cyanide cadmium plated, baked, and the delayed brittle failure performance investigated

under sustained loads. After removal of the cadmium plating, the "mobile hydrogen" was determined on the ends of the broken notched tensile specimens.

The next figure, Fig. 2.7 shows the effect of the "mobile hydrogen" on stress rupture time. At first glance, it appears amazing that a hydrogen concentration, as low as that determined with these specimens is sufficient to induce embrittlement. This problem will be discussed in greater detail later in this chapter.

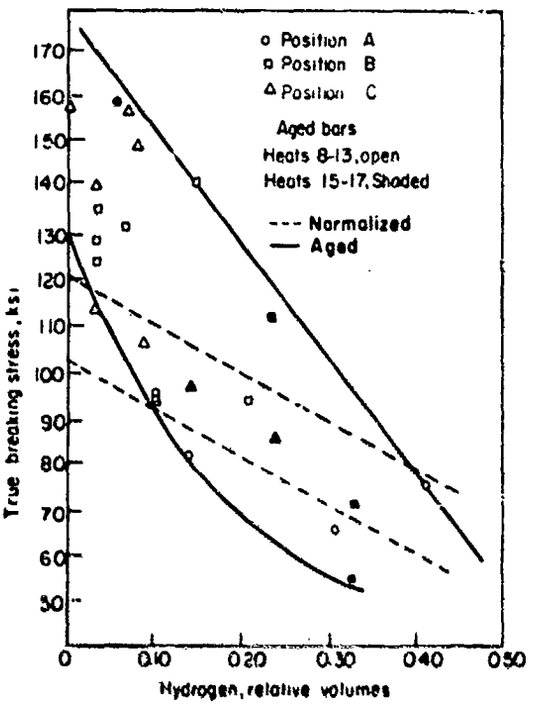

Fig. 2.6 – Effect of "residual hydrogen" in cast steel bars on the true breaking stress. Data are presented for bars aged at 360 C for 25 hours and for bars normalized at 890 C and cooled for 2 hours in still air. Specimens were taken from three different locations in the ingot.

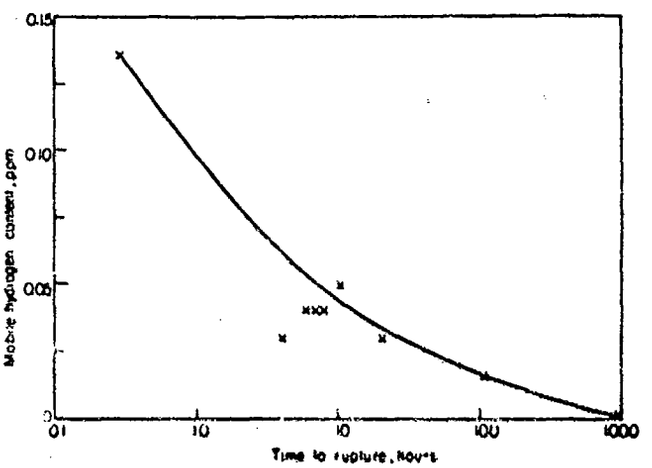

Fig. 2.7 – Effect of "mobile hydrogen" on the stress rupture behavior of notched steel specimens (3% Cr + 1% Mo). The applied load was 200 to 250 ksi. Specimens were cyanide cadmium plated and baked for 2 hours at 200 C.

Beck in conjunction with Devanathan and Stachurski[11] demonstrated that by skillful use of the permeation method important information about the relationship between hydrogen absorption and embrittlement can be obtained. They were interested in finding the reason for the drastic change in embrittlement, related to changes in the composition of cadmium plating baths.

They used appropriate model solutions to record permeation transients to determine the cause of the above findings. The model solutions approximated the standard plating baths, i.e., they had a corresponding pH and complexing agent but did not contain cadmium. Hydrogen permeation measurements indicated that the hydrogen concentration in the specimen is profoundly affected by preferentially adsorbed complexing agents.

Reported in the literature are tensile and bend ductility measurements on high strength steel specimens, plated with cadmium from the conventional cyanide bath, a fluoborate bath, and an amino butyric acid bath. Also available are sustained load delayed failure measurements on cadmium plated notch tension specimens and average survival times of cadmium plated specimens, which broke in less than 100 hours under sustained loads of 75 percent of the NTS of the unplated test bars. However, the number of available embrittlement measurements on e.g., ultra strength AISI 4340 steel cadmium plated from the above mentioned three plating baths are too limited to permit a statistical correlation. Therefore, an attempt was made to correlate embrittlement results by means of a histogram.

The plots were made in such a manner that the steady state permeation current determined for the CN containing solution was set to equal 100 percent absorption of hydrogen. The calculation of the absorption was made from the hydrogen permeation currents for the other two model solutions and was based on this value.

The differences in measurements obtained on unplated specimens and those on cyanide cadmium plated test bars of AISI 4340 steel from slow rate fracture deflection, tensile ductility measurements, and the fracture

stress after 100 hours under sustained load of 75 percent of the unplated NTS were set equal to 100. The results of corresponding mechanical measurements on specimens plated with cadmium from the fluoborate and amino butyric acid baths were then related percentage wise to those determined on cyanide cadmium plated test bars as described above.

The results of above described computations are presented in the histogram, Fig. 2.8, which strikingly demonstrates the intimate relationship between hydrogen absorbed in the structure of the steel diaphragm and the susceptibility to brittle fracture of the cadmium plated steel, determined by any one of the three different mechanical tests.

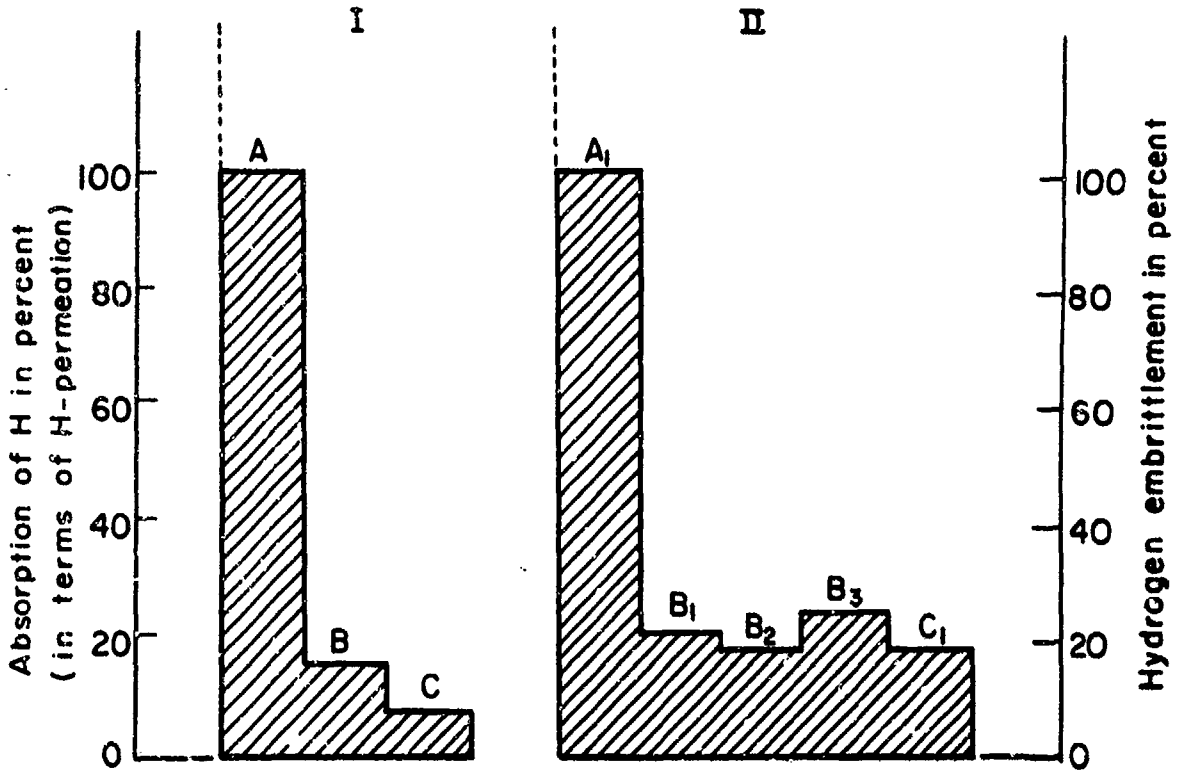

Fig. 2.8 – Hydrogen permeation compared with hydrogen embrittlement of AISI 4340 steel (260-280 ksi) plated from different cadmium baths

I Permeation measurements from Cd free solutions containing compounds used as complexing agents

- A CN solution
- B Ammonium fluoborate solution
- C Aminobutyric acid solution

II Hydrogen embrittlement measurements of specimens plated from different cadmium baths

- A_1 Cyanide bath, all mechanical tests
- B_1 Fracture deflection (fluoborate bath)
- B_2 Reduction in area (fluoborate bath)
- B_3 Fracture stress after 100 hours of sustained load at 75% of the unplated NTS (fluoborate bath)
- C_1 Fracture deflection (amino butyrate bath)

Detailed information in section 2.2.3

The average survival time was increased 200 times when the notched tension bars were plated from the aminobutyrate bath instead of the cyanide bath. An analysis was made of the complex trends of the hydrogen permeation transients recorded during the actual plating of cadmium from the above mentioned baths. This analysis revealed that hydrogen was introduced into the steel within an initial, rather short period of plating while the barrier effectiveness of the very thin plating was still negligible[11].

Other results clearly indicate that adsorption equilibrium, high hydrogen coverage, and spacing of the embrittling hydrogen atoms in vacancies of the bcc lattice and embrittlement are quickly accomplished by the cyanide species in contrast with the other two complexing agents.

Calculation of the maximum hydrogen concentration (C_O) on the galvanostatically polarized Armco iron membranes (-8 mA/cm^2) in cyanide, ammonium fluoborate, amino butyric acid and sodium hydroxide solutions were 1.45, 0.85, 0.63 and 0.18 ppm respectively. These values are in a remarkably good agreement not only with the embrittlement measurements plotted in the histogram, Fig. 2.8, but also with those of Beck and Jankowsky[24] who showed that the fracture deflections of specimens charged in a pure NaOH solution were much higher than those of specimens charged in a CN containing solution or plated with cadmium from the conventional cyanide bath.

Fig. 2.7 clearly indicates that embrittlement can be induced by very low hydrogen concentrations (mobile hydrogen). Very low concentrations of embrittling hydrogen were found also by an ultrasonic attenuation method[15]. The general agreement between the above calculated value, C_O, (for cyanide) and that determined for "mobile hydrogen" is considered to be strong support of the assumption that hydrogen embrittlement is induced by much lower quantities of hydrogen than that determined as total hydrogen.

A prerequisite for reliable calculation of the maximum hydrogen concentration is the determination of the hydrogen diffusion coefficient which, therefore, must be determined with the highest precision. The electrochemical permeation method alone satisfies this requirement. McBreen, Nanis and Beck,[12] have compared this method with the conventional manometric time lag method and have emphasized that the superiority of the electrochemical procedure lies in the fact that in addition to its much higher sensitivity, the boundary conditions are sharply defined. In contrast in the manometric method, as the pressure builds up at the diffusion side of the membrane (during the permeation process) and thus, the equilibrium concentration of the hydrogen does not remain constant. This gives rise to a situation with "shifting" boundary conditions and easily may lead to erroneous values for permeation rates and diffusion coefficient as well. In summary, it should be emphasized that the embrittlement determining hydrogen concentration depends on numerous variables. These variables consist primarily of the composition of the steel, its hardness, the hydrogen solubility and diffusivity. Very little is known about the relationship between the distribution of hydrogen inside the metal and its embrittlement behavior. The role of total and "mobile hydrogen" in embrittlement initiation is still open to discussion. At the present state of the art it is difficult if not, impossible to base a prediction of the susceptibility to brittle failure, or loss in ductility of any type of steel for a specified quantity of extracted hydrogen.

REFERENCES

[1] D. C. Carney, J. Chipman and N. J. Grant, "The Tin Fusion Method for the Determination of Hydrogen in Steel", *Trans AIME*, **188**, pp. 397-403 (1950).

[2] J. F. Martin, R. C. Takacs, R. Rapp and L. M. Melnick, "Evaluation of Methods for Determining Hydrogen in Steel", *ibid.*, **230**, pp. 107-112 (1964).

[3] M. Smialowski, Hydrogen in Steel, Addison-Wesley Publishing Co. Inc., Reading, Palo-Alto, London (1962).

[4] B. M. Shields, J. Chipman and N. J. Grant, "Thermal Conductivity Method for Analysis of Hydrogen in Steel", *Trans AIME*, **197**, pp. 180-184, p. 1551 (1953).

[5] E. Giegerl, "Electrometric Determination of Hydrogen in Steel by a Carrier Gas Method", *Archiv. Eisenhütt.* **33**, pp. 453-458 (1962).

[6] T. C. Franklin and N. F. Franklin, "Verification of the Coulometric Method of Analysis of Hydrogen in Iron", *J. Electroanalytical Chem.* **8**, pp. 310-311 (1964).

[7] S. C. Lawrence, Jr., "Detection and Control of Chemisorbed Hydrogen During Electrolysis, *Proc. Am. Electroplaters' Soc.*, **47**, pp. 135-137, p. 244 (1960).

[8] *"Proceedings of the First Biennial Hydrogen Corrosion and Embrittlement Symposium"*, Lawrence Electronics Co., Seattle, Washington (1967).

[9] Mildred N. Patterson, "A Study of the Lawrence Hydrogen Detection Gauge for Control of Production Electroplating Processes", BUWEPS, WEPTASK, RRMA-55038/010/IR-007080i, *USN Air Station, Alameda, Cal.* (Sept. 1964).

[10] P. Fischer and W. Beck, "Evaluation of the Lawrence Hydrogen Detection Gage for the Prediction of Hydrogen Embrittlement", Report No. NADC-MA-7052, Naval Air Dev. Center, Warminster, Pa. (Oct., 1970).

[11] M. A. V. Devanathan, Z. Stachurski and W. Beck, "A Technique for the Evaluation of Hydrogen Embrittlement Characteristics of Electroplating Baths", *J. Electrochem. Soc.*, **119**, pp. 886-890 (1963).

[12] J. McBreen, L. Nanis and W. Beck, "A Method for Determination of the Permeation Rate of Hydrogen Through Metal Membranes", *J. Electrochem. Soc.*, **113**, pp. 1218-1222 (1966).

[13] H. H. Shively, R. F. Heheman and A. R. Troiano, "Hydrogen Permeability in a Stable Austenitic Stainless Steel", *Corrosion*, **22**, pp. 253-256 (1966).

[14] H. H. Shively, R. F. Heheman and A. R. Troiano, "Hydrogen Permeability of a Stable Austenitic Stainless Steel Under Anodic Polarization", *ibid.*, **23**, pp. 215-217 (1967).

[15] H. T. Lord, B. B. Chick and G. P. Anderson, "Hydrogen in Alpha Iron, Determined via Ultrasonic Snook Effect", Final Tech. Report, Contract N00019-67-C-0331 Metals Res. Lab., Brown University, Providence, R. I. (Jan, 1968).

[16] R. F. Coe, N. Jenkins and D. H. Parker, "The Preparation and Evaluation of Primary Standards for the Determination of Hydrogen in Steel", British Welding Research Assoc., Rept. Misc. 11/65, Cambridge, England (1965).

[17] R. F. Coe, "Measurement of the Hydrogen Potential of Welding Consumables by Encapsulation", *Metal Construction and British Welding J.*, **1**, pp. 108-109 (1969).

[18] J. B. Seabrook, N. J. Grant and C. Carney, "Hydrogen Embrittlement of SAE 1020 Steel", *Trans. AIME*, **188**, pp. 1317-1321 (1950).

[19] "The Lawrence Hydrogen Detection Gauge", Rept. Ser. No. LR-AD-1575 Douglas Aircraft Co., Inc., Santa Monica, Calif. (Aug. 1962).

[20] G. T. Sink, "A Low Embrittlement Cadmium Plating Process", *Plating*, **55**, pp. 449-455 (1968).

[21] C. Simms, George A. Moore, and W. Williams, "The Effect of Hydrogen on the Ductility of Cast Steels", *Trans. AIME*, **176**, pp. 283-308 (1949).

[22] J. P. Hobson and C. Sykes, "Distribution of Hydrogen in Large Ingots and Forgings", *J. Iron Steel Inst.* **170**, pp. 118-122 (1952).

[23] P. I. Brittain, "The Protection of Very Strong Steels", Hawker Siddeley Aviation Ltd, Res. Rept. R. 240 (p. 4) **63**, England (Dec. 1963).

[24] W. Beck and E. J. Jankowsky, "The Effectiveness of Metallic Undercoats in Minimizing Plating Embrittlement of Ultra High Strength Steel", *Proc. Am. Electroplaters' Soc.*, **47**, pp. 152-159 (1960).

CHAPTER 3

MEASUREMENT OF HYDROGEN INDUCED AND CONTROLLED CRACK PROPAGATION

3.1 METALLOGRAPHIC TECHNIQUES

A diagram (Fig 1.6) was presented in the chapter on mechanical testing depicting delayed failure performance of notched embrittled specimens subjected to sustained loads. The diagram illustrates crack propagation in the sharply notched area of a statically loaded specimen under the joint action of stress and hydrogen. To obtain detailed information about propagation of the crack, Troiano et al.[1] made measurements of the crack size in notched specimens which were stressed at a fixed applied load for various times. In addition to the"heat tinting method", the metallographic sectioning method was used to determine crack depths. Each specimen was longitudinally sectioned and polished and the "effective radial crack depth" (the component normal to the applied stress) was measured at the extremities of the notch diameter. Crack growth then may be expressed by either of two geometrically related parameters: percent of notch cross sectional area, or radial crack depth. Representative photomicrographs of cracks (or crack patterns) from their publication are presented in Figs. 3.1 and 3.2.

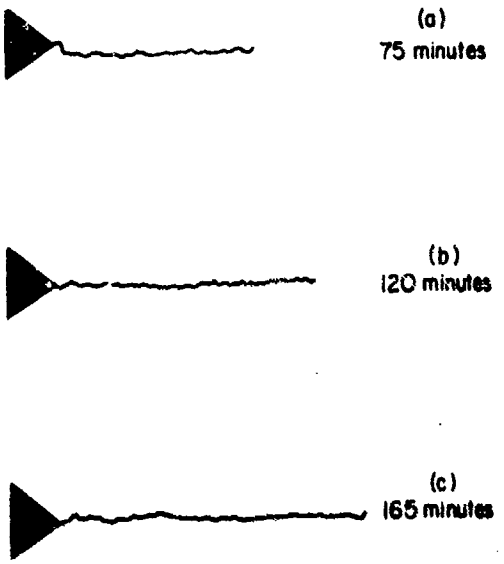

Fig. 3.1 – Cracks formed in notched specimens sectioned after static loading slightly above the lower critical stress limit for the indicated times (80 ksi). Longitudinal axial section, unetched (x 75). AISI 4340 steel, 240 ksi strength level, charged in 4% H_2SO_4 at 0.02 A/in^2 for 5 min at 80 F. Loaded 5 min after charging.

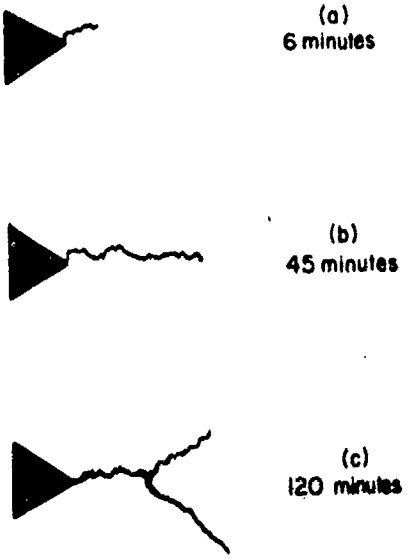

Fig. 3.2 – Cracks observed in notched specimens sectioned after static loading in the range of relatively slow crack propagation (175 ksi). Longitudinal axial section unetched (x75). AISI 4340 steel, 240 ksi strength level, charged in 4% H_2SO_4 for 5 min at 80 F. Loaded 5 min after charging.

The authors postulated that at the lower applied stress, the path of crack propagation remained in the notch plane, while at the higher applied stress, the advancing crack exhibited a tendency to branch and deviate from the notch plane, that is the plane normal to the applied tensile stress, passing through the notch diameter. This point of branching occurred at various positions, usually somewhat below the notch root. The plastic (permanent) opening of the crack, as evidenced by the crack width, was somewhat greater at the higher applied stress, but in both cases, it remained quite small even after considerable crack growth. In general, observations at high magnifications revealed the cracks to be continuous. However, occasional instances of apparent discontinuous growth or advanced

nucleation were observed. The crack originates at, or probably slightly below, the root of the circumferential notch and grows radially inward.

Fracture formation due to the action of hydrogen and stress, arises from the interaction of a number of complex factors such as notch geometry, hydrogen distribution, normal and shear stresses.

3.2 ELECTRICAL RESISTIVITY MEASUREMENTS

3.2.1 KELVIN DOUBLE BRIDGE MEASUREMENTS

With the serious limitations of the metallographic method in mind, Troiano et al. [2-4] developed an electrical resistance method for the measurement of crack propagation. In contrast to the metallographic method, which requires measurements on a series of different specimens, the electrical method permits determination of a complete crack propagation curve from only one specimen. The procedure is based on an empirically established relationship between crack area and the change in resistance of the notch section of the specimen used for the sustained load test. The electrical resistance is measured across the notch section by means of a precision Kelvin double bridge; its balance is determined by a galvanometer.

Figure 3.3 illustrates the manner in which the notched specimen is incorporated into the bridge circuit. The concentric loading members serve as current leads. The two knife edge potential leads, attached to the specimen on opposite sides of the notch, approximately 0.10 in. apart, define the resistance gage length. Each lead is free to move relative to the other, but remains fixed with respect to the specimen. With the exception of the range of comparatively small crack areas (below about 20 percent when expressed in percent of notch area), the relationship between resistance increase and the percent of notch area is linear. The dependency shows that the resistance increase measured under an applied stress is primarily the result of the geometric alterations of the specimen.

The action of tensile stress on the crack also affects resistance properties. Experimental results on hydrogenerated specimens are presented in Fig. 3.4. This curve reveals the same characteristic features as those shown in Chapter 1 (Fig. 1.6). Hence, the electrical resistance method is as suitable for the study of the kinetics of crack

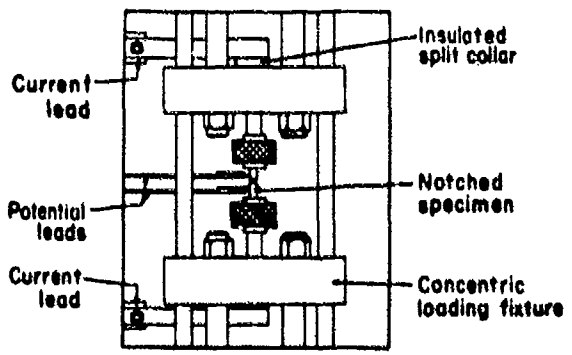

Fig. 3.3 – Experimental arrangement for measurement of the notch section electrical resistance under an applied tensile load.

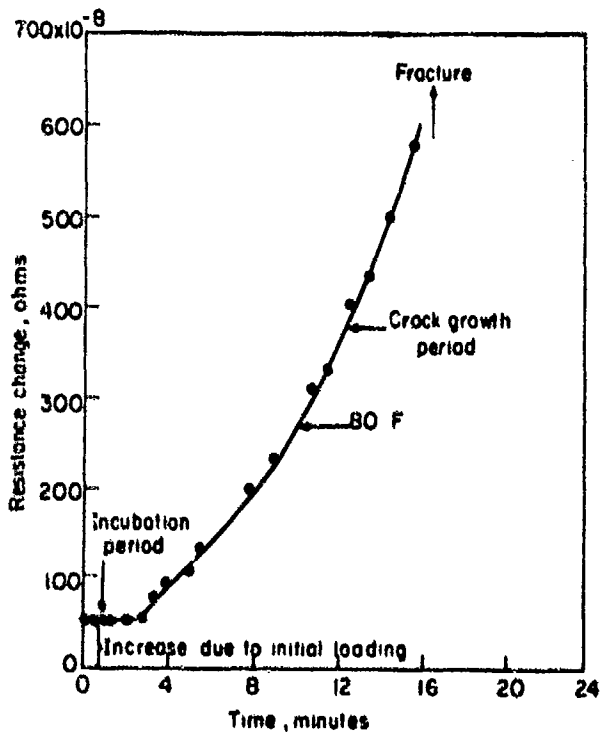

Fig. 3.4 – Resistance increase as a function of time for a uniformly hydrogenated, notched specimen. Tested in the stress range of delayed failure.

initiation and propagation as a pure mechanical or metallographic procedure. The typical resistivity-time curve in the figure again indicates the existence of an incubation period for crack initiation and a period of controlled crack propagation. On the basis of resistance measurements, the failure process may again be divided into three distinct stages: (1) the incubation phase, (2) the period of relatively slow crack propagation, and (3) catastrophic failure with extremely rapid crack growth. The appearance of the fracture as well as the resistivity curves clearly differentiate between these latter two statges.

From resistivity measurements, Troiano[3] proved that crack growth is a discontinuous process. He demonstrated this discontinuity by recording resistivity curves at low temperatures where the hydrogen diffusion rate is slowed down, as shown in Fig. 3.5.

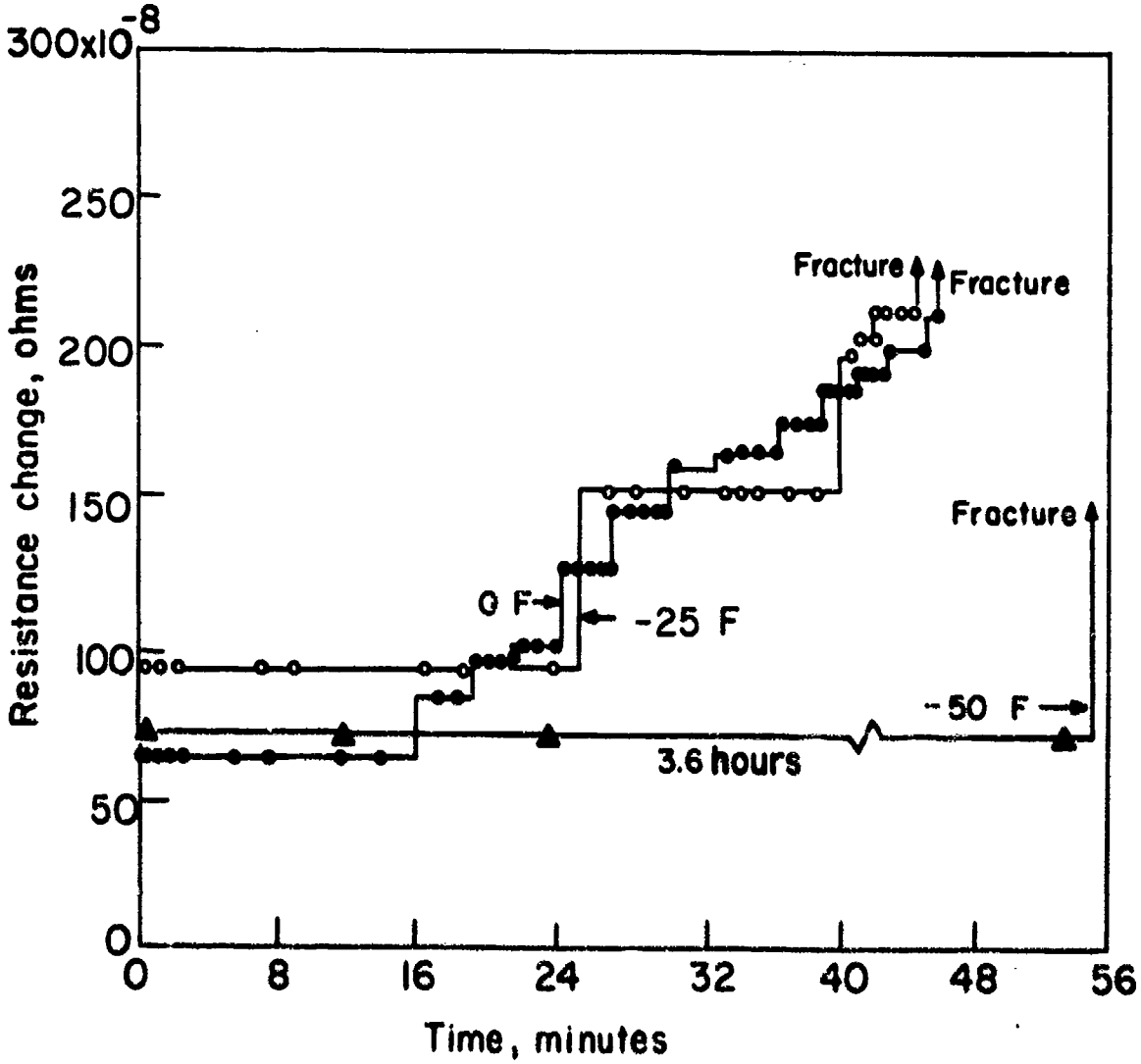

Fig. 3.5 – Resistance increase as a function of time and temperature for uniformly hydrogenated notched specimens, tested in the stress range of delayed failure.

It is apparent from the abrupt resistance increase that the cracks propagate in a discontinuous manner. A plateau of constant resistance is formed after each step. These plateaus according to Troiano are secondary incubation periods. As the temperature is lowered, the plateaus become longer and the individual crack extensions become larger. Thus, fewer discontinuous crack propagation steps are needed to achieve failure. Finally, at -50 F the first crack propagates instantaneously through the specimen.

The same resistivity procedure was employed by Steigerwald[5, 6] who used a center notched, precracked tension specimen as shown in Fig. 3.6. The center notch was made in accordance with ASTM recommendations[7]. A blank 1-3/4 in. wide and between 0.1 and 0.08 in. thick was sheared from sheet stock and a center notch 0.60 in. in length was produced with a jeweler's saw. After heat treatment, the specimens were precracked in tension-tension fatigue to produce a 3/4 in. center notch. This type of specimen has the advantage[8] of offering an initial crack of a comparatively small area from which crack growth may begin. Hence, scatter in the data is minimized. In addition, the very severe notch acuity tends to maximize the embrittlement and thus simplifies certain analyses of the embrittlement mechanism.

Resistivity measurements were made by means of the device shown in Fig. 3.7. The specimen again is made one leg of the Kelvin-Wheatstone double bridge,[6] used for measuring resistance increases resulting from crack extension. The apparatus is capable of detecting crack extensions exceeding 0.003 in. Steigerwald made measurements in numerous liquid and gaseous environments using the resistance method and the above described specimen. In general, measurements were made on specimens surrounded by practically non-conducting liquids or vapors. The use of alternating current, or better, high frequency current in conjunction with a modified measuring set-up would be required to avoid electrolytic processes in a conducting liquid.

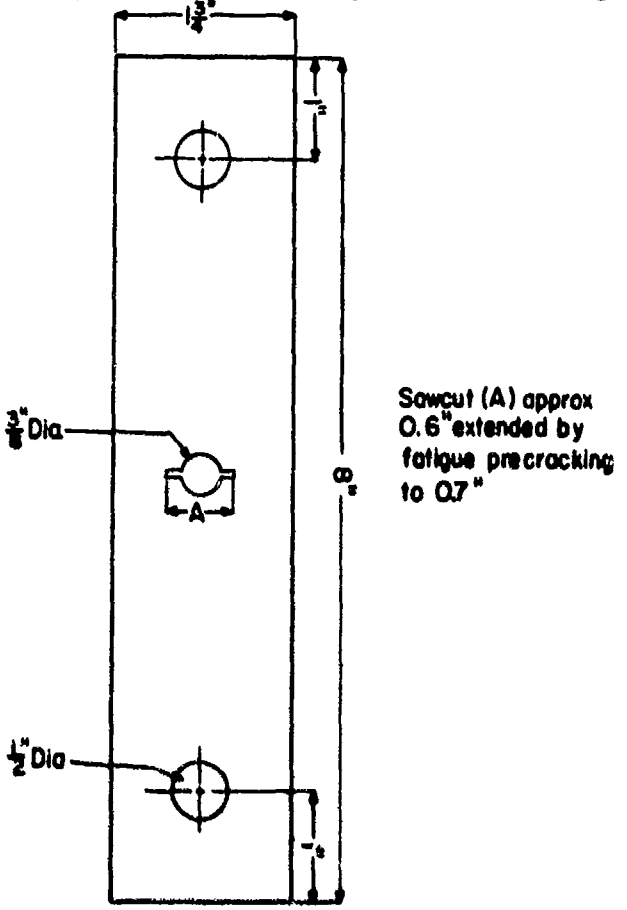

Fig. 3.6 – Center notched precracked tension specimen

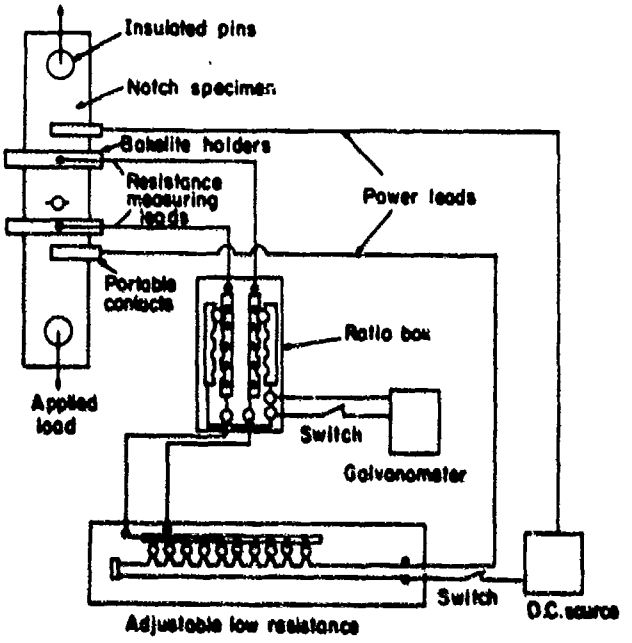

Fig. 3.7 – Schematic diagram of resistance apparatus used to study crack initiation and growth characteristics.

A good example of what occurs in an almost non-conducting liquid[9] is shown in Fig. 3.8. These curves disclose details of the kinetics of slow crack growth in specimens exposed to high purity distilled water (more details are given in the chapter on hydrogen embrittlement in aqueous environments). The data plotted in the figure indicate that if there are incubation periods, they must have been less than one minute, which is the time limit of the sensitivity of the experimental set-up. At the higher applied stresses crack growth was relatively rapid, while at the lower loads a slow growth occurred initially, and crack extension ultimately led to catastrophic failure. All curves exhibited some discontinuities.

Fig. 3.9 presents typical crack propagation behavior in a gaseous environment[10]. Water vapor was added to dry argon gas to produce gas environments having dew points of -3F and -7F. As shown in the figure, extensive crack growth occurred at a dew point of -3F while at a dew point of -7F there was no indication of delayed failure after 1200 minutes. On this basis, the critical dew point required to initiate fracture in AISI 4340 steel (400 F temper) was determined to be -3F. It follows from these results that the critical water vapor content is very low, less than 0.065 g of water vapor per cubic foot of gas. The above facts furnish a striking illustration of the contribution of environmental factors to service failures in ultra high strength steel. Practical examples of the important role played by the environmental conditions are cases of delayed failure of high strength steel pressure vessels produced by the joint action of moisture and internal pressure. Puzzling results occasionally obtained with sustained load-delayed failure tests performed under atmospheric conditions may be explained by differences in the moisture content of the ambient air.

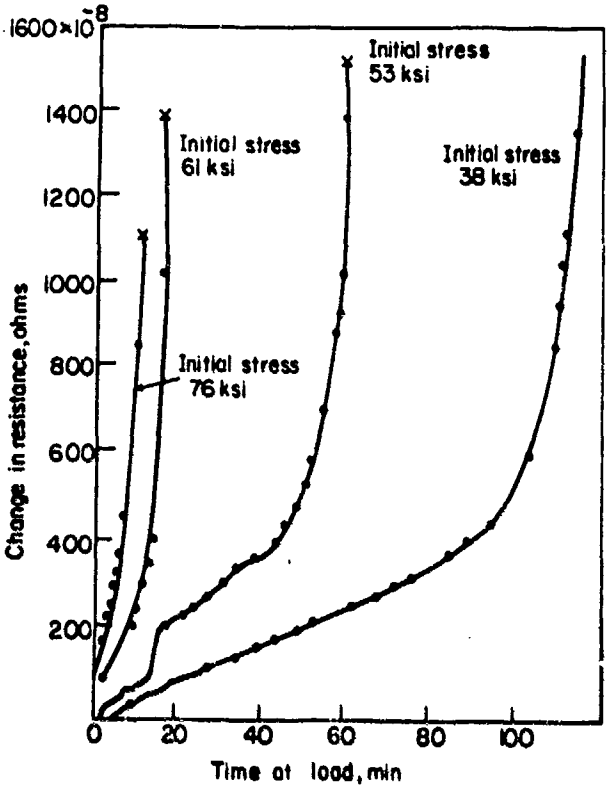

Fig. 3. 8 – Crack propagation curves in 300M steel (600 F temper) in distilled water.

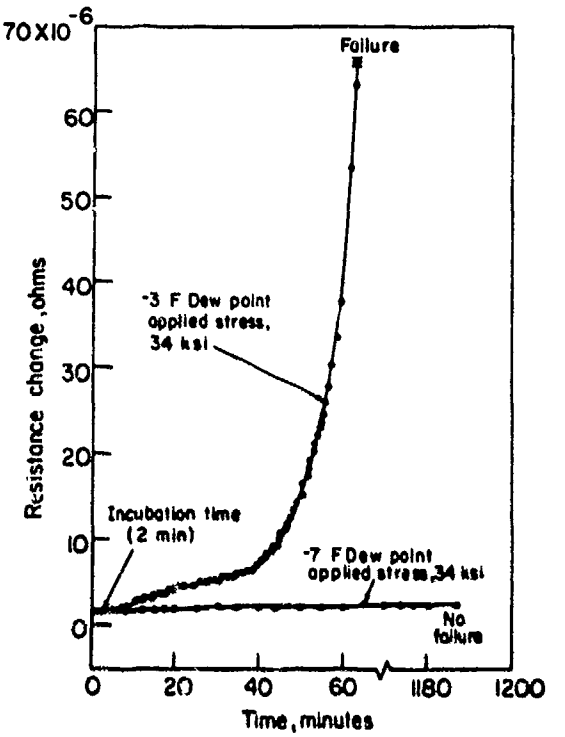

Fig. 3.9 – Effect of addition of water vapor on susceptibility of AISI 4340 steel (400 F temper) to cracking in dry argon gas environments at 68 F.

3.3 MODIFIED ELECTRICAL POTENTIAL TECHNIQUES

Two main disadvantages found in the Kelvin double bridge method are:

- the specimen may become heated because of the high current used, and
- conducting solutions require alternating current to minimize electrolytic effects.

Anctil et al[11] reduced these drawbacks by using a modified electrical potential technique and an alternating current source. Potential field changes were measured continuously across the propagating crack with a sensitive milliohmmeter using the ammeter-voltmeter measurement method. A signal from the milliohmmeter was fed into an X-Y recorder to obtain load-potential drop or potential drop-time curves. At constant current flow the voltage drop was measured and converted to resistance. With a given geometry and constant current, the potential drop across the crack will be an accurate indication of its size. Effects of resistivity on magnitude of the potential drop can be considered, and experimental calibration of potential drop with crack size can be made. For calibration, Anctil et al. used data for razor thin slits in an aluminum foil. Johnson et al. and Che-Yu Li[12-16] showed that calibration is sensitive to the initial crack starter geometry, and that calibration for a wide range of crack lengths is feasible only for simple geometries. Another drawback of this method is discussed later.

Johnson and Willner[15] used the electrical potential method with precracked center notched specimens to show that dry hydrogen gas at atmospheric pressure produces substantial hydrogen embrittlement in martensitic high strength steel (type H-11 steel). Even at comparatively low stresses, subcritical crack growth rate was high. Similar effects were produced by water vapor in dry argon or nitrogen. By introducing a relatively low concentration of oxygen into the gas phase, crack growth was arrested very quickly. These investigators attribute the inhibiting role of oxygen to its preferential adsorption at the crack tip which leads to the formation of a high energy barrier. This hypothesis is confirmed by the fact that oxygen arrested cracks may be restarted by water, hydrogen, or water vapor after removal of the oxygen from the gaseous environment. Fig. 3.10 clearly shows the effect of oxygen in arresting crack propagation in a pure hydrogen atmosphere.

They also made crack propagation studies in argon with varied relative humidities. As shown in Fig. 3.11, a practically steady state of crack propagation was attained at about 60 percent relative humidity.

Stress intensity at the crack tip was kept constant by appropriate manipulation of the load. The stress intensity factor, K, was computed by the conventional uncorrected Irwin formula.

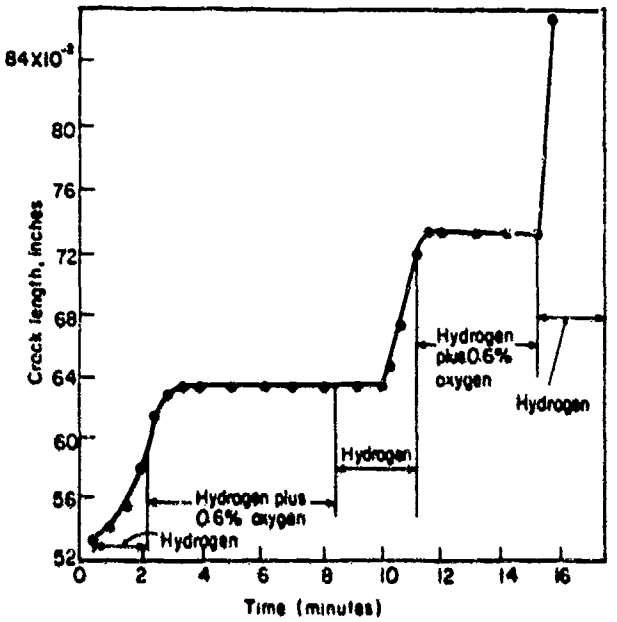

Fig. 3.10 – Subcritical crack growth in pure hydrogen and a hydrogen-oxygen mixture (H-11 Steel, 260-280 ksi strength level).

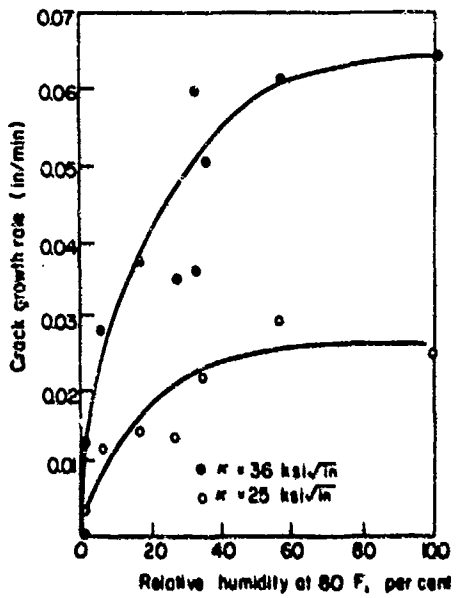

Fig. 3.11 – Crack growth rate versus relative humidity of argon gas. (H-11 Steel, 260-280 ksi strength level).

The Arrhenius plot of Fig. 3.12 shows the effect of temperature on crack growth. If the atmosphere is maintained saturated with water vapor, rate of crack growth varies exponentially with temperature. There appears to be only a slight difference in the crack propagation rate in water and water saturated argon. Apparently, when the relative humidity is high, water vapor condenses at the crack tip. The fact that an increase in relative humiuity above 60 percent has no additional effect on crack growth rate, as shown in Fig. 3.11, is also explained by Johnson by capillary condensation of water.

An energy of activation for crack growth of 9000 cal/mole agrees with values for diffusion of hydrogen in iron. According to Johnson, this may indicate that crack formation in gases, induced by humidity, is affiliated with hydrogen embrittlement.

The similarity of the curves in Fig. 3.12 with adsorption isotherms may also indicate that adsorption of water molecules on active sites on the steel surface plays an important role in the mechanism which controls formation and propagation of brittle cracks in humid atmospheres.

According to Srawley and Brown[17], Anctil's method[11] has the disadvantage of having a built-in power supply which is limited to 100 mA, and therefore, lacks sufficient sensitivity to make it generally useful in fracture testing. Therefore, they used a voltmeter-amplifier combination with an appropriate external current supply so that the output may be varied over a wide range. The method appears easily adaptable to all types of specimens used to

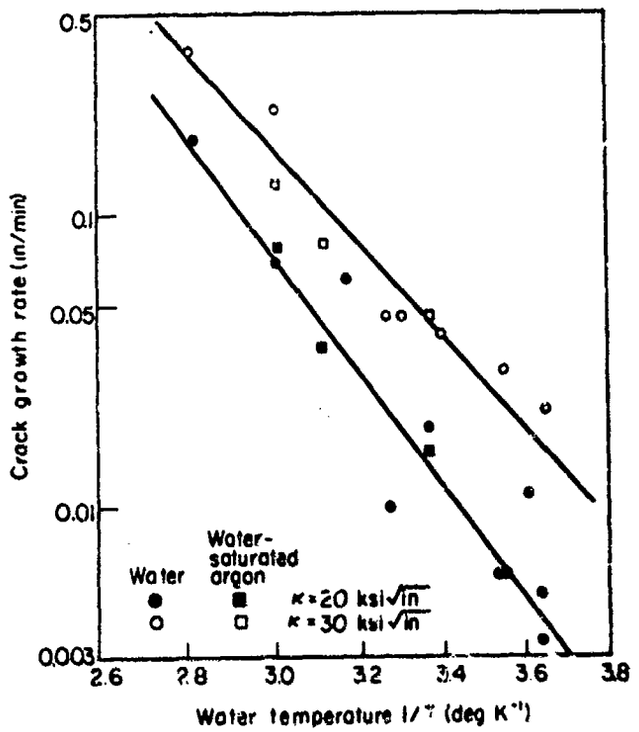

Fig. 3.12 – Crack growth rate as a function of water temperature. Activation energy approximately 9000 cal/mole. H-11 steel, 260-280 ksi strength level.

measure fracture toughness. The necessary instrumentation, which is commercially available, permits automatic recording of the potential change. Calibration curves relating potential change to crack extension are easy to establish. This method has not been used as yet for studies of the propagation of hydrogen induced brittle cracks. Its application to this field would be of great interest.

3.4 STRAIN ENERGY RELEASE RATE AND PROPAGATION RATE OF HYDROGEN CONTROLLED CRACKS

Recently, Van der Sluys[18] published an interesting report on steady state crack extension in high strength AISI 4340 steel. By using fracture mechanics extensively, this investigator succeeded in eliminating, or at least minimizing, a number of variables which frequently cloud results obtained in the field of slow crack propagation.

In linear elastic fracture mechanics, crack length, "a", is interrelated with the strain energy release rate, G, as follows:

$$G = 1/2\, P^2 \frac{\partial (1/M)}{\partial a} \tag{3.1}$$

where P is the load per unit thickness, and M the spring rate (load/deflection) of the specimen per unit thickness. Determination of the relation between 1/M (compliance) and crack length must be made very accurately in order to obtain reliable values of $\partial 1/M/\partial a$. G can also be obtained by an analytical method based on elasticity theory. Van der Sluys obtains the crack propagation rate, da/dt, from

$$\frac{da}{dt} = \frac{C}{P} \frac{d\delta}{dt} \tag{3.2}$$

where δ is the deflection, t the time, and $C = 1/\partial(1/M)/\partial a$. A tapered, double cantilever beam specimen of AISI 4340 steel (R_c 50), was used to achieve constant G level over a relatively long crack extension length. The specimen has a double edge notch with straight sides and a slightly rounded base. With this notch configuration, the length of the crack front was held more constant than with a V-shaped notch. The net stress was raised sufficiently to control

the direction and path of the crack. The rate of crack growth was determined as a function of G and environment. The G level was maintained at a constant value, independent of crack length. Also the dependency of activation energy for crack propagation on G level was studied and the effects of cathodic and anodic polarization and pH on the rate of crack growth at various G levels were evaluated.

The interesting results obtained will be discussed in detail in the chapter on distinguishing between hydrogen embrittlement and stress corrosion cracking (Chapter 6).

Hartbower, Gerberich and Crimmins[19, 20] monitored crack growth both by crack opening displacement measurements with a displacement (strain) gage, and an acoustic method employing a stress wave analysis technique. The acoustic method is based on the fact that elastic waves emanating from a propagating crack can be monitored by piezo-electric accelerators (piezo-electric transducer technique). The first of the two measurements is very suitable for crack length determinations, but less sensitive than the second method which has been used extensively by the above investigators for the determination of crack growth rate in specimens subjected to sustained load. They made measurements on low alloy steel single edge notched tensile specimens, heat treated to high strength levels, and hydrogenated by cathodic charging followed by cadmium plating from a cyanide bath. The effects of baking and environment (water and air) on subcritical crack growth rate of the hydrogenated specimens were studied.

3.5 ELECTRON FRACTOGRAPHY

Electron fractography also has been used to study the propagation of cracks induced by hydrogen[21]. Preliminary results obtained with this method indicate that hydrogen embrittlement is a failure process involving both cleavage and plastic fracture, and is initiated by the accumulation of excess hydrogen at preferred sites within a material. It is hoped that more information will be obtained with the 1 MEV microscope now being used by U.S. Steel scientists[22].

REFERENCES

[1] W. J. Barnett and A. R. Troiano, "Crack Propagation in the Hydrogen Induced Brittle Fracture of Steels", *Trans. AIME*, **209**, 488 ff (1957).

[2] A. R. Troiano, "The Role of Hydrogen and Other Interstitials in the Mechanical Behavior of Metals", *Trans. ASM*, **52**, 64 ff (1960).

[3] A. R. Troiano, "Embrittlement of Hydrogen and Other Interstitials", *Metal Progress*, **77**, 114 ff (1960).

[4] W. J. Barnett and A. R. Troiano, "Crack Propagation in the Hydrogen Induced Brittle Fracture of Steel", WADC Tech. Note 55-405 Air Force Materials Lab (WPAFB) Dayton, Ohio, (1955).

[5] E. A. Steigerwald, "Delayed Failure of High Strength Steels in Liquid Environments", *Proc. ASTM*, **60**, 750 ff (1960).

[6] E. A. Steigerwald and G. L. Hanna, "Initiation of Slow Crack Propagation in High Strength Materials", *Proc. ASTM*, **62**, 885 ff (1962).

[7] "Fracture Testing of High Strength Sheet Materials", Report of Special ASTM Committee, *ASTM Bulletin No. 243*, p. 18 ASTM Philadelphia, Pa. (1960).

[8] G. L. Hanna, A. R. Troiano and E. A. Steigerwald, "A Mechanism for the Embrittlement of High Strength Steels by Aqueous Environments", *Trans. ASM*, **57**, 660 ff (1964)

[9] G. L. Hanna and E. A. Steigerwald, "Influence of Environment on Crack Propagation and Delayed Failure in High Strength Steels", Tech. Documentary Report No. RTD-TDR-63-4295 p. 24, Air Force Materials Lab (WPAFB) Dayton, Ohio (Jan. 1964).

[10] "The Slow Growth and Rapid Propagation of Cracks", Second Report of a Special ASTM Committee on Fracture Testing of High Strength Metallic Materials, *Mater. Res. Std.*, **1**, p. 392 (1967).

[11] A. A. Anctil, E. B. Kula and E. DiCesare, "Electrical Potential Technique for Determining Slow Crack Growth", *Proc. ASTM*, **63**, 799 ff (1963).

[12] H. H. Johnson, "Calibrating the Electrical Potential Method for Studying Slow Crack Growth", *Mater. Res. Std.*, **5**, 442 ff (1965).

[13] G. G. Hancock and H. H. Johnson, "Subcritical Crack Growth in AM 350 Steel", *ibid*, **6** 431 ff, (1966).

[14] G. G. Hancock and H. H. Johnson, "Hydrogen, Oxygen, and Subcritical Crack Growth in a High Strength Steel", *Trans. AIME*, **235**, 513 ff (1966).

[15] H. H. Johnson and M. A. Willner, "Moisture and Stable Crack Growth in a High Strength Steel", *Applied Materials Research*, **4**, p. 34 (1965).

[16] Che-Yu Li and R. P. Wei, "Calibrating the Electrical Potential Method for Studying Slow Crack Growth", *ibid.*, **6**, 392 ff (1966).

[17] J. E. Srawley and W. F. Brown, Jr., "Fracture Toughness Testing and Its Applications", *ASTM STP 381* Fracture Toughness Testing Methods, 175 ff (1965).

[18] W. A. Van der Sluys, "Mechanism of Environment Induced Subcritical Flaw Growth in AISI 4340 Steel", *Eng. Fracture Mech.*, **1**, pp. 447-462 (1969).

[19] C. E. Hartbower, W. W. Gerberich and P. P. Crimmins, "Mechanisms of Slow Crack Growth in High Strength Steels", Aerojet-General Corp., Tech. Rept. AFML-TR-67-26, Vol. 1, Sacremento, Cal. (Feb. 1967).

[20] C. E. Hartbower, W. W. Gerberich and P. P. Crimmins, "Monitoring Subcritical Crack Growth by Detection of Elastic Stress Waves", *Welding J.*, **47**, Research Suppl. p. 18 (Jan 1968).

[21] H. C. Burghard, Jr., "Electron Fractography of Metals and Alloys", *ASM Tech. Report No. H21* (1964).

[22] R. M. Fisher, "Million Volt Metallography", *Metal Progress*, **93** (2) pp. 66-69 (1968).

CHAPTER 4

EFFECT OF HYDROGEN ON FATIGUE STRENGTH AND LIMIT

4.1 HIGH STRESS, LOW CYCLE FATIGUE

According to Sachs et al.,[1] the lack of attention paid to the effect of hydrogen on the fatigue properties of high strength steel is a result of the fact that the fatigue limit is usually lower than the lower critical stress in sustained loading. They postulated that if hydrogen embrittlement affects fatigue strength and life at all, it should be evident during low cycle fatigue at comparatively high stress. They also emphasized the increasing importance of low cycle fatigue as a limiting design factor in various engineering applications and concluded that under these conditions, a better knowledge of the hydrogen embrittlement effect would be of considerable practical significance.

Rotating beam type specimens fabricated from two heats of AISI 4340 steel, heat treated to strength levels between 210 and 290 ksi were used for their investigation. It was necessary to gear down the fatigue machines to speeds ranging from 45 to 2500 rpm, because any hydrogen effect completely faded out at relatively high speeds. At 2500 rpm only severe hydrogen embrittlement affected the fatigue properties.

Fatigue data were obtained for unembrittled and embrittled, and smooth and notched AISI 4340 steel specimens tempered to various strength levels. Hydrogen was introduced by cyanide cadmium plating (coating thickness on the gage section 0.0003 in.). The data presented in Figs. 4.1 and 4.2 represent two types of conditions (a) as heat treated and ground or machined surface, and (b) cadmium plated after heat treating and finishing.

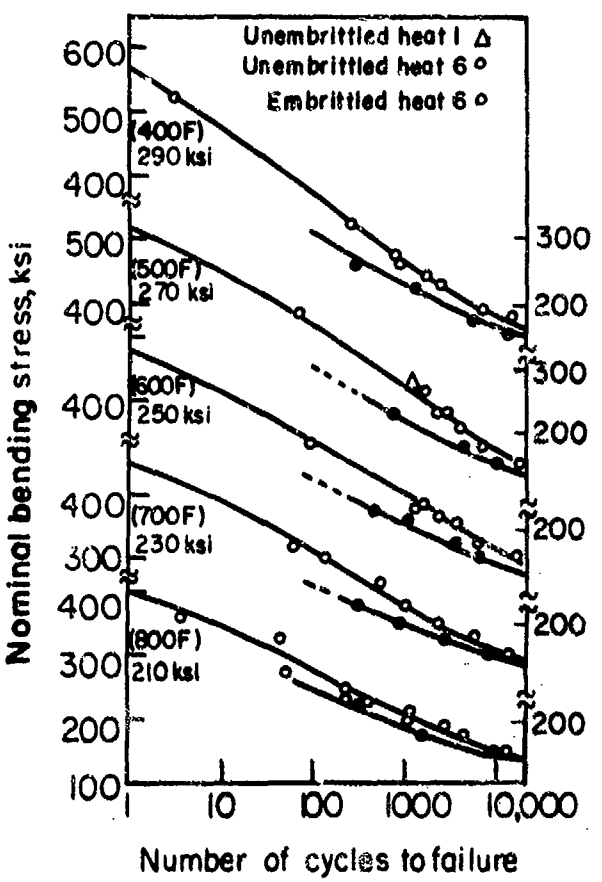

Fig. 4.1 – S-N curves for smooth rotating beam specimens, unembrittled and embrittled (by cadmium plating). AISI 4340 steel tempered to various strength levels.

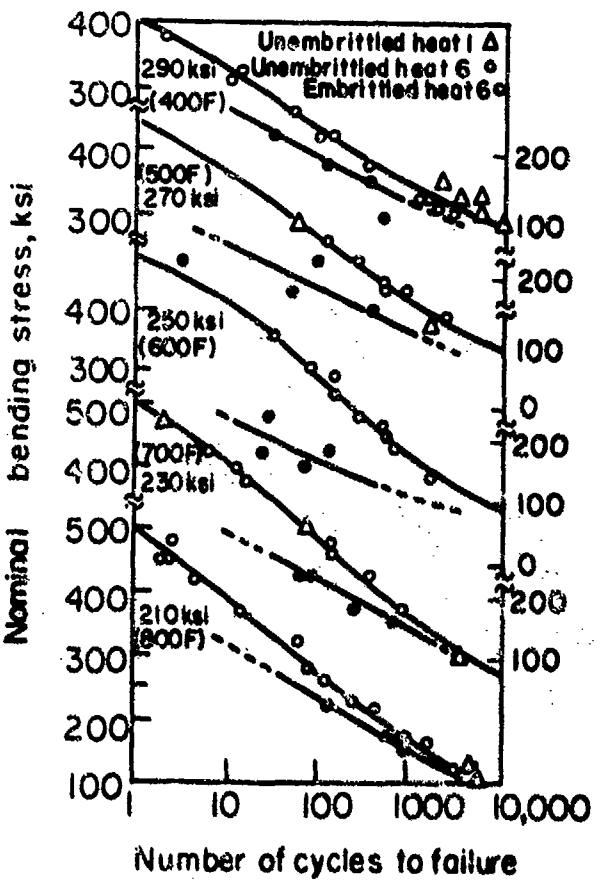

Fig. 4.2 – S-N curves for notched (K_t = 7) unembrittled and embrittled AISI 4340 steel rotating beam specimens tempered to various strength levels.

Sachs summarized the experimental results as follows:

- In all instances, the hydrogen effect decreases as the number of cycles increases, and gradually fades out at about 10,000 cycles.
- In general, this effect appears to be considerably larger for notched than for smooth specimens.
- The greatest reduction in strength was observed on specimens heat treated to a strength level of about 250 ksi.

In addition to the mechanical studies just described, Sachs made crack propagation measurements in the notched area. Plated and unplated fatigue specimens were run for various numbers of cycles at constant stress and were used for the crack propagation analysis. The crack depth was determined by longitudinally sectioning the specimens along two planes less than 90^{o} to each other, taking photomicrographs of the four crack areas thus exposed, and measuring the crack depth.

The average values of crack depth are plotted in Figure 4.3 as a function of the number of cycles. The data clearly reveal crack initiation after very few cycles. The crack grows in the radial direction until at least one half of the specimen life is expended. Finally, the crack penetration in the embrittled specimen becomes much more marked, until the rest of the section suddenly fractures, probably within less than one cycle, by what is actually a static phenomenon. The cracked surface in hydrogen containing fatigue specimens revealed comparatively deep valleys and high peaks.

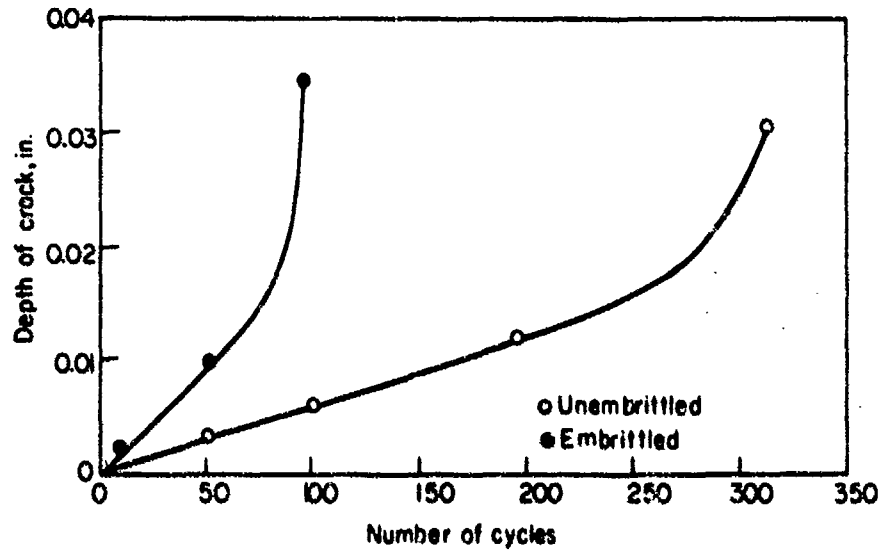

Fig. 4.3 – Comparison of the initiation and depth of radial cracks in notched area (K_t = 7) of unembrittled and embrittled (by cadmium plating) specimens as a function of the number of cycles. AISI 4340 steel fatigued at a cycling stress of 224 ksi.

4.2 LOW STRESS, HIGH CYCLE FATIGUE

The fatigue behavior of cyanide cadmium plated or cathodically charged high strength steel (NTS 230 ksi) was studied by Gurklis, McGraw and Faust[2]. Sheet flexure fatigue specimens were cut to 2.62 and 3.32 in. lengths from 0.5 in. wide, 0.025 in. and 0.040 in. thick stock so that the natural frequency of their vibration, when supported as beams, was 800 cps. They were fatigued over an electromagnet which could be tuned to half this frequency and could flex the specimens over any desired amplitude. A block diagram of the electro-mechanical system is shown in Fig. 4.4.

About 3.5 hours produced a 10 million cycle run out. The stress was calculated from the deflection of the vibrating specimen. Deflection measurements were made with an optical magnifier when the panel was optically frozen in the position of maximum deflection with a stroboscopic light adjusted to the same frequency.

The S-N curves for cathodically precharged spring steel which had either been stored in air at room temperature, or in a mixture of dry ice and acetone prior to fatigue testing, are shown in Fig. 4.5. Charging was carried out in dilute sulfuric acid at 80 F at 5 A/ft^2 for 2.5 minutes. The fatigue limit was about 5 ksi lower for specimens stored in the freezing mixture than for those stored at room temperature. Results indicate that hydrogen embrittlement causes a small loss of fatigue strength.

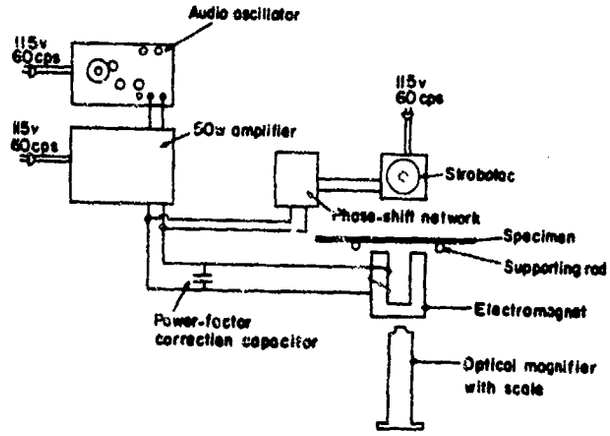

Fig. 4.4 – Block diagram showing the essential features of the electronic system for an electromagnetic fatigue testing apparatus.

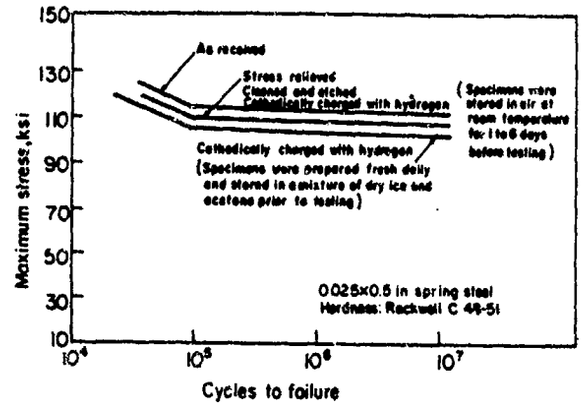

Fig. 4.5 – Effect of cathodic charging on the fatigue strength of spring steel.

Fig. 4.6 gives fatigue results for baked and unbaked cadmium plated specimens. Stress relief at 475 F for one hour had practically no effect on the fatigue limit of the spring steel, nor did cleaning and anodic etching processes. Cadmium plating reduced the fatigue limit by slightly more than 15 per cent. The reduction was essentially independent of coating thickness, within the plate thickness range studied. Baking of the plated steel at 375 F for 4 and 24 hours, or at 525 F for 24 and 72 hours, respectively, did not restore the original fatigue strength of the plated steel specimens.

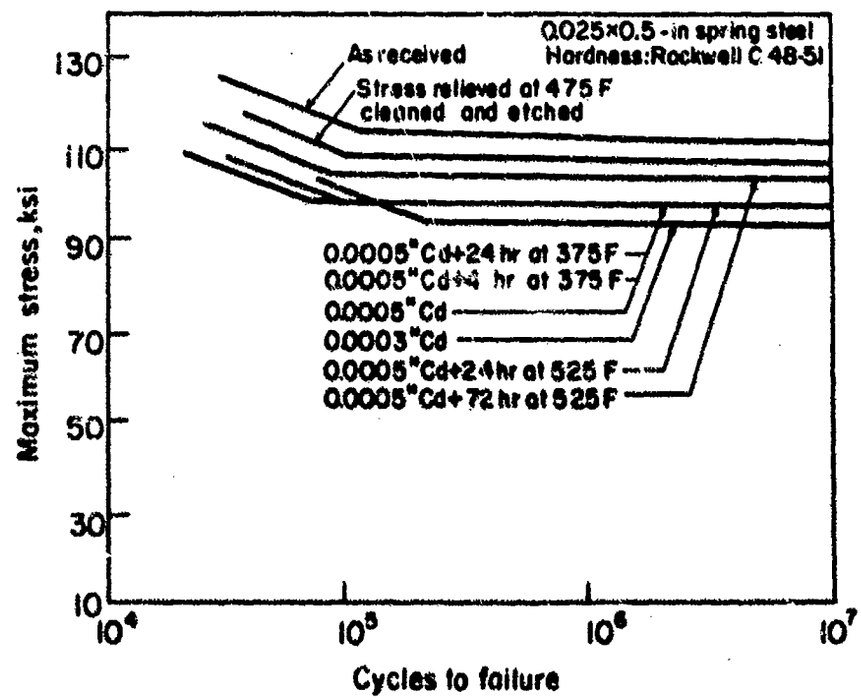

Fig. 4.6 – S-N curves for baked and unbaked cadmium plated spring steel.

Beck and Jankowsky[3] studied the effect of hydrogen on delayed brittle failure and fatigue strength of notched specimens prepared under the same conditions. The stress rupture behavior is given in Fig. 4.7. Lower critical stress is about 140 ksi for the following processes

- Plating (1) cadmium, (2) tin, or (3) tin-cadmium alloy (30-70) from fluorate baths.
- Phosphatizing treatment at 160 F for 5 min.
- Cyanide cadmium plating, 30 min. bake at 340 F after plating.

Data for the stannate tin and duplex tin-cadmium plating (process C) indicate a markedly decreased lower critical stress of about 30 ksi as compared with measurements for the above processes.

The fatigue strength and limit data for H-11 steel specimens, which were plated with duplex tin-cadmium, tin-cadmium alloys, or phosphatized are given in Fig. 4.8. The 50 tin + 50 cadmium alloy was mechanically plated after a copper immersion and phosphatizing pretreatment.

The experimental results presented in both figures may be summarized as follows:

In Fig. 4.7 the delayed cracking is quite marked in the duplex coating and is definitely controlled by the tin phase of the plating. Delayed cracking is less marked on the fluoborate plated specimens and is characterized by a relatively long induction period. The phosphatizing treatment, applied prior to mechanical plating, resulted in considerable embrittlement, in contrast to the slight embrittlement induced by the coppering treatment.

The values plotted in Fig. 4.8 clearly display the significantly reduced fatigue limit of the phosphatized specimens. Though the agreement between static (Fig 4.7) and dynamic behavior of the plated high strength steels is only qualitative in nature, it supports the conclusion that the presence of embrittling hydrogen in notched specimens also adversely affects fatigue strength and limit. The reduction in fatigue limit is seen to progress in the sequence of duplex coating, alloy plating from a fluoborate bath, and phosphatizing.

The coppering pretreatment induced relatively little embrittlement, since the mechanically plated specimens showed the same fatigue behavior as the phosphatized. It is concluded that the reduction in fatigue strength and limit displated by the mechanically plated specimens is due only to the embrittling phosphatizing.

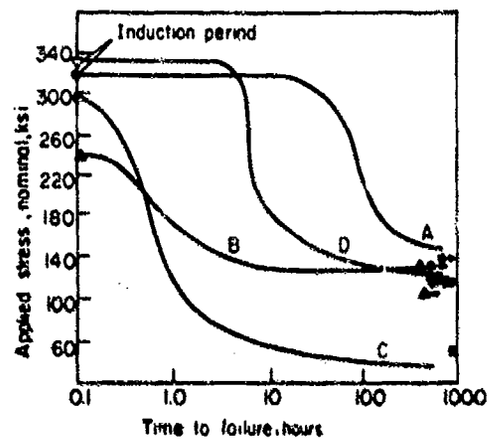

Process:

A. Fluoborate Plating
   1. Cadmium 2. Tin 3. Tin-cadmium alloy (30-70)
   Curves for plating processes 1, 2, and 3 are superimposed
B. Phosphatizing Treatment
C. Stannate tin and duplex tin-cadmium plating (50-50 diffused at 340 F, 30 min.)
D. Cyanide cadmium plating

Fig. 4.7 – Delayed failure results for AISI 4340 steel (NTS unplated 360 ksi, K_t = 4.0) for phosphatizing treatment and different plated coatings (coating thickness - 0.3 mil)

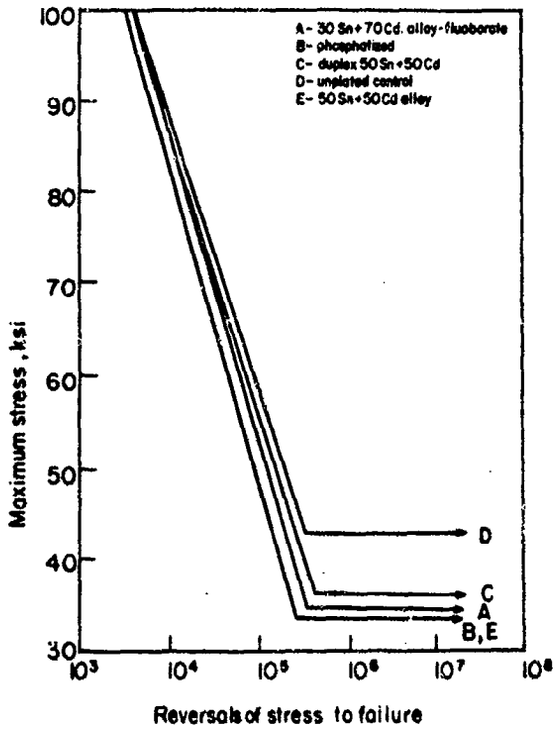

Fig. 4.8 – Fatigue failure results for notched rotating beam specimens for phosphatizing treatment and different plated coatings (0.3 mil). H-11 steel, NTS unplated ~ 380 ksi, K_t = 4.0, stress ratio -1.0, R. R. Moore fatigue machine speed 10^4 cpm. Per cent reduction in fatigue limits, A 20%, C 16%, E 23%.

W. Beck [4] comprehensively investigated the effect of cathodic charging and cadmium plating on the fatigue behavior of high strength steels. Some pertinent results will be discussed in this chapter.

Sheet flexure and rotating beam fatigue specimens fabricated from AISI 4340 steel and H-11 hot work die steel were employed in this study. Specimens longitudinal to the grain direction were taken from plate material or cylindrical bar stock and heat treated to a strength level of 260-280 ksi. The K_t of the notch in the flexural fatigue specimen was 2.8 (the highest that can be practically achieved with this type of design), but in the cylindrical specimen, it was increased to 4.2. The notched and unnotched sheet flexure specimens were similar in configuration and the double edge notch was symmetrically located at both sides.

All sheet fatigue experiments were made in Krouse sheet flexural fatigue machines. The test cycles were completely reversed tension-compression with zero mean stress (R = -1.0). In order to avoid hydrogen losses and to minimize scatter, the runs with cathodic charging were made under conditions of continuous cathodic polarization during fatigue testing. As shown in Fig. 4.9, this was accomplished by surrounding the cathodic specimen with a coil platinum wire anode. It was kept in position by a Lucite frame, fastened rigidly to the specimen holder of the machine.

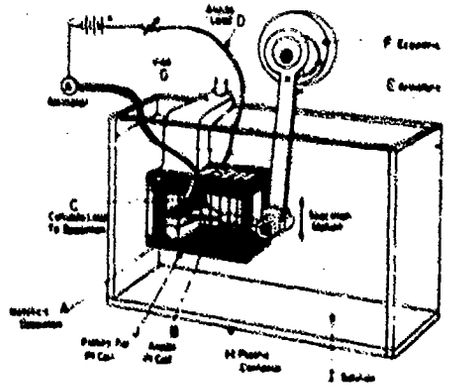

Fig. 4.9 – Krouse flexural fatigue machine and accessary for continuous charging of specimen during test.

The notched rotating beam specimens were fatigued in R. R. Moore machines in air with zero mean stress. Prior to plating or charging, the specimens were degreased anodically in a hot alkaline cleaning solution, rinsed, dipped in 50 per cent hydrochloric acid at room temperature for 50 seconds, rinsed, and then plated or cathodically polarized. Cadmium was plated from a conventional cyanide bath containing brightener at 20 A/ft^2 for 16 minutes. The average thickness of the plating, measured on the unnotched portion of the specimens was 0.0005 in. Sheet specimens were polarized cathodically in a 0.025N sodium hydroxide +0.2N sodium cyanide solution at the same current density used for plating. The cyanide compound is the effective embrittlement accelerator used in the cadmium plating bath. Runs were also made with specimens plated after charging in 0.1N sulfuric acid at 20 A/ft^2 for 60 minutes at room temperature. A number of cadmium plated specimens was baked at 375 F for 24 hours. Baking was begun immediately after completion of plating.

Specimens that were to be cadmium coated by vacuum deposition were cleaned by dry blasting with 120-grit aluminum oxide at 90 psi pressure, which was followed by glow discharge treatment in a vacuum chamber. A deposition time of 20-25 minutes was required to obtain a coating thickness of 0.0005 in. Since the number of tests was not sufficient to provide statistically reliable S-N curves, or make possible the establishment of scatter bands, the curves presented in Figs. 4.10 and 4.11 can be regarded as a fairly accurate estimate of the fatigue strengths and limits for the sheet specimens.

As shown in Fig. 4.10, the fatigue limit of notched AISI 4340 steel specimens, cathodically charged in the alkaline solution, is reduced to 45 per cent of the untreated control value. The fatigue limit of cyanide cadmium plated H-11 steel specimens, is diminished 30 per cent (Fig. 4.11). The fatigue strength of specimens precharged in the very embrittling sulfuric acid is appreciably below that of those plated only with cadmium in the relatively low-cycle high-stress range.

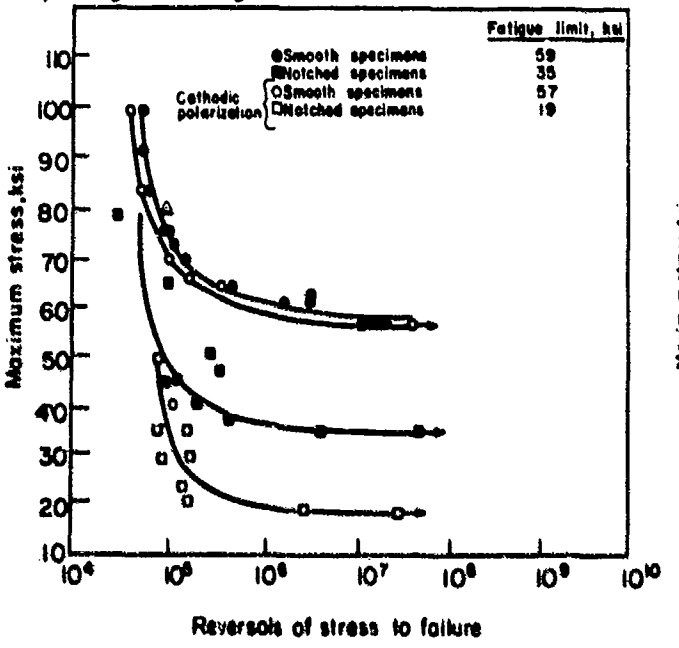

Fig. 4.10 -- Sheet flexure fatigue results for 4340 steel. Specimens immersed in 0.025N NaOH/0.20N NaCN solution with and without cathodic polarization. UTS 280 ksi, K_t = 2.8, stress ratio = -1, machine speed 1.75 x 10^3 cpm.

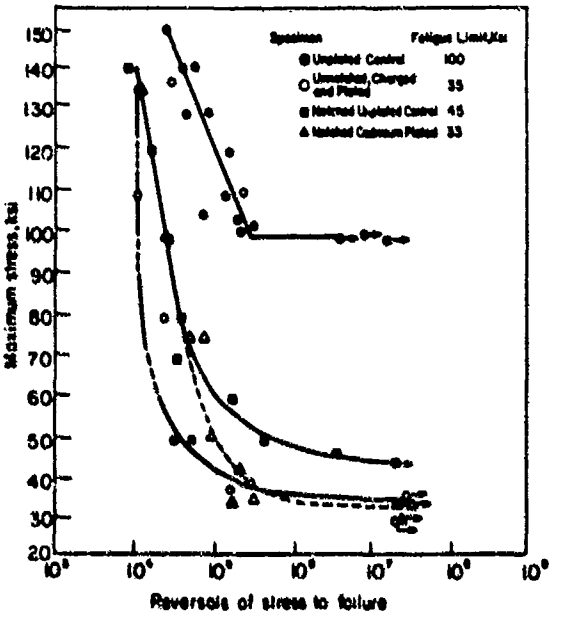

Fig. 4.11 -- Sheet flexure fatigue results for H-11 steel. The unnotched specimens were cathodically charged in 0.1N H_2SO_4 followed by cyanide cadmium plating. UTS 280 ksi, K_t = 2.8, stress ratio = -1.0, machine speed 1.75 x 10^3 cpm.

The results obtained for notched rotating beam specimens, presented in Fig. 4.12, clearly display the significant effect of various surface treatments on the fatigue limit. The fatigue limit is reduced about 20 per cent on the cyanide cadmium plated steel. The blast pretreatment raised it about 25 per cent (discussed in section 4.3), while baking increased it about 5 per cent above that of the unbaked plated specimen.

The effectiveness of hydrogen in reducing low stress, high cycle fatigue strength, as established by Beck et al.,[3, 4] was confirmed by a number of other investigators. Harrison and Smith[5] observed that this effect not only occurred in electrolytically charged or plated specimens, but also in high strength steel notched specimens charged by exposure to hydrogen gas at a temperature of 1000 C.

Russian investigators,[6] found that the number of cycles to fracture is inversely proportional to the current density applied to smooth sheet flexure specimens polarized cathodically during fatiguing in 3 per cent NaC1 solution at a constant stress.

Wedden[7] has ascribed the reduction in fatigue strength to the embrittling effect of hydrogen on steel. If this is true, removal of the embrittling hydrogen atoms should enhance the fatigue behavior of steel. This was observed by Heller and Janicke[8] who succeeded in markedly increasing the low stress, high cycle fatigue limit by annealing hydrogen containing high strength steel at 200 C and 400 C, as pictured in Fig. 4.13. Disregarding the limited effect of the annealing temperature, the hydrogen effect is superimposed on the normal effect of repeated stress in determining the fatigue behavior of the steel.

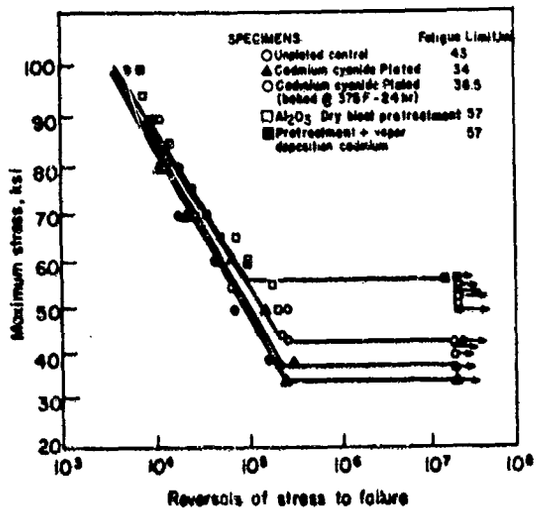

Fig. 4.12 – Rotating beam fatigue results for H-11 steel showing the effect of different plating treatments. All specimens were notched, UTS 280 ksi, $K_t = 4.2$, stress ratio = -1.0, machine speed 10^4 cpm.

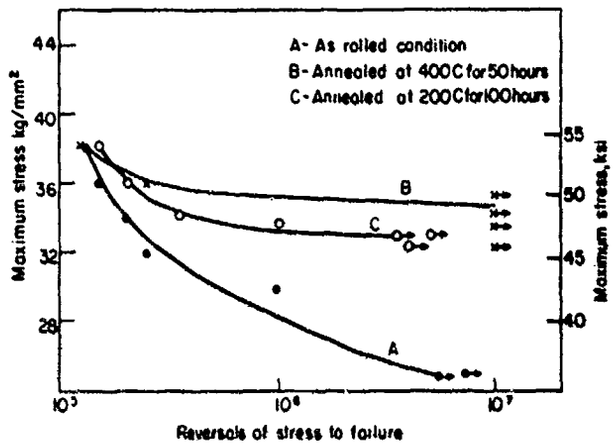

Fig. 4.13 – Effect of hydrogen removal on fatigue strength of high strength, abrasion resistant unnotched steel specimens. The hydrogen content of the specimens in the as-rolled condition and those annealed at 200 C for 100 hours was 2.8 and 0.8 ml/100g Fe respectively (STP).

Beck et al. found that removal of hydrogen from steel by vacuum melting improved the fatigue limit of cyanide cadmium plated steel which is in agreement with the above findings.

4.3 MECHANISM OF REDUCTION OF FATIGUE LIMIT BY HYDROGEN

One of the factors involved in the mechanism which determines the decrease in fatigue limit of notched cyanide cadmium plated specimens is the stress concentration, since the effect on unnotched specimens is in general slight.

It is conceivable that the coating itself exerts a detrimental effect on the fatigue strength of the substrate metal, since it has been shown that the cracks in chromium electrodeposits may act as stress raisers on the surface of

the substrate[9]. In contrast to a chromium electrodeposit, the cadmium layer[4] was found to be free of crack-inducing residual tensile stresses. The increase in the fatigue limit of the vacuum plated specimens (Fig. 4.13) is solely the result of the compressive stresses introduced into the steel surface during the blast cleaning treatment. Identical results were obtained recently by Wedden, who applied a sprayed aluminum coating subsequent to a blast treatment[7].

It is well known from hydrogen embrittlement studies, that the presence of cyanide effectively stimulates introduction of hydrogen into steel during any type of cathodic treatment[10], whereas vacuum deposition does not induce embrittlement[11]. These facts, along with the beneficial effect of baking, are considered strong indications of a definite relationship between the embrittling effect of hydrogen and the reduction of fatigue strength and limit.

Sachs[1] did not attempt to advance a mechanism to explain the hydrogen effect. He labeled the reduction of the low cycle fatigue strength for cyanide cadmium plated specimens simply a hydrogen-embrittlement phenomenon.

The facts summarized above are considered an indication that high stress, low cycle fatigue failures are caused by increasing internal stresses in much the same way as deformation by static straining. Electron microscopic studies[12] have given fairly conclusive evidence that this mechanism is basically correct. This type of fatigue failure then becomes, in effect, analogous to a delayed static fracture. Hence, in accordance with the theory of Troiano[13] at stresses applied in the range of delayed fracture, the reduction in fatigue life would only be dependent on the development of a critical hydrogen concentration in the area of highest triaxial stress. This would be attained rather quickly after cathodic treatment in a cyanide-containing solution, as indicated by the experimental facts (Fig. 4.11).

It is more difficult to propose a mechanism which determines the low stress, high cycle fatigue behavior of notched hydrogen-containing specimens. This phenomenon cannot be discussed on the basis of a predominantly static phenomenon because, from a mechanical point of view, it is hardly possible to ignore the combined effect of stress and high cycling on the fatigue behavior of the metal. Wood and Bendler[14] suggested the concept that, in the presence of sharp notches on the surface of specimens subjected to cyclic stressing, abnormal lattice distortions are produced within the slip zones and, by their transformation into narrow fissures, the metal is weakened mechanically and ultimately collapses locally. Apparently absorbed hydrogen accelerates this transformation.

There seems to be little doubt that in any mechanism which determines the detrimental effect of hydrogen on the fatigue behavior at any degree of cycling, the acceleration of the formation of fatigue cracks because of embrittlement of the steel matrix will play an important role[15].

In context with this discussion, recently published observations by Spitzig et al[16] are of considerable interest. According to these investigators, the acceleration of the propagation rate of fatigue cracks (high stress, low cycles) in a dry hydrogen atmosphere is the result of progressive, localized embrittlement in microscopic regions in the vicinity of the crack tip. The above hypothesis of the hydrogen accelerated transformation of abnormal lattice distortions into narrow fissures, if slightly modified, might then explain the role of hydrogen in accelerating the rate of crack propagation in Spitzig's experiments. The experiments of this investigator and others indicate that there are two environments instrumental in the generation of the embrittling hydrogen atoms. One environment requires the strict exclusion of moisture, whereas the other is totally dependent upon the presence of moisture.

In the first environment hydrogen atoms are generated by the catalytic effectiveness of freshly formed steel surfaces (presence of moisture adversely affects hydrogen adsorption) to activate dissociation of adsorbed hydrogen molecules (activated adsorption) whereas hydrogen generation is the result of electrolytic processes in the second environment.

4.4 FATIGUE OF ROLLING SURFACES ACCELERATED BY HYDROGEN

Interesting observations concerning water (hydrogen) accelerated fatigue of rolling steel surfaces were reported by Grunberg, Jamieson and Scott[17]. They observed that rolling bearings are subjected to surface fatigue failure which is initiated by the formation of pits, resulting from the repeated compression-tension cycles during the rolling action. The so-called "pitting life", that is, the time which elapses before the first pit appears, is greatly dependent on the environment in which stressing occurs. Different lubricants produce different pitting lives under identical conditions of stressing. For example, the presence of water in petroleum lubricants causes acceleration of pit formation, accelerates the propagation of cracks once they have been formed, and often leads to complete fracture of ball bearings.

Grunberg et al. conducted experiments to determine the cause of this phenomenon. They used a special four ball wear test apparatus which simulates the rolling and sliding action occurring in angular contact ball bearings. All balls were made of ultra high strength steel. High unit loads were used and failure occurred on the running track of the driving ball.

Runs were made with lubricants in a dry state, and containing "neutral" or tritium labeled water for the purpose of measuring the quantity of hydrogen absorbed by the stressed material. The total hydrogen content in the driving ball, obtained by high temperature vacuum extraction, was found to be greater by a factor of more than 100 than the hydrogen equivalent of the tritium present. This difference was explained to be due to hydrogen generated by the cracking of the oil in the presence of water. Hence, acceleration of pitting and fatigue crack growth is the result of hydrogen embrittlement.

In addition to the moisture hypothesis, attempts were made to explain hydrogen production as a thermal phenomenon, induced by the comparatively high surface temperature of friction (400 to 500 C) of the heavily loaded balls (300 to 500 kg.) for rather long periods. Confirmation of this hypothesis was seen in the fact that rolling surface fatigue, which is accelerated by hydrogen embrittlement, was more marked in the relatively thermally unstable paraffinic oils, than in the more stable naphthenic oils. The investigators conclude that hydrogen penetration is the controlling factor in crack initiation during rolling surface fatigue of steel.

The delayed failure behavior and fatigue strength and limit of vacuum degassed steel will be reported in a later chapter.

REFERENCES

[1] G. Scheven, G. Sachs and K. Tong, "Effects of Hydrogen on Low Cycle Fatigue of High Strength Steel", *Proc. ASTM*, **57**, pp. 682-697 (1957).

[2] J. A. Gurklis, L. D. McGraw and C. L. Faust, "Hydrogen Embrittlement of Cadmium Plated Spring Steel", *Plating*, **47**, pp. 1146-1154 (1960).

[3] W. Beck and E. J. Jankowsky, "Effect of Tin-Cadmium Electrodeposits on Corrosion and Mechanical Behavior of Steel", *Proc. 2nd International Congress on Metallic Corrosion*, New York, pp. 669-675 (1963).

[4] W. Beck, "Effect of Cathodic Charging and Cadmium Plating on the Fatigue Behavior of High Strength Steels", *Electrochem. Technol*, **2**, pp. 74-78 (1964).

[5] J. D. Harrison and G. C. Smith, "Effect of Hydrogen on the Fatigue Behavior of Mild Steel Bar and Weld Metal", *British Welding J.*, **14**, pp. 493-502 (1967).

[6] V. I. Tkachev and R. I. Kripyakevich, "Hydrogen Embrittlement and Fatigue", *Fiziko-Khimicheskaja Mekhanica Materialov*, **1**, (6) pp. 688-692 (1965).

[7] P. R. Wedden, "Effect of Plating on Fatigue", *Trans. Inst. Metal Finishing*, **38**, p. 175 (1961).

[8] W. Heller and W. Janicke, "Effect of Removal of Hydrogen on the Mechanical Properties of Steel", *Stahl und Eisen*, **83**, pp. 145-154 (1963).

[9] R. A. F. Hammond and C. Williams, "The Effect of Electroplating on Fatigue Strength", *Met. Rev., J. Inst. Metals*, **5**, pp. 165-223 (1960).

[10] W. Beck and E. J. Jankowsky, "Effectiveness of Metallic Undercoats in Minimizing Plating Embrittlement", *Proc. Am. Electroplaters' Soc.*, **47**, pp. 152-159 (1960).

[11] P. J. Clough, "Functional Surfaces by Vacuum Metallizing", *Metals Eng. Quarterly*, **1**, pp. 7-14 (1961).

[12] W. A. Wood, "Fracture", *Proc. International Conference on Atomic Mechanisms of Fracture*, p. 412 (1959).

[13] A. R. Troiano, "The Role of Hydrogen and Other Interstitials in the Mechanical Behavior of Metals", *Trans. ASM*, **52**, pp. 54-80 (1960).

[14] W. A. Wood and H. M. Bendler, "Effect of Superimposed Static Tension on the Fatigue Process in Copper Subjected to Alternating Torsion", *Trans. AIME*, **224**, pp. 18-33 (1962).

[15] R. J. Walter and W. T. Chandler, "Effects of High Pressure Hydrogen on Metals at Ambient Temperature", Final Report Contract NAS 8-19, Rocketdyne Div., North American Aviation, Inc., Conoga Park, Calif. (Feb. 1969).

[16] W. A. Spitzig, P. M. Talda and R. P. Wei, "Fatigue Crack Propagation and Fractographic Analysis of 18Ni (250) Maraging Steel Tested in Argon and Hydrogen Environments", *Eng. Fracture Mech.* **1**, pp. 155-165 (1968).

[17] L. Grunberg, D. T. Jamieson and D. Scott, "Hydrogen Penetration in Water Accelerated Fatigue of Rolling Surfaces", *Phil. Mag.*, **8**, (93) pp. 1553-1567 (1963).

CHAPTER 5

EFFECT OF MICROSTRUCTURE AND COMPOSITION ON HYDROGEN EMBRITTLEMENT AND HYDROGEN STRESS CRACKING

5.1 THE ROLE OF MICROSTRUCTURE

The role of microstructure in the hydrogen induced brittle failure phenomenon is not understood clearly, therefore, only a brief discussion of some pertinent cases is included in this chapter. The possible differences in hydrogen embrittlement susceptibility of steels with bainitic, pearlitic, ferritic and martensitic structures, and the effects of retained austenite were discussed by Elsea and Fletcher[1]. In view of the above uncertainties, suffice it to quote their report and to summarize a few additional results of studies.

Cain and Troiano[2] and Slaughter et al.[3] performed sustained load delayed failure measurements on notched AISI 4620 and 4140 steel specimens, heat treated to different strength levels. The measurements were made after cathodic charging, cadmium plating and normalization of the hydrogen distribution by thermal treatment for 30 minutes at 300 F. They found, as depicted in Fig. 5.1 that at a nominal tensile strength of 100 ksi, a normalized structure (mixed ferrite and pearlite) was more susceptible than either tempered martensite or tempered bainite.

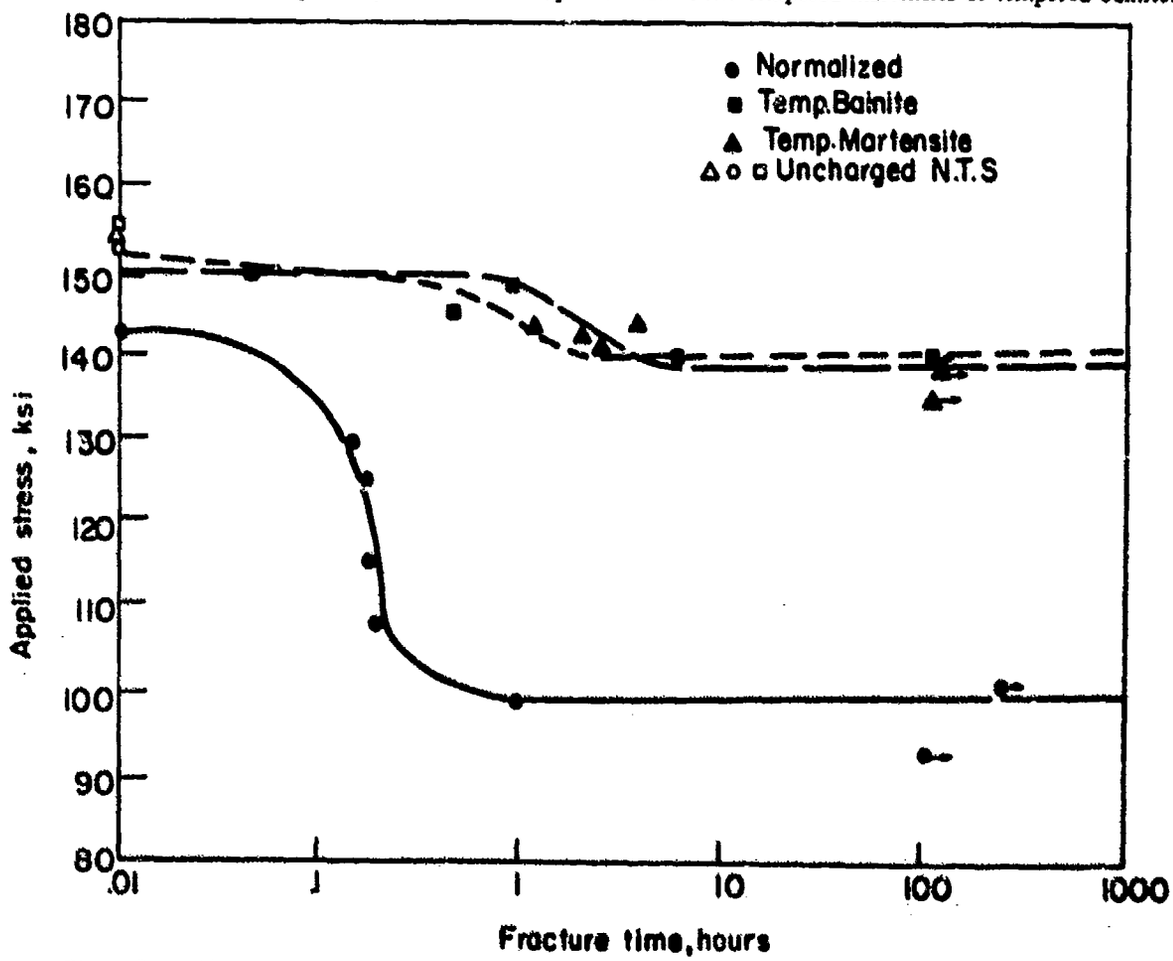

Figure 5.1 – Measurements showing low resistance to delayed fracture of a normalized structure (mixed ferrite and pearlite) as compared with tempered bainite and tempered martensite (AISI 4620 steel, nominal strength level 100 ksi). Specimen charged cathodically and cadmium plated. Hydrogen distribution normalized by annealing for 30 min. at 300 F.

At the higher strength level of 120 ksi, tempered and austempered bainite respectively, were less resistant to delayed brittle failure than tempered martensite. At a strength level of 140 ksi, the pearlitic structure was less resistant than tempered bainite and tempered martensite (Figs. 5.2 and 5.3).

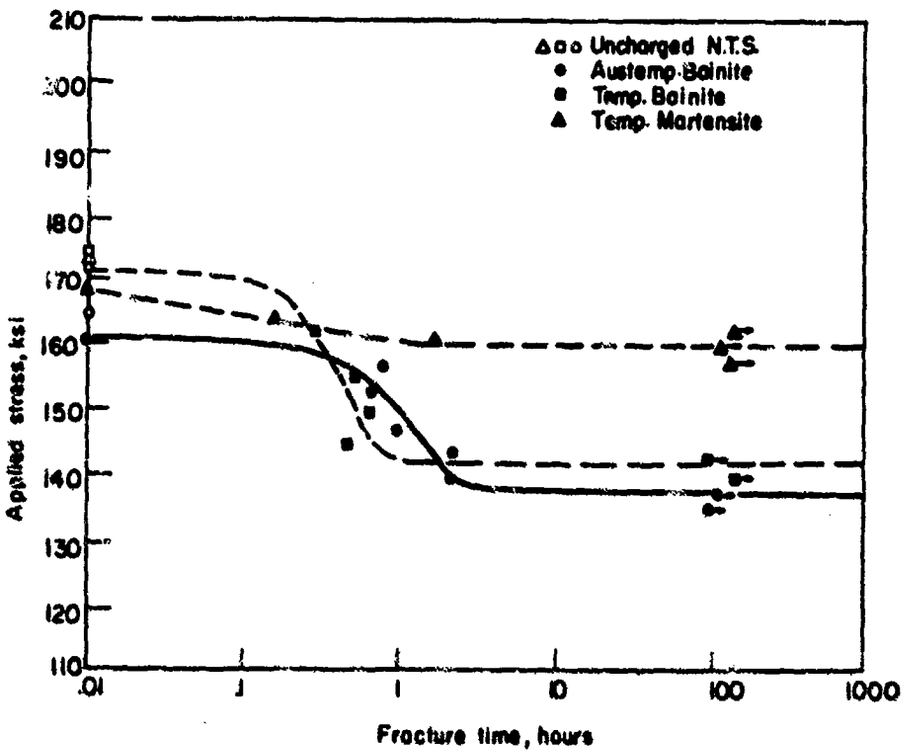

Fig. 5.2 – Measurements showing low resistance to delayed fracture of tempered and austempered bainite as compared with tempered martensite (AISI 4620 steel, UTS 120 ksi). Specimen cathodically charged and cadmium plated. Hydrogen distribution normalized by annealing for 30 min. at 300 F.

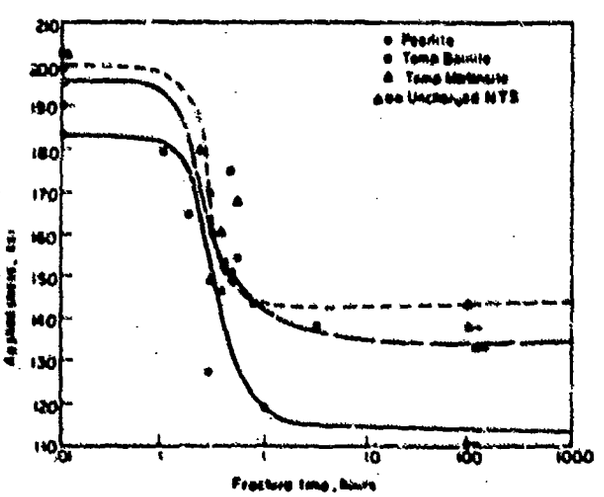

Fig. 5.3 – Measurements showing low resistance to delayed fracture of a pearlitic structure as compared with tempered bainite and tempered martensite (AISI 4140 steel, UTS 140 ksi). Specimen charged cathodically and cadmium plated. Hydrogen distribution normalized by annealing for 30 min. at 300 F.

Thus, Cain and Troiano concluded that the resistance of a material to delayed failure cannot be judged on the basis of strength alone. It appears that microstructure exerts an even greater influence on hydrogen susceptibility than strength level. These conclusions are strongly supported by the behavior of maraging steels (to be discussed later), which despite their extremely high strength, have a remarkably high hydrogen tolerance.

Boniszewski and Baker[4] made studies of notched specimens of vacuum melted 9Ni-7Mn high strength steel. The specimens were charged in one atmosphere of hydrogen at 950C for 30 minutes and subsequently quenched. The susceptibility to hydrogen stress cracking was increased considerably by the introduction of twinned martensite (produced by rapid quenching) into the martensitic structure.

Benjamin and Steigerwald[5] investigated delayed failure behavior of a number of high strength steels in distilled water and a 3N NaCl solution using center notched precracked specimens. Results obtained with 9Ni-4Co steels, (HP 9-4-45 and HP 9-4-25) at the same strength are included in their report. Martensitic HP 9-4-45 has a twinned martensitic structure with a high concentration of carbides at platelet boundaries as well as within the platelets. Conversely, the bainitic HP 9-4-25 is not twinned and has a more uniform distribution of the carbides and no indicated preference for precipitation at platelet boundaries. They stated these differences are sufficient to suggest that the delayed failure kinetics in these steels are regulated by martensite or carbide morphology or both. The twinned structure or the preferential carbide distribution in the HP 9-4-45 martensite provides a network of high energy boundaries which could produce a preferred path for crack propagation, thus accelerating the rate of crack growth.

Benjamin and Steigerwald emphasize that if composition alone was the primary cause of the observed differences in the kinetics of delayed failure, the various structures in the 9Ni-4Co steels would exhibit comparable behavior. However, the appreciably difference in failure kinetics produced by heat treatment or changed carbon content indicates the significance of structural control and is in agreement with the findings of Cain and Troiano[2].

The acceleration of crack propagation by the presence of twinned martensite in the microstructure of the high strength 9Ni-4Co alloy agrees well with the above reported results obtained by Boniszewski et al.[4] on the 9Ni-7Mn alloy. The fact that this investigator employed specimens which contained a rather high quantity of hydrogen* indicates again that the mechanism which controls fracture kinetics is hydrogen stress cracking and not stress corrosion cracking (See Chapter 6).

5.2 AUSTENITIC VERSUS MARTENSITIC STRUCTURE

Blanchard and Troiano[6] studied the hydrogen embrittlement susceptibility of several fcc alloys. In order to induce embrittlement, they had to intensify electrolytic charging conditions materially. The effect of strain rate on ductility of a 72Ni-28Fe alloy is plotted in Fig. 5.4 which shows decreasing embrittlement with increasing cross head speed.

*The hydrogen extracted at 650 C after quenching reached a steady value of approximately 4 cc (STP) per 100g Fe (containing 0.1 percent carbon).

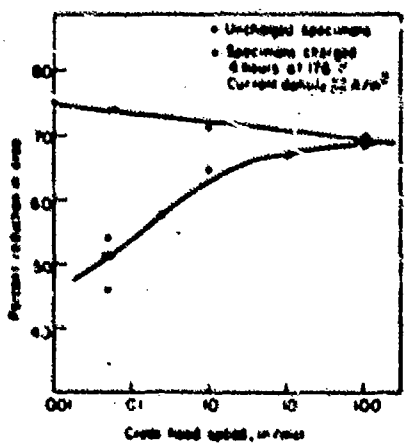

Fig. 5.4 – Effect of cross head speed on fracture ductility of an austenitic 72Ni-28Ni alloy. Electrolytically charged with hydrogen in 2N H_2SO_4 containing a promotor, followed by cadmium plating.

The next figure depicts increasing ductility of charged austenitic 80Ni-20Cr alloy with increasing aging (baking) time, and complete restoration of ductility at 1000 minutes. From these and other results Blanchard and Troiano conclude that austenitic alloys are definitely susceptible to hydrogen embrittlement.

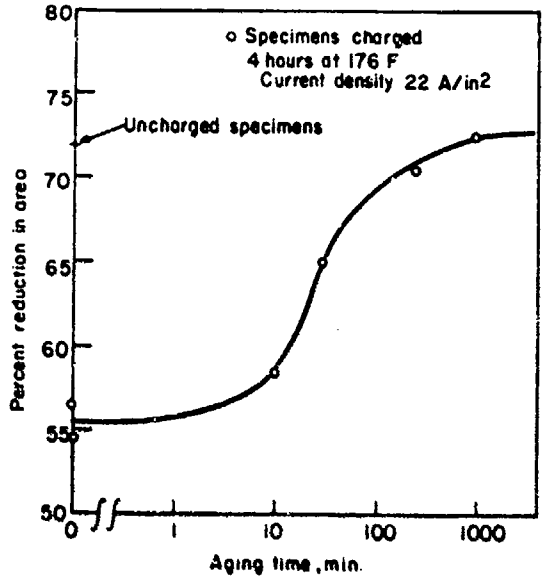

Fig. 5.5 – Recovery of ductility of a hydrogenated 80Ni-20Cr austenitic alloy with aging (250 F). Charged electrolytically with hydrogen in 2N H_2SO_4 with a promotor, followed by cadmium plating.

These conclusions were confirmed by Whiteman and Troiano[7] who found that fcc type 310 stainless was embrittled by hydrogen in the same way as a low alloy bcc steel, However, the amount of hydrogen necessary to produce this phenomenon in the fcc structure was one to two orders of magnitude greater. In addition, there is strong resistance for penetration of hydrogen to any appreciable depth. This inhibition of hydrogen introduction and penetration is probably due to the presence of oxide coatings and the decreased diffusivity of hydrogen in high Ni, high Cr or high Ni+Cr iron alloys (discussed later).

Hobson and Hewitt[8] reported that with increasing cold working of austenitic Cr-Ni steels, austenite is transformed to martensite as a result of ausforming, and that the susceptibility to hydrogen embrittlement is increased. On the other hand, Beck and Jankowsky[9] showed that in an ausformed low alloy steel, sensitivity to brittle fracture was slightly less than in a steel with a tempered martensitic structure.

Eisenkolb and Ehrlich[10] and Popov[11] demonstrated the sensitivity of austenitic steels to embrittlement and hydrogen absorption by experiments with specimens that were charged cathodically in dilute acidic and alkaline solutions in the presence of promotors. The degree of embrittlement was found to be rather low and ductility was quickly restored by room temperature aging. Eisenkolb et al. conclude that ferritic and martensitic steels are more prone to embrittlement than austenitic structures and that the hydrogen bond is stronger in the bcc than in the fcc lattice. These investigators assume that the total quantity of hydrogen introduced into an austenitic steel is concentrated in a thin layer underneath the surface of the specimen, and apparently is caused by the high resistance of the fcc lattice to hydrogen penetration. This in agreement with the findings of Whiteman and Troiano[7].

Benson et al.[12] found that martensite is formed in 300 series unstable austenitic steels by strain induced plastic deformation at room temperature. This material becomes very susceptible to hydrogen embrittlement. Conversely, stable austenite does not transform and therefore, is not affected by embrittlement.

In this context, experiments conducted by Lagneborg[13] with austenitic stainless steel alloys with 18 percent chromium and various concentrations of nickel are of appreciable interest. According to this investigator, alloys with 18 percent chromium and with nickel contents up to 35 percent, most probably will be used for the cladding of fuel elements in fast steam-cooled nuclear reactors now being developed. In these studies, tension specimens were charged with hydrogen in a molten salt bath of pure $KHSO_4$ at temperatures of 280 to 290 C for 4 days

at rather high current densities. Hydrogen embrittlement was only observed when the nickel content was either less than 15 percent or greater than 35 percent. The susceptibility to embrittlement of the materials with nickel contents below 15 percent was attributed to the unstable austenite that transformed to martensite during deformation. (More details about the embrittlement behavior of stainless steels is given in the next chapter.)

5.3 SUSCEPTIBILITY OF LOW ALLOY AND STAINLESS STEELS

In 1964, Elsea and Fletcher[1] reported on the effectiveness of a wide variety of alloying additions, comprising both substitutional and interstitial elements, for increasing the resistance of steel to hydrogen induced delayed brittle failure. In addition to AISI 4340 steel, they reported about the effectiveness of chromium and nickel additions as hydrogen embrittlement retarders in AISI 1020 and 4140 steels. They also summarized reports about hydrogen damage afforded certain stainless steels.

In 1966, Groenevelt et al.[14] submitted new facts pertinent to this subject matter. They evaluated delayed hydrogen stress cracking of specimens under sustained load. Several steels were tested, which were designated by NASA to be suitable for use in space application. Specimens were stressed to 80 percent of the yield strength of the alloy, and charged electrolytically under stress under three hydrogen charging conditions designated:

- Very severe
- Moderately sever
- Mild

Evaluation of resistance to hydrogen stress cracking was based on the assumption that a failure delay exceeding 200 hours indicated no susceptibility.

The results compiled in Table 5.1 are instructive and permit a preliminary rating of various alloys with respect to their sensitivity to hydrogen stress cracking.

TABLE 5.1 – SUSCEPTIBILITY OF VARIOUS ALLOYS TO HYDROGEN STRESS CRACKING FOR DIFFERENT CHARGING CONDITIONS

GROUP 1

Not susceptible to failure after 200 hours of sustained load under very severe charging conditons:

Alloy 718*	(180 ksi uts)
Waspalloy	(190 ksi)
Rene 41	(200 ksi)
U-212 Steel	(180 ksi)

GROUP 2

Failed only under very severe charging conditions:

17-7PH Stainless steel	(200 ksi)

GROUP 3

Failed under moderately severe charging conditions:

AM-355 Stainless Steel	(180 ksi)
18Ni Maraging steel	(260 ksi)
AISI 8740 Steel	(180 Ksi)

GROUP 4

Failed under mild charging conditions:

AISI H-11 Tool Steel	(260 ksi)
17-4PH Stainless Steel	(200 ksi)

*Ni base alloy developed by Inconel (Ni-19Cr-18Fe-5Nb-3Mo-0.8Ti-0.6Al)

Hydrogen determinations were also performed, using the tin-fusion vacuum extraction method. However, in numerous cases, there was no clear cut relationship between total hydrogen content and susceptibility to hydrogen stress cracking, Groenevelt concluded that hydrogen distribution within the sample is a more important factor than total hydrogen content in determining susceptibility to failure.

High susceptibility to delayed failure of notched AISI 4340, 4130 and 1020 steel specimens, tested under sustained load after cathodic charging was reported by J. W. Srawley[15]. Results on 1020 steel agree well with those of Seabrook[16], who observed a rapid decrease in the tensile ductility with increasing quantity of total hydrogen.

Bressanelli[17] worked with 410 stainless steel specimens embrittled by immersion in a 50 percent HCl solution, containing the promotor, SeO_2. He reported that considerably higher stress levels could be maintained for a given time in samples slowly cooled as compared with those quenched rapidly. Isothermal holding within the martensite transformation range after austenitizing improved cracking resistance after subsequent tempering at 900 F, as compared with samples directly quenched and tempered at 900 F. According to Bressanelli extended holding in the martensite range during hardening appears to decrease susceptibility to hydrogen cracking of marquenched material* by producing a non-uniform crack propagation retarding distribution of M_3C. Conversely, because of the uniform distribution of M_3C in direct quenched and tempered material, very little stress relief would occur ahead of an advancing crack and the overall crack propagation rate would be high.

Figure 5.6 shows striking differences between the embrittlement response of oil quenched and marquenched material. A partial explanation of the complex embrittlement behavior of the oil quenched material is suggested in a later section.

*Marquenching consists of austenitizing at 1800 F for 10 minutes, followed by quenching in salt at 700 F, holding at this temperature for 10 minutes, and finally slow air cooling to room temperature.

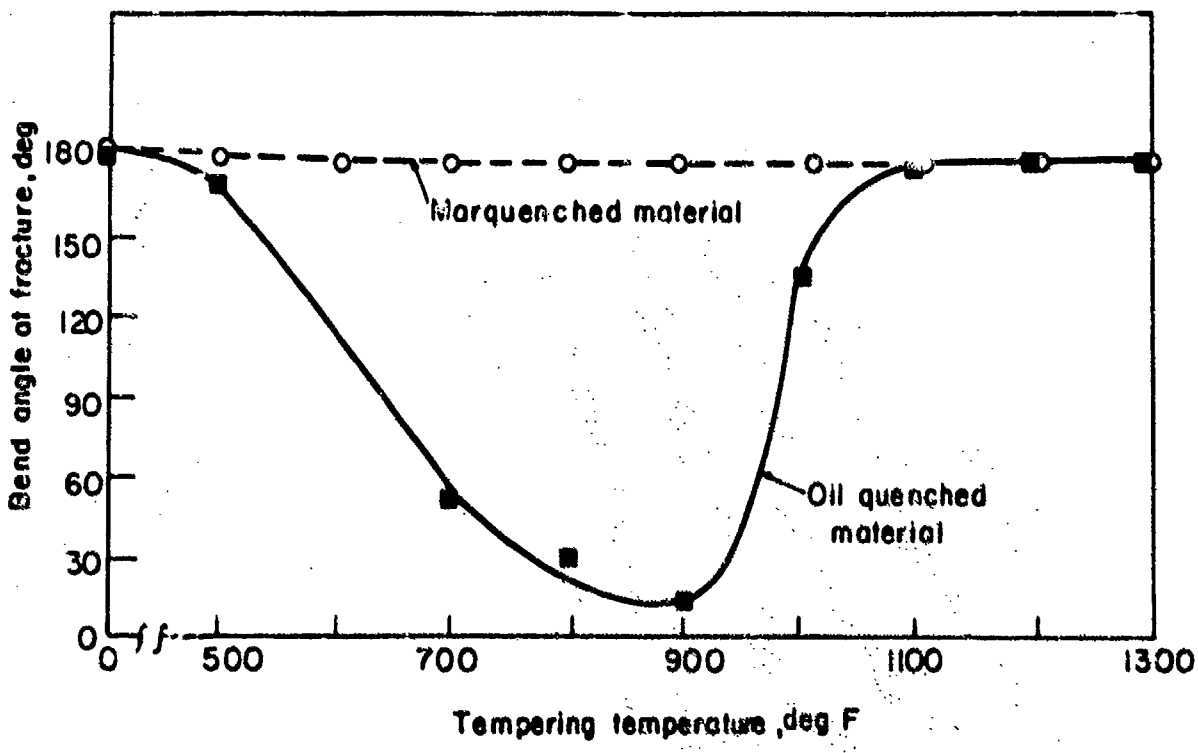

Fig. 5.6 – Effect of tempering temperature on embrittlement response of marquenched and oil quenched 410 stainless steel. Tempering time 2 hours. Embrittlement procedure - 20 min. immersion in 1:1 HCl containing the promotor, SeO_2

The marked delay in the loss of ductility for the marquenched and tempered material as compared with the rapid breakdown for the oil quenced and tempered material is shown in Fig. 5.7.

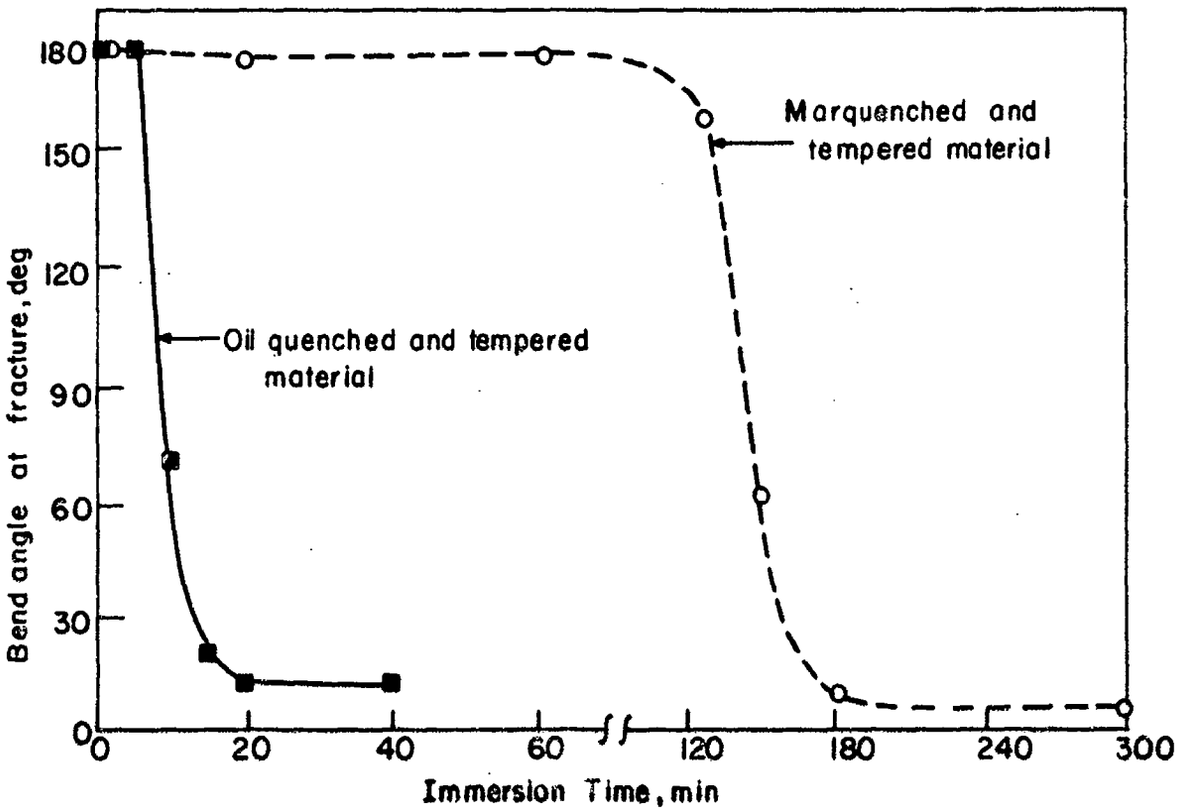

Fig. 5.7 – Plot showing a marked delay in loss of ductility for the marquenched and tempered as compared with oil quenched and tempered 410 stainless steel. Tempering temperature 900 F. Embrittled by 20 min. immersion in 1:1 HCl solution containing the promotor SeO_2.

Lillys and Nehrenberg[18] thoroughly studied the problem of the effect of tempering temperature on embrittlement of martensitic stainless steels. Their studies were instigated by those of Uhlig[19, 20], who demonstrated on hardenable stainless (such as 13 Cr martensitic stainless steel) that cathodic polarization accelerates crack propagation when they are immersed and stressed in a 3 percent sodium chloride solution. Therefore, the failure is classified as "hydrogen embrittlement".

Lillys and Nehrenberg evaluated the hydrogen embrittlement of 410, 420 and 436 stainless steels. In their study of these hardenable steels, bent beam specimens were stressed well below the elastic limit in a 0.1N sulfuric acid solution with arsenic as the promotor, charged cathodically, and the time to cracking recorded. These investigators discovered that times to failure vary with tempering temperature. They reported that embrittlement tendency in these steels heat treated to high strength levels, is a minimum at the temperature at which cementite begins to form (500 F) and is a maximum when an incoherent chromium carbide is formed at the parent austenite grain boundaries at tempering temperatures around 900 F. These structural changes may explain the results plotted in Fig. 5.6.

Recently, Raymond and Kendall[21] discovered that 17-4PH stainless steel bolts, which are used on the thrust chamber oxidizer and fuel valves of the Titan III, failed in a brittle fashion.* They proved that the failure was

*The marked susceptibility of 17-4PH to hydrogen stress cracking observed by Raymond and Kendall compares favorably with the findings of Groenevelt et al. (See Table 5.1).

due to hydrogen stress cracking. These bolts, which in general have a hardness between R_C 42 and 47, can be made more resistant by decreasing the hardness to about R_C 40 by overaging. Of more general interest are that results of tests obtained by these investigators on bolts subjected to cathodic polarization, which was accomplished in a very simple way by coupling with aluminum. Plating the bolts with a heavy nickel-cadmium coating was found to be effective in preventing failures. Anodizing the aluminum or insulating the aluminum/steel interface with a lubricant was beneficial under controlled laboratory conditions, but, by careless handling, the dissimilar metal couple can easily be reactivated and failure by hydrogen stress cracking can occur.

Some time ago, Suss[22] studied the susceptibility of the 17-4PH alloy to stress cracking after subjecting it to various aging treatments. This alloy is also used at various temperatures up to 600 F, for many important applications in pressurized water reactor systems. Frequently, cracking was observed under service conditions and ascribed to stress corrosion. Suss used notched strip material, which after aging at different temperatures, was stressed as a four point loaded beam with a uniformly applied stress across the surface. The specimens were placed in aqueous solutions, pH of 5 and 10, and exposed to a temperature of 600 F in autoclaves. It is the considered opinion of Suss that despite the comparatively high exposure temperature, the resultant failures are mainly transgranular brittle failures induced by hydrogen. This investigator emphasizes that, as a result of secondary aging during testing, the hardness of the alloy, and thus the susceptibility to hydrogen stress cracking is increased. All brittle failures occurred at a stress of 165 ksi at the root of the notch. A striking example is the increase in hardness from R_C 34.5 to 36.8 after 700 hours exposure in the autoclave.

5.4 BENEFICIAL EFFECTS OF SILICON AND CHROMIUM ADDITIONS

Studies by Sachs, Klier, and Muvdi[23] revealed the beneficial effect on embrittlement by addition of 1.5 percent silicon to various types of low alloy steels, heat treated to strength levels between 240 and 280 ksi. The next figure depicts the remarkable resistance of the Hy-Tuf Steel to delayed brittle cracking at any value of the notch-stress concentration (K_t). Similar results were obtained for UHS-260 steel. A possible reason for the enhanced resistance of the silicon containing steels will be discussed in Section 5.6.

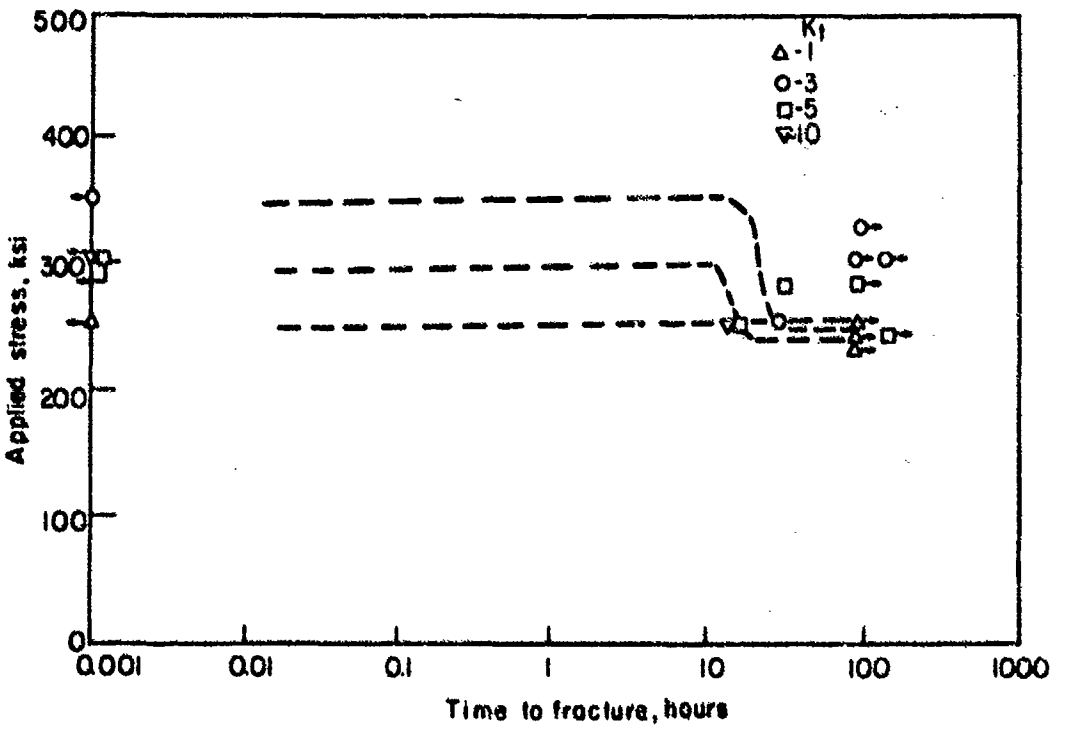

Fig. 5.8 – Beneficial effect of the addition of silicon (1.5%) as shown by the marked delay in fracture time and the high values of lower critical stress for Hy-Tuf steel (260-280 ksi) embrittled by cadmium plating. Data are shown for 4 different notch-stress concentrations.

Beck and Jankowsky[24] studied the effect of the chromium content on the stress rupture life of notched specimens. Fig. 5.9 vividly illustrates the beneficial effect of increasing chromium concentrations on the embrittlement sensitivity expressed in percent of notch tensile strength of the unplated specimen. The tendency to delayed brittle cracking is seen to decrease markedly up to a chromium concentration of about 8 percent. When this limiting value is exceeded, the favorable effect is overshadowed by rapidly increasing notch sensitivity, and the resistance to cracking falls accordingly. Mechanisms suggested for explaining the beneficial effect of chromium will be discussed in Section 5.6.

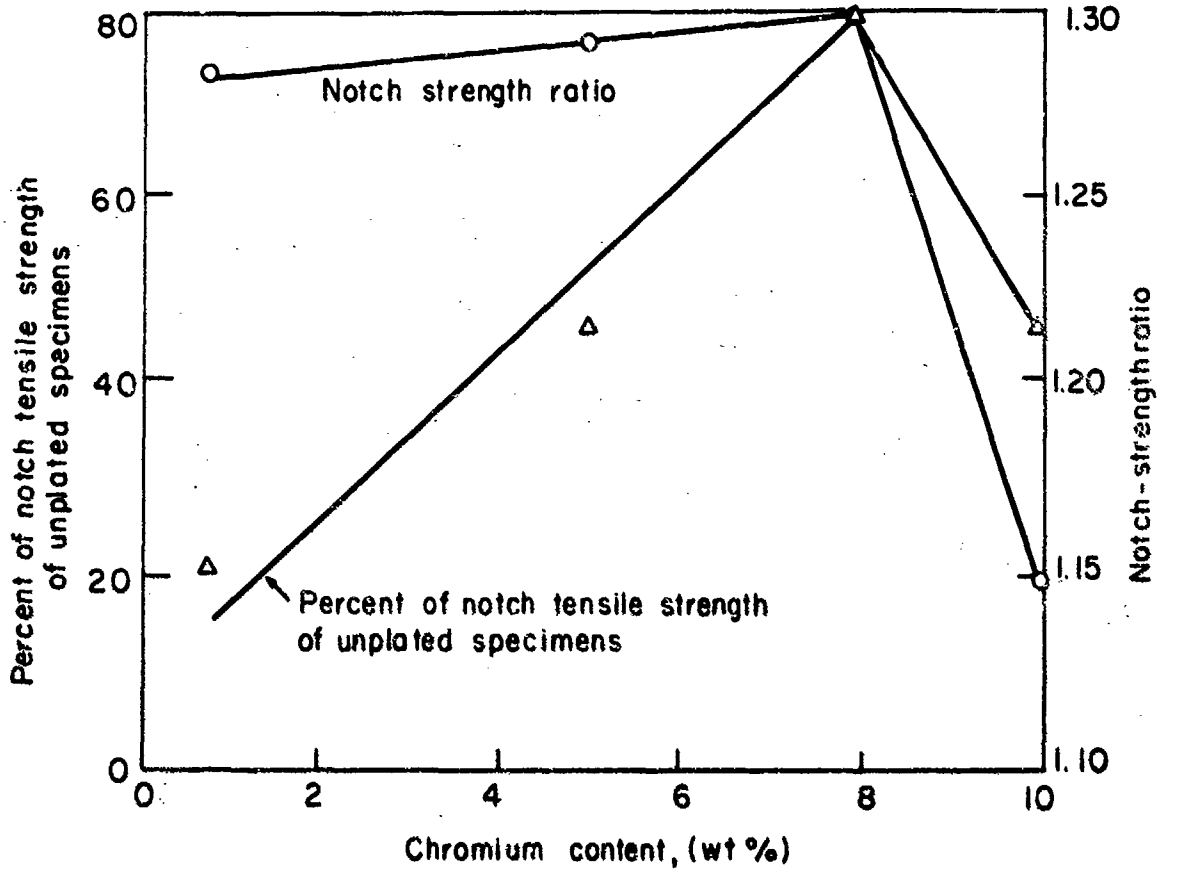

Fig. 5. 9 – Beneficial effect of increasing chromium concentration on the notch tensile strength (NTS) of cadmium plated steel (260-280 ksi). NTS is primarily controlled by notch sensitivity when the chromium concentration exceeds 8 percent.

5.5 MARAGING STEELS, AND STEELS DEHYDROGENATED BY REFINED MELTING TECHNIQUES

The precipitation hardening ultra high strength (in excess of 300 ksi) steels, commonly designated "maraging steels", show remarkable resistance to hydrogen stress cracking and are very desirable for the production of components to withstand high stresses. Large sections can be hardened with slow cooling rates minimizing internal stresses. Components can be machined in the relatively soft as-transformed state and the full properties developed subsequently by a moderate temperature aging treatment. Ductility and notch toughness of these steels have received considerably attention, particularly the 18Ni-8Co-5Mo alloys[25].

The cracking response to hydrogen of a steel of this composition has been studied recently by Gray and Troiano[26]. Specimens used had an ultimate tensile strength of 290 ksi, a yield strength of 285 ksi, an elongation of 11 percent and reduction in area of 53 percent. The ratio of notch tensile to tensile strength was 1.4. A comparison of the tensile ductility of this type of steel with AISI 4340 was made after charging cathodically in a 4 percent

sodium hydroxide solution saturated with sodium cyanide. The results are plotted in Fig. 5.10. It is apparent that 4340 steel is embrittled severely when charged at 20 MA/in^2 for as little as 5 minutes. With maraging steel, however, charging times of 9 to 12 hours are required to achieve the same loss of ductility.

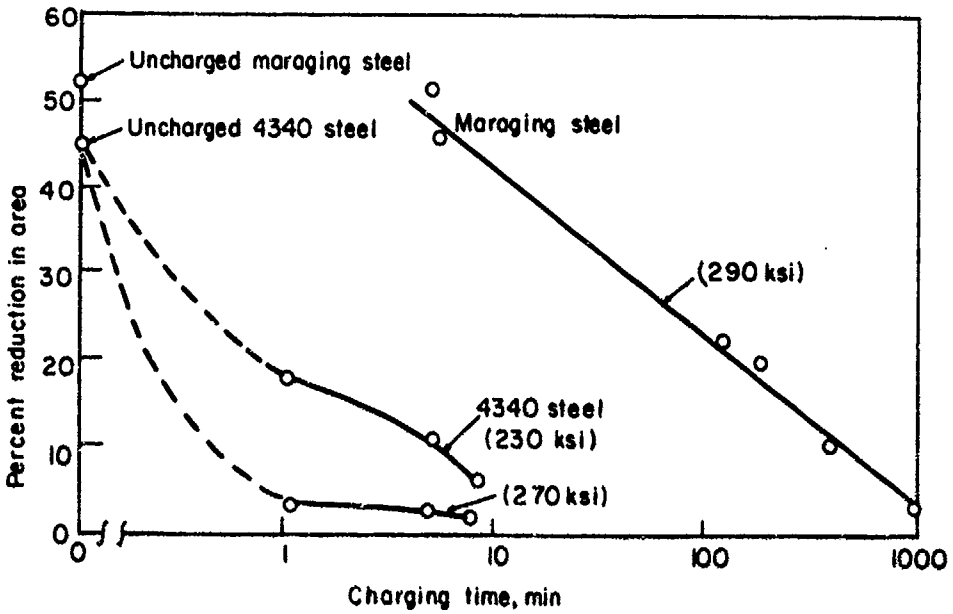

Fig. 5. 10 – Marked resistance of maraging steel to embrittlement as compared with AISI 4340 steel, is indicated by the increased charging times necessary to reduce tensile ductility.

The two steels also display different recovery characteristics, as depicted in Figure 5.11. Besides its increased resistance to embrittlement, maraging steel regains ductility much faster than AISI 4340 steel. Under similar conditions of hydrogenation, AISI 4340 steel required 24 hours of baking at 300 F to recover, while the maraging steel recovered in about 10 minutes. Recovery is difficult only if the maraging steel is severely charged with hydrogen.

In addition to the above described experiments, vacuum fusion analysis was performed on hydrogen charged bars after various aging times. In Figure 5.12 the effect of increasing baking time is portrayed. The hydrogen contents are given on the recovery curves for the two types of steels. It is apparent that hydrogen is present in substantially greater quantities in maraging steel than necessary to achieve the same relative embrittlement as in AISI 4340 steel. The above investigators conclude that maraging steel, even at very high strength levels, tolerates rather great quantities of hydrogen in terms of ductility loss and propensity to static brittle failure.

Boniszewski[27], also showed that maraging steel with 18 percent nickel has superior resistance to hydrogen embrittlement, when compared with medium carbon low alloy, high strength steel in the as-quenched condition*. These data substantiate the results obtained by Gray and Troiano.

DiBari[28] recently reported that maraging steel appears to be less susceptible to plating embrittlement than AISI 4340 steel. Hydrogen embrittlement studies on maraging steel were also performed by Parkins and Haney[29] and by Leckie and Loginow[30]. Hartbower et al.,[31] using the highly sensitive acoustic technique of stress wave analysis, did not find any susceptibility to hydrogen stress cracking on strongly hydrogenated 18Ni maraging steel. Mechanisms for the beneficial effect of a high nickel content are suggested in section 5.6.

*This steel was quenched rapidly from high temperature and was in the microstructural condition to be found in the weld heat affected zone immediately after welding. The material was austenitized in 1 atmosphere of hydrogen.

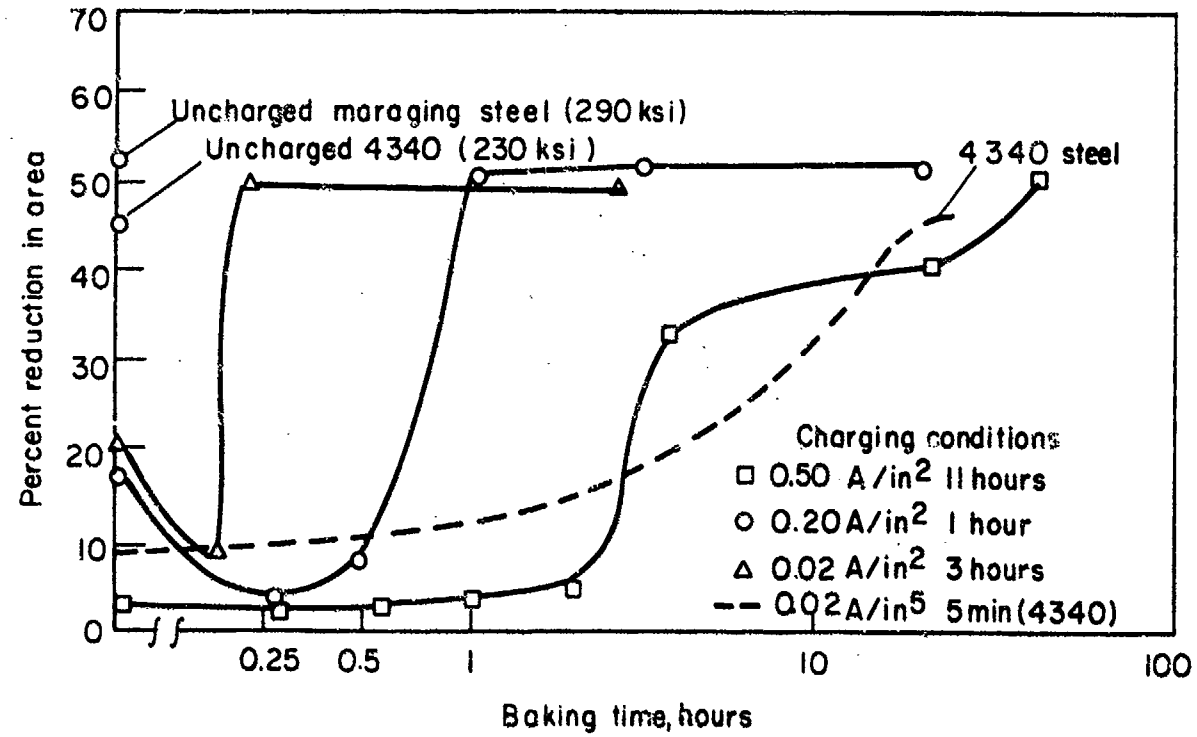

Fig. 5.11 – High rate of recovery of ductility of maraging steels as compared with AISI 4340 steel, is indicated by the much shorter baking times required to regain ductility. Baking temperature 300 F.

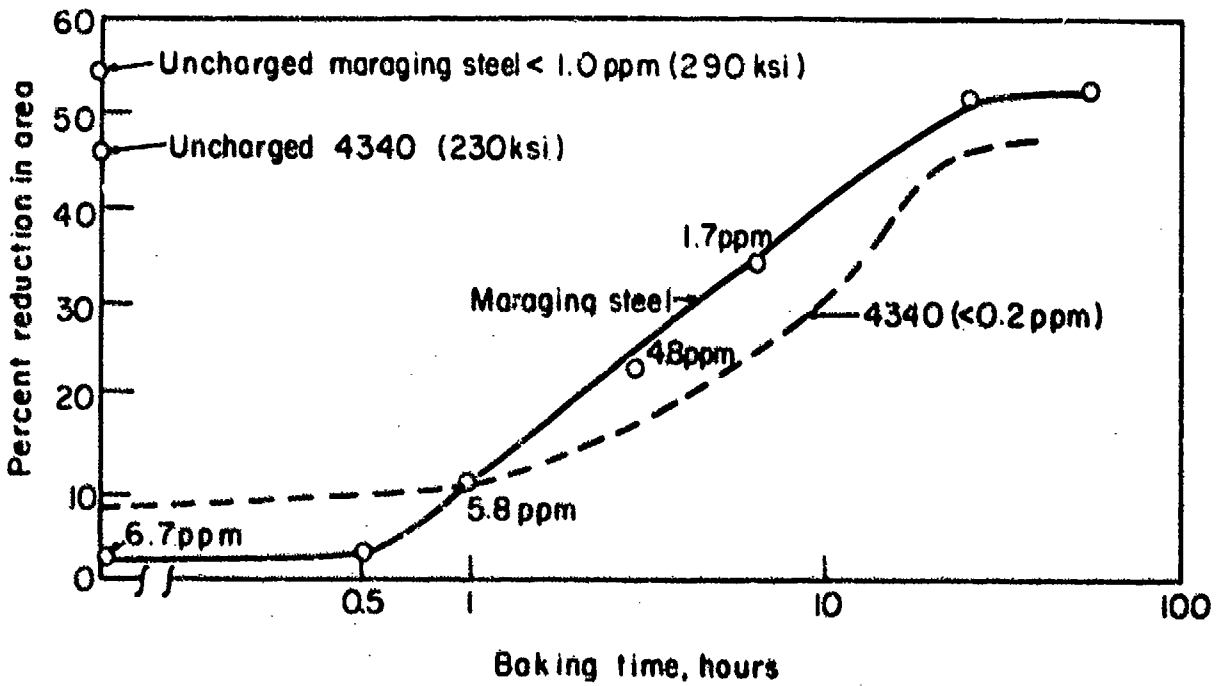

Fig. 5.12 – High hydrogen tolerance of maraging steel as compared with AISI 4340 steel is indicated by the larger quantities of hydrogen required to produce the same degree of embrittlement. Baking temperature 300 F.

Sustained load experiments were performed with notched specimens plated with cadmium from the cyanide bath by Hatfield[32] and by Dowty Rotol, Ltd., in Great Britain[33] and confirmed the comparatively low sensitivity of the 18 Ni maraging steel to hydrogen stress cracking[34,35].

Besnard[36] did not determine hydrogen embrittlement but found that as the purity of iron increased, for example, in the sequence Armco iron, electrolytic iron, and zone refined iron, the quantity of absorbed hydrogen decreased progressively in the same order. In these experiments, the iron was annealed for 24 hours at 850 C, in a stream of dry, high purity hydrogen. This investigator showed that embrittlement promotors when added to an electrolytic charging bath are effective on Armco or electrolytic iron, but not on the highest purity zone refined iron. Embrittlement behavior of Armco iron was also studied by Perlmutter and Dodge[37].

Beck et al.[38] reported that extraction of residual hydrogen by a refined melting technique enhanced the ductility of a steel[39]. This improvement, according to the above mentioned investigators is the reason that cadmium plated vacuum melted steel appears to be less prone to brittle cracking than air melted steel. Results of pertinent measurements are depicted in Fig. 5.13. The curves indicate that the highest values for the lower critical stress are obtained for those steels which were purified by double vacuum remelting. Similar findings were made by Brittain,[40] who reported that a high strength Cr-Mo-V steel, when made up with air melted steel could not sustain loads approximately half as large as those carried by the same alloy made from vacuum melted steel. The specimens were hydrogenated by cadmium plating.

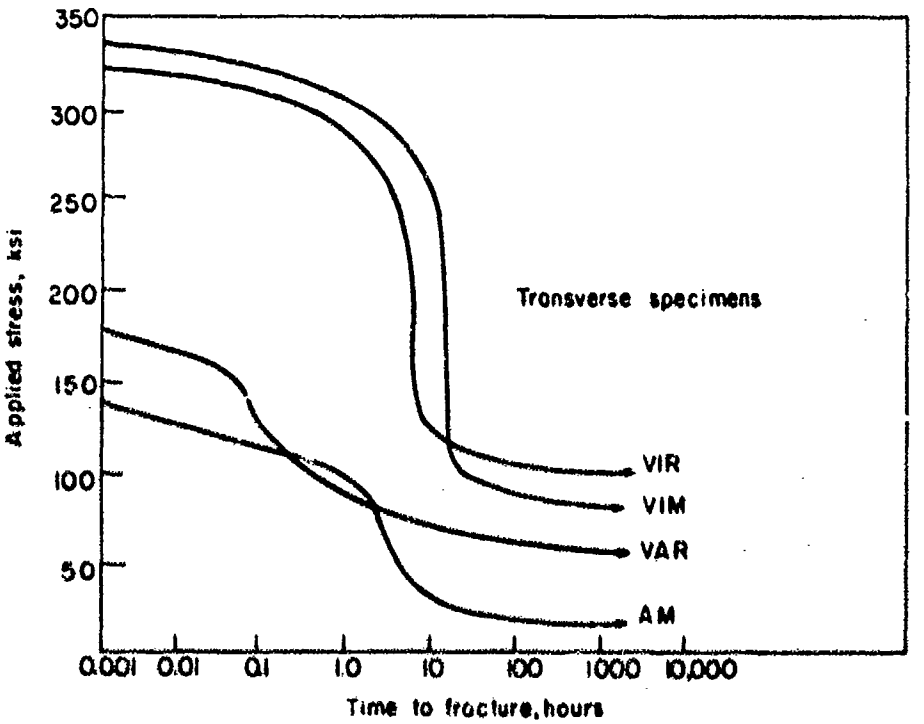

Fig. 5.13 – Improvement of upper and lower critical stress by refinement of melting technique. Hydrogenation by cadmium plating of high strength AISI 4340 steel.

AM	–	Electric Furnace Air Melt, heat No. 1
VAR	–	Part of heat No. 1 vacuum remelted as consumable eletrodes.
VIM	–	Vacuum induction melted, heats No. 2 and 3.
VIR	–	Part of heats No. 2 and 3. Vacuum remelted as consumable eletrodes.

Results obtained by Fransson et al.[41] who worked with cathodically charged bent beam specimens, carrying a single edge notch, did not agree with those summarized above. These investigators take issue with the conclusions drawn by Beck that the vacuum treatment "per se" is the reason for the decrease in sensitivity to delayed fracture. This statement made by Fransson is a rather odd one, because as was mentioned above, Beck discussed the the improved resistance to hydrogen cracking in the light of an "indirect" effect. And it was emphasized that the enhanced resistance to delayed failure was due solely to vacuum extraction of (embrittling) hydrogen from the steel prior to plating. Actually, Fransson indirectly proved this hypothesis to be correct, by demonstrating that introduction of hydrogen into the specimen in quantities greatly exceeding those diffusing into the steel during cadmium plating, overshadowed the favorable effect of the removal of residual hydrogen. In addition, it should be emphasized that differences in the geometry of a test specimen notch configuration and acuity, and type of load application, markedly affect the quantity of hydrogen charged into the steel, and thus its embrittlement characteristics.

5.6 GENERAL CONSIDERATIONS OF THE EFFECTS OF THE ALLOYING ELEMENTS

A number of attempts were made to explain the reduced susceptibility to hydrogen cracking accomplished by addition of silicon or chromium to steel. The beneficial effect of chromium, may be discussed in the light of a hypothesis, advanced by Troiano[42] to explain the increase in tensile ductility, accomplished by addition of iron or chromium to nickel. Troiano suggested that the electrons of hydrogen in solution in a transition metal join the d band of the metal. If the alloying metal being added has fewer electrons in the third band than the solvent metal, then the repulsive forces between the metallic cores will be lower, hydrogen added to the system will not produce as great an energy increase, and embrittlement will not be as great. Chromium fulfills the requirements of such a hypothesis since it has only five electrons in its third band compared with six for iron. Therefore, as the chromium content of an iron alloy system is raised, the repulsive forces and the embrittlement produce by hydrogen atoms introduced into the system should decrease.

The experimental alloys mentioned above[37] contained 0.4 percent vanadium which also fits this hypothesis. Therefore, it should also add to the beneficial effect of chromium.

According to Boniszewski,[27] the improvement of the resistance to cracking is related to the alpha phase ferrite in maraging steel. Troiano[26] advanced the opinion that the key to the diminished susceptibility of maraging steels to hydrogen damage most probably lies in the structure. These steels have small grains, and a fine distribution of precipitate particles. It may be that much of the introduced hydrogen is adsorbed on internal interfaces, including surfaces of precipitate particles. Troiano theorized that the high dislocation density of the maraging steels and attendant creation of vacancies may be involved in bonding a substantial quantity of this hydrogen. Since this hydrogen is not in solid solution, it is in an innocuous state. The effects of alloying elements on hydrogen diffusivity in steel has been studied by various investigators[43-47].

REFERENCES

[1] A. R. Elsea and E. E. Fletcher, "Hydrogen Induced, Delayed Brittle Failures of High-Strength Steels", *DMIC Report 196*, p. 106 Batelle Memorial Institue Columbus, Ohio (1964).

[2] W. M. Cain and A. R. Troiano, "Steel Structure and Hydrogen Embrittlement", *Petroleum Engineer*, pp. 78-82 (May 1965).

[3] E. R. Slaughter, E. E. Fletcher, A. R. Elsea and G. K. Manning, "An Investigation of the Effects of Hydrogen on the Brittle Failure of High-Strength Steels", *WADC Tech. Report 56/83*, Air Force Materials Lab. (WPAFB), Dayton, Ohio (Apr. 1956).

[4] T. Boniszewski and R. G. Baker, Hydrogen Embrittlement in Low Carbon, Nickel and Manganese Steels", *British Welding J.*, **12**, pp. 349-362 (1965).

[5] W. D. Benjamin and E. A. Steigerwald, "Environmentally Induced Delayed Failures in Martensitic High Strength Steels", Technical Report AFML-TR-68-80, Air Force Materials Lab. (WPAFB) Dayton, Ohio (Apr. 1968).

[6] R. A. Blanchard and A. R. Troiano, "Hydrogen Embrittlement of Several Face-Centered Cubic Alloys", WADC Tech. Report 59-172 pp. 94-121 Air Force Materials Lab (WPAFB) Dayton, Ohio (1959).

[7] M. B. Whiteman and A. R. Troiano, "Hydrogen Embrittlement of Austenitic Stainless Steel", *Corrosion*, **21**, pp. 53-56 (1965).

[8] J. D. Hobson and J. Hewitt, "The Effect of Hydrogen on the Tensile Properties of Steel", *J. IRSI 173*, pp. 131-140 (1955).

[9] W. Beck and E. J. Jankowsky, "Delayed Brittle Failure in Cadmium Plated Steels", *Metal Progress*, **84**, pp. 92-95 (1963).

[10] F. Eisenkolb and G. Ehrlich, "The Absorption of Hydrogen, Cathodically Charged into Austenitic Steels", *Archiv. Eisenhütt.*, **25**, pp. 187-194 (1954).

[11] K. V. Popov and Ye. P. Neckay, "Hydrogen Embrittlement of Metals with a fcc Lattice Structure", *J. of Electrochem. (USSR)* pp. 97-101, (1966).

[12] R. B. Benson, Jr., R. K. Dann and L. W. Roberts, "Hydrogen Embrittlement of Stainless Steel", *Trans. AIME*, **242**, pp. 2193-2205 (1968).

[13] R. Lagneborg, "Hydrogen Embrittlement in Austenitic Steels and Nickel Base Alloys", *J. IRSI*, **207** *(3)* pp. 363-366 (1969).

[14] T. S. Groenevelt, E. E. Fletcher and A. R. Elsea, "A Study of Hydrogen Embrittlement of Various Alloys", Batelle Memorial Institute Report (to NASA) Contract Number NAS 8-20029, Columbus, Ohio (June 1966).

[15] J. E. S. Srawley, "Hydrogen Embrittlement Susceptibility of Some Steels and Non-Ferrous Alloys", NRL Report 5392 Naval Research Lab., Washington, D. C. (1959).

[16] I. B. Seabrook, N. J. Grant and D. Carney, "Hydrogen Embrittlement of SAE 1020 Steel", *Trans. AIME*, **188**, pp. 1317-21 (1950).

[17] J. P. Bressanelli, "Effects of Heat Treatments on the Resistance to Hydrogen Embrittlement of Type 410 Stainless Steel", *Trans. ASM*, **58**, pp. 3-13 (1965).

[18] Peter Lillys and A. E. Nehrenberg, "Effect of Tempering Temperature on Stress Corrosion Cracking and Hydrogen Embrittlement of Martensitic Stainless Steels", *Trans. ASM*, **48**, pp. 327-355 (1956).

[19] H. H. Uhlig, "Action of Corrosion and Stress on 13% Cr Stainless Steel", *Metal Progress*, **57**, pp. 486-487 (1950).

[20] I. Matsushima, D. Deagan and H. H. Uhlig, "Stress Corrosion and Hydrogen Cracking of 17-7 Stainless Steel", *Corrosion*, **22**, pp. 23-27 (1966).

[21] L. Raymond and P. Kendall, "Hydrogen Stress Cracking of 17-4PH Stainless Steel", Report No. SAMSO, T. R. 67, p. 59, Aero Space Corp., El Segundo, Calif. (August 1967).

[22] H. Suss, "Stress Corrosion and Hydrogen Embrittlement Properties of 17-4-HP in 600°F Waters", G. E. Knolls Atomic Power Laboratory for U. S. AEC, Contract No. W-31-109, Eng. -52, (August, 1967).

[23] E. P. Klier, B. B. Muvdi and George Sachs, "The Response of High Strength Steels in the Range of 180,000 to 300,000 psi to Hydrogen Embrittlement from Cadmium Electroplating", *Proc. ASTM* **58**, pp. 597-621 (1958).

[24] Walter Beck and Edward J. Jankowsky, "Delayed Brittle Failure in Cadmium Plated Steels", *Metal Process* **84**, pp. 92-95 (1963).

[25] R. B. Setterlund, "Stress Corrosion Cracking of Maraging Steel", *Materials Protection*, **4**, pp. 27-29 (1965).

[26] H. R. Gray and A. R. Troiano, "How Hydrogen Affects Maraging Steel", *Metal Progress*, **85**, pp. 75-78 (1964).

[27] T. Boniszewski, "Hydrogen Induced Delayed Cracking in Maraging Steel", *British Welding J.*, **12**, pp. 557-565 (1965).

[28] G. A. DiBari, "Electroplating on 18% Nickel Maraging Steel: Relative Resistance to Hydrogen Embrittlement", *Plating* **52**, pp. 1157-1161 (1965).

[29] R. N. Parkins and E. G. Haney, "Stress Corrosion Cracking of 18% Ni Maraging Steel in Acidified Sodium Chloride Solution", *Trans. AIME* **242**, pp. 1944-1953 (1968).

[30] H. P. Leckie and A. W. Loginow, "Stress Corrosion Behavior of High Strength Steels", *Corrosion*, **24**, pp. 291-297 (1968).

[31] T. Hartbower, Gerberich and Crimmins, "Monitoring Subcritical Crack Growth by Detection of Elastic Stress Waves", *Welding J.*, **47**, Research Suppl., pp. 1-18 (1968).

[32] P. Hatfield, "Investigation of the Susceptibilityoof MMS-211, 18% Nickel Maraging Steel to Hydrogen Embrittlement", Report 513-472 McDonnel Aircraft Corp., St. Louis, Mo. (June 1966).

[33] W. M. Imrie, "An Examination of a Maraging Steel Die Forging", Dowty Rotol Ltd, Report 64/9006 Gloucester, England (April 1964).

[34] L. R. Scharfstein, "Stress Corrosion Cracking of 18% Ni Maraging Steel", *J. IRSI* **202**, pp. 158-59 (1964).

[35] Lauchner and Herfert, "Plating Components of 18% Ni Maraging Steels in Low Hydrogen Baths", Metal *Progress*, **90**, p. 85 (1966).

[36] Simone Besnard, "Absorption of Hydrogen and Low Temperature Hydrogen Embrittlement of Iron, as Affected by its Purity", *Annales de Chimie*, **6** (3/4) pp. 245-283 (1961).

[37] D. D. Perlmutter and B. P. Dodge, "Effects of Hydrogen on Properties of Metals", *Ind. Eng. Chem.*, **48**, pp. 885-893 (1956).

[38] W. Beck, E. J. Jankowsky and W. H. Golding, "Fatigue and Delayed Brittle Failure of Vacuum Melted and Cadmium Plated Steel", *Corrosion Science*, **7**, pp. 709-715 (1967).

[39] P. Blanchard and A. R. Troiano, "Delayed Failure and Notch Tensile Properties of a Vacuum Melted 4340 Steel", WADC. Technical Note 58-176 Air Force Materials Lab. (WPAFB) Dayton, Ohio (1958).

[40] P. I. Brittain, "Protection of Very Strong Steels – The Cadmium Plating of a 5% Cr-Mo-V Steel", Hawker Siddeley Aviation Ltd., Res. Progress Report No. R 240/P5/64 England (April 1964).

[41] Artur Fransson, Sten Nilsson and Holger Henriksson, "Hydrogen Embrittlement in Air-Melted and in Vacuum Remelted High Strength Steel", *Jernkontorets Ann.* **152**, pp. 501-515 (1968).

[42] A. R. Troiano, "The Role of Hydrogen and other Interstitials in the Mechanical Behavior of Metals", *Trans. ASM* **52**, pp. 54-80 (1960).

[43] W. Geller and Tak-Ho-Sun, "Effect of Alloying Additions on the Hydrogen Diffusion in Iron", *Archiv. Eisenhütt.* **21**, pp. 423-430 (1950).

[44] F. Erdmann - Jesnitzer and A. Petzold, "Effect of Si content on Fish Scale Formation in Enamel Coatings", ibid., **31**, pp. 479-84 (1960).

[45] H. Bennek and S. Klotzbach, "Effect of Alloying Additions on Hydrogen Diffusivity in Iron", *Stahl und Eisen*, **61**, pp. 597-606, 624/630 (1941).

[46] John O'M. Bockris, M. Fullenwider and E. Gileadi, Hydrogen Embrittlement Resulting from Corrosion, Cathodic Polarization and Electroplating", Electrochemistry Lab., U. of Penna., Contract No. N156-46659 First Quarterly Report, (August 1965).

[47] John O'M. Bockris, M. Genshaw and P. K. Subramanyan, "Hydrogen Embrittlement Resulting from Corrosion, Cathodic Polarization and Electroplating", Electrochemistry Lab., U. of Penna., Contract No. N-156-67-C-1941 Third Quarterly Report (Dec. 1967).

CHAPTER 6

THE PROBLEM OF DIFFERENTIATING BETWEEN STRESS CORROSION CRACKING AND HYDROGEN STRESS CRACKING

Despite the great similarity between the fracture phenomena of hydrogen stress cracking (HSC) and stress corrosion cracking (SCC), they might be controlled by different fracture mechanisms, and the limiting conditions for the occurrence of these two types of cracking appear different.

According to Fletcher, Berry and Elsea[1] SCC is a process in which a crack propagates, at least partially, by stress induced corrosion of a susceptible metal at the advancing tip of the crack. There is convincing evidence that the cracking results from electrochemical corrosion of a metal subjected to tensile stresses.

HSC may be initiated by the impregnation of a metal with hydrogen from the gas phase, and from various electrochemical and chemical processes. According to Troiano[2] certain conditions must prevail before HSC will occur. They are a critical combination of hydrogen and stress in a susceptible material at a location suitable for crack nucleation under conditions permitting absorption of the hydrogen by the steel.

6.1 EFFECTS OF VARIOUS PARAMETERS ON HSC AND SCC

The effects of various parameters on both types of cracking may be summarized as follows:

6.1.1 STRENGTH LEVEL

A minimum ultimate tensile strength of about 100 ksi and a minimum yield strength of about 80 ksi are required for initiation of HSC. Conversely, SCC is encountered in steels of all strength levels.

6.1.2 COMPOSITION AND STRUCTURE

All high strength steels, having bainitic, pearlitic, ferritic, martensitic or austenitic structure are susceptible to HSC. Martensitic structures are much more sensitive to HSC than austenitic. Maraging steel is only slightly susceptible to HSC.

6.1.3 APPLIED STRESS

The directionality of the applied stress plays the same role in SCC as in HSC. Compressive stresses give protection against SCC as well as HSC.

6.1.4 GENERAL FACTORS

Both HSC and SCC are environment dependent. Anodic polarization causes SCC but has a beneficial effect on HSC. However, cathodic polarization produces the opposite effect, i.e., it causes a decrease in SCC and an increase in HSC. Systems with a high oxidation potential exert the same beneficial effect on HSC as anodic polarization. HSC can be induced by exposure to high pressure hydrogen.

6.1.5 EFFECT OF TEMPERATURE

Maximum susceptibility to HSC occurs at about room temperature. At temperatures appreciably below or above room temperature, susceptibility to HSC is markedly reduced and finally disappears completely. SCC can be produced at room as well as elevated temperatures.

6.2 EXPERIMENTS ELUCIDATING DIFFERENCES BETWEEN HSC AND SCC

A number of investigators have studied the effect of changes in pH, potential, and environment on the mechanism of fracture in steels. Van de Pluyr[3] subjected double cantilever beam specimens to anodic and cathodic polarization in solutions adjusted to three pH levels 2.4, 9.3, and 11.7. Appropriate ratios of hydrochloric acid or

sodium hydroxide were used to prepare the solutions which were maintained at 80 ± 0.5 F. Specimens were made of AISI 4340 steel heat treated to a yield strength of 217 ksi, with a fracture toughness of K_{I_C} = 51.5 ksi $\sqrt{in.}$ The specimens were fatigue precracked and side notches were used to maintain plane strain conditions along the crack front. Two levels of strain energy release rate, G, were used, 10 and 30, where G = 10 represents a very low value.

The results of the polarization experiments are plotted in Figs. 6.1a to 6.1c. The increase in rate of crack growth as the potential becomes more negative indicates that a hydrogen embrittlement mechanism prevails. This is also supported by the decreasing crack rate, as polarization becomes more anodic. Very little or no effect is observed in the range between -1v and +1v and is due to the fact that at these low voltages the discharge potentials for H^+ or OH^- have not been attained. As shown in Fig. 6.1c in solutions with a pH = 11.7, the trend of the anodic branch of the polarization curve for G = 30 is slightly different from Figs. 6.1a and 6.1b because of the increase in the crack growth rate.

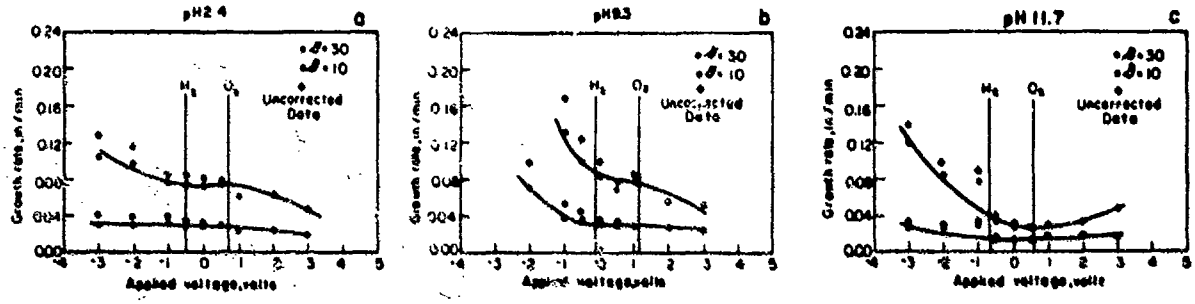

Fig. 6. 1 – Crack growth rate dependency on applied voltage and loading (two strain energy release rates). Precracked tapered double cantilever notched beam specimen, AISI 4340 steel, UTS 260 ksi, K_{I_C} = 51.5 ksi $\sqrt{in.}$), test temperature 80 F, pH = 2.4, 9.3 and 11.7.

In addition to the above solutions Van der Sluys also made crack propagation studies in distilled water and summarizes his findings as follows:

- In a distilled water environment, the primary mechanism of subcritical flaw growth appears to be hydrogen embrittlement.
- Under conditions of cathodic charging in aqueous environments, (pH 2.4 to 11.7), the primary mechanism of subcritical flaw growth appears to be hydrogen embrittlement.
- Under conditions of anodic polarization, both the mechanisms of hydrogen embrittlement and stress corrosion appear to operate. However, the hydrogen embrittlement mechanism dominates at relatively low pH's and low anodic voltages, while the stress corrosion mechanism becomes more marked as either the pH or the anodic voltage is increased.
- To avoid subcritical flaw growth, the use of an impervious coating is recommended to prevent the electrolyte from coming in contact with the steel in the flawed region.

More definite statements concerning the control of the cracking mechanism can be made when the polarization experiments are performed under galvanostatic conditions and in place of the applied voltage, the polarizing current is taken into consideration. This was the approach of Bhatt and Phelps[4, 5] who succeeded in delineating the current and pH ranges over which each of the two cracking mechanisms is operative.

Fig. 6.2 shows the effect of polarization with pH (pH 1, 6.5, 12.5) on the time to failure in aerated 3 percent sodium chloride solutions. Bent beam specimens, used in these tests were 0.67 in. wide and 0.020 in. thick cut to a length calculated from a relationship between: 1) the strain in the outer fiber at the center of the specimen; 2) the specimen thickness; 3) the modulus of elasticity of the steel; and 4) the holder span. In all experiments, the stress level used was 75 percent of the yield strength. The 3 percent sodium chloride solutions were adjusted to the desired pH by the addition of dilute hydrochloric acid or sodium hydroxide prior to the initiation of the polarization experiments. It was preferred to make the limited pH changes rather than to work with buffered solutions, which may give rise to undefined effects on the failure times.

The current circuit consisted of an auxiliary platinum electrode, an unpolarizable reference electrode, the specimen, electrical equipment for impressing anodic or cathodic currents on the stressed specimen and for measuring polarizing current and solution potential. As depicted in Fig. 6.4 at pH = 6.5, increased anodic polarization decreases the cracking time drastically, whereas small cathodic currents lengthen it. Thus, cracking in this region is

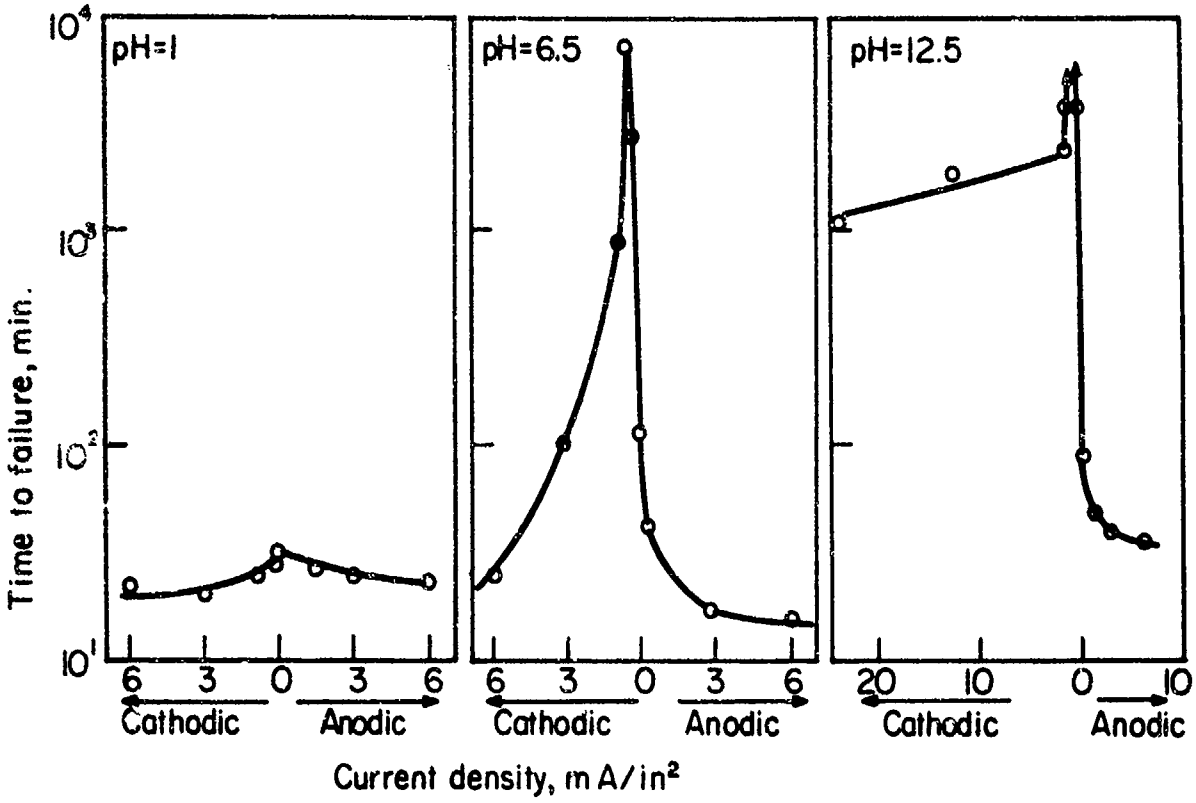

Fig. 6.2 – Effect of anodic and cathodic polarization with pH on time to failure in aerated 3% NaCl solution at room temperature. Unnotched bent beam specimens stressed to 75% yield strength of a specially alloyed martensitic stainless steel (USS 12Mo-V, UTS 260 ksi).

caused by an active path (stress corrosion). The potentials measured during these experiments are more positive than the estimated reversible hydrogen potential, hence the reduction of water to form hydrogen would not be expected to occur. At higher cathodic current densities, the cracking time became shorter and the potential is more negative than the reversible hydrogen potential. In this region, the cracking is caused by hydrogen embrittlement. Moreover, in other experiments, permeation of hydrogen through steel membranes is detected when the potential is more negative than the reversible hydrogen potential in a solution with a pH = 6.5, and is considered convincing evidence of hydrogen entry into the steel.

From these results, it appears that this mechanism can be expected to prevail as soon as the electrochemical surface reactions permit introduction of hydrogen into steels, which are very susceptible to hydrogen embrittlement.

The interpretation of the results at pH = 1 is similar, with the notable exception that the potential without applied current is appreciably more negative than the reversible hydrogen potential. Because, increasing anodic and cathodic polarization both reduced cracking time, it is not possible to determine from the polarization measurements which cracking process was rate determining with no applied current. However, the fact that appreciable quantities of hydrogen evolved from the steel and permeation of hydrogen through the steel membrane was measured, makes it appear likely that the mechanism of cracking without polarization at this very low pH is hydrogen embrittlement.

The results obtained at pH = 12.5 are interesting because they include the only experiments in which the steel is found to be resistant to failure (with no applied current and with very weak cathodic current). The potential and pH conditions for these experiments are within the "passivation" zone of the pH - potential equilibrium diagram for iron. Apparently, at a pH 12.5 and 6.5 the chloride content of the solution is sufficient to cause localized breakdown of the passivating film and continue "active path" corrosion when the steel is polarized anodically.

Hughes[6], Steigerwald and Benjamin[7] have also proven that the differences in response to hydrogen stress cracking and stress corrosion cracking of two different steels in distilled water and a sodium chloride solution are reflected in their polarization behavior, as depicted in Figs. 6.3 and 6.4.

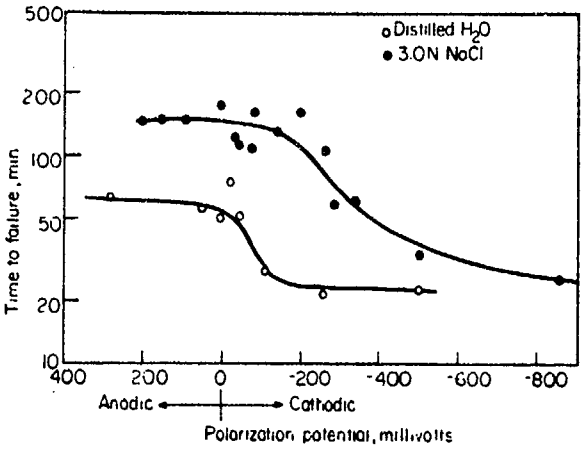

Fig. 6.3 -- Effect of impressed potential on delayed failure of AISI 4340 Steel (235 ksi) center-notched specimens (applied stress 50 ksi).

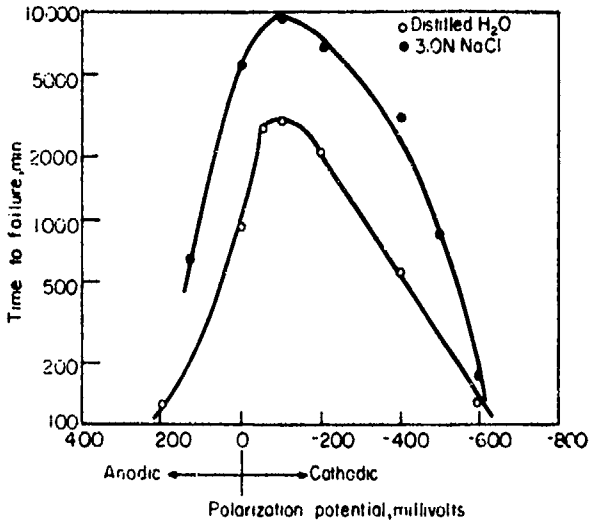

Fig. 6.4 -- Effect of potential on delayed failure of HP 9-4-45 steel (242 ksi) center-notch specimens (applied stress 120 ksi).

These figures show that the effect of polarization is markedly different in AISI 4340 and HP-9-4-45 steels. Application of a cathodic potential to the 4340 steel produced a decrease in the failure time in both distilled water and chloride environments, which is consistent with a hydrogen embrittlement failure mechanism as was also found by Van der Sluys. In the HP-9-4-45 steel, which is susceptible to SCC, the application of a slight cathodic potential produces an increase in failure time (cathodic protection). However, as the potential becomes more cathodic the rate of delayed failure brought about by hydrogen embrittlement is accelerated.

6.3 FRACTURE APPEARANCE

According to Phillips, Kerlin, Rawe and Whiteson[8] great difficulty has been encountered in attempts to distinguish between the appearances of fractures caused by stress corrosion and hydrogen embrittlement because the two types of failures appeared to exhibit a remarkably similar fracture appearance. They stress that it would be of great importance in failure analysis if this approach could be refined so that it could be used for differentiating these two failure mechanisms.

With this goal in mind, these investigators performed sustained load tests to produce failure as a result of either stress corrosion or hydrogen embrittlement. A flat tensile specimen was used with a circular hole as a stress raiser. Hydrogen embrittlement was induced by cadmium plating from the cyanide and fluoborate baths, respectively. For inducement of stress corrosion, specimens were spring loaded and subjected to alternate immersion in deionized water. All experiments were performed at 50, 75 and 90 percent of the yield strength with AISI 4340, 433M and D6AC steels, with ultimate strengths of 277, 224, and 289 ksi, respectively.

They concluded from their work that the features associated with stress corrosion fracture are:

- Predominantly surface nucleation of intergranular fracture.
- Intergranular regions showing pronounced secondary cracking or deep crevices.
- A relatively great amount of oxidation or corrosion attack at the nucleus.
- Less marked hairline indications on the intergranular surfaces than observed on hydrogen embrittlement fractures.

The features associated with hydrogen embrittlement are:

- Predominantly sub-surface nucleation of intergranular fracture.
- Evidence of dimples and marked hairline indications in the intergranular regions.

The scanning electron microscope has been used at the Naval Air Development Center to provide useful information for distinguishing these two types of failures[9]. Scanning electron micrographs showing fracture

surfaces considered to be typical of these failures are shown in Fig. 6.5. The work to date using fracture appearances should be considered preliminary with the final picture still to be completed.

Matsushima, Deegan and Uhlig[10] emphasized that, depending on environment, stainless steel may fail either by HSC or SCC, but that there are no compelling reasons to believe that hydrogen in any form enters the mechanism of SCC in austenitic alloys.

The examples given above seem to indicate that certain media favor only one type of cracking or the other. Taking this into consideration along with the differences in behavior of the two types of cracking under impressed (polarizing) currents, various authors have concluded that SCC and HSC are controlled by different fracture mechanisms.

It is significant to consider, that the pH at the tip of an advancing crack is quite lower than that measured near the opening of the crack[11]. Brown[12] has suggested that at the crack tip, hydrogen embrittlement may contribute to SCC or even replace it as the failure mechanism as a result of initiation of the hydrogen evolution reaction.

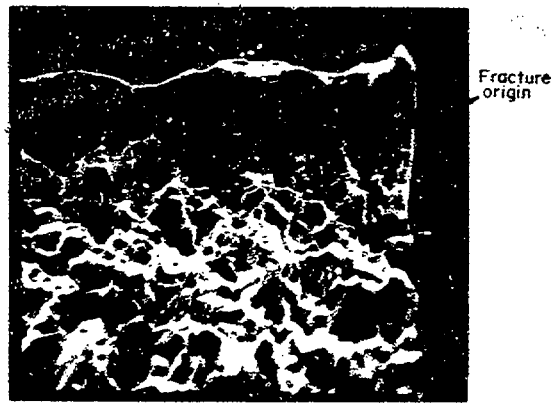

Hydrogen Embrittlement Failure X500
Note sub-surface fracture origin with shear lip extending to surface

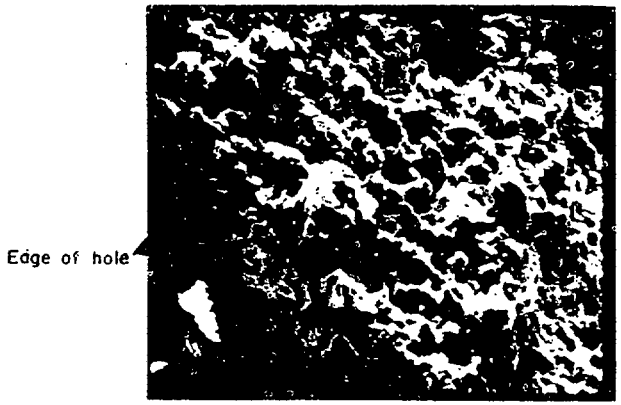

Stress Corrosion Failure X500
Intergranular fracture originates at the edge of the hole

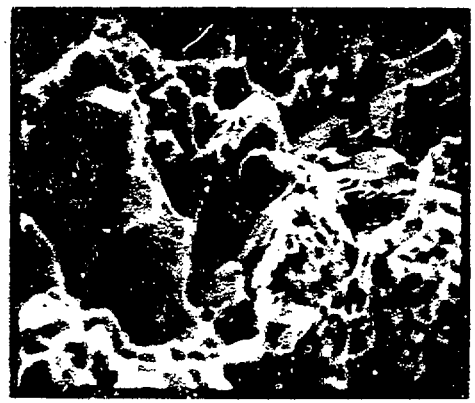

Intergranular Fracture mode in hydrogen embrittlement failure X2000

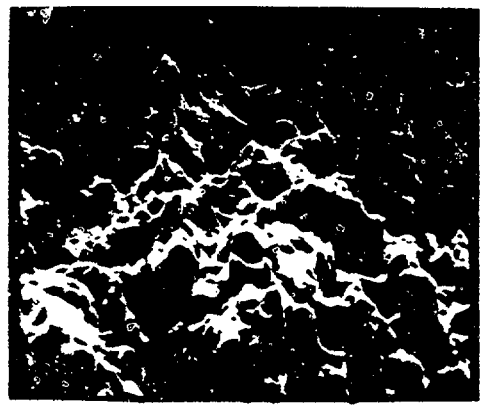

Intergranular Fracture mode in stress corrosion failure X1000

Fig. 6.5 — Scanning electron micrographs of typical hydrogen embrittlement and stress corrosion failures in high strength steel.

REFERENCES

[1] E. E. Fletcher, W. E. Berry and A. R. Elsea, "Stress Corrosion Cracking and Hydrogen Stress Cracking of High Strength Steel", DMIC Rept. 232, Battele Memorial Institute, Columbus, Ohio (July, 1966).

[2] A. R. Troiano, "The Role of Hydrogen and Other Interstitials in the Mechanical Behavior of Metals", *Trans. ASM,* **52**, pp. 54-80 (1960).

[3] W. Alan Van der Sluys, "Mechanism of Environment Induced Subcritical Flaw Growth in AISI 4340 Steel", *Eng. Fracture Mech. 1,* pp. 447-62 (1969).

[4] H. J. Bhatt and E. H. Phelps, "Effect of Solution pH on the Mechanism of Stress Corrosion Cracking of a Martensitic Stainless Steel", *Corrosion,* **17** (9) pp. 430-434t (1961).

[5] H. J. Bhatt and E. H. Phelps, "The Effects of Electrochemical Polarization on the Stress Corrosion Behavior of Steels with High Yield Strength", Paper presented at the Third International Congress on Metallic Corrosion, Moscow, (May 1966).

[6] P. C. Hughes, "Delayed Fracture of a 5% Cr Tool Steel," *IRSI,* **204**, pp. 385-87 (1966).

[7] W. D. Benjamin and E. A. Steigerwald, "Stress Corrosion Cracking Mechanisms in Martensitic High Strength Steels", Technical Report AFML-TR-67-98, TRW, Equipment Laboratories, TRW Inc. Cleveland, Ohio (1967).

[8] A. Phillips, V. Kerlin, B. A. Rawe and B. V. Whiteson, "Electron Fractography Handbook, Supplement I", Technical Report AFML-TR-416, Douglas Aircraft Co., Inc., Santa Monica, Calif. (Dec. 1966).

[9] I. Shaffer, J. A. Hoffner, W. A. Sipes unpublished work, Metallurgical Division Naval Air Development Center, Warminister, Pa.

[10] Y. Matsushima, P. Deegan and H. H. Uhlig, "Stress Corrosion and Hydrogen Cracking of 17-7 Stainless Steel", *Corrosion,* **22**, pp. 23-27 (1966).

[11] B. F. Brown, C. T. Fujii, and E. P. Dahlberg, "Methods for Studying the Solution Chemistry Within Stress Corrosion Cracks", *J. Electrochemical Soc.,* **116**, No. 2, pp. 280-290 (1966).

[12] B. F. Brown, "Concept of the Occluded Corrosion Cell", *Corrosion,* **26**, pp. 249-250 (1970).

CHAPTER 7

EMBRITTLEMENT IN LIQUID METALS, ORGANIC COMPOUNDS AND AQUEOUS ENVIRONMENTS

7.1 LIQUID METAL EMBRITTLEMENT

The phenomenon of embrittlement by liquid metals and organic compounds has a number of features in common with hydrogen embrittlement. Therefore, it seems appropriate to discuss some of these similarities. The similarity of the relationship between applied stress and time to failure is illustrated in Fig. 7.1.

Rostocker et al.[1] rightly emphasized the basic similarity of this type of delayed failure to that encountered in static loading of hydrogen embrittled high strength steel or titanium. Typical in this regard are results also obtained with steel wetted with molten indium, zinc, tellurium and particularly, cadmium.

It is interesting to note that the decrease of the surface energy term for iron, wetted by lithium is of the same magnitude as Petch[2] found in his studies with hydrogen. As in the case of hydrogen adsorption, the magnitude of surface energy reduction by the wetting is sufficient to produce significant reduction in ductility. Both hydrogen and molten lithium produce embrittlement of approximately the same magnitude[3]. Moreover, liquid metal embrittlement is similar to hydrogen embrittlement in that it is not restricted to one crystallographic structure, and the degree of embrittlement increases with increasing strength of the metal substrate.

Also, as can be seen from Fig. 7.2, the small but significant reduction in fatigue strength for mercury coated specimens[4], strongly resembles the decreased fatigue strength and limit of notched specimens, hydrogen embrittled by cyanide cadmium plating[5] (see Chapter 4).

Rostocker[1] emphasized that the ability of liquid metal wetting to cause failure under static loading conditions must be regarded to be of fundamental importance. Liquid metal embrittlement resembles hydrogen embrittlement and stress corrosion cracking and there is strong reason to assume that all three of these phenomena are similar in nature.

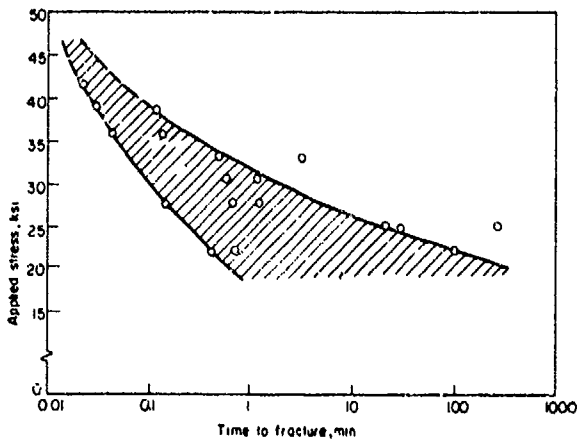

Fig. 7.1 – Delayed failure behavior of statically loaded AISI 4130 steel (R_C-44) wetted with molten lithium at 200 C.

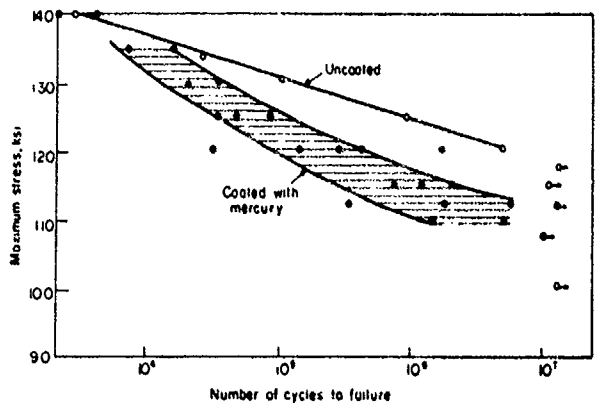

Fig. 7.2 – Fracture behavior of mercury coated AISI 4340 steel (190 ksi) fatigued in axial loading (stress ratio 0.75).

PRECEDING PAGE BLANK

7.2 EMBRITTLEMENT BY LIQUID ORGANIC COMPOUNDS

It has been established that certain organic liquid compounds induce time dependent fracture in high strength steels. Some results obtained by Steigerwald[6] are pictured in the bar diagram, Fig. 7.3. The fracture times were considerably longer in the organic compounds and in dry air than those in distilled water or in the recording ink (an aqueous solution). Although no direct correlation is apparent between the nature of the environment and the failure time, specimens immersed in closed ring structure compounds of low dielectric constants are capable of sustaining the applied load for the longest time period. Taking into consideration the remarkable effectiveness of distilled water in inducing delayed failure, it cannot be decided whether the organic liquid itself is involved in the control of crack formation or the presence of water in the compounds which are hygroscopic.

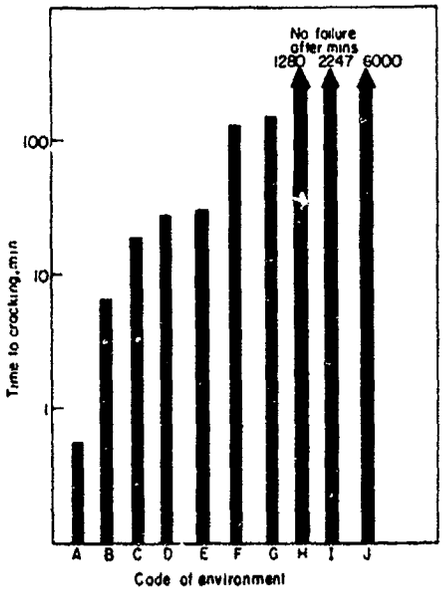

Environment

A	–	Recording ink	F	–	Acetone
B	–	Distilled water	G	–	Lubricating oil
C	–	Amyl alcohol	H	–	Carbon Tetrachloride
D	–	Butyl alcohol	I	–	Benzene
E	–	Butyl acetate	J	–	Dry air

Fig. 7.3 – Effect of various environments (liquids and dry air) on delayed failure of 300-M (295 ksi) steel specimens, notched, precracked and loaded to 75% of NTS.

7.3 HYDROGEN EMBRITTLEMENT IN AQUEOUS ENVIRONMENTS

This problem has been studied thoroughly by Hanna, Troiano, and Steigerwald[7]. Steigerwald[8, 9], used a sharp center-notched precracked tension specimen fabricated of AISI 4340 and 300-M low alloy martensitic steels, heat treated to a high strength level. After heat treatment, a minimum of 0.006 in. was ground off each side of the specimen to remove any decarburized layer, and after tempering, oxides were removed by a light sand blast. The notch was kept continuously wetted by the liquid from an adjacent reservoir.

The effects of distilled water and some other aqueous solutions on the delayed failure characteristics of the steels are depicted in a more detailed manner in Fig. 7.4.

The curves show the relationship of the applied stress versus the time to failure. The stress at the crack tip greatly exceeds the applied stress since the fatigue precrack acts as a very severe stress riser. The notched tensile strength plotted at zero time corresponds to the notched strength obtained in a conventional tension test conducted at a crosshead speed of 0.05 in/min. The results in Fig. 7.4 indicate that both recording ink and distilled water produced a considerable variation in delayed failure. The most noteworthy aspect, however, is the relatively rapid rate at

which the crack propagated in the presence of the liquid environment. At a nominal stress of 55 ksi (300-M steel) failure occurred in less than 1 minute when recording ink surrounded the crack.

The results obtained with the recording ink deserve attention, because as mentioned in an earlier chapter, ink staining techniques are employed to determine critical crack lengths. Although this technique does not alter values of the fracture toughness, it should be used with caution when applied to determine energy release rates for the conditions governing crack growth. It should always be kept in mind that such staining solutions do influence the stress necessary to the growth of a crack, because they themselves induce delayed failure.

Fig. 7.5 shows delayed failure curves for AISI 4340 and 300-M steels. The 300-M steel was used at two strength levels, 226 ksi (1025 F temper) and 187 ksi (1150 F temper). The range of stress over which delayed failure occurred was considerably greater for the material tempered at 1025 F than that tempered at 1150 F. The shape of the delayed failure curve for AISI 4340 steel differs markedly from that for the 300-M steel.

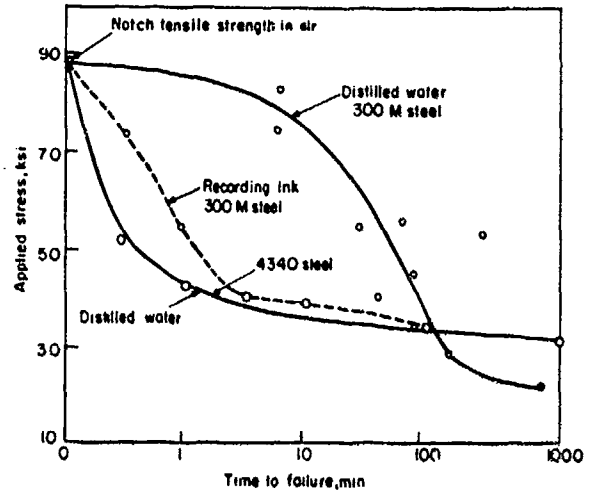

Fig. 7.4 – Delayed failure times for 300-M (295 ksi) and AISI 4340 (205 ksi) steels. Center notched precracked thin specimens stressed in liquid environments.

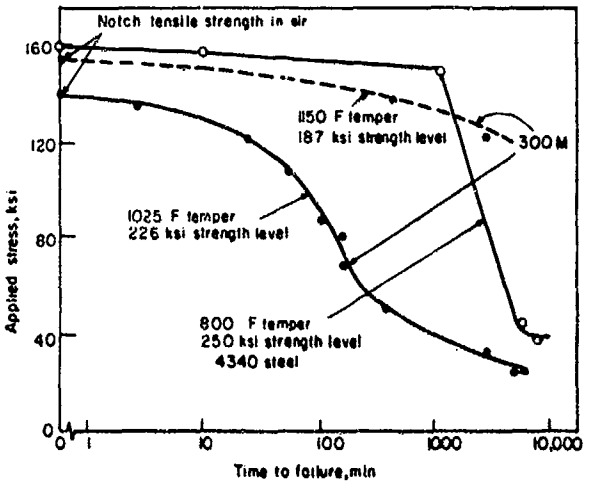

Fig. 7.5 – Delayed failure curves for AISI 4340 and 300-M steels in distilled water. Tests conducted with thin center notched precracked specimens.

The delayed failure behavior of H-11 steel exposed to distilled water is presented in Fig. 7.6. The general nature of the fracture behavior of this steel is similar to that of the 300-M steel.

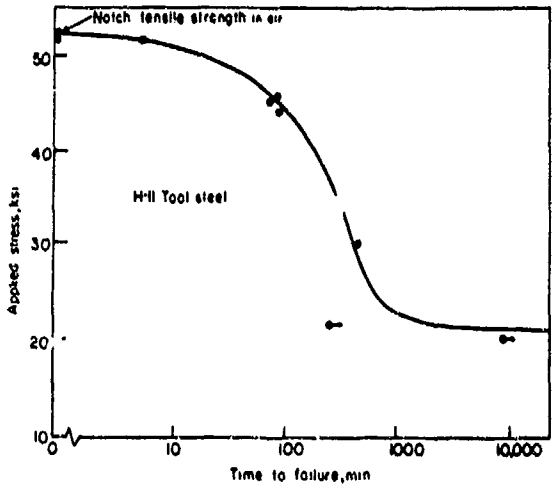

Fig. 7.6 – Delayed failure of H-11 tool steel (295 ksi) in distilled water. Thin center notched precracked specimens.

Fig. 7.7, depicts delayed failure behavior in distilled water for AISI 4340 and 300M steels at different temperatures. The decreased time to failure with increasing temperature is clearly seen.

Test data presented in Fig. 7.8 show the effects of a dry and a humid gas atmosphere and that of distilled water and ambient air. It is evident that gaseous environments containing water vapor also exert a strong embrittling effect on high strength steels.

Although the dew points of air and wet argon are different (35 F and 45 F, respectively), the delayed failure behavior of both steels in these atmospheres is almost the same as in distilled water. However, the delayed failure curve in dry argon (dew point - 11 F) is quite different from those obtained in the other media. In contrast to the lower critical stress obtained for experiments in dry argon, those for the other media are identical and considerably lower. No corrosion products were visible on the exposed surfaces.

The results clearly demonstrate the marked effect of moisture on the delayed failure behavior of high strength steels. Moreover, Hanna et. al.[7] succeeded in greatly decreasing the fracture time by the application of a cathodic potential, and the addition of the embrittlement accelerator, arsenic trioxide, to the distilled water. The phenomena discussed above indicate that the rate controlling process of embrittlement in distilled water is absorption of cathodically generated hydrogen.

Fig. 7.9 is instructive because it shows the effect of strength level on crack growth rate measured by resistance change. The steel at the lower strength level exhibits a much slower crack growth rate and distinct discontinuous growth with temporary stops several minutes long.

Yamaoka and Wranglen[10] conducted a detailed electrochemical study of processes associated with the cracking of stressed high strength, low alloy martensitic steel wires in conductivity water at room temperature. The wires, having a composition very similar to AISI 4340 steel, were subjected to sustained tensile loading. Data indicated that time to fracture is reduced by more than one power of ten by immersion in water as compared with tests in dry air. They observed that addition of an embrittlement accelerator, in this case sodium sulfide, reduced the fracture time by another factor of ten which agrees with Steigerwald's findings described above. Application of a cathodic current of about 1 mA/cm^2 reduced the fracture life by about two powers of ten. Therefore, it was concluded that hydrogen embrittlement is operative in the delayed fracture of steels subjected to static loading in high purity water. Conditions faborable for the generation of hydrogen were also clearly indicated by a slow change of the potential of the stressed wire to a potential more cathodic than the reversible hydrogen potential calculated for the pH of the water used in embrittlement studies.

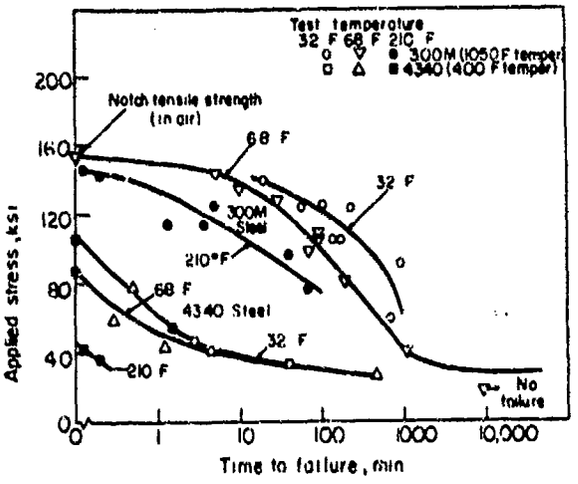

Fig. 7.7 – Decrease in failure time with increasing temperature in distilled water for AISI 4340 and 300M steels. Center notched precracked thick sheet specimens used for tests.

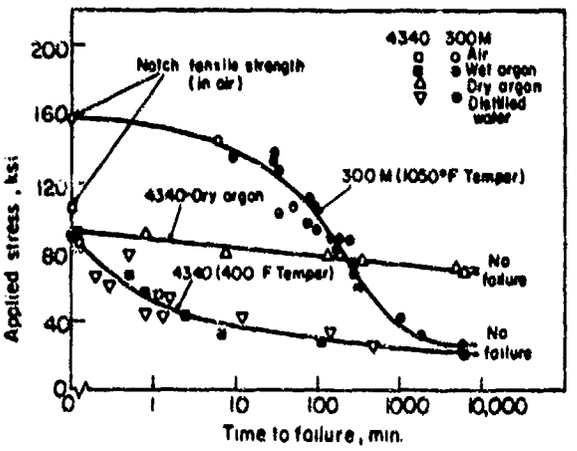

Fig. 7.8 – A comparison of delayed failure data for high strength steels subjected to dry and wet argon and distilled water environments at ambient temperature. Thick center notched precracked specimens.

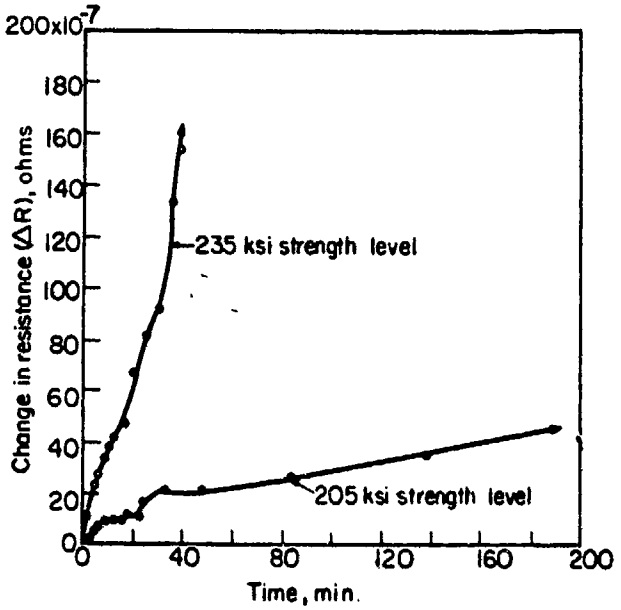

Fig. 7.9 – Effect of strength level on crack propagation rate in AISI 4340 steel (200 ksi) in distilled water at ambient temperature. Applied stress 160 ksi, center notched cylindrical specimens. Electrical resistivity method used for measurements.

Brittle failures observed during hydrostatic tests with tap water of high strength solid fuel rocket chambers are of great practical interest. The tests were made in full size cylindrical missile casing vessels, 6 ft. long with a diameter of 3 ft. 4 in., and fabricated of H-11 vacuum melted steel with a hardness of R_C 50-51. Tests were also performed on sub-size test vessels (6 sq. ft. interior area). The hydrogen content of the vessel steel before fabrication of the cases was 1.2 - ± 0.1 ppm. Full scale size vessels failed on hydrostatic testing at a stress lower than they should withstand. All of the sub-size vessels, which displayed no weld or other defects, also failed. Cracks had clearly originated in the parent metal from spots in the vessels on their inside surfaces and there was clear evidence of pitting corrosion. The failures occurring in the sub-size vessels, had features typical of a hydrogen initiated fracture. Shank et. al.[11] made interesting speculations on the embrittlement controlling mechanism. They surmised that galvanic action, a prerequisite for local hydrogen generation, is a factor in the failures originating in the parent metal in both types of vessels. They considered that the anodic areas are represented by the pits formed at different locations. Because of the small total area of the pits, the ratio of cathode to anode area is high, and thus, the current density at the anodes would be high also. The cathodic current density would be greatest in the region immediately surrounding the anodes. Hydrogen would be generated at these locations and permeate into the steel. The pitted areas provide points of considerable stress concentration. The maximum regions of triaxiality of stress would be just adjacent to the location of the pits and the embrittling hydrogen charged into the steel by galvanic action would diffuse to these regions, in accordance with the mechanism suggested by Troiano. Ordinarily, such galvanic processes do not produce very much hydrogen. The overall hydrogen level could be very small, but the local hydrogen concentration around the pits should be very high. Cracks should grow in size from the point of maximum triaxiality bordering the pits and after attainment of the necessary crack length, catastrophic failure would occur.

The above examples show clearly that essentially the same hydrogen generating corrosion mechanism is responsible for triggering delayed cracking in tap water as in distilled water. High purity distilled water is a poor electrolytic conductor and therefore, a local cell mechanism, as a source for hydrogen generation, would hardly be expected. Steigerwald[8] did not specify the pH and conductivity of the distilled water used in his experiments. Thus, making the very probable assumption that the water was in equilibrium with the ambient atmosphere, the pH must have been about 5.8 due to dissolved CO_2, which makes the water conductive. This assumption is strongly supported by Steigerwald's observations for solutions where the pH was varied from 4.8 to 9.0 by buffer additions. He found practically the same time dependent fracture behavior in these solutions with good conductivity as in the distilled water he used.

Cracks were found in ultra high strength AISI 4340 steel, exposed in boiling 3.5 percent NaCl solution[12]. Logan et al., used a hollow tension specimen developed by NBS. Under an applied stress of 200 ksi, the specimens failed in 80 to 600 minutes in a brittle fashion. Light and electron micrographs through the fracture and of the fractured surface, respectively showed that the fracture had originated within the wall of the tube and not at its surface. Analysis of the gases in the interior of the tube showed hydrogen to be present in all cases. These investigators inferred that failure of the high strength steel was caused by hydrogen embrittlement. Because of the fact that under room temperature conditions evidence of hydrogen diffusion associated with brittle failure was also obtained, it appears justified to conclude that the hydrogen generation was again the result of the corrosive action of the aggressive sodium chloride solution on the steel.

7.4 HYDROGEN EMBRITTLEMENT IN HEAVY WATER

Wood[13] made a comparative study of hydrogen and deuterium embrittlement. Small ring specimens were subjected to slow bending in a so called "crushing test". Embrittlement was generally expressed by the deformation at fracture, or percent decrease in deformation (corresponding to percent decrease in fracture height). This test in essence is a constant rate bend test. Thus, it was not discussed separately in the chapter dealing with testing. The ring specimen is subjected to compression and finally "crushing" between flat anvils.

In Wood's investigation, embrittlement was produced by cathodic charging or electroplating. Although plating embrittlement will be discussed in detail in a special section, it is taken into consideration here for the purpose of comparison of the action of hydrogen with deuterium.

The plating bath was made from hydrogen free compounds with D_2O as the solvent. To avoid pick up of water, it was imperative to carry out the handling, pouring and electrolysis of all D_2O solutions in an inert atmosphere chamber containing dry helium. The effect of plating time on the magnitude of the embrittlement produced by cadmium plating from a cyanide bath is pictured in Fig. 7.10. The resulting embrittlement in steel is less for cadmium plating from a "D_2O bath" than from a "H_2O bath".

Figure 7.11 also shows that the embrittlement caused by deuterium is less than that caused by hydrogen when chromium and copper are plated.

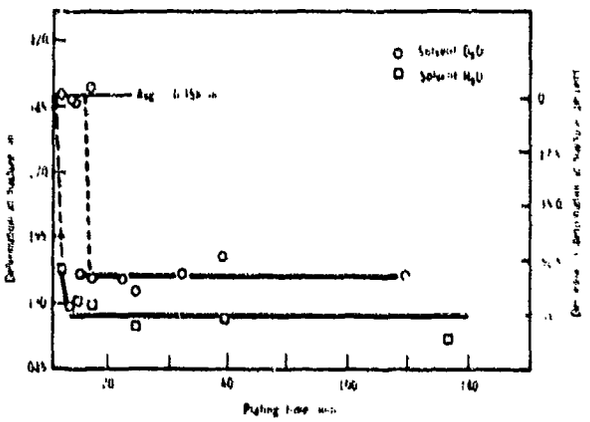

Fig. 7.10 – Comparison of the effect of plating times for D_2O and H_2O cadmium plating baths on deformation of AISI 4340 steel rings, 260-280 ksi.

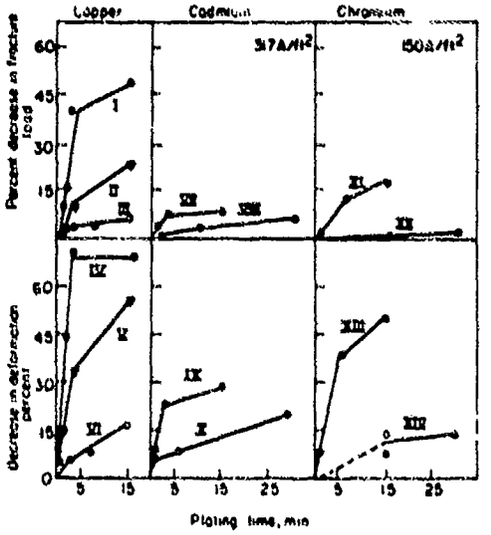

Fig. 7.11 – Effect of plating time on percent decrease in fracture load or percent decrease in fracture height (deformation) for specimens plated with Cu and Cd from cyanide baths and Cr from a conventional chromic acid bath for H_2O and D_2O plating bath solvents.
NOTE: Copper curves – I, IV - 34.4 A/ft²
II, III, IV, VI - 17.2 A/ft²

Wood found that the electroplating processes introduced more deuterium into the steel than hydrogen (analysis by high temperature vacuum extraction), and speculated that the differences between the action of hydrogen and deuterium during the process of embrittlement are due to differences in their physical properties. (Electrolytically introduced deuterium diffuses through steel more slowly than "light" hydrogen).

Differences in embrittlement resulting from charging with hydrogen and deuterium are clearly pictured in Fig. 7.12. Data obtained by Mahorter and Jankowsky [14] show that there is a decrease in ductility until very low strain rates are reached. Then the ductility for the hydrogen charged specimens increases while the ductility for the deuterium charged specimens continues to decrease (in the limits of the experimental testing). The reason for the apparent anomally, i.e., the increase in ductility, is that it is no longer controlled by the strain rate but by the higher out-diffusion rate of hydrogen.

As mentioned previously lower temperatures lessen the embrittlement effect of hydrogen, which is the result of the decrease in the diffusion rate of hydrogen. Fig. 7.13 is similar with respect to the suppressed inflection point (Fig. 7.12) and indirectly supports the assumption that deuterium has a slower diffusion rate in steel than hydrogen. The reason for this is the presence of the neutron in the deuterium nucleus [15].

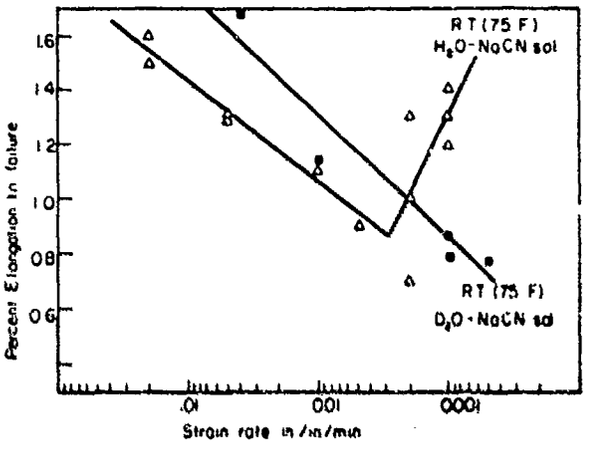

Fig. 7.12 – A comparision of the effect of hydrogen and deuterium and strain rate on tensile ductility at room temperature. Precharged at 20 A/ft²

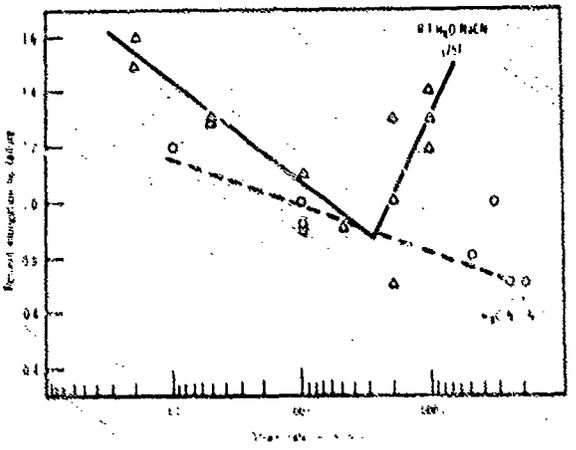

Fig. 7.13 – Effect of testing temperature and strain rate on the tensile ductility of AISI 4340 steel specimen (260-280 ksi) after charging (20 A/ft²) in an aqueous NaCN solution

As discussed in the chapter dealing with hydrogen determinations, the correlation of "total" hydrogen with loss in ductility is problematic and therefore, the disagreement between hydrogen content and loss in ductility found by Wood, cannot be construed as being inconsistent with the results of the mechanical measurements.

7.5 EMBRITTLING EFFECT OF HYDROGEN ON NEUTRON IRRADIATED REACTOR STEELS

7.5.1 HYDROGEN GENERATION IN A PRESSURIZED WATER REACTOR SYSTEM

Three reactions which represent potential hydrogen sources in a pressurized water reactor system are:

- Dissociation of hydrogen from water at the steel vessel inner surface.
- Radiolytic decomposition of water
- Corrosion reactions

Reaction 1 - According to Harries and Broomfield [16] a small fraction of hydrogen exists in an atomic form in a pressurized water reactor. These hydrogen atoms produced by a catalytic decomposition of water on the steel surface, may be adsorbed on and diffuse through the steel wall at the temperature and pressure conditions of operation of the reactor system.

Reaction 2 - Numerous studies[17] have been made in order to elucidate the "primary hydrogen atom yield" in the radiolysis of aqueous solutions. The following reaction of the solvated proton in the regions of high ionization density (rapid recombination of solvated protons and electrons, respectively) is considered possible and could be largely responsible for the primary hydrogen atom yield.

$$---e_0^- + H_3O^+ \rightleftharpoons H + H_2O \qquad (7.1)$$

However, Harries and Broomfield emphasized that in a pressurized reactor system, operating at 250 to 315 C with purified water, all the available evidence suggests the probability of the occurence of radiolytic reactions to be very remote.

Reaction 3 - As will be discussed in greater detail in a later chapter, mild and low alloy steels may react with high temperature high pressure water to produce magnetite and hydrogen according to the reaction:

$$--- 3Fe + 4H_2O \rightleftharpoons Fe_3O_4 + 8H \qquad (7.2)$$

The generated hydrogen atoms, may, (a) all recombine to form molecules in the water and then distribute themselves between the water and the available vapor space, (b) all diffuse through the steel in the nascent form and then some recombine to form molecular hydrogen.

Harries and Broomfield calculated (Eq. 7.2) hydrogen equilibrium concentrations ranging from 0.1 up to 1.3 ppm for different water temperatures and vessel wall thicknesses. In consideration of the work by Tackett, Brown and Esper[18], the calculations were based on a corrosion rate of 75 mdm* corresponding to a hydrogen evolution rate of 75 x 10^{-5} cm^3/hour (STP). Therefore, it may be assummed that the corrosion reaction furnishes most of the hydrogen involved in the embrittling process.

Finally, it is worthwhile mentioning that an analysis of water at the Westinghouse Yankee plant indicates a similar hydrogen concentration range during the operation of this type of reactor, and a higher range after prolonged shut down[19]. The analysis presented above, reveals the probability of formation of atomic hydrogen under conditions prevailing in a pressurized water reactor system.

The embrittlement behavior of an irradiated reactor steel, when charged with hydrogen, was studied thoroughly by Rossin, Blewitt and Troiano[20]. The pearlitic, tough and ductile 212-B steel was selected for this study because it is used extensively for boiling water or pressurized water nuclear reactors. Neutron radiation hardens this steel, raises its yield and tensile strength and makes it brittle at room temperature. The effect of increased yield strength on delayed fracture might well be the same if the hardening were caused by irradiation rather than by appropriate heat treatments. The purpose of the investigation was to determine whether or not this steel would become susceptible to hydrogen embrittlement after irradiation. This type of failure would have serious reactor safety implications.

Notched specimens were exposed to neutron radiation high enough to embrittle the pressure vessel steel, and the delayed failure characteristics of the irradiated, hydrogen charged steel were determined. The encapsulated specimens were irradiated in a CP-5 reactor to 3 x 10^{19} RDU in which the NDT was raised to 100 C. The most intense cathodic charging condition selected was 100 mA/in^2 for 20 hours in a 4 percent sulfuric acid solution poisoned with sodium arsenate (disregarding the notch, the gage area of the subsize tension specimen was about 1 square inch).

Despite the extreme conditions of hydrogen charging and considerable irradiation hardening, the reduction in the lower critical stress was not significant. Since irradiation increases the yield, tensile and notched tensile strength (NTS), the loss in NTS due to hydrogen does not even bring this parameter back to the unirradiated level (See Fig. 7.14). The net effect is still one of strengthening. Thus, the necessary conditions for catastrophic delayed failure do not exist in 212B reactor pressure vessel steel. About 8 ppm of hydrogen (determined by outgassing at 150 C) was found in the charged specimens. This amount is far more than necessary for embrittling ultra high strength steel (e.g. AISI 4340 steel) and is also much greater than one would expect to find in practice as a result of any aqueous corrosion reaction. The condition of heavy charging was chosen to determine how irradiated steel would perform with a high hydrogen content. Apparently, the critical concentration for hydrogen cracking of this relatively low strength type steel must be much higher than for the high strength steels, if it can be embrittled at all. For higher strength reactor steels the embrittlement behavior may be quite different.

*milligrams/square decimeter/month

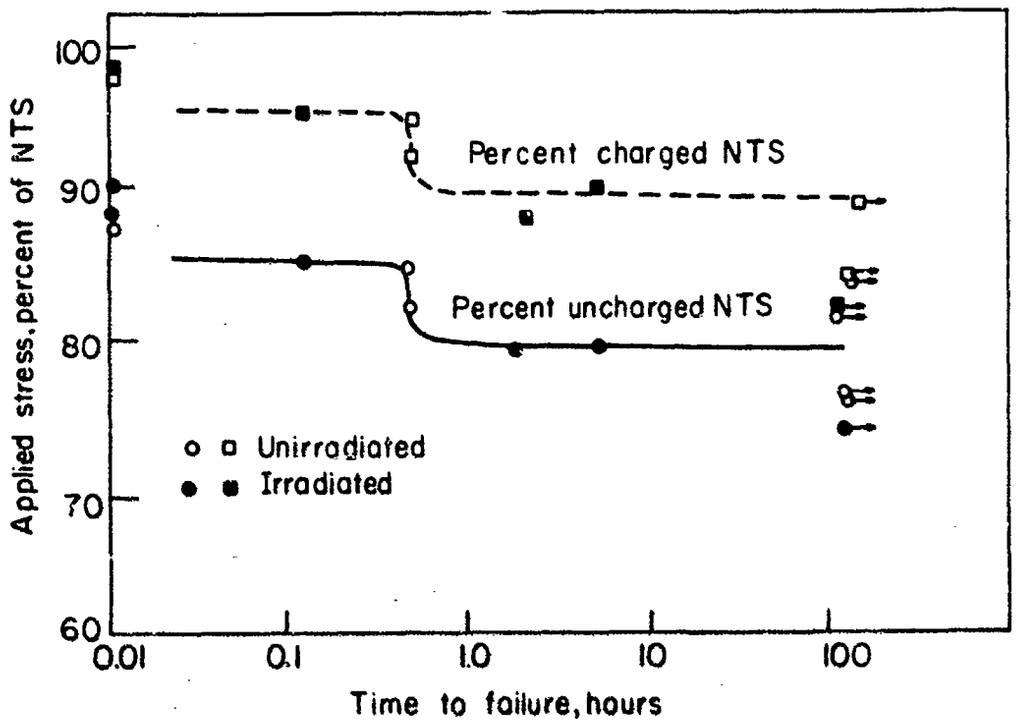

Fig. 7.14 – Behavior of uncharged and strongly hydrogen charged, irradiated and unirradiated 212-B reactor steel in the range of delayed failure. Radiation conditions, 3 x 10^{19} RDU

The aforementioned results are in excellent agreement with those obtained by Harries[21] at Harwell on an irradiated 1 percent chromium, 0.5 percent molybdenum pressure vessel steel. Smooth tension specimens were exposed for 107 days, one group in contact and another isolated from the water at 250 C in the "out of pile" and "in-pile" sections, respectively of a high pressure water loop. The purpose of the investigation was to study whether or not exposure under pressure water reactor operating conditions at 250 C (a) produced gross structural defects such as blisters or cracks due to increased hydrogen absorption in the steel, or (b) affected kinetics of the hydrogen-carbon reaction in the steel in such a way that hydrogen attack could occur. Hydrogen induced structural defects and attack would then be manifested as reduction in tensile ductility. The specimens were tested at a cross head speed of 0.02 in/min. five hours after shut down of the reactor. The irradiation was about 1.0×10^{19} n/cm^2 (fission). The tensile strengths were considerably increased, and it was, therefore, concluded that no attack or structural defects were produced.

7.6 THE EFFECT OF HYDROSTATIC PRESSURE

In a recent study dealing with the effect of hydrostatic pressure (up to 8250 psig) on hydrogen solubility in steel, Nanis and DeLuccia[22], used a permeation method similar to that of Devanathan, Stachurski and Beck. This work was done to assess the effect of electrolytic hydrogen on corrosion reactions at a pressure of 8250 psig, which corresponds roughly to a depth of 18,400 feet.

Nanis and DeLuccia[22] found a marked increase in hydrogen solubility (permeation current) with increasing pressure. Results plotted in Fig. 7.15 are significant, because they demonstrated pressure/solubility relationship for hydrogen in Armco iron serves as an important index of embrittlement problems, which may be encountered in the ocean at great depths. If the behavior of Armco iron may be taken as indicative of that of steel in general, it should be expected that hydrogen solubility will be enhanced with increasing pressure, corresponding to ocean depths beyond the 14,000 foot mark.

The authors of this remarkable report determined that there is no effect of the hydrostatic pressure on hydrogen diffusivity, and that the hydrogen solubility is proportional to the pressure at least up to 6000 psi. The increased solubility of hydrogen in steel at elevated pressures and comparatively low temperatures (21 C and lower) necessitates an increased concern for the role of hydrogen in environmental cracking of high strength steels destined to be used in the deep ocean environment.

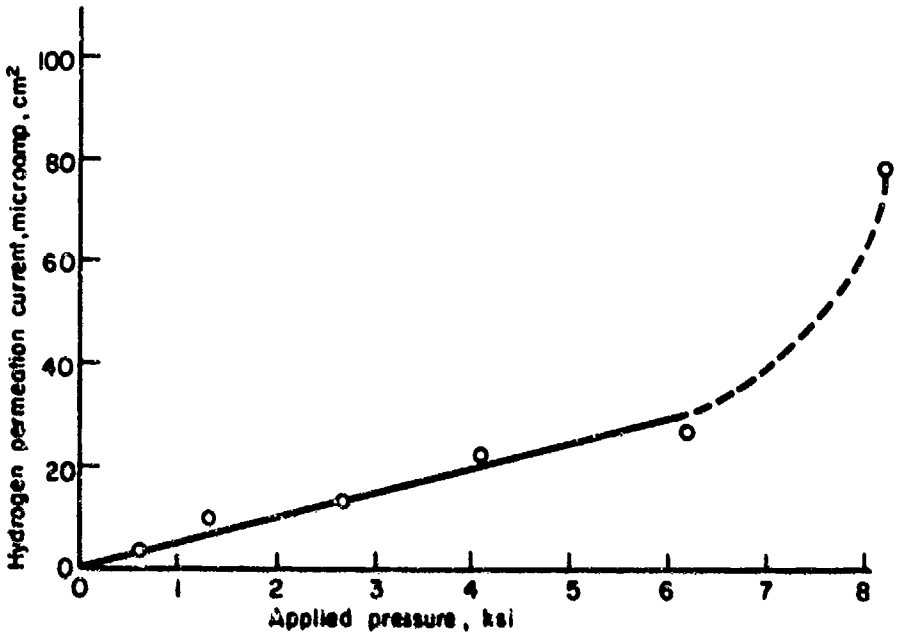

Fig. 7.16 – Effect of hydrostatic pressure on permeation (solubility) of hydrogen in Armco iron. Charged in 0.10N H_2SO_4 + 0.001N HCl at 21 C.

REFERENCES

[1] W. Rostocker, J. M. McCaughey and H. Markus, *"Embrittlement by Liquid Metals"*, Reinhold Publishing Corp. New York, 1960.

[2] Petch, N. J. *Phil. Mag.*, **8** (1), pp. 186-190 (1956).

[3] Ref. [1], p. 65.

[4] ibid., p. 87.

[5] W. Beck, "Effect of Cathodic Charging and Cadmium Plating on the Fatigue Behavior of High Strength Steels", *Electrochem. Technol.*, **2**, pp. 74-78 (1964).

[6] E. A. Steigerwald, "Delayed Failure of High Strength Steel in Liquid Environments", *Proc. ASTM*, **60**, p. 758 (1960).

[7] G. L. Hanna, A. R. Troiano and E. A Steigerwald, "A Mechanism for the Embrittlement of High Strength Steels by Aqueous Environments", *Trans. ASM*, **57**, pp. 658-671 (1964).

[8] E. A. Steigerwald, "Delayed Failure of High Strength Steel in Liquid Environments", *Proc. ASTM*, **60**, pp. 750-760 (1960).

[9] E. A. Steigerwald, "Influence of Environment on Crack Propagation and Delayed Failure in High Strength Steels", Technical Documentary Rept. RTD-TDR-65-4225, pp. 23, 25 Air Force Materials Lab. (WPAFB) Dayton, Ohio (Jan. 1964).

[10] H. Yamaoka and G. Wranglen, "An Electrochemical Study of the Cracking of Stressed High Strength Low Alloy Martensitic Steels In Water", *Corrosion Science*, **6**, pp. 113-127 (1966).

[11] M. E. Shank, C. E. Spaeth, V. W. Cooke and J. E. Coyne, "Solid-Fuel Rocket Chambers for Operation at 240,000 psi and Above", *First Part, Metal Progress*, **76** (5) pp. 74-81 (Nov. 1959), *Second Part* **76**, (6) pp. 84-92 (Dec. 1959).

[12] H. L. Logan and J. W. D. Wehrung, "Embrittlement of High Strength AISI 4340 Steel in Boiling NaCl Solution", *Corrosion*, **22**, pp. 265-269 (1966).

[13] G. B. Wood, "A Study of Embrittlement of High Strength Steels by Hydrogen Isotopes", *J. Electrochem. Soc.* **110**, (8) pp. 867-885 (1965).

[14] R. G. Mahorter and E. J. Jankowsky, "An Investigation of the Mechanism of Hydrogen Embrittlement by the Use of Heavy Water", Report No. NAMC-AML (3)-R360FR 101 Naval Air Development Center, Warminster, Pa. (June 1962).

[15] P. M. S. Jones, R. Gibson, and F. H. Evans, "The Permeation and Diffusion of Hydrogen Isotopes Through Steel", Part 3, Maraging Steel, Atomic Weapons Res. Establishment, UK Atomic Energy Authority.

[16] D. R. Harries and G. H. Broomfield, "Hydrogen Embrittlement of Steel Pressure Vessels in Pressurized Water Reactor Systems", *J. of Nuclear Materials*, **9** (3) pp. 327-338 (1963).

[17] M. Chouragni and J. Sutton, "Origin of Primary Hydrogen Atom Yield in Radiolysis of Aqueous Solutions", *J. Physic. Chemistry*, **70**, pp. 2111-2120 (1966).

[18] E. E. Tackett, P. E. Brown and R. T. Esper, Westinghouse Rept. WAPD-LSR (C) - 134, (1955).

[19] "Evaluation of YANKEE Vessel Cladding Penetrations", Report WCAP-2855 Westinghouse Atomic Power Division, Pittsburg, Pa. (1965).

[20] A. D. Rossin, T. H. Blewitt and A. R. Troiano, "Hydrogen Embrittlement in Irradiated Steels", *Nuclear Engineering and Design*, **4**, pp. 446-458 (1966).

[21] D. R. Harries, "Hydrogen Embrittlement of a 1 wt %Cr, 0.5 wt % Mo Pressure Vessel Steel in High Pressure Water", *J. of Nuclear Materials*, **12** (1) pp. 24-29 (1964).

[22] L. Nanis and J. DeLuccia, "Effects of Hydrostatic Pressure on Electrolytic Hydrogen in Iron", *ASTM STP* **445** – Materials and the Deep Sea (1969).

CHAPTER 8

DELAYED CRACKING IN STEEL WELDMENTS

8.1 THE NATURE OF DEFECT FORMATION IN WELDMENTS

There is much confusion in the terminology of crack formation in weldments and therefore, the following definitions and explanations may be helpful. The terms "microcracks, microfissures and hairline cracks" may be used interchangeably and are used to characterize defects associated with high cooling rate of weld metal and hydrogen embrittlement. In general, these defects are located in transverse planes across which large tensile stresses are known to act during cooling of the weld[1-3].

The so-called "cold cracking" of steel weldments, the result of the presence of hydrogen[4] in either the weld or the heat affected zone, (HAZ), may be initiated at temperatures below 150 C and the cracks may propagate for several hours after reaching ambient temperature. The crack tends to propagate from a finite point of initiation, and its length is governed by the extent of the residual stress field. The stress direction has a decided influence upon the path of cracking while the degree of cracking is affected by the magnitude of the stress prevailing in the presence of hydrogen. Weldments with residual stresses below a critical level show no major cracking, but may contain a number of microcleavages[5].

According to Vaughan and deMorton[6], cold cracking in weld metal is similar to that produced by charging steel with hydrogen and is a cleavage failure. The crack itself appears to consist of elementary cleavages which can be identified with fissures which are formed continuously ahead of one another in a propagating crack.

In contrast to cold cracking, the phenomenon called "hot cracking" is produced by causes other than the accumulation of hydrogen, e.g., internal stress. However, when the hydrogen content and restraint of the weld metal are high enough, the hot cracks may propagate in a manner similar to cold cracks.

Cracking occuring in the HAZ of high tensile steel welded joints is frequently designated "underbead cracking" or "hardened zone cracking"[7]. It may occur shortly after the weld reaches room temperature or several hours afterwards. Weld metal cracking cannot be entirely separated from underbead cracking. There are cracks which start near the fusion line in the HAZ, but finish in the weld metal, whereas other specimens crack deep in the underbead area.

Crack susceptibility of a weld increases with the tensile strength of the steel. This tendency is also observed in the so-called "root cracking" which is frequently found in the first layer of a high strength steel weld of severe restraint[7]. It has been shown that the high hydrogen content of the weld metal is the most important factor promoting the formation of fissures[4]. Cracking may be either transgranular or intercolumnar. The transgranular fissures are the result of cleavage cracking induced by a combination of high hydrogen content and internal stresses. An example of such a fissure is shown in Fig. 8.1. The fissures are very narrow and sometimes are seen to pass through large spherical inclusions. They probably form below 200 C.

Intercolumnar fissures are also caused by the joint action of hydrogen and internal stresses, but they appear to be associated with non-metallic particles lying between the columnar cyrstals. An example of such a fissure is given in Fig. 8.2.

Fig. 8.1 – Transgranular hydrogen induced fissure in weld metal deposited from titania covered electrode without preheating (X500).

Fig. 8.2 – Intercolumnar hydrogen induced fissure in weld metal deposited from titania covered electrode without preheating (X500).

Considerable literature exists on the formation of fish eyes. Years ago, Zapffe and Sims[8, 9] reported the appearance of shiny white haloes (fish eyes) on weld metal fracture surfaces. They demonstrated that their appearance was associated with hydrogen in the weld metal, just as the appearance of flakes in wrought steels is due to hydrogen absorbed in steel. Later it was confirmed that fish eyes generally appear on fracture faces of weld metals deposited from high hydrogen electrodes. Heat treatments that remove hydrogen from the weld metal tend to eliminate fish eyes from the fracture faces. Recently, Boniszewski[10] used the electron microscope to resolve the details of their formation. The dark "pupil" was found to contain a large plate-like inclusion and the bright "iris" surrounding it, to consist of cleavage facets that have undergone some plastic deformation. However, it has been found that fish eyes are not necessarily always initiated by hydrogen[11].

8.2 SOURCES OF HYDROGEN

Hydrogen is introduced into weldments because molecular hydrogen and hydrogen bearing compounds (water vapor) dissociate into atomic hydrogen in the welding arc. Molten weld metal absorbs atomic hydrogen in proportion to the hydrogen partial pressure in the arc atomsphere[12].

The hydrogen content of the weld metal at the time of solidification[13] can be calculated rather accurately from the partial pressure of hydrogen in the arc atmosphere and Sieverts solubility data for 2820 F. There is good correlation between hydrogen content of the arc atmosphere and the extent of underbead cracking in a crack sensitive steel.

High hydrogen content in the core wire and moisture content in the electrode coating also promote the formation of fissures in beads[14, 15]. When a bead is deposited in a hydrogen bearing atmosphere, the hydrogen concentration in the molten pool is high. During the welding cycle, the HAZ is subjected to temperatures which greatly accelerate the diffusion of hydrogen. Although the time of holding at elevated temperature is limited by the nature of the welding cycle, it is reasonable to assume that it is of sufficient length for the HAZ metal near the fusion line to attain a hydrogen concentration almost equal to that found in the weld metal.

Interante and Stout[16], published data showing the effects of hydrogen in gas-metal arc weldments. Their tests were performed primarily with low chemistry HY 80 steel, which was subjected to various heat treatments. With a dry argon atmosphere, cracks were not produced even at the highest restraint. However, susceptibility to delayed cracking was found to increase with the hydrogen content of the welding atmosphere.

The quantity of hydrogen, in free or combined form, appears to act in a cumulative manner in their range of concentrations shown in Fig. 8.3, for a given restraint level. The time required to initiate a crack becomes shorter as the hydrogen content increases.

The HY 80 steel used for the study was annealed, spheroidized, normalized, tempered, spray quenched, tempered, and then spray quenched. Its nominal composition is 0.18% C, 0.18% Si, 0.30% Mn, 2.25% Ni and 1.22% Cr. Number 2 welding electrode contains 0.05% C, 1.32% Mn, 0.55% Si, 1.3% Ni, 0.43% Mo, 0.15% V, 0.5 ppm H, and low concentrations of P, S, N and O.

Fig. 8.4 shows the effect of water vapor on time to appearance of the first crack in an argon-hydrogen welding atmosphere. It is evident that the susceptibility to delayed cracking is increased by the presence of water vapor in the welding atmosphere. It was discovered that the restraint levels required to cause cracking are inverse functions of the hydrogen content (from 0 to 5 percent) of the welding atmosphere containing 1 percent water vapor[16].

8.3 TEST METHODS PROPOSED FOR THE DETERMINATION OF CRACKING SUSCEPTIBILITY OF STEEL WELDMENTS

Various approaches and types of specimens are used for quantitative evaluation of crack susceptibility. A description and salient features of the more important test procedures follow.

8.3.1 BEND TEST (SIX BEAD, THREE LAYER WELD ON PLATE)

This procedure is a comparatively simple bend test, which was developed in the laboratories of the McKay Company by DeLong[17]. The investigator stated that a slow bend test of a multipass weld is capable of simulating weakness in a weldment. The tests are easy to run and the specimen is inexpensive and requires no machining. The test results show distinct differences in hydrogen response under varied conditions. In addition, testing for hydrogen induced brittle failures can be made because the slow bend test allows adequate time for migration of hydrogen to areas of high stress concentrations located within the weld bead.

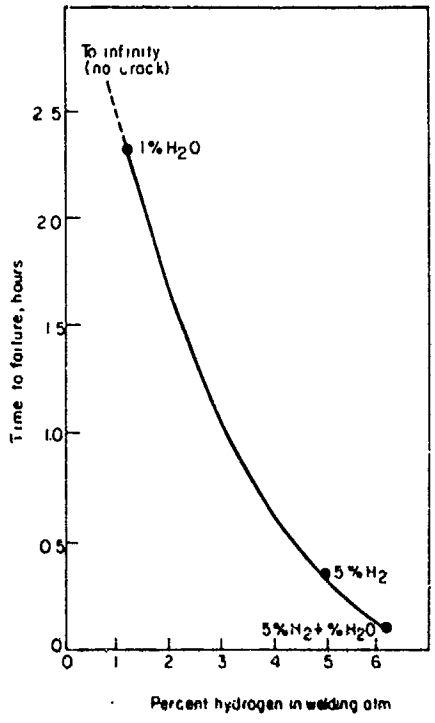

Fig. 8.3 – Effect of hydrogen concentration in welding atmosphere on the time delay of cracking in HY-80 steel (low chemistry) welded with alloy No. 2 electrodes at at a restraint level of 8 in.

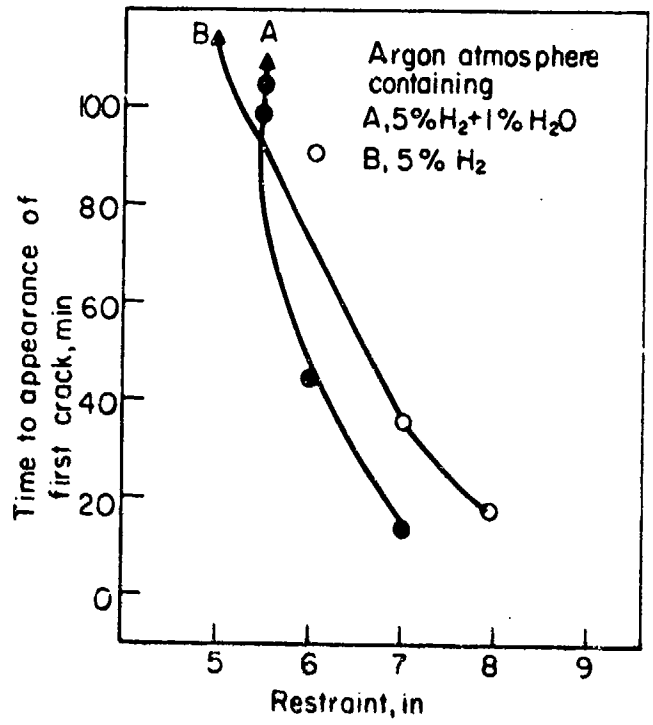

Fig. 8.4 – Effect of water vapor on time of appearance of the first crack in an argon-hydrogen welding atmosphere.

The test specimen consists of a six bead, three-layer weld on 1/2 or 5/8 in. thick plate which is 1-1/2 in. wide and about 8 in. long. Use of the test should be restricted to welds of 140 ksi minimum yield strength. There are three beads in the first layer, two in the second, and one in the third. A cross section of the test weldment is shown in Fig. 8.5.

A summary of the welding procedure is as follows:

1. Baseplate - HY 140 steel from USS
2. Preheat temperature - 200 F
3. Interpass temperature - 250 F
4. Welding time per bead - 55-70 seconds
5. Electrode size - 5/32 in.
6. Current - 160 amperes
7. Voltage - 24 volts
8. Bead Length - 6 to 6-1/2 in.
9. Typical time cycle for welding 6 beads with 250 F interpass is approximately 110 minutes.
10. Heat input of 37,500 joules per inch, ± 10%.

The specimen is bent in a power driven hydraulic press. The test procedure consists of 3 bending stages as shown in Fig. 8.5.

Stage 1 – the specimen is bent for approximately 14 seconds on a 14 in. radius mandrel which produces approximately 3 percent fiber elongation in the last bead weld.

Stage 2 – a second bending on a one in. radius mandrel to increase the fiber elongation to 15 to 20 percent in the mid-section of the weld.

Stage 3 – a final bending to complete fracture as a free bend (about 120 seconds).

According to DeLong in the bend test, plastic strain caused by stressing the test sample over the yield point and the complex high stresses associated with straining, act as a substitute for the complex high stresses of a cruciform or heavy restrained joint. Hydrogen significantly reduces the bend angle and fiber elongation in the bend test. If sufficient hydrogen is present to cause visible flaws, their formation during bending further reduces bend angle and fiber elongation.

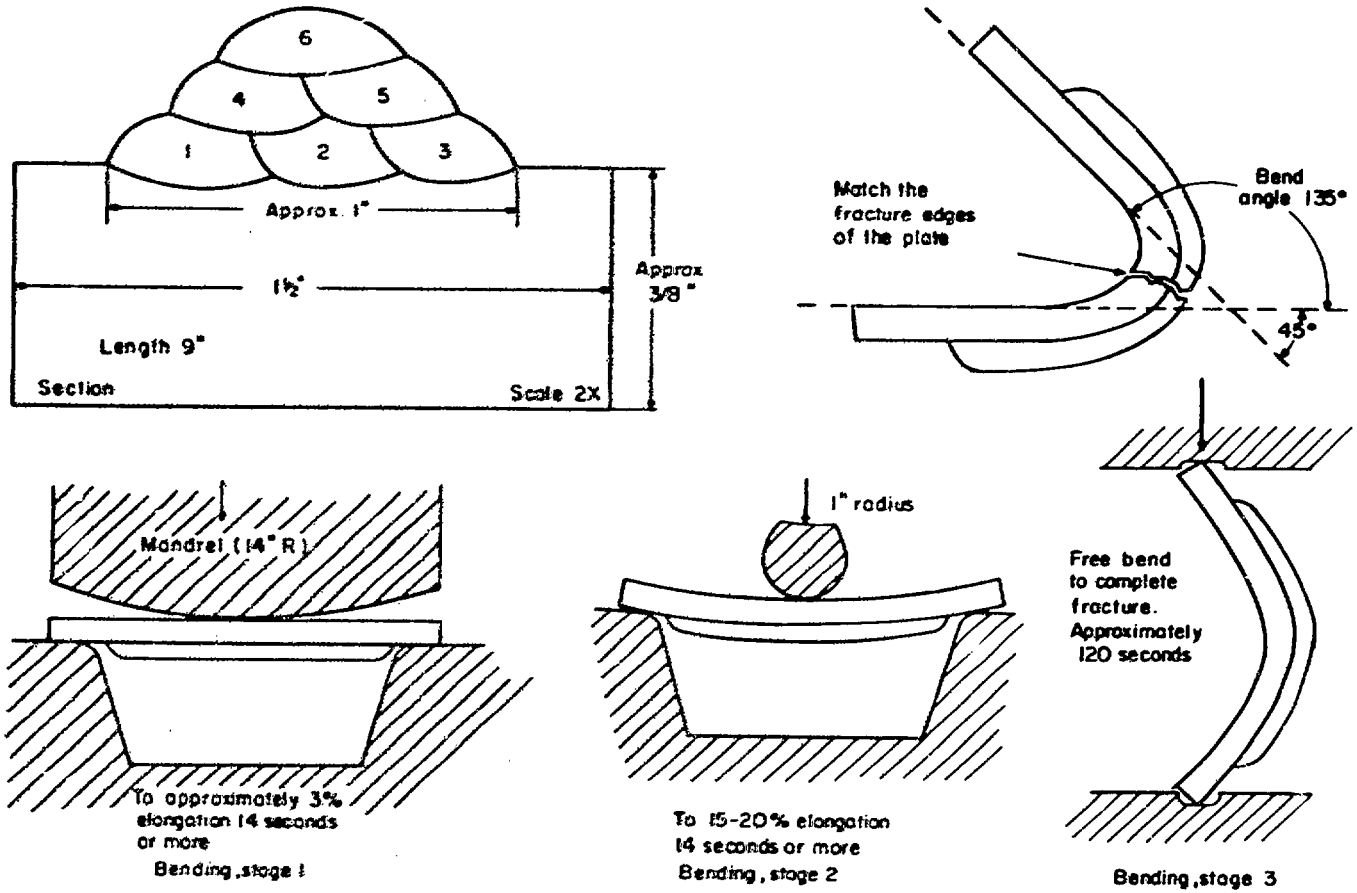

NOTES:

1. After welding, bends may be made hot (250 F in some cases), at room temperature, and after various aging times at room or elevated temperature.
2. Bend angle is based upon the angle where the final major fracture occurred through the plate, as shown by matching the fractured edges of the plate after full fracture (see illustration above).
3. Fiber elongation – measured on the top weld bead number six by means of scribe marks 1/2 in. apart on top surface. The top surface is finished with a belt sander before painting with layout ink and scribing.
4. Rockwell C hardnesses are taken on a cross section of the specimen in an area which has had a minimum bend (under 3% elongation. Six readings are taken on each side of the cross section on beads 4, 5, and 6, and averaged.

See text for welding and testing details.

Fig. 8.5 – Details of bend test for welded strips.

The bend test can be used to advantage in the following areas:

- Studies to determine effects of specific alloying elements and impurities, and allowable moisture and hydrogen levels;
- Studies to establish required preheat and interpass temperatures, and base material-weld metal compatibility;
- Specification testing requirements, where this type of test may be used as a substitute for the cruciform test;
- Quality control applications such as lot comparisons and the determination of the effect of exposure of electrodes to dehydration under various conditions.

8.3.2 BEND TEST (NOTCHED SPECIMEN)

This method is also based on bend testing however, the test specimen is notched. Flanigan, Bocarsky and McGuire [3] designed a specimen which consists of a bead-on-plate weld deposited along the major center line of a 4 in. x 9 in. x 3/4 in. blank [3]. The axis of the weld lies in the direction of rolling. The transverse notch (1/16 in. radius) is cut to a depth of 0.020 in. below the surface of the plate. The notch terminates in the weld metal at the center line of the weld.

During testing, the specimen is bent as a centrally loaded simple beam with the notched side in tension, at a cross head speed of 0.4 in./min. Bending is continued up to a sudden and complete fracture and the bend angle at fracture is a measure of ductility of the weld itself. It is necessary to render the material outside the weld so notch-sensitive that it becomes unable to withstand the propagation of cracks originating in the weld. This is achieved by using a sufficiently low test temperature.

8.3.3 LEHIGH RESTRAINT TEST (MECHANICAL GAGE MEASUREMENTS)

Although various test procedures are used for determining the effect of hydrogen on weld metal cracking, the Lehigh Restraint Test is considered one of the most significant [18, 19]. This sensitive test makes it possible to evaluate the effect on hydrogen cracking of weldments for a number of variables such as restraint, welding conditions, microstructure, steel composition, and preheating. The specimen design allows variations of the restraint against which the weld contracts during cooling. The problem of varying the restraint was solved by cutting slots into the sides and ends of the plate specimen. The degree of prevailing restraint is then determined by the distance between opposite slots. Additional details of the design can be found in Fig. 8.6.

The measurements of the constrictions across the weld groove and the crack formation in the deposited weld metal are of predominant interest. The contractions during welding and cracking are continuously indicated on dials of special mechanical gages, which are fastened to pins at the mid-point of the weld, one on top, and one at the bottom of the test plate. Cracking is readily picked up by these gages.

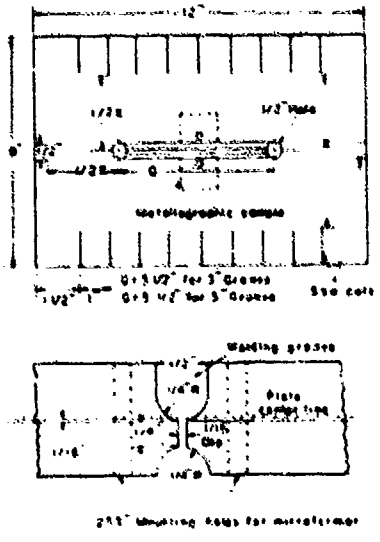

Fig. 8.6 – The Lehigh restraint test specimen.

8.3.4 RESTRAINT TEST (USING TRANSDUCER)

Interante and Stout[16] improved the technique of evaluating groove contraction, onset of cracking, and delayed cracking time using the restraint test. They employed a differential transformer type of transducer across the mid-point of the welding groove. On one side of the groove, the transducer is attached by a brass mount, fitted into a hole in the plate adjacent to the mid-point of the groove. The core inside the transducer is spring loaded against a brass bar similarly attached to the opposite side of the weld groove. This mount is fitted with an adjustment bolt by which a recorder pointer is set at the desired position on the recorder chart, and the output from the transducer fed into a multipoint recorder. Cracking response of multiple specimens may be evaluated by means of this improved technique. Cracking is indicated by a change in the output voltage and movements as small as 0.0001 in. can be recorded.

8.3.5 MODIFIED RESTRAINT TEST

The effects of a restraining force and hydrogen on root cracking of various high strength steel welds ranging in strength from 50 to 80 kg/mm^2 (71-114 ksi) have been studied also by Nakamura et al.[20] who developed a special tensile restraint cracking test procedure.

8.4 THE PROBLEM OF SAMPLING AND DETERMINATION OF HYDROGEN IN THE WELD METAL

The method of sampling may greatly affect the results of hydrogen determination in the weld deposit and is a very critical factor for achievement of accurate analyses[15]. This is clearly depicted in Fig. 8.7.

It is concluded from this figure that the quenched sample data are more truly representative of the hydrogen content of the liquid weld metal, than data from the air cooled specimens. The latter procedure might be more useful in an investigation of hydrogen retained under practical conditions of welding. A commonly accepted practice is to report the measured gas volume on the basis of 100 g deposited or fused metal.

Christensen[15] has discussed the possibility of estimating the fractional hydrogen losses by appropriate calculations, if it is inferred that the initial hydrogen distribution immediately after solidification is uniform.

It may be assumed that the average hydrogen content per unit mass of weld metal does not vary much from layer to layer. A very tentative assumption has been made also that single bead test data, reported on the basis of fused metal, are representative of the highest hydrogen content that can be expected in multilayer deposits from the same electrode.

Welding engineers frequently refer to three types of hydrogen[15]. A diffusible fraction which is released on prolonged storage at or close to room temperature, a residual fraction which is recovered at elevated temperatures, and the fixed hydrogen obtained by subtraction of the diffusible plus residual hydrogen from the total hydrogen. The vacuum fusion method is used for the analysis of total hydrogen. Frequently, the diffusible hydrogen is collected at about 45 C over a period of 48 hours. More specifically the diffusible hydrogen is defined as that volume of gas extracted at 45 C during a 48 hour period from a bead deposited on mild steel under specified conditions of welding. The residual hydrogen content may then be defined as that volume of gas completely extracted at 650C from samples. Previously degassed at temperatures which generally do not exceed 45C. However, Stout considers it necessary to extend the time of evolution of diffusible hydrogen to 72 hours[16].

Blake[21] adopted the following procedure of preparation of samples for analysis by the vacuum extraction technique. The original weld, cooled to -78 C, is first cut to remove 1 to 1-1/2 in. "run on" and "run off" pieces from each end. The weld deposit is then cut away from the parent plate while three jets of liquid carbon dioxide (CO_2) are sprayed over the weld. The sample is machined in a shaping machine and kept at a low temperature by two jets of liquid CO_2. After machining it is enveloped in solid CO_2 and taken to the laboratory for analysis. According to Blake, the entire machining and setting up process takes about 35 minutes.

It is rather difficult to establish limiting values for the critical hydrogen content necessary to impart mechanical damage to the weld metal. Generally speaking, increasing quantities of diffusible hydrogen in mild steel weld metal lead to decreasing ductility. Although it has been suggested[15] that microfissures develop on rapid cooling of weld metal containing more than 12 ml of hydrogen per 100 g of metal, a truly critical hydrogen content depends primarily on cooling rate and restraint. Flanigan[22] determined that after air cooling, the residual hydrogen content was about 4 ml/100 g, whereas specimens quenched immediately following completion of welding showed a hydrogen content of about 15 ml/100 g of weld metal.

Temporary loss of mechanical properties are associated with the diffusible fraction of hydrogen, which will be eventually released by ambient aging. Permanent defects such as weld metal fissures, under-bead and toe cracks,

as well as porosity, are frequently correlated with the fixed hydrogen. The possible role that the diffusible fraction may also play in these cases should be considered. It was also suggested that studies be made to determine the correlation between the total hydrogen content of the weld metal with the water content of the electrode coating[15]. Fig. 8.8 shows a plot of the total hydrogen versus the water content of the coating, determined by a combustion method.

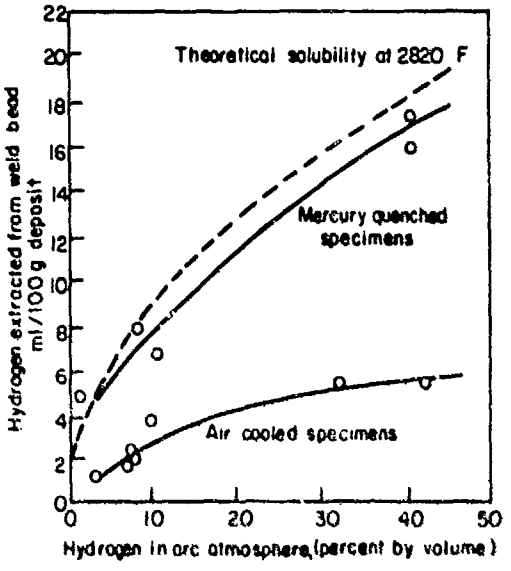

Fig. 8.7 – The effect of the method of sampling weld metal on accuracy of hydrogen determinations.

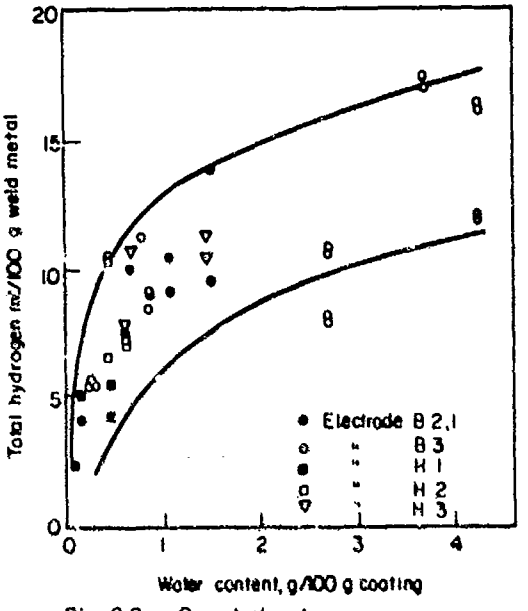

Fig. 8.8 – Correlation between water content of the welding electrode coating and total hydrogen content of the weld metal.

Data in the range of low water contents are residual values, that is, the electrodes have been dehydrated as recommended by the manufacturer, prior to testing. The higher levels represent electrodes in the as-delivered condition; water contents above 1 percent have been obtained by exposure to a humid atmosphere. The measured hydrogen contents are seen to scatter within a band of parabolic shape as would be expected from theoretical considerations. Any increase in the water content of the coating will result in a proportional increase of the partial pressure in the gas and water vapor ($H_2 + H_2O$) system. Based on the experimental evidence, the investigator concluded that the water content of the coating gives a reasonable indication of the total hydrogen content of the weld metal, if the data are applied to one group of electrodes. Fig. 8.8 is instructive in this context.

The relationship of underbead cracking to total and diffusible hydrogen contents are shown in Fig. 8.9. The extraction experiments were conducted with single bead deposited on a 1 in. plate of a carbon-manganese steel. As

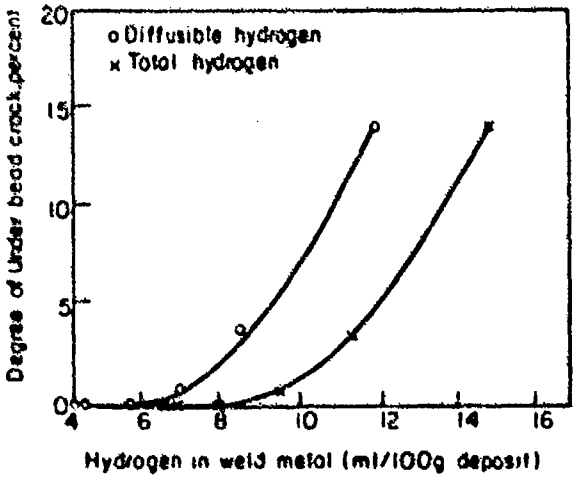

Fig. 8.9 – Example of relationship between under-bead cracking and weld metal hydrogen contents.

seen in the curves, cracking commences at a total hydrogen concentration above 8 ml/100 g of deposit. However, at the same concentration of diffusible hydrogen there is an increased tendency to cracking[23, 14].

8.4.1 THERMAL CONDUCTIVITY METHOD FOR DETERMINATION OF HYDROGEN IN WELDMENTS

A carrier gas-thermal conductivity method was used for the analysis of hydrogen in weldments[14, 23]. Hydrogen, which evolves from the weld at 600 C, is carried in a stream of pure argon gas, through a furnace and then to a catharometer cell. The catharometer consists of two matched heat sensing elements (thermistors), which are housed in two separate cells heated to the same temperature. The highly thermoconductive hydrogen carried from the weld absorbs heat from the thermistor when it is introduced into one of the cells and is recorded as an electrical signal. The volume of hydrogen that produces a certain decrease in heat content is then obtained from the differential electrical measurement, using the argon (hydrogen free cell) as the reference cell.

Tentative recommendations for the determination of the total hydrogen content on single beads of weld metal were issued by the International Institute of Welding[24]. A method based on hydrogen encapsulation has been suggested by British investigators[25].

8.5 MITIGATION OF EMBRITTLEMENT AND FISSURE FORMATION IN WELD METAL AND THE HAZ

8.5.1 EFFECT OF COOLING RATE AND PRE-HEAT AND POST-HEAT TREATMENTS

Preheat and interpass temperatures or both have a strong effect on cooling rate and the release of hydrogen from the weld. With slower cooling rate a greater proportion of hydrogen is released, which can appreciably help to prevent hydrogen cracking in critical situations.

This phenomenon confirmed by the seemingly strange observation that during summer, tension test results on welded specimens passed the requirements but failed consistently during the winter. This phenomenom can easily be related to a more complete dissipation of hydrogen in the summer due to slower cooling.

The effect of cooling rate on some mechanical properties of weld tensiles is vividly illustrated in Table 8.1. The results show that all five types of welds have considerably reduced ductility when cooled rapidly, although only two of them, E217 and E437, had shown fissuring in a single bead test[26].

It is of the utmost importance in welding practice to pay attention to the rate of cooling in the weld beads. When high cooling rates prevail, preheating up to 100 C is essential. Low ductility of rapidly cooled welds is frequently associated with minute intergranular cracks, however, embrittlement can occur without actual fissuring. Once regions of the weld are reduced in ductility, hydrogen can intensify embrittlement, especially when associated with macro-contractional stresses, as demonstrated by the hard zone cracking in the welding of high tensile steels. In this respect, it should be emphasized that rapid cooling, in addition to impeding the diffusion of hydrogen, may also raise the thermal stresses which affect the weld during cooling[27]. Sufficiently severe stresses along with a sufficient concentration of hydrogen will promote fissuring. On the other hand, welds with low hydrogen concentrations are immune to embrittlement even when quenched immediately after welding.

Increasing the time interval between completion of welding and quenching also decreases the extent of fissure formation, regardless of subsequent rapid cooling of the weld metal deposit[27]. Rollason[26] found that welds will fissure if cooled to 100 C in less than 1 minute but will not fissure at this temperature at a longer cooling time interval.

Two instructive examples of the effect of cooling rates follow.

Example 1

Stout et al.[10] attempted to eliminate cracking by accelerating the escape of hydrogen to the atmosphere by various postheating cycles applied to restraint specimens. Experimental results are plotted in Fig. 8.10 and are typical of postheating data. Postheating temperatures, required for complete elimination of delayed cracking, decrease with the elapsed time after completion of the welding procedure.

Example 2

Experimental results of bend tests showing the effect of rapid cooling on the ductility of single bead welds are compiled in Table 8.2. Single beads were deposited on 1/2 in. mild steel and tested by slow bending over a 1-1/2 in. mandril until they cracked. Specimens tested were either in the as-welded condition or heat treated for 1 hour at 650 C. Rapid cooling produced a decrease in ductility in the welds from all four types of electrodes. All welds except the molybdenum free E217 weld completely recovered on heat treatment. Only in the case of the E217 weld, low ductility was not associated with fissuring.

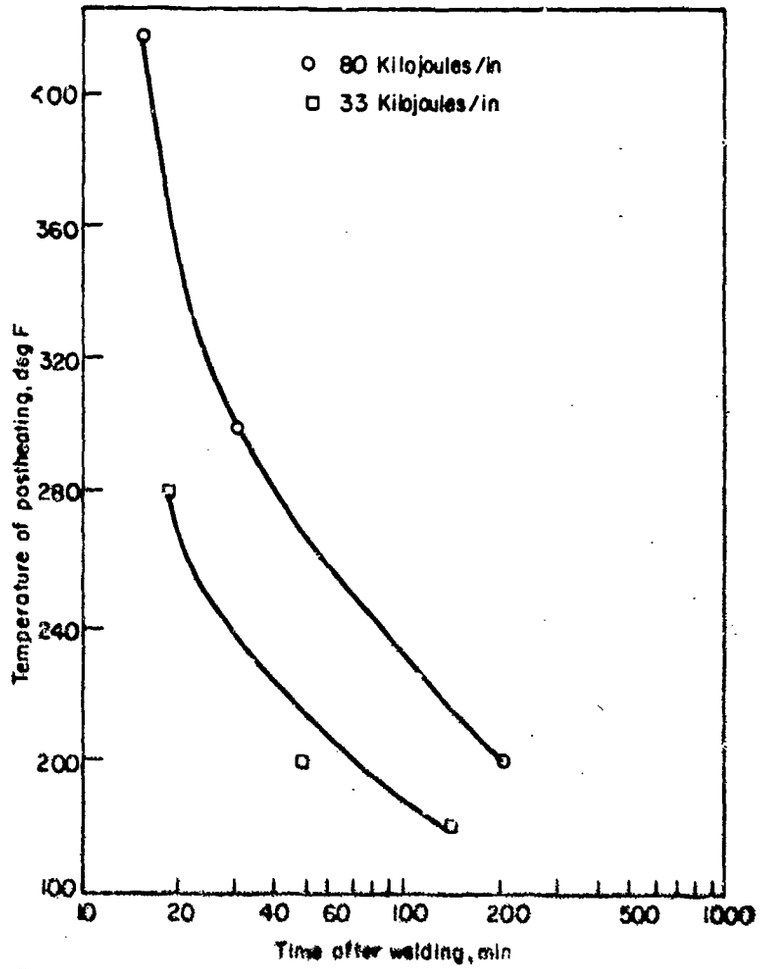

Fig. 8.10 – Time required to eliminate delayed cracking in T-1 steel, at different postheating temperatures immediately after welding. Steel was welded with allow No. 2 electrode at two heat input levels in argon with 1% H_2O.

8.5.2 MISCELLANEOUS METHODS FOR MITIGATION OF FISSURING

8.5.2.1 Dehydration of Welding Electrode Coating

As stated previously, the water content of an electrode coating is strongly involved in the control of the hydrogen concentration in the deposited weld metal[14]. Hence, dehydration of an electrode represents a method of increasing mechanical stability of the deposited weld metal or of the HAZ.

8.5.2.2 Dehydrogenation and Dehydration of The Welding Atmosphere

Crack free weld deposits have been obtained with commercially pure argon arc atmospheres[15]. See Section 8.2 for a detailed discussion of the role of hydrogen and water vapor in crack formation.

8.5.2.3 Reducing Impurities in Parent Metal

British investigations[28, 29] showed that high strength carbon-manganese steels, highly purified by a combination of basic electric melting and vacuum degassing, were strongly susceptible to hydrogen induced HAZ cracking, when sulfur was present in concentrations less than 0.01 percent. However, the removal of sulfur seems to be of doubtful value because DeLong[30] has found that hydrogen has a detrimental effect even in metals of very high purity. It is conjectured that the above finding would be true for the removal of phosphorus and silicon.

TABLE 8.1 – EFFECT OF RAPID COOLING ON TENSILE PROPERTIES

Welds deposited from E217 and E437 electrodes contain approximately 20 ml of H_2 per 100 g of sample
Welds deposited from E645 electrodes contain approximately 3 ml of H_2 per 100 g of deposit

Electrode	Cooling	Heat Treatment	Yield Point, ksi/sq. in.	UTS ksi/sq. in.	Elongation, %	Reduction of Area of %	Fracture
E217	Normal	As welded	62.3	75.0	27	45	Haloes present
	Rapid	As welded	67.0	71.5	6	12	Extensive brittle areas
	Normal	16 h at 650 C.	51.1	63.8	40	70	Cup and cone
	Rapid	16 h at 650 C.	52.6	63.2	29	40	Many brittle areas
E217-Mo	Normal	As welded	80.4	93.2	18	33	Haloes present
	Rapid	As welded	80.0	80.0	2	4	Extensive brittle areas
E437	Normal	As welded	58.2	63.8	31	45	Haloes present
	Rapid	As welded	58.2	63.8	11	17	Brittle areas
	Normal	1 h at 650 C.	53.8	64.3	38	65	Cup and cone
	Rapid	1 h at 650 C.	51.5	63.8	25	37	Partially brittle
E645	Normal	As welded	67.7	75.5	33	65	Cup and cone
	Rapid	As welded	73.0	76.2	10	16	Extensive brittle areas
E645-Mo	Normal	As welded	78.6	87.1	26	62	Cup and cone
	Rapid	As welded	87.6	91.0	9	17	Extensive brittle areas
	Normal	16 h at 650 C.	69.7	76.8	32	73	Cup and cone
	Rapid	16 h at 650 C.	76.8	83.8	21	36	Partially brittle

TABLE 8.2 – BEND TEST RESULTS SHOWING EFFECT OF RAPID COOLING AND HEAT TREATMENT ON DUCTILITY OF SINGLE-BEAD WELDS

Electrode	Cooling	Heat Treatment	Angle of Bend
E217	Air Cooling	As welded	180°
	Rapid	As welded	18°
	Rapid	1 h at 650°C.	70°
E217-Mo	Air Cooling	As welded	180°
	Rapid	As welded	11°
	Rapid	1 h at 650°C.	180°
E645	Air Cooling	As welded	180°
	Rapid	As welded	44°
	Rapid	1 h at 650°C.	180°
E645-Mo	Air Cooling	As welded	180°
	Rapid	As welded	40°
	Rapid	1 h at 650°C.	180°

8.6 EFFECT OF MICROSTRUCTURE AND COMPOSITION ON HYDROGEN CRACKING

8.6.1 EMBRITTLEMENT EFFECT OF MICROSTRUCTURE OF METAL TO BE WELDED

Carbon segregation enhances hydrogen induced crack formation[16]. It has been found that the susceptibility to delayed cracking of acicular microstructures and finer carbide structures decreases with decreasing carbon content[31]. A uniform microstructure, one which does not have relatively soft phases at the boundaries between rigid columnar grains, also enhances resistance to delayed cracking, whereas twinned martensite has a detrimental effect[32].

8.6.2 EFFECT OF ALLOYING ELEMENTS OF THE WELD METAL

The composition of the weld metal alloy must be carefully chosen to minimize cracking susceptibility. Manuel[33] presented a case history involving welds in a channel of a reactor charge effluent exchanger, operated at a temperature of 950 F and a partial hydrogen pressure of 375 psi. Because of an insufficient, chromium and molybdenum content, the weld had a very short service life. The differences in the effect of concentration of five common alloying elements on the production of weld fissures[26] is clearly shown in Fig. 8.11.

A summary of the effects of concentration of alloying elements on the production of weld fissures is as follows:

Molybdenum - Addition of this metal to the E217 deposit containing 0.55 percent manganese results in a reduction in the number of fissures. Sound deposits are obtained with approximately 0.80 percent molybdenum (see Table 8.2). However, further additions cause an increase in fissured deposits.

Chromium and Vanadium -- Small additions of either of these metals cause a reduction in the number of fissures, with a minimum being reached at about 0.35 percent. Any further addition increases the number of fissures.

Nickel The number of fissures remains unchanged and high when nickel is added[34]. The mechanism of delayed hydrogen failures in the high nickel maraging steels has been elucidated by Toy and Phillips[35].

Manganese -- Deposits with very low concentrations of manganese are not fissured. However, when the manganese content is raised above 0.15 percent, the number of fissures increases rapidly to a maximum at about 0.55 percent. Increasing the manganese content to 0.85 percent has no additional effect. Although not shown in the figure, no additional effect was noted up to a concentration of 1.85 percent.

All specimens were air cooled after welding. The number of fissures was estimated from sections of the bead etched in 50 percent hydrochloric acid. The approximate hydrogen content was 21 ml/100 g of welding electrode.

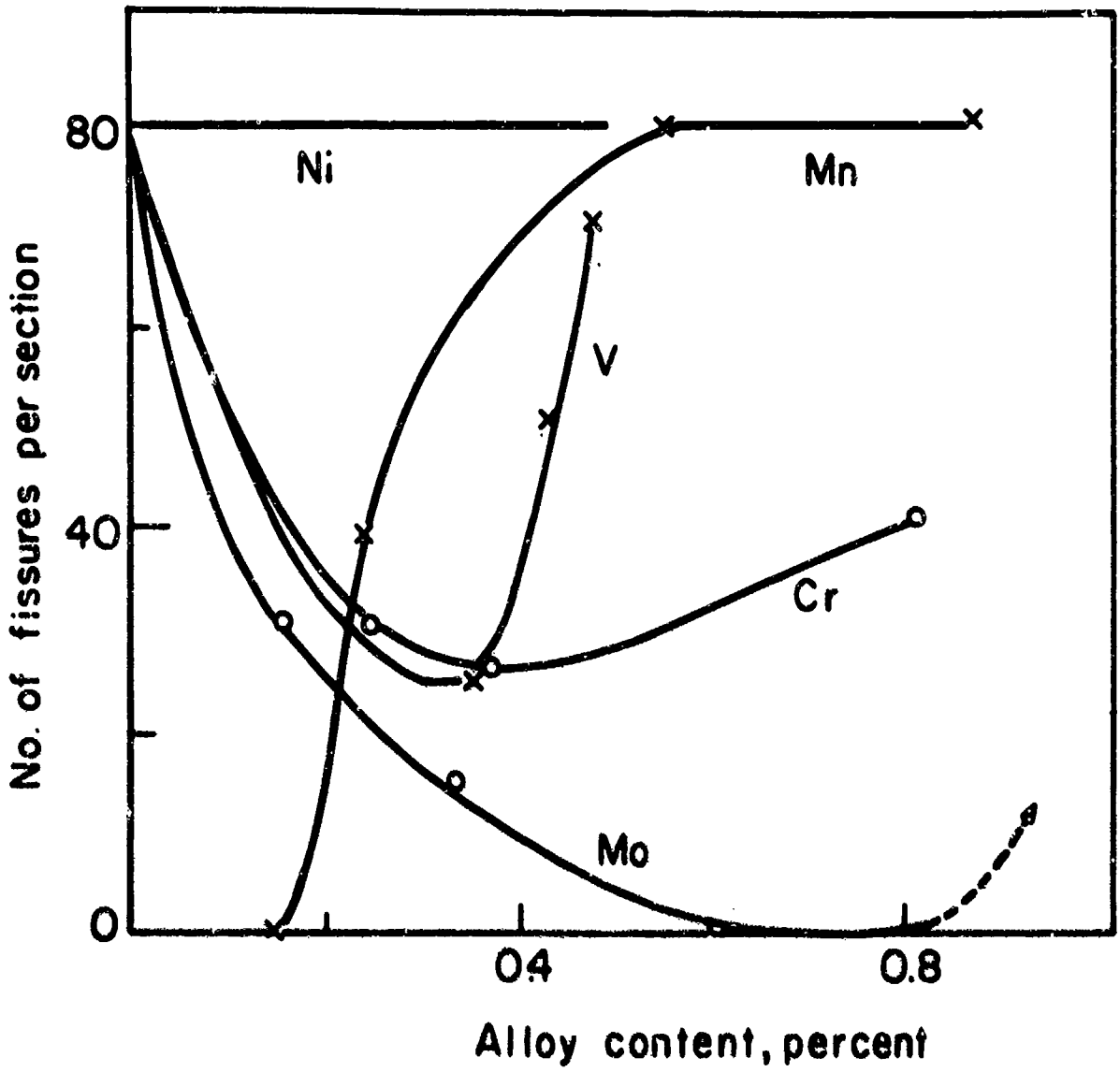

Fig. 8.11 – Relationship of the concentration of common alloying elements to the number of weld fissures.

REFERENCES

[1] A. E. Flanigan, and M. Kauffman, "Microcracks and the Low Temperature Cooling Rate Embrittlement of Welds", *Welding J.*, **30**, Research Suppl. **3**, pp. 613-622 (1951).

[2] A. W. Steinberger, and J. Stoop, "Studies of the Crack Sensitivity of Aircraft Steels", *ibid.*, **31**, pp. 527-542 (1952).

[3] A. E. Flanigan, S. I. Bocarsky, and B. M. McGuire, "Effect of Low-Temperature Cooling Rate on the Ductility of Arc Welds in Mild Steel", *ibid.*, **29**, pp. 459-466 (1950).

[4] A. E. Flanigan, "An Investigation of the Influence of Hydrogen on the Ductility of Arc Welds in Mild Steel", *ibid.*, **26**, pp. 195-214 (1947).

[5] M. D. Mallett, and P. G. Rieppel, "Underbead Cracking of Welds Cathodically Charged with Hydrogen", *ibid.*, **29**, pp. 343-347 (1950).

[6] H. G. Vaughan, and M. E. DeMorton, "Hydrogen Embrittlement of Steel and its Relation to Weld Metal Cracking", *British Welding J.*, **4**, pp. 40-61, (1957).

[7] A. E. Flanigan, and Z. P. Saperstein, "Isothermal Studies on the Weld Metal Microcracking of Arc Welds in Mild Steel", *Welding J.*, **35**, Research Suppl., pp. 541-550 (1956).

[8] C. A. Zapffe, and C. E. Sims, "Fish Eyes in Steel Welds Caused by Hydrogen", *ibid.* **19**, pp. 377-395 (1940).

[9] C. A. Zapffe, "Fish Eyes" *Metal Progress*, **42**, pp. 201-206 (Aug. 1942).

[10] T. Boniszewski, "Hydrogen Entrapment in Mild Steel Weld Metal with Micropores", *Metal Construction and British Welding J.*, **1**, pp. 269-276 (1968).

[11] T. Boniszewski, and E. D. Brown, "Fissures in Refined Regions of Multirun Weld Metal", *British Welding J.*, **13**, pp. 18-32 (1966).

[12] J. T. Berry, and R. C. Allan, "A Study of Cracking in Low Alloy Steel Weld Joints", *Welding J.*, **39**, Research Suppl., pp. 105-116 (1960).

[13] D. G. Howden, and D. R. Milner, "Hydrogen Absorption in Arc Melting", *British Welding J.* **10**, pp. 304-316 (1963).

[14] G. R. Salter, "Hydrogen Absorption in Arc Welding", *ibid.*, pp. 316-325.

[15] N. Christensen, "The Role of Hydrogen in Arc Welding with Coated Electrodes", *Welding J.* **40**, Research Suppl., pp. 145-154 (1961).

[16] C. G. Interante, and R. D. Stout, "Delayed Cracking in Steel Weldments", *ibid.*, **43**, pp. 145-156 (1964).

[17] W. T. DeLong, "The Role of Hydrogen and the Control of Hydrogen-Caused Difficulties in Weld Deposits with Minimum Yield Strength of 140 ksi", Document AD 467814, Defense Documentation Center, Cameron Station, Alexandria, Va. (1965).

[18] R. D. Stout, S. S. Tor, L. G. McGeady, and G. E. Doan, "Quantitative Measurement of the Cracking Tendency in Welds", *Welding J.*, **25**, Research Suppl., pp. 522-531 (1946).

[19] E. P. Beachum, H. H. Johnson, and R. D. Stout, "Hydrogen and Delayed Cracking in Steel Weldments", *ibid.*, **40**, pp. 155-159 (1961).

[20] H. Nakamura, M. Inagaki, and J. Mitami, "Cold Cracking in Multi-Layer Welds of Low Alloy High Strength Steel", *ibid.*, **47**, pp. 35-46 (1968).

[21] P. D. Blake, "Effect of Diffusible Hydrogen on the Mechanical Properties of Weld Metal", *British Welding J.* **5**, pp. 16-18, (1958).

[22] A. E. Flanigan, "An Investigation of the Influence of Hydrogen on the Ductility of Arc Welds in Mild Steel", *Welding J.*, **26**, Research Suppl. pp. 193-214 (1947).

[23] *Jubilee Annual Reports*, Australian Defense Standard Laboratories, Department of Supply (1966/1967).

[24] "Determination of Total Hydrogen Contents in Weld Metal", Document II W (HS-8-58/ex. Doc. II-6-57) of Commission II. Arc Welding (Sub - Commission A - Hydrogen in Weld Metal) of the International Institute of Welding (1958).

[25] F. R. Coe, "Measurement of the Hydrogen Potential of Welding Consummables by Encapsulation", *Metal Construction and British Welding J.*, **2**, pp. 108-109 (1969).

[26] E. C. Rollason, and R. R. Roberts, "Effect of Cooling Rate and Composition on the Embrittlement of Weld Metal", *J. Iron Steel Inst.* pp. 105-112 (1950).

[27] J. Bland, "Effect of Quench Time on Weld Metal", *Welding J.*, **28**, Research Suppl. pp. 216-226 (1949).

[28] N. Smith, and B. Y. Baynall, "The Influence of Sulphur on Heat Affected Zone Cracking of Carbon-Manganese Steel Welds", *Metal Construction and British Welding J.*, **2**, pp. 17-23 (1969).

[29] J. Hewitt, and J. D. Murray, "Effect of Sulphur on the Production and Fabrication of Carbon-Manganese Steel Forgings", *ibid.*, pp. 24-31.

[30] W. T. DeLong, "Eliminating Hydrogen Cracking", *Metal Progress*, **94** (5), pp. 74-78 (1968).

[31] T. Boniszewski, F. Watkinson, R. G. Baker, and H. F. Tremlett, "Hydrogen Embrittlement and Heat Affected Zone Cracking in Low-Carbon Alloy Steels with Acicular Micro Structures", *British Welding J.*, **12**, pp. 14-36 (1965).

[32] J. L. Kae, "Mechanical Properties, Microstructure and Susceptibility to Cracking in the HAZ of Controlled-Rolled Niobium Treated, Low Carbon, Manganese Steels", *ibid.*, **15**, pp. 395-407 (1968).

[33] R. W. Manuel, "Hydrogen Service Failures of Welds With Insufficient Alloy Content", *Corrosion* **17**, pp. 435t-436t (1961).

[34] F. Watkinson, "Hydrogen Cracking in High Strength Weld Metals", *Welding J.*, **48**, Research Suppl. pp. 417-424 (1969).

[35] S. M. Toy, and A. Phillips, "Stress Corrosion Characteristics of Maraging Steel Weldments in Air and Pentaborane", *ibid.*, **49**, pp. 497-504 (1970).

CHAPTER 9

SULFIDE CORROSION HYDROGEN STRESS CRACKING IN THE PETROLEUM AND GAS INDUSTRIES

9.1 SULFIDE CORROSION HYDROGEN STRESS CRACKING

Sulfide corrosion hydrogen stress cracking has been the concern of engineers and metallurgists in the petroleum and gas industries for many years. Bartz and Rawlins and other early investigators[1-4], reported striking examples of damaging effects of hydrogen generated by sulfide corrosion of steel.

The complexity of the subject matter is strikingly illustrated by reports issued by the Technical Unit Committees of NACE (National Association of Corrosion Engineers). In 1952, the Technical Practices Committee 1-G issued the first report on field experience with the cracking of high strength steels in sour gas and oil wells[5]. This report presents a number of cases dealing with field experiences, field tests, and preventive measures.

In 1954, this committee issued a more detailed report, dealing with sulfide corrosion cracking of oil production equipment[6]. The importance of the three main factors in sulfide corrosion stress cracking is considered in this report: (1) the relative susceptibility of the materials to cracking; (2) the severity of the environment; and (3) the severity of the mechanical stresses to which the material is subjected.

An increase in hardness or yield strength also tends to cause an increase in susceptibility to cracking. Failures have been experienced with N-80 tubing and casing, 9 percent nickel steel tubing, valves, some carbon steel fittings, and both carbon steel and stainless steel (AISI 304 and 316) pipe lines.

As regards environmental factors, the Committee emphasized that the minimum concentration of H_2S required to produce cracking of a very susceptible material has not been precisely defined, but apparently is quite low. However, according to Hudgins and other investigators[7-11] 0.5 ppm H_2S in solution is sufficient to crack oil field tubular steels rather quickly. The tendency of a given environment to promote cracking diminishes with increasing temperature. Changes in environmental conditions which lead to a weakening of the protective ferrous sulfide film should be considered undesirable. Among other significant chemical and physical factors in the environment are acidity and oil wettability, because an increase in the relative wettability of the metal surface by the oil decreases the tendency for the occurrence of corrosive attack.

In consideration of mechanical factors and test conditions, the Committee suggested that laboratory and field testing strip type specimens, loaded as beams, should be stressed to values near the yield strength, or slightly above, in order to obtain failures in a reasonable time. Because of the problem of data reproducibility multiple testing is required for accurate comparisons. The same type specimens should be employed in field test as in laboratory tests. Specimens are usually inserted in the flowline near the well head and are securely mounted to prevent movement in the flowline. The minimum time generally used in such tests is two weeks, and the maximum time may range up to several months.

The Committee's report also contains a valuable presentation of field test data, and a description of preventive measures used by various operators.

The most recent report of NACE Technical Unit Committee T-1B,[12] issued in 1963, on corrosion in oil and gas well equipment contains recommendations on materials for sour service. The susceptibility of a number of materials to sulfide corrosion stress cracking is presented in this report. AISI 400 series stainless steels become resistant to sulfide stress cracking, if given well controlled heat treatments to reduce internal stresses and hardness. Monels at all hardness levels are resistant to stress cracking and show excellent resistance to general corrosion. The same is true for Inconel below a Brinell hardness level of 375. Hard facing materials, Stellites, Colmonoy and cemented carbides have proved to be resistant to corrosive attack. For API* N-80 tubing and casing, special heat treatment conditions and a minimum tempering temperature of 610 C are required. The yield strength of this steel should be limited to 90 ksi maximum, to provide an adequate margin of safety. Chromium-molybdenum steels have also shown satisfactory behavior.

*American Petroleum Institute

The susceptibility of tubing materials, threaded and coupled joints, integral joints and particularly the problem of materials specification for valves are also discussed in this report. It is imperative to keep highly localized stresses in valve bodies and components to a minimum. In valve components, where high strength, wear resistance, etc. are essential, materials such as Inconel, K-Monel, Hastalloys, Stellites and cemented carbides have proven satisfactory. A tentative NACE specification[13] published in 1963, outlines the requirements under which most valves should perform satisfactorily from the point of view of sulfide stress cracking.

In addition to the above Committee reports a number of pertinent papers will be next discussed. Baldy and Bowden[14] studied the susceptibility of martensitic structures to sulfide corrosion stress cracking. They used test bars made from API Grade N-80 tubing. Specimens were produced with 0 to 100 percent martensite using appropriate prequenching temperatures. The test specimens were four point loaded bent beam bars with a constant load between loading points. They were immersed in a bath of distilled water saturated with hydrogen sulfide and carbon dioxide. All specimens were loaded to various stress levels below the yield strength.

The susceptibility of a steel with 80 ksi minimum yield strength to sulfide corrosion stress cracking, was found to fall into the three following categories depending on the percentage of martensite present:

- From 0 to approximately 35 percent martensite, the steel is not susceptible,
- From 35 to about 80 percent martensite, the permissible load carrying capacity to avoid failure decreases with increasing martensite,
- Above 80 percent martensite, very low stresses will cause failure.

Baldy[15] developed an experimental alloy containing Mn-Mo-V which meets API 5A grade N-80 requirements and, according to laboratory experiments, it can be used to advantage in sulfide wells.

Cauchois, Didier and Herzog[16] developed a Cr-Al-Mo alloy (APS 10 M4 steel) with a thermodynamically stable ferritic structure with highly dispersed fine carbides. The resistance of this alloy against sulfide stress cracking, determined by field tests, appreciably exceeds that of the conventional N-80 steel.

An excellent study of the susceptibility to sulfide corrosion stress cracking of AISI 4140 Allen head cap screws and stud bolts was made by Warren and Beckman[17]. The bolting material was heat treated to provide specimens with hardnesses in the range of R_C 20 to R_C 55. The cap screws were loaded on bars, whereas the bolts were loaded in individual sleeves. Holes were drilled in both types of jigs to permit free circulation of the corrosive environment around the bolts. Stresses were applied to the bolts by tightening them in the jigs until their elongations reached certain predetermined values. Three test environments based on the H_2S-H_2O system were used. Tests in two environments were conducted under similar H_2S pressures (250 psi) but at different temperatures 40 C and 120 C, respectively in autoclaves. Tests in the third environment were performed with H_2S at atmospheric pressure and room temperature. The bolts were exposed in the water saturated vapor rather than the liquid phase in all three environments and were examined periodically for failures. The microstructure of the quenched and tempered bolts was tempered martensite.

A plot of the minimum bolting stress required for failure versus the bolt hardness is given in Fig. 9.1. Results demonstrate that the critical stress below which sulfide cracking does not occur is largely a function of the hardness of the material. No bolting failures occurred at hardness values less than R_C 27 even at applied stresses approaching the yield point

As shown in Fig. 9.2, the cracking susceptibility was greatly reduced by raising the test temperature from 40 to 120 C. On the other hand, heavy plastic pre-straining of AISI 4140 bolts increased their susceptibility to sulfide cracking at high levels of applied stress[18-21].

Additional data in the curves in Fig. 9.3 also depict a marked reduction in cracking time caused by increased bolt hardness. The number of bolt failures for each hardness level occurring at a given exposure time was plotted as a percentage of the total number of bolt failures in that hardness range. The data represented bolt failures which took place at applied stress values ranging from 15 to 125 ksi. Analysis of the data disclosed that the effect of hardness on failure time largely overshadows any effect of applied stress and pre-stressing.

As shown in Fig. 9.4, an increase in applied stress reduced the time to failure of the R_C 39-43 bolts, but did not appreciably affect the time to failure of bolts in the two lower hardness ranges.

There was no apparent correlation between the corrosion rate in the aforementioned three environments and the incidence of sulfide stress cracking. The formation of fractures was noted at four principal locations: (1) in the threaded portion between the nut and the unthreaded shank (gauge failure); (2) in the threaded portion engaged in the nut (nut failure); (3) in the unthreaded shank (shank failure); and (4) in the minimum cross-section at the base of the cap (head failure). In the case of nut failures, the restraint by the nut thread caused multiple cracking. Cracking in the uniformly martensitic microstructure was found to be occasionally either intergranular or transgranular.

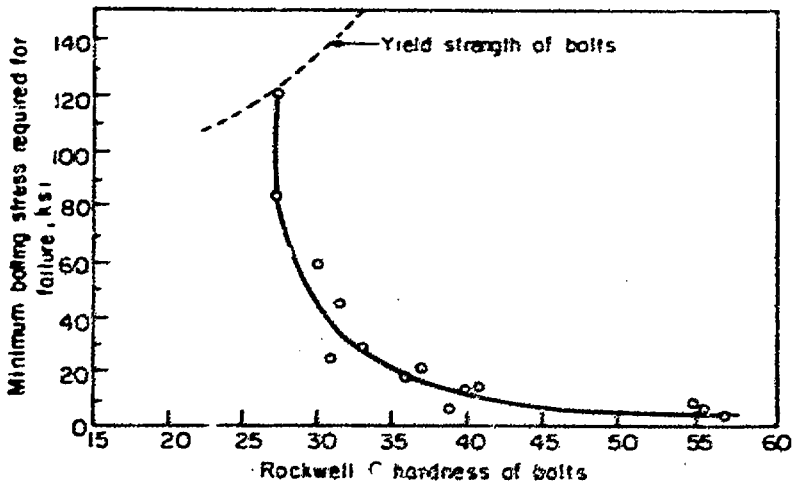

Fig. 9.1 – Minimum bolting stress required to produce cracking of AISI 4140 steel bolts of different hardnesses in a H_2S-H_2O vapor system at 40 C and 250 psi partial pressure of H_2S. Time to failure ranged from 56 hours to 9 months.

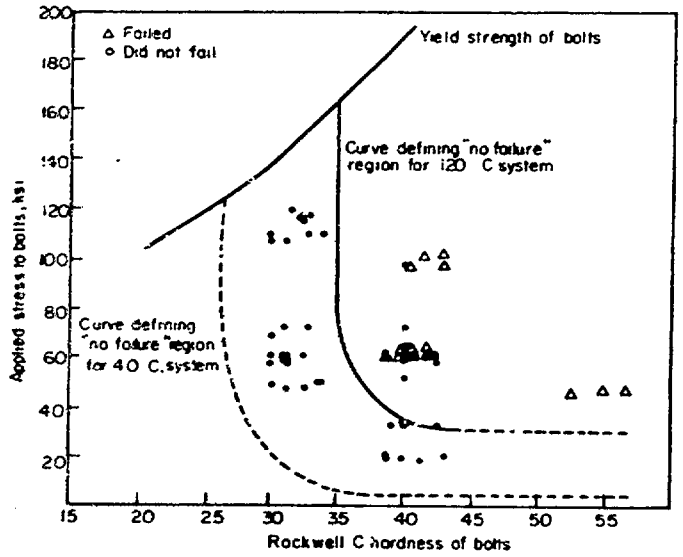

Fig. 9.2 – Cracking susceptibility of AISI 4140 bolts of different hardnesses exposed up to 1 year in a pressurized H_2S-H_2O system at 40 and 120 C.

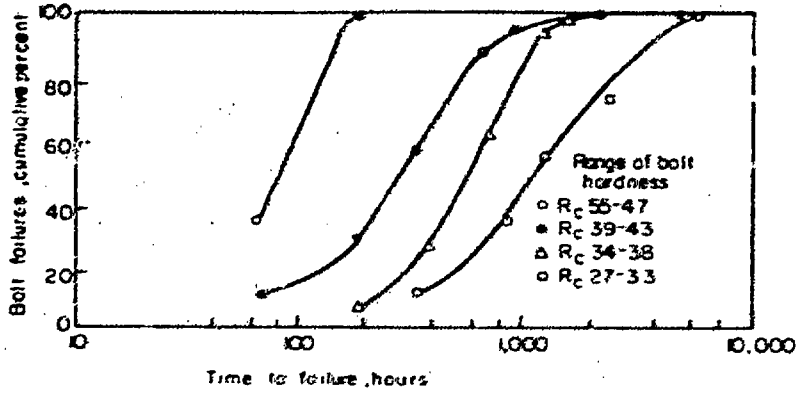

Fig. 9.3 – Effect of hardness on time to failure of AISI 4140 bolts, exposed in a pressurized H_2S-H_2O system at 40 C.

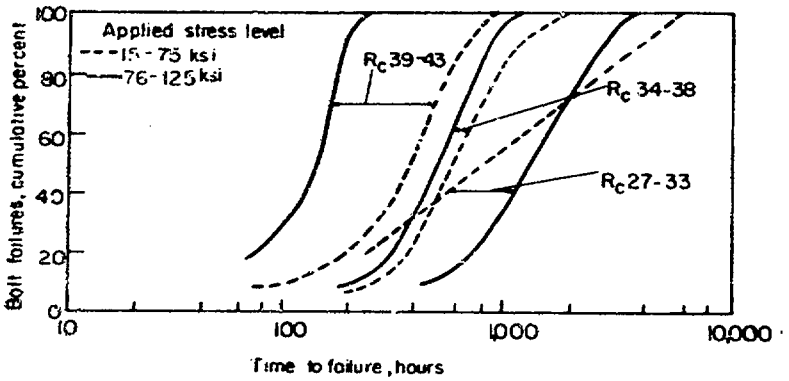

Fig. 9.4 – Effects of applied stress and hardness on time to failure of AISI 4140 bolts, exposed in a pressurized H_2S-H_2O system at 40 C.

Warren and Beckman[17] performed numerous experiments to prevent bolting failures in H_2S-H_2O environments. Primarily, the effectiveness of three procedures was studied: (1) addition of corrosion inhibitors; (2) use of metallic coatings; and (3) use of other alloys for manufacturing bolts. Protection by inhibitors will be discussed in the next section.

Seven different types of metallic coatings were applied to the bolts prior to their exposure to the H_2S-H_2O systems. The hardness and strength level of these bolts were sufficient to ensure cracking of uncoated specimens. The results of this study are summarized in Table 1. While most of the coatings were effective in increasing bolt life, they did not provide consistent reliable protection against hydrogen stress cracking. The relatively heavy nickel plating (0.005 in. thick) gave good protection. Despite its effectiveness in these tests, nickel plating was rejected as a method of preventing bolting failures in the field because the making and breaking of threaded joints materially increases the probability of mechanical rupture of the coating.

TABLE 9.1 – EFFECT OF METALLIC COATINGS ON THE SUSCEPTIBILITY OF TYPE 4140 BOLTS TO SULFIDE CORROSION CRACKING

Environment	Type of Coating(1)	Number of bolts Exposed(2)	Number of Bolts Failed	Avg. Time To fracture (Hours)	Exposure Time Unfailed Bolts (Hours)
H_2S-H_2O at 40 C 250 psi	No coating	4	4	500	–
	Cd	2	2	1100	–
	Zn	2	2	1100	–
	Cr	2	2	1400	–
	Pb	2	2	1400	–
	Brass	2	0	–	8200
	Ni	4	0	–	8600
H_2S-H_2O at room temp. Atm. press.	No coating	5	5	250	–
	Zn	2	2	500	–
	Brass	2	2	600	–
	Al	3	2	1700	11,000
	Cd	2	2	7600	–
	Pb	2	1	8400	14,000
	Cr	2	1	14000	14,000

(1)All coatings were electrodeposited having a minimum thickness of 0.002 in., except Al which was a sprayed paint coating applied in 3 successive light layers, and the Ni coating which was 0.005 in. thick.

(2)All bolts were heat treated to a hardness level of R_C 38-42 and stressed to 55-65 ksi.

Substitute materials, such as 316 stainless in the annealed condition, K-Monel, Inconel and Inconel X, were immune to sulfide cracking even at high levels of hardness and applied stress (R_C 32-36 and 100 - 125 ksi).

In summary, the hydrogen embrittlement theory of bolt cracking is strongly supported by the following facts: (1) the decrease in cracking tendency with increasing test temperature; (2) the correlation between hardness and susceptibility to cracking; (3) the effectiveness of corrosion inhibitors and (4) the effectiveness of corrosion resistant metallic coatings.

Hudgins et al[7] as well as other investigators[20-22], used a stressed notched C-ring similar to that developed by Williams, Beck, and Jankowsky. In general their results confirmed those obtained by Warren and Beckman. In addition, they also agreed that hydrogen is the primary factor involved in sulfide corrosion

stress cracking of high strength steels. Treseder and Swanson found a rather drastic increase in time to failure for H_2S concentrations below 30 to 40 ppm, or for higher H_2S concentrations when the pH is increased to 9.5. Warren and Beckman[17] recommend maintaining hardness below the R_C 27 level and bolt stresses to 40 ksi, while Treseder and Swanson, considering the difficulty in controlling bolt stresses, prefer that the hardness be less than R_C 20.

Recently, Schenck, Schmidtmann and Klarner[23] studied the effect of natural gas on the cracking behavior of high strength steel. The H_2S content of German natural gases was found to range between 0.5 and 1 percent. Hydrogen penetration into spring loaded cylindrical specimens was studied for the H_2S containing gases when the dew point was varied over a wide range. The effect of H_2S containing liquids with a varied pH was also investigated. These investigators recommended drying the gases as effectively as possible, because desulfurization is not economically feasible. They noted that at a dew point of a gas, which is approximately 20 C below the lowest operating temperature at the inside wall of the pipe line, the H_2S content no longer exerts a corrosive effect on the steel. They also found it highly desirable to maintain the gas pressure inside the line as low as possible. In addition, they recommended that the hardness of the pipe steel be as low as possible.

A number of German investigators are in agreement with the recommendations of Schenck et al. Naumann,[24] conducted delayed failure tests under sustained loads in humid gases containing H_2S, and in aqueous solutions of H_2S. A beneficial effect was obtained by drying the gases or by increasing the pH above 10. A marked decrease was observed in the susceptibility to delayed cracking with decreasing H_2S concentration. He emphasized the importance of the formation of a protective iron sulfide coating. Corresponding results were obtained by other German investigators[25-27]. Embrittlement in humid environments containing H_2S can be completely excluded by alloying 14 percent chromium to the steel[28].

Snape[29, 30] studied sulfide corrosion hydrogen stress cracking in some medium and low alloy steels, types 4600, 47353 to 47367. In addition, N-80 B and D, and a great number of other low alloy steels were tested. Strength level of the medium alloy steel was varied from 155 to 260 ksi, and for the low alloy steel it was varied from 100 to 280 ksi. The smooth three-point loaded beam specimens were immersed in a dilute NaCl solution saturated with H_2S and experiments were performed over a wide pH range. Stress rupture tests and hydrogen determinations were made on specimens with the hydrogen introduced into the steel by cathodic charging at different current densities as well as on specimens hydrogenated in a sulfide containing medium. The embrittlement effects of these treatments on the steels were basically identical, clearly indicating again that sulfide stress cracking is essentially hydrogen embrittlement. Additional evidence in favor of this conclusion was obtained by metallographic examination, which showed that the mode of crack growth for specimens exposed in H_2S media, is precisely the same as that in specimens embrittled by cathodic charging. A number of other findings of this investigator are in excellent agreement with those mentioned above. By a special heat treatment called "intercritical hardening", Snape et al[31] succeeded in increasing the strength, ductility, and resistance to sulfide stress cracking of AISI 4340 and similar steels.

Bates[32] studied comprehensively sulfide stress cracking of high-yield-strength steels in sour crude oils. It is his considered opinion that the yield strength of steels is more important for determining sulfide stress cracking performance than the hardness. In anticipation that the petroleum industry might be interested in using ASTM-A-157, Grade F and A-517, Grade B steels for large welded storage tanks, sulfide cracking studies were performed on nine structural steels exposed to sour gas, oil, and brine in crude oil storage tanks. The steels were: ASTM A-517 F, A-517 B, A-302 B, A-441, A-242, A-285, A-537, AISI 4130, and 635 stainless.

Two types of specimens were used: (1) a machined smooth tensile specimen loaded in a stressing ring, which afforded a precise knowledge of the applied stress; and (2) a tuning-fork specimen, that applied realistic stresses to as-welded and as-rolled plate surfaces, by bolting the ends of the tines together.

The tuning forks can be stressed to a definite level, or beyond the yield point, and cold worked by bending the tines outward. Cold worked tuning forks were also welded by placing a weld bead on the outside of one tine at its base, and then stressed by closing the tines completely. Tuning fork specimens are pictured in Fig. 9.5.

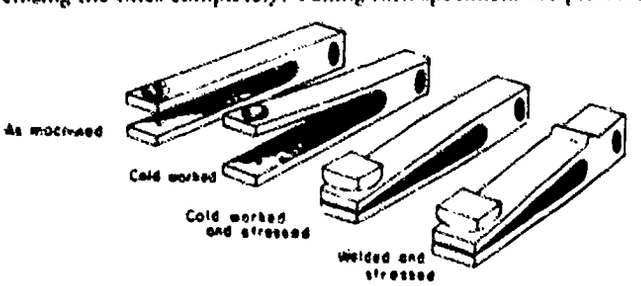

Fig. 9.5 – Tuning-fork specimens used for sulfide cracking studies.

The tension specimens were tested in both the welded and unwelded conditions. Welded tension specimens* were machined from butt-welded 1/2 in. plate, so that the heat affected zone on one side of the weld was approximately in the center of the specimen-gauge length. Most welded specimens were stressed to 75 percent of the yield strength, some to 80 percent whereas unwelded specimens were stressed to a specified level either below the yield strength or slightly above it. Specimens were exposed in two crude oil storage tanks, one contained a moderate concentration of H_2S representing a very corrosive environment, while the other contained a low sulfide concentration representing a moderately corrosive environment. Additional exposure tests were performed in two separating tanks. Specimens were periodically inspected visually and were considered to have failed if they fractured, or contained a crack visible under low magnification.

The effect of increasing yield strength on the frequency of failure of all specimens in sulfide containing test media is summed up in Fig. 9 6. Increasing yield strength is shown to decrease resistance to sulfide stress cracking. AISI type 635 stainless (183 to 202 ksi yield strength) had about 80 percent failure frequency. All steels in the 112 to 128 ksi yield strength range, ASTM A-517 F steel, A-517 B steel, AISI 4130 steel, and quenched and tempered ASTM A-302 (modified) steel, had about 20 percent failures, whereas ASTM A-441 steel and A-242 steel (52 to 56 ksi yield strength) had only about 5 percent failures. The fact that ASTM A-285 (35 ksi yield point) steel is practically immune to cracking whereas type 635 stainless is highly susceptible is in good agreement with observations made in the petroleum indusry.

*Additional details on welded specimens are given in Chapter 8.

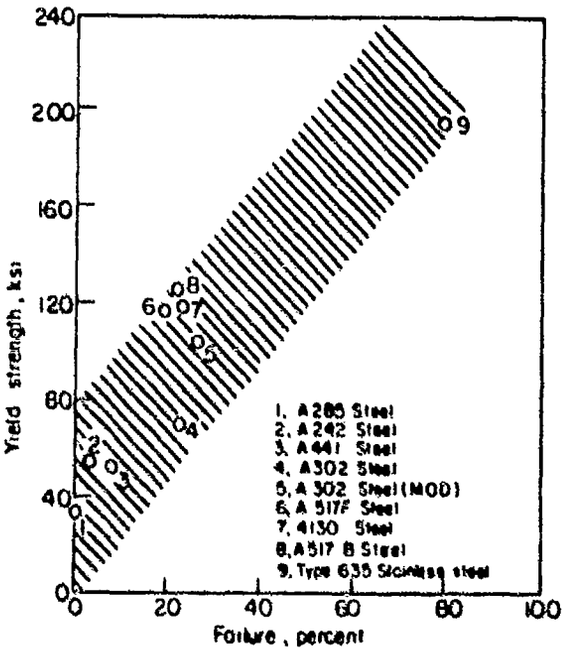

Yield Strength (ksi)	Steel
183 to 202	9
112 to 128	4, 5, 6, 7 and 8
52 to 56	2, 3
35	1

Fig. 9.6 – Relationship of fracture frequency to yield strength of smooth tension specimens exposed to a test media containing sulfide.

A plot of failure incidence of 112-128 ksi yield strength steel versus H_2S concentration in different environments illustrates that high strength steels will crack at low sulfide concentrations (Fig. 9.7).

High yield strength and the hydrogen disulfide content of the crude oil are important factors in the sulphide stress cracking of steels. The same is true for weldments where the cracks were formed in or immediately adjacent to the heat affected zone, as pictured in Fig. 9.8 [33]. Post weld heat treatments reduced the hardness markedly, and therefore, lessened cracking susceptibility (See Chapter 8).

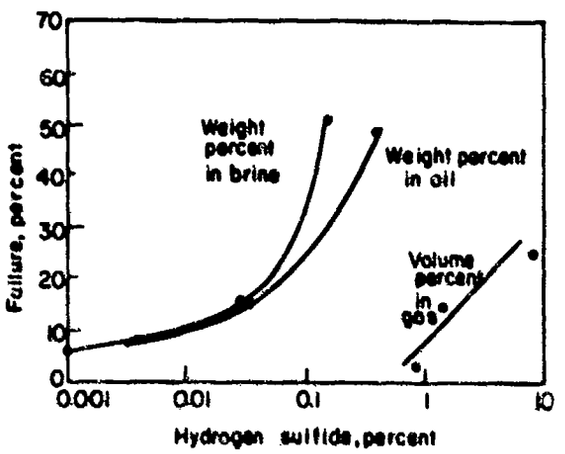

Fig. 9.7 – Effect of H_2S concentration on frequency of cracking of 112 to 128 ksi yield strength steels in sour crude oils, brine and gas.

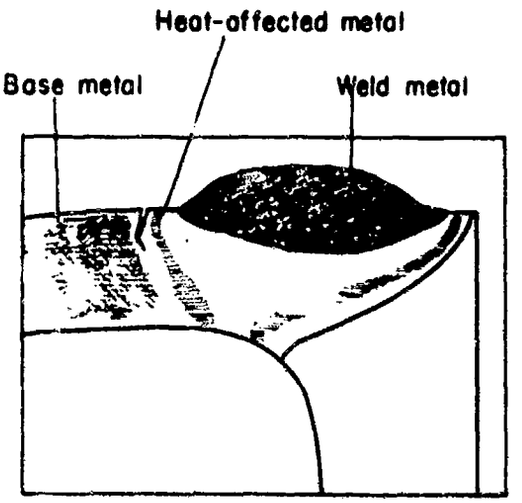

Fig. 9.8 – Tuning fork specimen in ASTM A-517 B steel cracked in the heat affected zone, adjacent to the weld, after exposure to a sulfide containing test medium. Etched in Nital (X9).

An interesting result was obtained with large U-bend specimens fabricated of the susceptible ASTM A-527 F steel and coated with a coal tar epoxy. No failures were observed during an exposure time of 12 months in an acidic H_2S saturated solution. Coated specimens, which had a hole drilled through the coating (1/8-in. diameter) into the metal at the point of maximum stress, failed between 11 and 12 months, while uncoated specimens failed overnight. This result clearly demonstrates that even a defective, but otherwise good coating, can markedly prolong the life of a susceptible steel.

Hydrogen problems are also encountered in the field of hydrogen treating processes [34]. For example, cadmium plated coil valve springs in reciprocating compressors and impellers used in hydrosulfurization and hydrogen cracking processes were hydrogen damaged. Cracking was initiated when pressurized recycle gas contained H_2S and acidic moisture. A high cracking incidence was found for low alloy structural steel and precipitation hardening stainless steels with yield points above 100 ksi.

9.2 EFFECTIVENESS OF ORGANIC CORROSION INHIBITORS

There are divided opinions concerning the effectiveness of organic corrosion inhibitors in reducing hydrogen sulfide corrosion. However, there can be no doubt that this type of inhibition is closely related to retardation of both the dissolution rate of iron and hence, the hydrogen evolution reaction. (Discussed in detail in the Chapter on Mechanisms)

Bradley and Dunn [35], working in the laboratories of the Shell Development Company, exposed high strength steel in a H_2S absorption pilot plant. They found that corrosion, and hence, blister and crack formation were more effectively inhibited by water soluble, oleophobic, imidazoline type substances than by water dispersable amine type corrosion inhibitors.

Warren and Beckman [17] evaluated two inhibitors, Duomeen T and tetraethylenepentamine, (TEPA), two low vapor pressure amines. The addition of either of these inhibitors to the liquid phase of the 40 C, 250 psi,

H_2S-H_2O system, markedly reduced the corrosion rate for short time exposures (100 to 400 hours). Cracking tests were performed in the liquid phase of pressurized H_2S-H_2O systems at 40 C with about 500 ppm of the inhibitor added. Hardness and stress level of the test bolts were sufficient to insure cracking in the absence of any inhibitor.

Results of the experiments showing the cracking behavior of AISI 4140 bolts in inhibited and uninhibited systems are shown in Fig. 9.9. TEPA reduced the percentage of bolt failures form 100 to 40 percent. In spite of this favorable result, the above investigators conclude that the practical significance of these tests is limited, because the number of bolts tested was insufficient for a reliable statistical evaluation. Moreover, neither inhibitor was 100 percent effective in preventing failure.

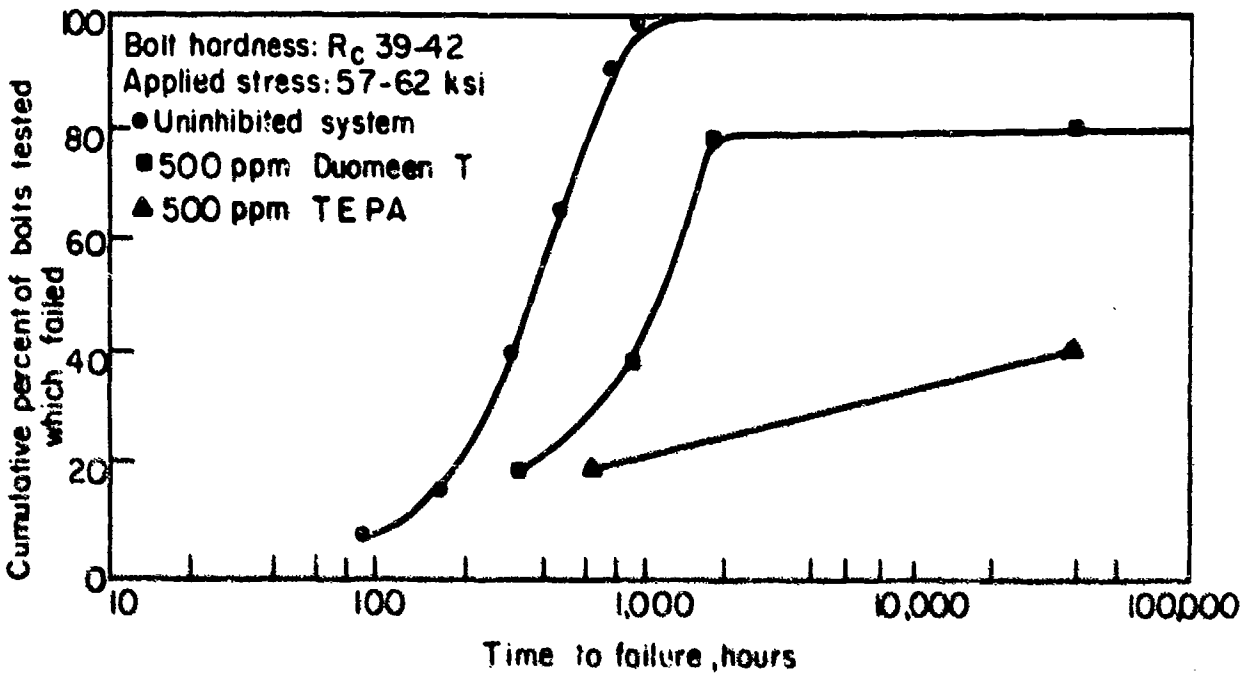

Fig. 9.9 – Effectiveness of Duomeen T and TEPA (tetraethylene pentamine) in reducing cracking susceptibility of AISI 4140 bolts, exposed in a pressurized H_2S-H_2O system at 40 C.

Riggs and Radd[36] and Keeney et al.[37] also showed he close relationship between inhibition of corrosion in hydrogen sulfide containing systems and reduction in susceptibility to sulfide stress cracking. The stress rupture life of highly stressed notched C-rings was significantly longer when the corrosion inhibitor, alkyl propylene diamine salicylate, was added to an aggressive NaCl brine, saturated with H_2S.

Bates[32] established a definite relationship between inhibition of general corrosion of high strength steel and its cracking incidence in sour crude oils. He emphasized that the inhibitors used in his investigation did not entirely prevent cracking (similar to results obtained by Warren and Beckman[17]) and suggested that chemical inhibition should not be used as the sole preventive measure.

REFERENCES

[1] M. H. Bartz and C. E. Rawlins, "Effects of Hydrogen Generated by Corrosion of Steel", *Corrosion*, **4** (5), pp. 187-206 (1948).

[2] W. A. Bonner, H. P. Burnham, G. Y. Conrad: and T. Skei, "Industry Probes Means of Mitigating Hydrogen Attack on Steel in Refinery Equipment", *Oil and Gas J.*, **52** (5), pp. 100-103, 120, 131 (1953).

[3] T. Skei, A. Wachter, W. A. Bonner and H. D. Burnham, "Hydrogen Blistering of Steel in Hydrogen Sulfide Solutions", *Corrosion*, **9** (5), pp. 164-172 (1953).

[4] W. A. Bonner and H. D. Burnham, "Air Injection for Prevention of Hydrogen Penetration of Steel", *ibid.*, **11** (10), pp. 447t-453t (1955).

[5] "Field Experience with Cracking of High Strength Steels in Sour Gas and Oil Wells", A Report of Technical Practices Committee 1-G of NACE, *ibid*, **8** (10), pp. 351-354 (1952).

[6] "Sulfide Corrosion Cracking of Oil Production Equipment", Report of Technical Unit Committee 1-G of NACE on Sulfide Stress Corrosion Cracking, *ibid.*, **10** (11), pp. 413-419 (1954).

[7] C. M. Hudgins, R. L. McGlasson, P. Mehdizadeh, and W. M. Roseborough, "Hydrogen Sulfide Cracking of Carbon and Alloy Steels", *ibid.*, **22**, pp. 238-251 (1966).

[8] *Proc. 2nd International Congress on Metallic Corrosion*, pp. 364-374 (1963).

[9] C. M. Hudgins, Jr., "A Review of Sulfide Corrosion Problems in the Petroleum Industry", *Materials Protection*, **8**, (1) pp. 41-47 (1969).

[10] E. C. Greco and W. B. Wright, "Corrosion of Iron in an H_2S-CO_2-H_2O System", *Corrosion*, **18** (3), pp. 11qt-124t (1962).

[11] J. B. Sardisco, W. B. Wright and E. C. Greco, "Corrosion of Iron in an H_2S-CO_2-H_2O System, Corrosion - Film Properties on Pure Iron", *ibid.*, **19** (10), pp. 354t-359t (1963).

[12] "Recommendations on Materials for Sour Service", A Report of NACE Technical Unit Committee T-1B on Corrosion in Oil and Gas Well Equipment, Mater. Protection, **2** (3), pp. 89-95 (1963).

[13] "Tentative NACE Specifications No. 50 - "Nominal Weight Loss and Imminent Cracking Conditions", No. 51 - "Severe Weight Loss and Imminent Cracking Conditions"; No. 60 - "Tubular Goods", *ibid.* pp. 95-99 (1963).

[14] M. F. Baldy and R. C. Bowden, Jr., "The Effect of Martensite on Sulfide Stress Corrosion Cracking", *Corrosion*, **11** (10), pp. 417t-422t (1955).

[15] M. F. Baldy, "Sulfide Stress Cracking of Steels for API Grade X1-80 Tubular Products", *ibid.*, **17** (11), pp. 509t-513t (1961).

[16] L. Cauchois, J. Didier and E. Herzog, "A Special N-80 Steel Tubing, Developed in France to Resist Sulfide Stress Cracking in Sour Gas Wells", *ibid.*, **13** (4), pp. 263t-269t (1957).

[17] D. Warren and G. W. Beckman, "Sulfide Corrosion Cracking of High Strength Bolting Material", *ibid.*, **13** (10), pp. 631t-646t (1957).

[18] J. B. Fraser and G. G. Eldredge, "Influence of Metallurgical Variables on Resistance of Steels to Sulfide Corrosion Cracking", *ibid.*, **14**, pp. 524t-530t (1958).

[19] C. N. Bowers, W. J. McGuire and A. F. Wihe, "Stress Corrosion Cracking of Steel Under Sulfide Conditions", *ibid.*, **8** (10) pp. 333-341 (1952).

[20] A. E. Schütz and W. D. Robertson, "Hydrogen Absorption, Embrittlement and Fracture of Steel", *ibid.*, **13** (7), pp. 437t-458t (1957).

[21] R. S. Treseder and T. M. Swanson, "Factors in Sulfide Corrosion Cracking", *ibid.*, **24** (2), pp. 31-37 (1968).

[22] I. S. Shparber, A. V. Shreider and N. P. Zhuk, "Hydrogen Absorption of Steel in Alkaline Sulfide Electrolytes", *Zashchita Metallov*, **3** (11), pp. 73-78 (1967).

[23] H. Schenck, E. Schmidtmann and H. F. Klarner, "Sustained Load Tests on Steels with A Minimum Yield Strength of 30 kg/mm^2 in H_2S Containing Solutions and Gases", *Stahl und Eisen*, **87**,(3), pp. 136-146 (1967).

[24] F. K. Naumann, "Sustained Load Tests on High Tensile Strength Steels Exposed to H_2S Containing Gases and Liquids", *ibid.*, **87** (3) pp. 146-153 (1967).

[25] W. Dahl, H. Stoffels, H. Hengstenberg and C. Daren, "Hydrogen Induced Embrittlement", *ibid.*, pp. 123-136.

[26] F. K. Naumann and W. Carius, "Fracturing of Steels Exposed to an Aqueous Solution of H_2S", *Archiv. Eisenhutt*, **30** (6) pp. 233-238 (1959).

[27] F. K. Naumann and W. Carius, "Absorption of Hydrogen and Fracturing of Stressed Steel Parts Exposed to H_2S Containing Solutions", *ibid.*, **30** (6), pp. 361-370 (1959).

[28] E. E. Hofmann, E. Martin and H. Kupper, "Hydrogen Embrittlement of Steels in Humid, H_2S Containing Environments", *ibid.*, **39**, pp. 677-682 (1968).

[29] E. Snape, "Sulfide Stress Corrosion of Some Medium and Low Alloy Steels", *Corrosion*, **23**, pp. 154-172 (1967).

[30] E. Snape, "Roles of Composition and Microstructure in Sulfide Cracking of Steel", *ibid.*, **24**, pp. 261-282 (1968).

[31] E. Snape, F. W. Schaller, R. M. Forbes Jones, "Method for Improving Hydrogen Sulfide Accelerated Cracking Resistance of Low Alloy Steels", *ibid.*, **25**, pp. 380-388 (1969).

[32] J. F. Bates, "Sulfide Cracking of High Yield Strength Steels in Sour Crude Oils", *Mater. Protection*, **8** (1), pp. 33-36 (1969).

[33] M. Watanabe and Y. Mukai, "About Corrosion Cracking of High Strength Steel Induced by H_2S", Osaka Univ. Technical Report 16 740, pp. 671-685 Japan (1966).

[34] G. B. Kohut and W. J. McGuire, "Sulfide Stress Cracking Causes Failure of Compressor Components in Refinery Service", *Mater. Protection*, **7**, pp. 17-22 (1968).

[35] B. W. Bradley and N. R. Dunn, "Corrosion Measurements in a Hydrogen Sulfide-Water Absorption Pilot Plant", *Corrosion*, **13** (4), pp. 239t-242t (1957).

[36] O. L. Riggs and F. J. Radd, "Physical and Chemical Study of an Organic Inhibitor for Hydrogen Sulfide Attack", *Corrosion*, **19** (1), pp. 1t-8t (1963).

[37] R. R. Keeney, R. M. Lasater and J. A. Knoze, "New Organic Inhibitor Retards Sulfide Corrosion Cracking", *Mater. Protection*, **7**, pp. 23-26 (1968).

CHAPTER 10

DAMAGING EFFECTS OF HIGH PRESSURE HYDROGEN AT ELEVATED AND AMBIENT TEMPERATURES

Since a comprehensive report[1] dealing with the embrittlement of steel by high pressure hydrogen at and above ambient temperatures was published in 1964, only the more recent findings will be discussed in this chapter. The results confirm that hydrogen embrittlement, induced by high pressure hydrogen at ambient temperature, reveals all the features typical of embrittlement by electroytically generated hydrogen. However, the adverse effect of high pressure hydrogen at elevated temperatures in many cases is not caused directly by absorbed hydrogen atoms, but by an irreversible chemical reaction, in which hydrogen atoms are involved. To avoid confusion, the last mentioned process will be designated "hydrogen attack." It is clear that "hydrogen attack" differs from hydrogen embrittlement defined previously. Thus, some striking cases of "hydrogen attack" will be presented for completeness of studies and postulations made concerning this process.

10.1 HYDROGEN ATTACK AT HIGH TEMPERATURES AND PRESSURES

As early as 1938, Naumann[2] considered the possibility of formation of CH_4 in connection with the hydrogen attack of unalloyed steel. However, it was not until recently that Podgurski[3] postulated that the reaction between hydrogen and cementite proceeds predominantly on grain boundaries and is as follows:

$$Fe_3C + 2\,H_2 \rightarrow CH_4\uparrow + 3\,Fe \qquad (10.1)$$

This investigator extracted CH_4 quantitatively from hydrogen attacked steel specimens. The above reaction would explain why hydrogen attack of steel is associated with decarburization which, as a rule, is followed by formation of internal fissures, resulting in a permanent loss in ductility and strength. Decarburization may also be accomplished at ambient pressure, but the temperature must be above 625 C.

Allen et al.[4] analyzed the kinetics of the attack of steel by hydrogen in terms of a chemical rate process. From the reaction of hydrogen with cementite, they derived an equation for calculation of the time necessary to attain a given CH_4 pressure. Results obtained by this equation are only in fair agreement with the experimental facts. This type of calculation does not consider a number of intermediate reactions which are part of the overall mechanism of hydrogen attack. For the methane reaction to occur inside the steel, the following sequential steps must take place: (1) hydrogen adsorption on the metal (2) hydrogen absorption into the metal (3) diffusion to the reaction sites. Carbon is furnished to these sites of high activation energy by migration of carbon atoms.

They attempted to calculate the quantity of CH_4, C_m, produced for a reaction time from the following equation.

$$C_m = C_0\,[\exp(-A)] \qquad (10.2)$$

where C_0 is the initial carbon concentration, and A a complex function of the rate constant k_1 of the CH_4 reaction and hydrogen concentration as a function of the hydrogen pressure and the reaction time. Results of numerical evaluation of Eq. 10.2, plotted in Fig. 10.1 indicate an initial rapid increasing rate of reaction between carbon and hydrogen. After an optimum value is attained, steady state is approached rapidly.

The rate of the methane reaction is primarily determined by the rate at which carbon is furnished to the reaction sites, and therefore, it is concluded that the availability of carbon atoms at internal reaction sites is rate controlling.

Steuben and Geiger[5] calculated the maximum depth of hydrogen attack, represented by fissuring to be a function of the square root of the hydrogen pressure and of the reaction temperature.

Vitovec[6] emphasized that the intensity of the hydrogen attack depends on the carbon content in solid solution, and on the rate of hydrogen absorption, and hence, on the partial pressure of the ambient gas. It is his

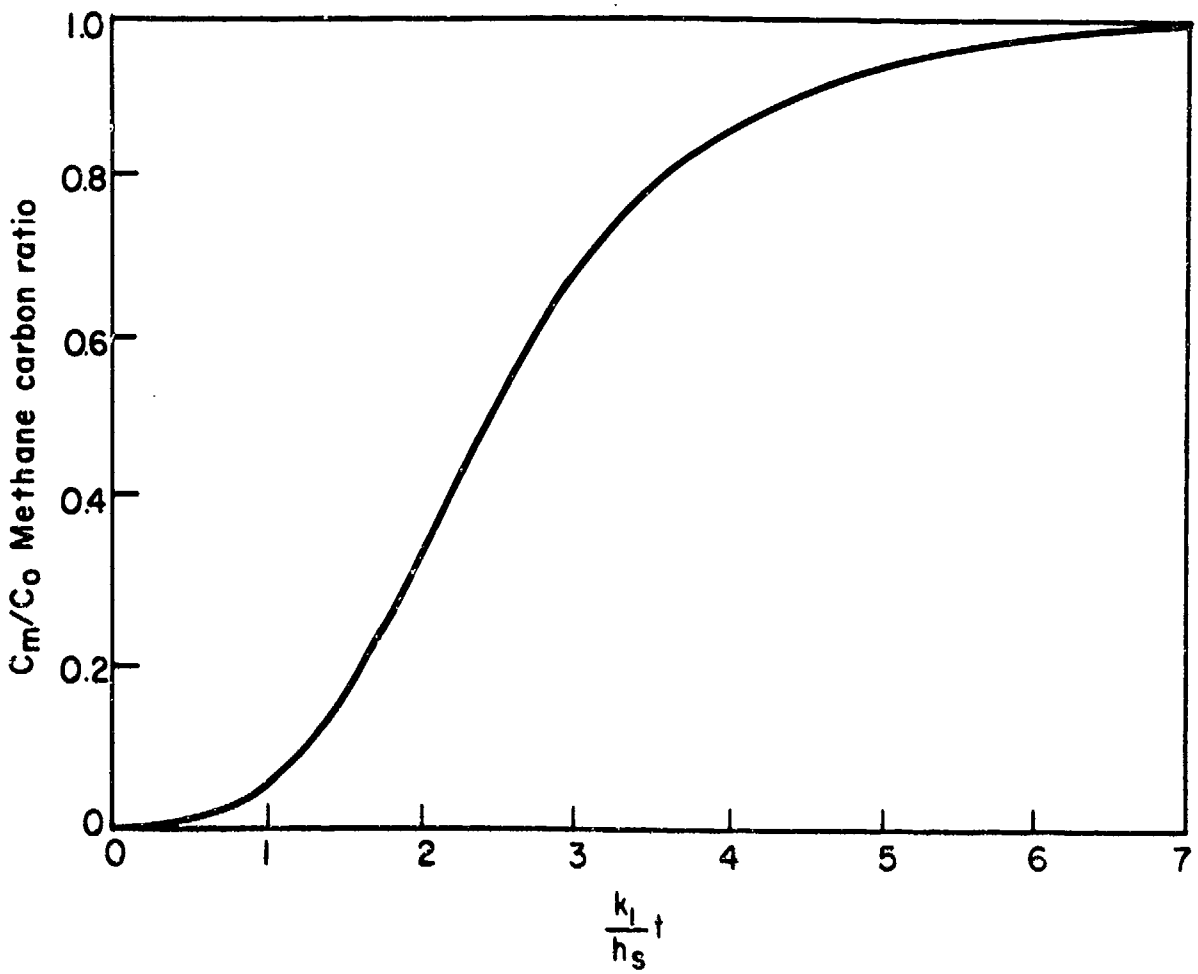

Fig. 10.1 – Relationship of the ratio C_m/C_o (the calculated methane concentration and the initial carbon concentration respectively) to the variables t, exposure time, k_1, rate constant of the methane reaction, and h_s, hydrogen solubility.

considered opinion that the growth of large fissures is preceeded by the formation of cavities, and the rate of propagation of the fissures along grain boundaries determined by a vacancy condensation mechanism. Furthermore, the effects of the methane pressure and of an applied tensile stress on the rate of fissure propagation are additively superimposed.

Thoma et al.[7] have examined the microstructure of hydrogen attacked steel and confirmed that the fissures nucleate at carbide particles and grow by consumption of carbon in the particle and growth continues by migration of fresh carbon atoms to the fissure. This explains why the steel is weakened not only by fissure formation, but also by removal of carbon from the steel structure, which finally leads to complete decarburization.

Most of the aforementioned work deals with engineering steel. Thoma et al. also investigated the stress rupture properties of very low carbon steel, attacked by hydrogen. Results obtained with this material were compared with those on steel which contained only a small quantity of carbon but in concentration sufficient to make it susceptible to hydrogen attack. The comparison was made between Ferrovac E, a vacuum melted iron containing 90 ppm of C and approximately 0.1 per cent impurities and a "decarburized" Ferrovac with only about 10 to 15 ppm of carbon. Mildly notched flat specimens were exposed in autoclaves placed in a resistance heated furnace. The experiments in argon were performed at 538 C at a pressure of 100 psig and those in hydrogen at 900 psig at a temperature of 517 C.

After argon exposure the decarburized Ferrovac contained numerous large intergranular voids and the matrix was heavily deformed, whereas after hydrogen exposure for 100 hours, the formed fissures were confined to the immediate vicinity of the grain boundaries. No changes in the mechanical properties were noted after completion

of the tests. The iron with the higher carbon content was exposed to a hydrogen environment. After completion of the test, its tensile strength was markedly reduced and the carbide grains were completely removed. According to Thoma et al., these results prove clearly that the presence of carbide is prerequisite for hydrogen attack and that the rate of this process is controlled by the velocity of carbon migration.

Addition of carbide forming alloying elements (carbide stabilizer) such as Cr, Mo, W, Ta, V and Nb to steel, substantially increased the resistance to hydrogen attack[8,9]. Biscaro and Geiger[10] discovered that by alloying a low carbon steel (Ferrovac 1020) with a small quantity of Nb, the extent and depth of hydrogen induced fissures were reduced as a result of the formation of finely dispersed stable carbides.

Non-carbide forming elements such as nickel and cobalt are not effective for increasing resistance to hydrogen attack. Also, silicon, which is used to advantage for reducing susceptibility of steel to hydrogen embrittlement, has no beneficial effect on hydrogen attack.

Austenitic stainless steel[11,12] is rather resistant to damage by hydrogen attack while a coarse grained high carbon steel is more sensitive to this type of attack than a fine grained low carbon steel.

Instructive case histories of hydrogen attack of boiler steels were presented in 1964 at a meeting of the Research Committee on Boiler Feed Water of the American Society of Mechanical Engineers [13-22] . It was emphasized that the damaged boiler tubes were all located in areas of highest heat input and many of them showed evidence of severe corrosion attack. All leaking tubes were located within cyclone burners, and evidence was found that the failures concentrated underneath corrosion products formed at an area where the metal temperature was high. No attack was observed at the cold side of the tube.

It was also reported that hydrogen damage in boiler tubes was characterized by bulging and longitudinal cracking and by complete blow out of a tube section. A close interrelation between hydrogen attack and surface oxidation was noted by other investigators. Conditions were improved materially by incorporating an organic chemical in the boiler system, which was effective in dispersing corrosion products throughout the boiler water and preventing local surface attack.

It was also reported at the meeting that hydrogen attack occured at many different locations in boilers of a great variety of designs operating at pressures from 450 to 2700 psi and temperatures between 260 to 510 C. Low carbon steel was damaged less rapidly when the iron carbide was spheroidized, or with steel of relatively high oxygen content. Addition of carbon stabilizers was again shown to be beneficial.

The next figure, Fig. 10.2, strikingly depicts examples of hydrogen damage in boilers.

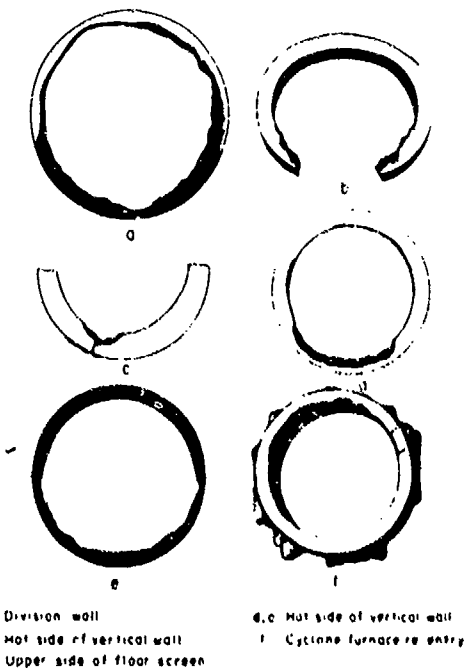

Fig. 10.2 – Hydrogen attack in boilers underneath corroded areas. Development of dark zones in areas where hydrogen attack occurred after etching with hot 1:1 HCl.

A plot showing the rapid increase in rate of hydrogen attack with increasing temperature is given in Fig. 10.3. Any cause which resulted in changes in the flow pattern within the boiler tubes was also a contributing factor and damage was found at backing rings and in bent-tube sections.

Ames and Smith designed an ingenious test loop for investigation of hydrogen attack[21] which is depicted in Fig. 10.4. The loop which takes water from the boilers is equipped with sections to which heat can be applied to

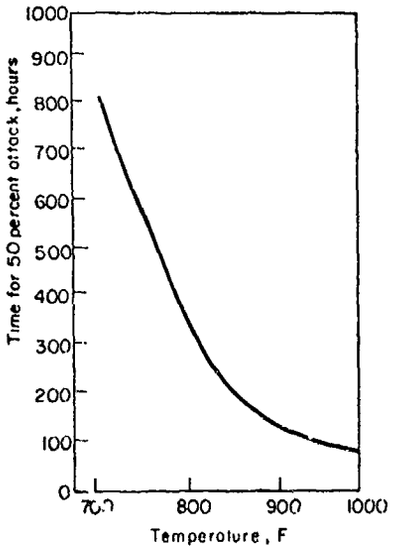

Fig. 10.3 – Plot showing relationship of increasing rate of hydrogen attack on boiler steel with increasing operating temperature.

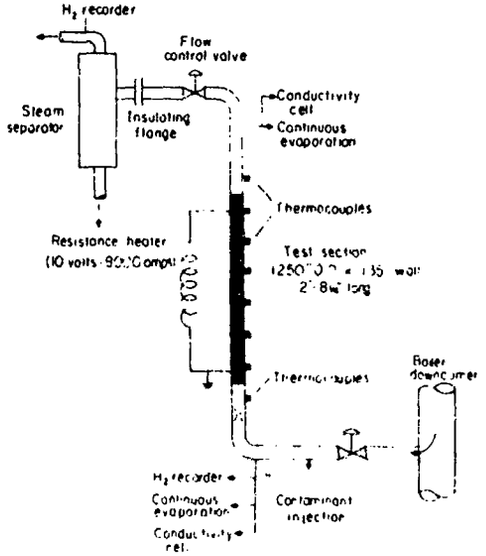

Fig. 10.4 – Embrittlement test loop used by Ames and Smith for the study of hydrogen attack.

simulate boiler conditions. Provisions are made for varying the rate of circulation and for adding contaminants to water flowing through the test sections. A large number of variables can be monitored in this device. With this set up, Ames and Smith established that an important contributing factor in hydrogen attack is contamination of the boiler water. Hydrogen attack of sections in the test loop was brought about by adding contaminants to the feed water which apparently precipitated in critical areas. It was concluded that hydrogen attack is the result of a combination of many factors, none of which can be singled out as a major factor responsible for the tube damage[22].

Hydrogen attack not only occurs on boiler walls and tubing bu. also in the synthetic ammonia process, in hydrogenation and dehydrogenation plants. In synthetic ammonia plants under working conditions where pressures range from (1500-2000 psi) the attack of coarse grained steels with ferritic and pearlitic structure is slight but becomes serious at temperatures exceeding 315 C.

10.2 EMBRITTLEMENT BY HIGH PRESSURE HYDROGEN AT AMBIENT TEMPERATURE

A number of cases will now be presented where true embrittlement is initiated in a high pressure hydrogen environment at ambient temperature. This problem has numerous important practical implications, e.g. in liquid fueled rocket engines. Since hydrogen is one of the most important fuels for hypersonic aircraft, long range space-craft, e.g., the Mariner, and very probably the nuclear rocket, it must be compatible with the many alloys (iron based and others) of the propellant system. As a rule, the investigations discussed below were made with high purity, carefully dried hydrogen.

The effect of high pressure hydrogen upon the tensile properties and fracture behavior of AISI 304 L stainless steel at room temperature was studied by Vennett and Ansell[23] and others[24,25]. The experiments were conducted on reduced section specimens and notched specimens. Exposure time and hydrogen pressure (up to 10 ksi) were varied over a wide range. It was found that high pressure hydrogen brought about a marked reduction in tensile strength and ductility. Increasing notch acuity and hydrogen pressure furthered the reduction in NTS, whereas exposure time was not a variable of significance. A prerequisite for mechanical damage was found to be a deformation induced transformation of the austenitic structure to a martensitic or ferritic structure, occurring during exposure of strained specimens to high pressure hydrogen. Conversely AISI 310, a stainless steel with a stable structure, does not transform and hence, there is only little or no loss in its tensile properties when deformed under the above described conditions.

Vennett and Ansell[23] discovered that with increasing hydrogen pressure as well as notch acuity, the mode of fracture changed from shear with a dimpled appearance to a predominantly dimpled structure, containing regions of quasi-cleavage and intergranular fracture.

In essence, these results were confirmed by Benson Jr., Dann and Roberts[26], who also investigated the mechanical properties of AISI 300 series stainless steels in a high pressure hydrogen environment at ambient temperature. They also found embrittlement of an unstable austenitic steel when strained plastically in the hydrogen environment, whereas a stable structure did not respond to hydrogen. The presence of hydrogen caused embrittlement at the martensitic structure and a definite change in the general fracture mode from a ductile to a quasi-cleavage type. These investigators suggested that hydrogen initiates microcracks in the martensitic structure.

Hofmann and Rauls and others [27-30] evaluated the effect of high pressure hydrogen on the tensile ductility of Armco iron and various steels. Their results shown in Fig. 10.5 can be interpreted in the light of a true hydrogen embrittlement mechanism.

As in the case of embrittlement produced electrolytically, ductility increased with increasing rate of testing and at temperatures exceeding ambient temperatures. Hofmann et al. confirmed that regardless of differences in the lattice structure both bcc and fcc structures were susceptible to hydrogen embrittlement.

Very recently, Walter and Chandler[31] presented the results of comprehensive tension tests on low alloy notched and unnotched specimens of high strength low alloy steels, stainless steels and other steels. Measurements were performed on specimens exposed to high pressure hydrogen at ambient temperature. Their results which offer a good picture of the present state of the art of hydrogen embrittlement of steels by high pressure, room temperature hydrogen are summarized as follows:

- The exposure time is not critical.
- Embrittlement increases with increasing pressure of the hydrogen gas environment, even when diluted with helium. However, small quantities of air added to hydrogen reduce the capability of the hydrogen to generate embrittlement.
- Decreasing the ratio of yield to ultimate strength facilitates the inducement of embrittlement.
- Increasing notch acuity, up to a limiting value, diminishes notch tensile strength and ductility.
- Non-stable types of AISI 300 series stainless steels are embrittled, but stable austenitic stainless steels are not.

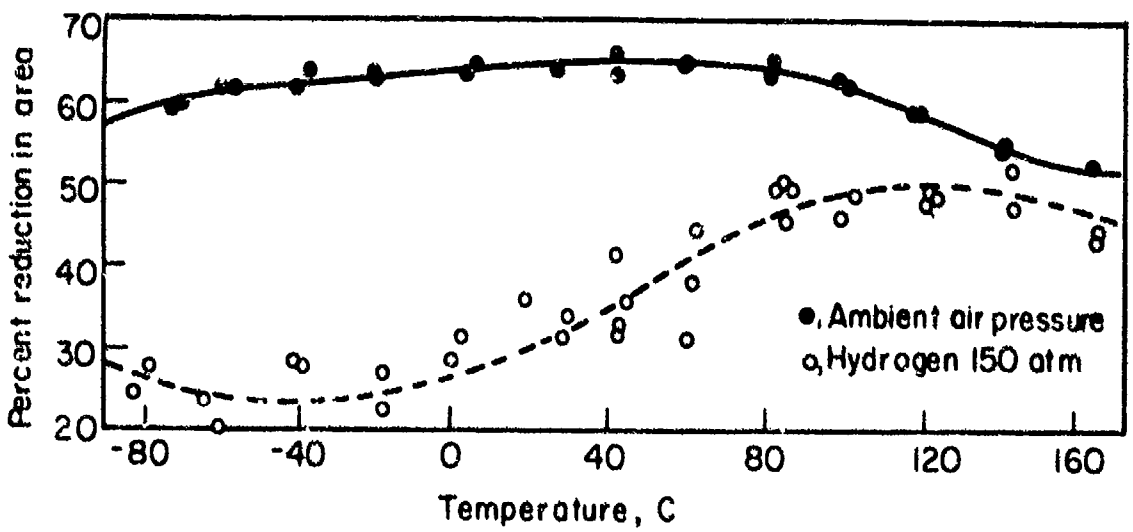

Fig. 10.5 – Effect of temperature on tensile ductility of an annealed steel exposed to air and hydrogen environments.

To explain some of the facts, summarized above, it may be assumed that the practically instantaneous accomplishment of embrittlement is the result of the high diffusivity of hydrogen atoms in a gaseous environment, particularly under conditions of increased pressure. Walter and Chandler demonstrated the exponential dependency of the tensile ductility on hydrogen pressure, which may indicate an effect on the strength of the H-H bond so that the increasing pressure gives rise to an increase in number of free hydrogen atoms available for adsorption at the solid interface.

The beneficial effect of the presence of air in the hydrogen environment, apparently is the result of a reinforcement of the oxide coating present on the steel, because Walter et al. demonstrated a markedly enhanced access of hydrogen to the metal surface after mechanical removal of the oxide barrier.

Lorenz[32] studied the effect of pressurized hydrogen on Inconel 718. Surface flawed specimens were subjected to sustained loads and flaw extension measurements were made by a polarized light technique. The effect of high purity hydrogen, pressurized to 5200 psig at ambient temperature, on the mechanical aspects of crack growth in Inconel was expressed in terms of initial and final crack sizes, applied stress levels, and calculated stress intensity parameters.

Marked hydrogen induced flaw extension and drastic reduction in fracture toughness, and hence, in the load carrying capacity of the Inconel specimens were found. Fractographic analysis of failed specimens did not reveal any definite trend in the behavior that could be traced to the metallurgical composition of the material.

REFERENCES

[1] E. E. Fletcher and A. R. Elsea, "The Effects of High Pressure – High Temperature Hydrogen on Steel", *DMIC Report*, **202**, Battele Memorial Inst., Columbus, Ohio (May 1964).

[2] F. K. Naumann, Techn. Mitteilungen Krupp, "Hydrogen Attack", pp. 207-243 (1938).

[3] H. H. Podgurski, "Trapping of Hydrogen in Cold-Worked Steel", *Trans. AIME*, **22**, pp. 389-394 (1961).

[4] R. E. Allen, R. G. Gansen, P. C. Rosenthal and E. H. Vitovec, "Analysis of Probable Mechanism of High Temperature Hydrogen Attack of Steel", *Proc. Am. Petrol. Inst.*, Div. of Refining, **42** (III), pp. 452-462 (1962).

[5] R. G. Steuben and G. H. Geiger, "Hydrogen Attack of Steel under Dynamic Exposure Conditions", *Corrosion*, **22**, pp. 309-319 (1966).

[6] E. H. Vitovec, "The Growth Rate of Fissures during Hydrogen Attack of Steels", *Proc. Am. Petrol. Inst.*, Div. of Refining, **44** (III), pp. 179-188 (1964).

[7] P. E. Thoma, E. H. Vitovec and G. A. Mullendore, "Effect of Hydrogen on the Creep Rupture Properties of Iron", *ibid.*, **46** (III), pp. 345-351 (1966).

[8] G. W. Coombs, R. E. Allen and E. H. Vitovec, "Hydrogen Attack", *Trans. ASME*, J. of Basic Eng., pp. 313-318 (1965).

[9] G. A. Nelson and R. T. Effinger, "Blistering and Embrittlement of Pressure Vessel Steels by Hydrogen", *Welding J.*, **34**, Research Suppl., pp. 12-21 (1955).

[10] R. E. Biscaro and G. H. Geiger, "Effects of Columbium Steel on Elevated Temperature Hydrogen Attack", *Corrosion*, **23**, pp. 289-296 (1967).

[11] H. K. Ehrig, "Attack of Hydrogen Nitrogen Mixtures on Steel", *Ind. Eng. Chem.*, **41**, pp. 2516-2541 (1948).

[12] I. A. Mullendore and A. Tralmer, "Hydrogen Plant Corrosion", *Proc. Am. Petrol. Inst.*, Div. of Refining, **47**, pp. 429-446 (1967).

[13] D. Y. Eposito and R. T. Harrington, "Case History: Hydrogen Damage Experience in a Boiler", *Trans. ASME*, J. Eng. Power, **86**, pp. 299-304 (1964).

[14] M. F. Nielsen, "Hydrogen Embrittlement, A Case History", *ibid.*, pp. 305-306.

[15] H. E. Bacon and E. L. Knoedler, "Case Histories of Hydrogen Damage in Boilers", *ibid.*, pp. 307-310.

[16] E. P. Partridge, "Hydrogen Damage in Power Boilers", *ibid.*, pp. 311-324.

[17] T. J. Finnegan, "Embrittlement in Boilers", *ibid.*, pp. 325-326.

[18] Y. B. Dick, "Experiences with Hydrogen Embrittlement in the Consolidated Edison System", *ibid.*, pp. 327-340.

[19] E. E. Galloway, "Hydrogen Damage in a 1250 psi Boiler", *ibid.*, pp. 341-343.

[20] R. H. Cook, "Hydrogen Damage to Two Boilers at Armstrong Power Station", *ibid.*, pp. 344-346.

[21] W. C. Ames, Jr. and R. I. Smith, "Hydrogen Embrittlement at Linden Generating Station", *ibid.*, pp. 347-349.

[22] D. E. Simon, "A Case History of Hydrogen Damage", *ibid.*, pp. 350-352.

[23] R. M. Vennett and G. S. Ansell, "The Effect of High Pressure Hydrogen upon the Tensile Properties and Fracture Behavior of 304L Stainless Steel", *Trans. ASM*, **60**, pp. 242-251 (1967).

[24] R. H. Cavett and H. C. van Ness, "Embrittlement of Steel by High Pressure Hydrogen Gas", *Welding J.*, **43**, Research Suppl., pp. 316-319 (1963).

[25] J. B. Steinman, H. C. van Ness and G. S. Ansell, "The Effect of High Pressure Hydrogen upon the Notch Tensile Strength and Fracture Mode of 4140 Steel", *ibid.*, **45**, pp. 221-224 (1965).

[26] R. B. Benson, Jr., R. K. Dann and L. W. Roberts, Jr., "Hydrogen Embrittlement of Stainless Steel", *Trans. AIME.*, **242**, pp. 2199-2206 (1968).

[27] W. Hofmann and W. Rauls, "Effect of High Pressure Hydrogen on the Ductility of Steel at Room Temperature", *Archiv. Eisenhutt*, **34**, pp. 925-934 (1963).

[28] W. Hofman and J. Vogt, "Delayed Failure of High Strength Low Alloy Steels in Air and High Pressure Hydrogen at Temperatures between 20° and 100°C", *ibid.*, **35** (6), pp. 551-559 (1964).

[29] W. H. Owens, "Effect of High Pressure Hydrogen on SAE 4140 and 1018 Steels at Ambient Temperatures", WADC Technical Report 66-269, Air Force Materials Lab. (WPAFB) Dayton, Ohio (Dec. 1966).

[30] H. Thielsch, *Defects and Failures in Pressure Vessels and Piping*, Reinhold Publishing Co., New York, pp. 355-365 (1965).

[31] R. J. Walter and W. T. Chandler, "Effects of High Pressure Hydrogen on Metals at Ambient Temperature", Contract NASA 8-19, Rocketdyne Research Division, Canoga Park, California (Feb. 1969).

[32] P. M. Lorenz, "Effect of Pressurized Hydrogen Upon Inconel 718 and 2219 Aluminum", Report prepared for Jet Propulsion Laboratory, P.O. No. EG-479375 and University of California at Berkeley, P.O. No. G845350 (Feb. 1969).

CHAPTER 11

EMBRITTLING EFFECT OF MOISTURE DURING HEAT TREATMENT

11.1 EMBRITTLING EFFECT OF MOISTURE

Zapffe[1] performed bend tests on AISI 414 stainless steel, hardened in dry helium, dry air, and steam at 1 atmosphere pressure, at temperatures ranging from 800 to 1100 C. The specimens surrounded by steam were critically embrittled. The metal fractured at very small bend angles, for hardening temperatures in the commercial range around 1000 C. The performance of AISI 410 and 430 stainless steels was similar. Both grades failed after hardening temperatures in a rather low range near 850 C, in a furnace atmosphere of steam at 1 atmosphere. At temperatures of full hardening, embrittlement was very severe.

In Fig. 11.1, results for several different grades of stainless steel are shown by shaded areas, which depict the difference in average bendability for heat treatments in dry air versus those in 1 atmosphere of water vapor. For AISI 410 stainless, the high bend value in dry atmosphere was reduced to a value as low as 10^{o}. Increasing carbon content rapidly increases the susceptibility to embrittlement, as is clearly shown by the low bendability limits for AISI 440-C steel. This grade is brittle even when hardened from a dry atmosphere. Its sensitivity to hydrogen is so great that slight amounts of moisture further reduce the bendability until a virtually glasslike condition is attained.

Bend values are also depicted for AISI 430 stainless, which is a widely used material belonging to the Class II steels which are not fully hardenable. The full bend for hardening from a dry atmosphere is reduced to values less than 60^{o} when steam is admitted to the furnace.

The above described steam phenomenon may be discussed in the light of the theory of the hydrogen potential of metal-steam reactions[2]. There is a well known process for producing hydrogen which involves the oxidation of iron by steam.

$$xFe + yH_2O \rightleftharpoons Fe_xO_y + yH_2 \qquad (11.1)$$

The subscripts x and y refer to unidentified proportions and permit the equations to be generally used for any given oxide.

By introduction of 1 atmosphere of steam into a closed container in the presence of iron, hydrogen would be developed in accordance with the above equation until equilibrium is attained. The theory of the hydrogen potential proposes that essentially such conditions prevail at the surface where steam-metal reactions proceed. Atomic hydrogen is generated from water at the instant it reacts with the metal, and then is absorbed into the steel. The calculation of the absorbed quantity, which is based on the thermodynamics of the reaction of moisture with iron, has the attributes of a pressure[2].

The effect of variation of the humidity of certain gases at room temperature on the hydrogen induced crack propagation of notched, high strength steel specimens subjected to sustained loading was discussed previously. Extensive work pertaining to the humidity effect was also done by Janiche et al.[3]. These investigators found a rapid decrease in the stress rupture life of notched high strength steel specimens with increasing humidity of the surrounding atmosphere. Time to cracking at a load of 185 kg/mm^2 (262 ksi) at 95 per cent relative humidity was about two powers of ten shorter than that at a humidity of only 20 per cent. Stress rupture life also decreased markedly with increasing steel hardness.

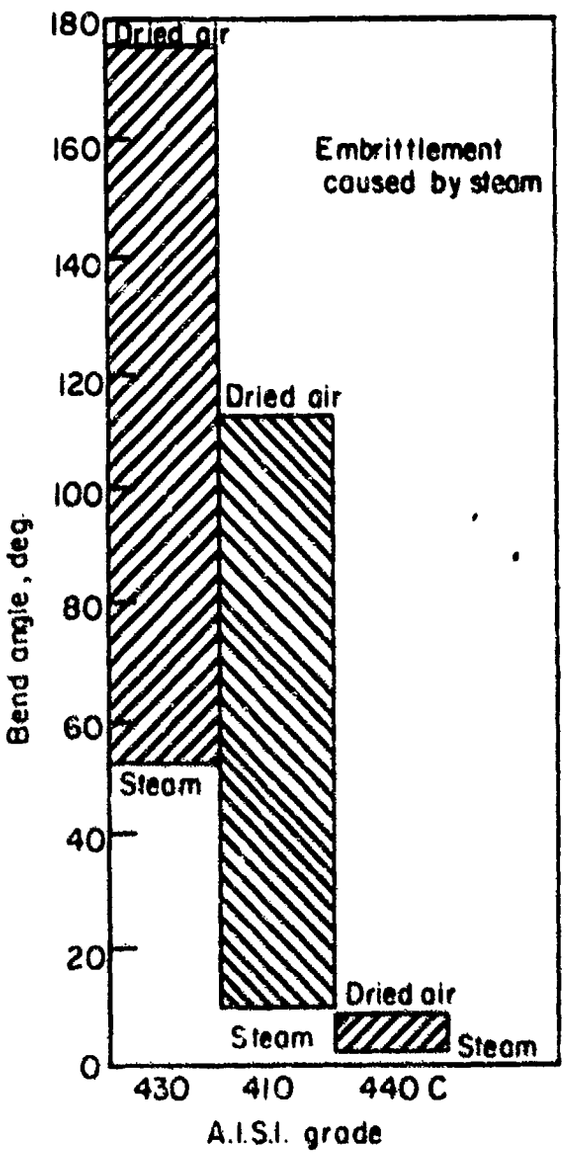

Fig. 11.1 – Bendability limits for three stainless steels given a hardening treatment in steam (1 atm. water vapor) or dried air.

REFERENCES

[1] C. A. Zapffe, "How Furnace Moisture Causes Embrittlement", *Iron Age*, Dec. 28 (1950).

[2] C. A. Zapffe, "Concept of the Hydrogen Potential in Steam-Metal Reactions", *Trans. ASME*, **40**, pp. 315-354 (1948).

[3] W. Janiche, W. Puzicha and H. Litzek, "An Investigation of the Stress Rupture Behavior of Low Alloy Steel", *Archiv. Eisenhutt.*, **36** (12) pp. 887-896 (1965).

CHAPTER 12

CAUSTIC CRACKING OF STEELS

12.1 CAUSTIC CRACKING OF STEELS

The problem of caustic cracking was studied recently rather thoroughly by Robins and Nel,[1] who emphasized its insidious nature. Caustic cracking at times progresses to a dangerous extent before indications for suspecting its existence have arisen. Indeed, in some instances, disastrous explosions have occured where evidence of its presence had either not been visible beforehand, or had not been recognized. It is commonly found in the riveted joints of boilers, and occasionally, at attachments for fittings and at the expansion of tube plates. It is not encountered where the construction is seamless or welded, except occasionally at attachments for fittings. There are also cases, where welded pipes carrying contaminated process steam, have been found to be susceptible to caustic cracking.

Microscopic examination of the damaged steel parts usually reveals the presence of one large fissure with associated secondary branching cracks taking an intergranular path through the ferrite-pearlite microstructure (Fig. 12.1).

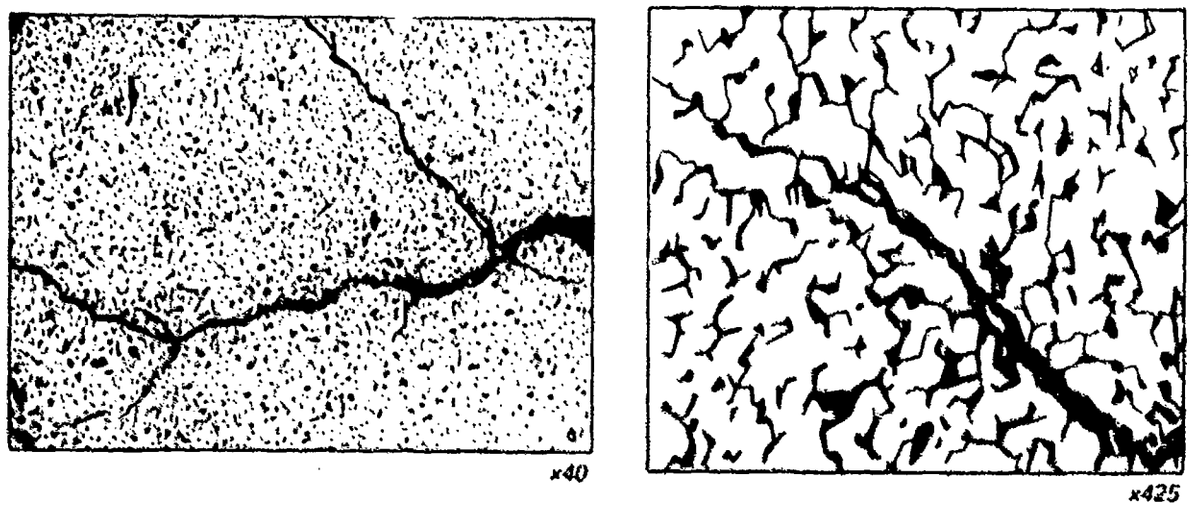

Fig. 12.1 – Caustic cracking of steel. Path of crack is intergranular through ferrite-pearlite microstructure with secondary branching cracks.

It has also been found that there is sometimes preferential attack on the carbide lamellae of the pearlite. It has been suggested that cracks of this particular type are associated with the action of caustic alkali, produced by the hydrolysis of sodium carbonate present in the boiler water[1].

It is known that strong sodium hydroxide solutions react with iron to form hydrogen. It was therefore suspected that there was a possible relationship between caustic cracking and hydrogen embrittlement. Experiments showed that appreciable damage to the steel only occurred when the concentration of the hydroxide solution exceeded the "tolerance levels" in the boiler water. It was established that, if the boiler water entered cavities invariably present in riveted seams, the subsequent loss of water vapor to the atmosphere resulted in a high concentration of the dissolved salt within the seams. When a seam, that has failed due to caustic cracking, is taken apart strongly alkaline deposits are generally found. In addition to the presence of caustic alkali in contact with the

affected part, the material must have been subjected to a tensile stress. Both practical experience and laboratory experiments indicate that the magnitude of this stress must approach closely, and most probably exceed the yield point[2].

Robins and Nel[1] emphasize that, although caustic cracking is a physical-chemical process falling under the general heading of stress corrosion or hydrogen embrittlement, the precise mechanism involved remains obscure. Therefore, they have performed a number of experiments to obtain more information about the mechanism which controls caustic cracking and to determine the effects of stress, corrosive environment, and steel quality.

Important information was obtained from exposure tests in autoclaves. The autoclaves used for these tests were designed for operation up to 350 C and 2,500 psi. Specimens were exposed as U-bend beams, stressed by means of a special jig. Exposure time was about 115 hours in a 50 per cent NaOH solution. In practice, caustic failure generally occurs in the boiler steam (200 - 250 C). For this reason, the runs were made at temperatures between 210 and 250 C. In addition to lead oxide and potassium permanganate, sodium silicate was used as a crack stimulator.

Three steels were tested, a fully killed carbon steel, designated FF, semi-killed steel, SF, and a rimming low carbon steel, RF. The effect of a number of variables on caustic cracking is compiled in Table 12.1.

The results show that the fully killed carbon steel, FF, cracked readily while the semi-killed steel, SF, showed only a slight tendency to crack. The rimming (low carbon) steel, RF was found to be most resistant to cracking attack. It was also confirmed that applied tensile stresses are particularly effective in initiating caustic cracking. In this regard, it was substantiated that caustic cracking only occurs in parts which have suffered some degree of plastic deformation. Caustic cracks always started at the surface of the steel.

It was concluded that the hydrogen embrittlement mechanism of caustic cracking is not in accordance with the experimental findings that specimens containing small cracks, previously exposed to caustic solutions, behave in a completely ductile fashion when bent slowly through 180°. The specimens stressed immediately after exposure to the caustic solutions were completely unembrittled, whereas specimens tested under conditions simulating actual steam boiler conditions, contained cracks filled with corrosion products. Robins and Nel[1] suggest, very appropriately, that the corrosive agent penetrates into the cracks as a result of capillary action. The crack propagates further into the interior of the steel and the corrosive action is then concentrated on the small anodic region at the crack tip. They suggest that this is a typical case of stress corrosion and hence conclude that the hydrogen embrittlement mechanism of caustic cracking should be abandoned in favor of this corrosion mechanism.

More light was shed on the mechanism of caustic cracking by experiments performed recently by Wenczel and Wranglen[2]. These investigators subjected stressed vacuum annealed high strength carbon steel wire to anodic and cathodic polarization at a temperature of 100 C in solutions of NaOH (20 to 60 per cent), using a potentiostatic technique. In general, they did not find a reduction in fracture strength or elongation under the cathodic conditions of hydrogen evolution. However, under anodic polarization there was a reduction in fracture strength. They conclude that caustic cracking is not caused by embrittlement by hydrogen, but by a stress corrosion phenomenon and are in agreement with those of Robins. Much additional work is required to unequivocally establish the controlling mechanism.

A more detailed discussion of the problem of differentiation between hydrogen embrittlement and stress corrosion was presented in Chapter 6.

TABLE 12.1 THE EFFECT OF STEEL COMPOSITION ON CAUSTIC CRACKING IN 50 PER CENT NaOH SOLUTION.

Spec. No.	Sodium Silicate % Equivalent	Exposure Temp. deg. C	% Max. Load	Exposure hr.	Remarks
SF14	0.3	210	100	112.30	No cracks after exposure and bending through 180°
SF15	0.3	210	91.0	112.30	
SF16	0.3	210	96.3	112.30	
SF17	0.3	210	97.9	112.30	
FF14	0.3	210	100	112.50	Large Cracks
FF15	0.3	210	89.3	112.50	Fine Cracks
FF16	0.3	210	96.3	112.50	Fine Cracks
FF17	0.3	210	98.0	112.50	Fine Cracks
FF68	3.0	250	100	24	Large Cracks
FF69	3.0	250	100	24	Large Cracks
FF70	3.0	250	80	24	Fine Cracks
FF71	3.0	250	80	24	Fine Cracks
SF23	3.0	250	100	24	No Cracks
SF24	3.0	250	100	24	No Cracks
RF19	3.0	250	100	24	No Cracks
RF20	3.0	250	100	24	No Cracks
FF67	4.0	250	100	24	Large Cracks
FF68	4.0	250	100	24	Large Cracks
SF21	4.0	250	100	98.30	Fine Cracks
SF22	4.0	250	100	98.30	Fine Cracks
RF18	4.0	250	100	98.30	No Cracks
RF18	4.0	250	100	98.30	No Cracks

N.B. 100% max. load is the peak in the stress-strain curve.

*The sodium silicate % equivalent is the amount of silicate present as a percentage of the NaOH in solution.

REFERENCES

[1] F. P. A. Robins and L. G. Nell, "A Contribution to the Study of Caustic Cracking", *Proc. 2nd. International Congress on Metallic Corrosion,* New York, pp. 172-183 (1963).

[2] J. Wenczel and J. Wranglen, "Electrochemical Studies on Stressed Steel Wires Exposed to Strong Sodium Hydroxide and Nitrate Solutions", *Corrosion Sci.*, **4**, pp. 137-158 (1964).

CHAPTER 13

CATHODIC PROTECTION OF STEEL TO MINIMIZE CORROSION

13.1 HYDROGEN EMBRITTLEMENT OF CATHODICALLY PROTECTED STEEL

Cathodic protection is often applied to steel parts that are exposed to corrosive environments in service. The objective is to maintain strength or load carrying capacity of the part by preventing corrosion which would reduce the effective cross sectional area. As strength levels and attendant design stresses of the steel are raised, it becomes progressively more important to protect against corrosion and avoid embrittlement. McEowen and Elsea[1] recently emphasized that in any cathodic protection system that is commercially feasible, the cathodic potential will usually be such that some atomic hydrogen is deposited on the surface of the steel cathode. This may cause loss in ductility in low to medium strength structural steels, or produce defects such as internal bursts, fish eyes, shatter cracks and blisters. When hydrogen enters high strength steel parts that are under a sustained tensile stress, hydrogen stress cracking may occur also. McEowen and Elsea considered gas transmission pipe lines to be subjected to most of the conditions necessary to produce hydrogen embrittlement. The steel pipe is under a sustained tensile stress in the circumferential direction as a result of the internal gas pressure and hydrogen is continually deposited on the cathodically polarized surface. Hydrogen stress cracking has not been a problem in pipe lines in the past, primarily because low strength level steels have been employed. However, it could become a problem with the trend toward the use of progressively higher strength steels in the manufacture of line pipe. The above investigators have estimated that at design or service stresses above a 150 ksi level, hydrogen embrittlement may become a problem in cathodically protected line pipes. McEowen[1] reported the occurrence of a limited number of failures on cathodically protected pipe lines during the last fifteen years, which were probably initiated by hydrogen. According to estimates of representatives of gas transmission companies, the minimum pipe to soil potential, required for adequate protection of coated pipe lines in most soils is -0.85 volt, but may exceed -1.50 volts at positions near the anode. They generally used the $Cu/CuSO_4$ half cell as the reference electrode. Current densities at holidays, usually range from about 3 to 100 mA/ft^2 but may be as high as 1000 mA/ft^2 near the anodes.

Bruckner and Miles[2] conducted a laboratory study in order to explore the possibility of inducing hydrogen embrittlement in hot rolled steel pipe sections subjected to cathodic polarization. They used three types of steel representative of API* grades A, B and M (N-80) with ultimate tensile strengths of 60.8, 70.6, and 115.9 ksi, and yield points of 38, 46.8, and 89.3 ksi, respectively. The cathode under study was placed in the center of a cylindrical glass jar along with the graphite anode which concentrically surrounded the cathode. Soil was placed in the space between the electrodes and saturated with the desired electrolyte. The cathode was made up of six ring sections cut from the as received pipes which were ground on the cut surfaces and assembled on a steel mandril, as shown in Fig. 13.1.

The rings assembled on the mandril were put under axial compression by means of a bolt and cap arrangement, thus closing the gap between cut and ground surface and providing essentially a continuous cathode. After completion of the polarization period, the sections were disassembled and placed vertically in a jig contained in a metal box filled with a dry ice-acetone mixture. At a temperature of -50 C, a load was slowly applied at a predetermined rate to provide plastic deformation in bending across the horizontal diameter.

The specimens were exposed for 2, 4, and 5 months. The potential affording cathodic protection to the steel was -0.85 volt versus the $Cu/CuSO_4$ reference electrode, and the corresponding cell current was 1 mA/ft^2. Two pH ranges of soil water were used, 7.2 to 8.4, and 2.5 to 3.5. For overprotection, a polarization potential of -1.32 volts was applied and maintained. A number of runs were made with mill scale removed. Some runs were conducted in solutions with the lower pH containing 5 g FeS per liter.

The results indicated that for steels A and B, bend ductility was reduced and crack formation was moderately severe, a behavior related to the formation of notches at the metal surface. When the mill scale was completely removed by mechanical means, there was evidence of hydrogen embrittlement, associated with severe

*American Petroleum Institute

crack formation in grade A steel. The presence of mill scale apparently diminished embrittlement appreciably by increasing surface resistance. The most embrittling conditions were noted for exposure at -0.8 volt in the low pH soil water containing FeS. Even with the mill scale present, excessive overprotection makes embrittlement worse under all conditions. Bruckner and Miles[2] state that the conditions of low and high sulfide concentration could be present in marsh soil, i.e. result of wetting with brackish water, or by the presence of sulfate reducing bacteria. According to the experimental data such conditions would practically assure embrittlement by hydrogen of numerous types of cathodically protected steels, including A and B steels.

Type M steel maintained a high embrittlement resistance, when closed tube sections internally stressed to near the yield point, were exposed under conditions of excessive cathodic protection. These conditions are considered to be very severe.

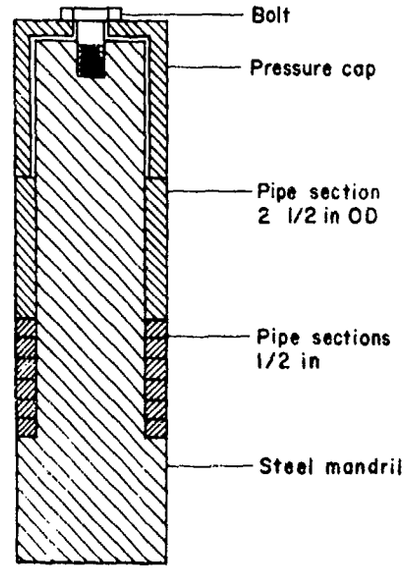

Fig. 13.1 – Schematic of assembly used in laboratory studies for hydrogen embrittlement in hot rolled steel pipe sections subjected to cathodic polarization.

The possibility of producing hydrogen embrittlement in high strength ship hull steels, under cathodic protection, was discussed by Geld and Acampora[3]. These steels are used extensively for submarines and deep diving vehicles. Based on experimental evidence, they conclude that dangerous conditions may be produced at breaks in paint coatings or dielectric shields covering the anodes and, as a result, high local current densities may be generated, particularly when relatively high protective currents are applied.

Hudson et. al[4] consider the electrochemical device used for measuring hydrogen permeation through iron membranes (Chapter 2), a suitable model for reproducing the electrolytic conditions prevailing on the outside surface of buried pipe, subjected to cathodic polarization. They polarized steel at the hydrogen entrance side galvanostatically. The polarization potential was maintained at -1.3 to -1.4 volts vs $Hg/HgSO_4$ electrode, which corresponds to a potential of -1.0 to -1.1 volts vs the $Cu/CuSO_4$ scale. This is close to the minimum potential of -0.85 volt vs $Cu/CuSO_4$ electrode maintained in cathodic protection systems. In the pH range from 4 to 9, the quantity of hydrogen permeating the steel membrane increased with cathodic polarization. Concentrations of total sulfide greater than 0.02 ppm (Na_2S added to Na_2SO_4 solution), increased the quantity of generated hydrogen.

REFERENCES

[1] L. J. McEowen and A. R. Elsea, "Behavior of High Strength Steels Under Cathodic Protection", *Corrosion*, **21**, pp. 28-37 (1965).

[2] W. H. Bruckner and K. M. Miles, "Studies of the Susceptibility of Cathodically Protected Steel to Hydrogen Embrittlement", *ibid.*, **15**, pp.591t-595t (1959).

[3] I. Geld and M. A. Acampora, "Current Densities: A Factor in Hydrogen Embrittlement of Cathodically Protected Steels in Sea Water", *Mater. Protection*, **7**, pp. 31-34 (1968).

[4] P. E. Hudson, E. S. Snavely, Jr., J. S. Payne, L. D. Field and N. Hackerman, "Adsorption of Hydrogen by Cathodically Protected Steel", *Corrosion*, **24** (7) pp. 189-196 (1968).

CHAPTER 14

CHEMICAL PROCESSING

14.1 SOME PARAMETERS CONTROLLING PICKLING EMBRITTLEMENT

This section deals principally with hydrogen embrittlement resulting from acid and cathodic pickling. Frequently it is necessary to pickle steel parts to remove heavy scale when mechanical means such as vapor blasting cannot be used. Hydrogen is generated during acid pickling and may embrittle the steel. Thus, embrittlement is closely associated with the hydrogen evolution reaction, which in turn is controlled by the dissolution rate of the steel exposed to a specific acid. The dissolution rate depends on the hydrogen ion concentration, the temperature and the characteristics of the steel. (The mechanism of hydrogen embrittlement control by pickling inhibitors is discussed in Chapter 18.)

Zapffe[1] et al. comprehensively studied the embrittlement of low carbon and stainless steel wires exposed to different acids. The test specimens were annealed, annealed cold-drawn, hardened, or in hardened cold-drawn conditions. They were pickled by immersion in 10 per cent H_2SO_4, and 50 per cent by volume HCl, 4N H_3PO_4 and CH_3COOH for increasing times up to 120 minutes. Bend angle measurements were made with the bend testing machine described previously in Chapter 1.

Cathodic pickling runs were made in 2.5N NaOH solution, generally at 122 F using 1 A/in^2 current density. The susceptibility of any type of cathodically pickled steel tested, increases in the following sequence:

- Annealed
- Annealed, cold-drawn
- Hardened
- Hardened, cold-drawn

Stainless steels with martensitic structure were found to be the most sensitive to hydrogen embrittlement. It was observed also that increasing the carbon content increases the susceptibility of any type of hardened steel. Annealed AISI 410 and 431 stainless steels resist embrittlement even when in the cold drawn condition. In general, stainless steels are less susceptible to acid pickling than they are to cathodic pickling. AISI 410 stainless is not susceptible in any condition. This is true also for AISI 1060, 1090, and 431 steels in phosphoric and acetic acids. However, 431 steel in the hardened and cold drawn condition, is embrittled in dilute sulfuric or hydrochloric acid. Types 440-C stainless and 1020 mild steels behave similarly to 431 steel (440-C contained 17.08% Cr, 0.52% Mo and 1.08% C).

The effect of cathodic pickling or acid pickling time on the embrittlement of AISI 1020, is illustrated in Figs. 14.1 and 14.2[2]. The similarity in the trends, the marked decrease in bend ductility of the two curves for the 1020 steel is striking. The marked differences in the rate of decrease in ductility are due to the differences in the mechanisms of the hydrogen evolution reaction.

Results of studies by Zapffe and Haslem on the dependency of ductility on the concentration of various acids are pictured in Figs. 14.3 and 14.4. Analysis of these curves, revealing rather unusual trends, may be based on the theory of the electrolytic dissociation of strong and weak acids[3].

According to this theory the hydrogen ion (hydronium ion) concentration for strong acids, such as sulfuric and hydrochloric, increases in dilute aqueous solutions because of their nearly complete dissociation into ions. (Strong and weak refer to the degree of ionization. Dilute and concentrated refer to relative concentrations). This explains why in a concentration range up to about 0.1N the bend ductility falls rapidly (Fig. 14.3). However, there is a limiting concentration, above which the dissociation increases only slightly. This is reflected in the fact that in the concentration range from 0.1N to about 10N, ductility decreases only slightly. However, when the acid concentration exceeds 10N, the hydrogen ion concentration rapidly decreases, and relatively high values of ductility are measured. It is evident from the data that a very large increase of the concentration of a strong pickling acid does not increase but decreases pickling effectiveness.

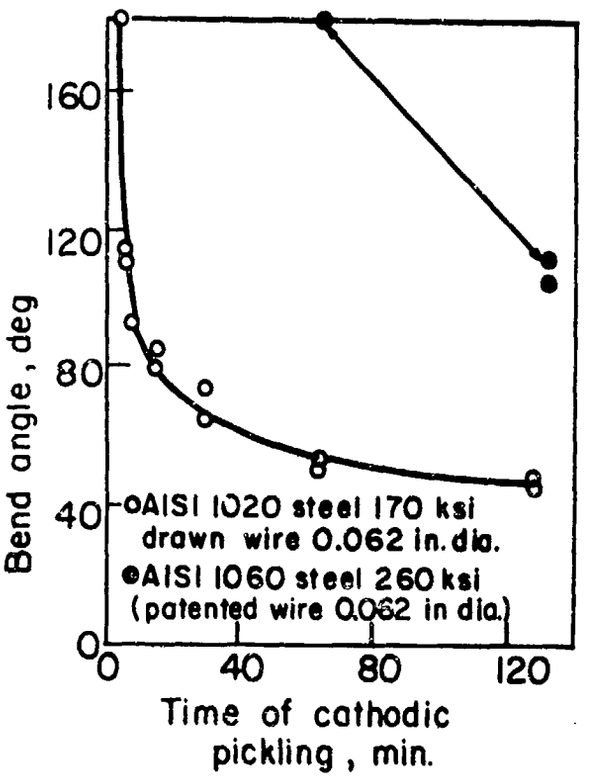

Fig. 14.1 – Effect of cathodic pickling on bend ductility of steel wires (2.5N NaOH, 1A/in^2 at 122 F).

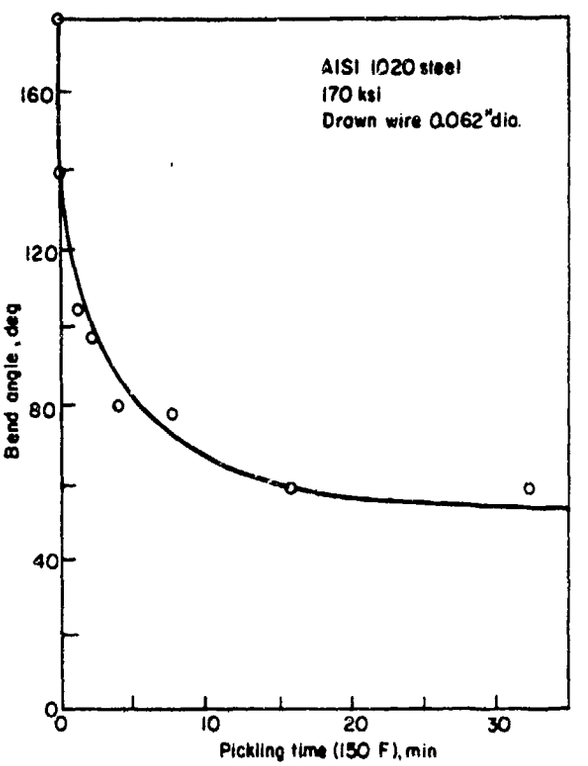

Fig. 14.2 – Effect of time of acid pickling (3.7N H_2SO_4) on bend ductility of cold drawn steel wire.

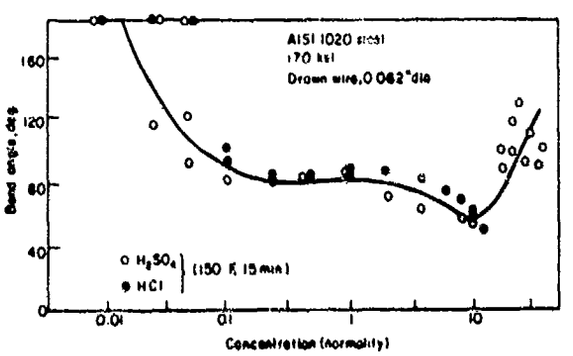

Fig. 14.3 – Effect of concentration of strong acids on bend ductility of cold drawn steel wire.

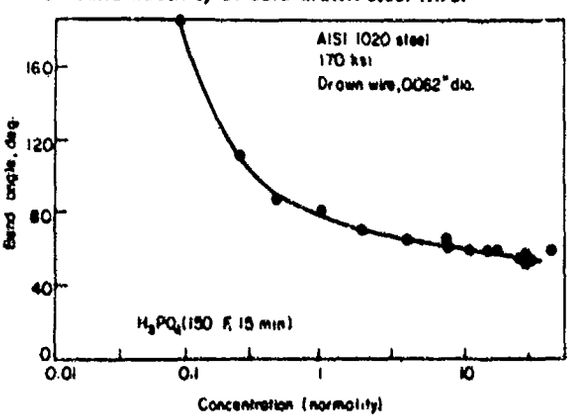

Fig. 14.4 – Effect of concentration of a weak acid on bend ductility of cold drawn steel wire.

On the other hand, relatively weak acids dissociate slightly and, thus, there are insufficient ions present to initiate the hydrogen evolution reaction until the acid concentration exceeds a limiting value (about 0.1N for H_3PO_4). From this limiting value up to a 1N concentration the bend angle rapidly decreases as can be seen in Fig. 14.4. For H_3PO_4, a weak acid, the concentration range where the effect on bend angle becomes very slight is between 1 and 10N, whereas for strong acids the range begins at a concentration as low as 0.1N. Also the rapid increase in ductility in strong acids in concentrations from 10 to 15N (Fig. 14.3) does not occur in the weak acid (Fig. 14.4).

Another important variable is the temperature as can be seen in Fig. 14.5. Embrittlement increases rapidly with increasing temperature up to about 100 F during sulfuric acid pickling. However, for temperatures above 100 F, embrittlement increases only very slightly with temperature. This is explained by the fact that in the temperature range between about 100 F and 180 F, there is practically an equilibrium state between hydrogen atoms diffusing into the metal to those diffusing out.

It has been emphasized that the presence of inclusions, particularly sulfide[4], increases hydrogen absorption and hence pickling embrittlement. Grain size may also effect hydrogen absorption[5].

Groenevelt et al.[6] reviewed the literature dealing with pickling and cleaning procedures as sources of hydrogen embrittlement. This review provides a valuable reference on these procedures.

14.2 CHEMICAL MILLING AND HYDROGEN EMBRITTLEMENT

This problem was studied by Convair Astronautics[7], using a free end-loaded bend test performed at a variety of bending speeds. The milled surface was made the tension side during testing. Longitudinal test specimens were fabricated from AISI 4340 steel test coupons, and heat treated to a hardness of R_C 52. The slender column specimens loaded in compression, were described in detail in Chapter 1.

The chemical milling was performed in the laboratory using baths similar to those employed commercially. The AISI 4340 steel was milled in the bath given below at a temperature of 140 F.

Chemical Milling Bath

HCl	– 15 volume per cent
HNO_3	– 17 volume per cent
H_3PO_4	– 31 volume per cent
H_2O	– 37 volume per cent
Fe	– 4g/liter

The milling rate at this temperature was about 1 mil/min. However, there was a small change in this rate depending on loading of the bath. The bath was replaced with a new solution when the milling rate decreased by a factor of 10 per cent. The bend test samples were chemically milled on one side only. Sheet materials, 0.050 gage and 0.060 gage, were milled to 0.040 gage. Immersion time in the milling bath was about 10 minutes for the removal of 10 mils of metal and 25 minutes for 20 mils of metal. The average values of the bend ductility of the steel, tested immediately after milling, as a function of testing speed are shown in Fig. 14.6.

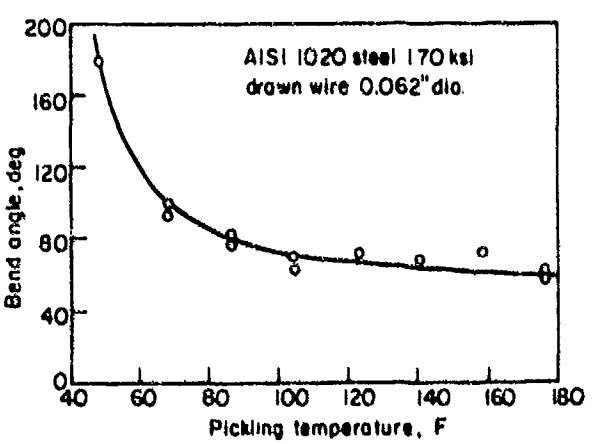

Fig. 14.5 – Effect of temperature of pickling acid on bend ductility of cold drawn steel wire (1N H_2SO_4 – 15 min.).

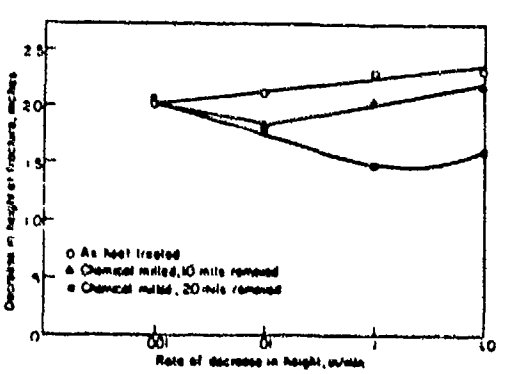

Fig. 14.6 – Dependency of the bend ductility on the rate of bending (decrease in height). Longitudinal slender column specimens, AISI 4340 steel, R_C52, milling temperature 140 F.

The removal of 10 and 20 mils of metal resulted in hydrogen embrittlement of the steel. As might be expected, more severe embrittlement was found in samples that were in the chemical milling bath the longer time. The effect of testing speed on bend ductility is somewhat unusual. Generally, hydrogen embrittlement in steels

shows up more readily at low rates of bending. However, the opposite appears to be true in this study and is especially seen where 20 mils of metal were removed. Embrittlement is severe at the higher rates of bending, but tends to decrease at the lower ones. This may be explained by the high diffusion rate of hydrogen in steel at ambient temperature. It seems entirely possible that the disappearance of hydrogen embrittlement at the slow testing speeds is simply related to the loss of hydrogen by diffusion from the steel during the longer times required for the test.

They concluded from their study that it appears that a delay period longer than 8 hours, but shorter than 33 hours is required for complete restoration of bend ductility. It is possible that the strain gradient established in the bend specimen during testing promotes the diffusion of hydrogen out of the steel and, if this is true, longer delay periods, or elevated temperature recovery treatments may be required to completely eliminate hydrogen embrittlement in unstressed specimens. As a consequence of these findings, it has been clearly established that hydrogen diffuses out of the milled bend samples during the test. In addition, the use of the free end loaded bend test to detect hydrogen embrittlement in chemically milled AISI 4340 steel sheet has been established and is considered to be more reliable than other types of bend tests employed to date[7]. Less embrittlement is produced in AISI 4340 steel from chemical milling than from cadmium plating, as would be expected. Consequently, embrittlement is more easily removed from chemically milled material. Another factor is the absence of the barrier action of the cadmium plate.

Hydrogen embrittlement produced by chemical milling of H-11 steel was studied by Ketcham at the Naval Air Development Center[8]. For this work, a transverse, double edge notched flat specimen was designed with a notch that could be milled from a radius of 0.030 to 0.050 in. Three heats were included in the study of the steel with strength levels ranging from 270 to 290 ksi. The chemical milling procedure is presented in the following table.

TABLE 14.1
CHEMICAL-MILLING PROCEDURE

- Vapor hone
- Chem-mill in a bath composed of H_2SO_4 + HNO_3, Temp. 140 F.
- Scrub to remove smut
- Water rinse

Specimens, which did not fail after 500 hours under a sustained load of 85 per cent of the notch tensile strength, were considered to have a stress rupture life of infinite length.

The results may be summarized as follows: The bath used for chemical milling in this study produces hydrogen embrittlement, however, complete recovery takes place at room temperature within one week, or by storage for 48 hours at room temperature followed by baking at 357 F for 4 hours. The results of the sustained load delayed failure tests are in good agreement with the bend tests performed by Convair Astronautics.

14.3 PAINT REMOVERS AND CLEANING COMPOUNDS

As has been stressed by a number of investigators, hydrogen embrittlement induced by acid pickling processes, chemical milling and phosphatizing has been a recognized problem for some time. Jankowsky and his colleagues[9] at the Naval Air Development Center, however, have rightly emphasized (1964) that until fairly recently little thought was given to the possibility that hydrogen embrittlement might also be produced by paint remover and cleaning materials that inadvertently come in contact with high strength steel parts. This situation could occur during routine overhaul and repair procedures normally considered safe from this problem.

A comprehensive study was made using the notched C-ring test procedure. These investigators used AISI 4340 steel heat treated to the 230 ksi strength level and in most experiments, the ring was prestressed to 75 per cent of its breaking strength. The geometric stress concentration factor of the shallow notch was about K_t=4. Test stresses of this magnitude have been generally accepted as realistic for hydrogen embrittlement testing by aircraft companies and government agencies.

Two different types of exposure tests were performed. In one test the ring was kept totally immersed in the paint remover or cleaning solution, while in the other test, the ring was dipped into the solution and then left in the air for the test period or until fracture occured. The first of the above test conditions (total immersion) represents situations which could exist if cleaning materials were trapped in a pocket which could not easily be rinsed out, and would represent a very unfavorable condition.

The purpose of the "dipping" test was to find out what might happen if the maintenance compound used on the steel was not properly rinsed away. This condition (dipping) is more likely to occur than that for total immersion. It must also be realized that it is quite possible for cleaning or paint stripping materials to be trapped in pockets (representative of the total immersion test), if inadequate masking is employed. A 200 hour life time was considered indicative that the specimens would not fail.

Dip tests were performed only on materials that failed the total immersion test as described above. Some representative results are compiled in Table 14.2.

The results clearly indicate that in the case of the highly acidic stripper S, the stress rupture life is negligibly short. All of the tested stripper materials, when used on cadmium plated rings are considered potentially dangerous. Only stripper H may be considered harmless on unplated rings. Hydrogen cracking induced by cadmium plating generally decreases markedly the failure time in alkaline paint stripper solutions. This was tentatively explained by the formation of embrittling cathodic hydrogen in the galvanic couple Fe/Cd. However, generation of hydrogen by chemical reaction of the complex stripping system with cadmium is also possible [10] *.

Useful information about the crack inducing mechanism in stripper solutions might have been obtained by pH measurements at the end of the exposure period along with exposure experiments with cadmium plated rings in pure alkaline solutions.

Based on his results Janowsky concluded that great care must be exercised in masking high strength steel parts on which paint strippers may drip, and that all cleaning and paint stripping materials should be rinsed off as soon as possible after use. He recommended that all materials that cause failure of cadmium plated notched C-rings, be prohibited for use on naval aircraft in any application where there is any possibility of these materials coming in contact with high strength steel parts.

*The mechanism is under further investigation at the Naval Air Development Center.

TABLE 14.2

STRESS RUPTURE LIFE OF NOTCHED C-RINGS EXPOSED TO DIFFERENT PAINT REMOVERS. AISI 4340 STEEL (230 ksi), PRESTRESSED TO 75% OF THE BREAKING STRENGTH, K_t=4.2. RESULTS OBTAINED ON TWO STATISTICALLY REPRESENTATIVE SPECIMENS.

Paint Remover Symbol	Initial pH	Surface Treatment	Test	Time to Failure Hours	Test	Time to Failure Hours
H	9.6	-	Total Immersion	>200	Dip	>200
		+		1.7		1.0
		+		25.2		1.4
I	10.4	-		3.6		200
		-	Total	6.8	Dip	40.0
		+	Immersion	3.0		1.6
		+		0.5		1.6
L	9.0	-		2.8		
		-	Total	4.8	Dip	>200
		+	Immersion	0.1		20.8
		+		1.2		3.4
S	<1	-		0.4		1.9
		-	Total	0.5	Dip	0.6
		+	Immersion	0.4		0.2
		+		0.5		1.9

Paint Remover		Surface Condition	
H	– Alkaline epoxy	-	Bare specimen
I, L	– MIL-R-8633A, (QPL)	+	Cyanide Cd plated (0.0005 in. coating)
S	– Acidic epoxy		

14.4 EMBRITTLEMENT OF HIGH STRENGTH STEELS BY PRETREATMENT WITH ETCHING PRIMERS

Recently Andrew and Spencer-Timms[11] have given rather convincing evidence that hardened 17-Cr steel is embrittled when treated with certain types of etching primers. These primers are used to improve the adhesion of subsequently applied paint coatings. An etching primer generally consists of a resin (epoxy or polyvinyl butyrate), an acid constituent, and a solvent. It is applied by dipping, brushing, or spraying, and air drying for 1 hour at room temperature. The primer used had an acid component of 3.5 per cent ortho-phosphoric acid. So called two-pack primers were also studied, and in contrast to the above single pack primers, are chromate pigmented.

Slow bend tests were performed on steels with an UTS of 280-300 ksi. The rate of bending was 180°/min. over a 0.5 in. diameter mandril. The specimen was 4 x 2 x 16 in. Results indicate that there was embrittlement; however, ductility was completely restored by baking for 1 hour at 100 C.

14.5 PHOSPHATIZING

Phosphate coatings are used to prevent corrosion of iron surfaces. Phosphatizing consists of chemically treating steel with a dilute acid phosphate solution, to produce an insoluble crystalline phosphate conversion coating on the surface.

An important application of this coating is for steel springs[12] and bolts, which are subsequently coated with an oil or paint film. If springs are stressed immediately after coating, or contain high residual stresses, they may fail in a delayed fashion as a result of hydrogen pick-up during phosphatizing.

Phosphatizing baths used for producing manganese or zinc base coatings (MIL-P-16232 C) have been found to be particularly embrittling, because they contain free acid. Another contributing factor is that the coatings are frequently post treated in hot chromic acid. The free acid content of manganese phosphatizing solutions exceeds that of the zinc phosphatizing solutions.

Bessey and Hawthorne[13] of Springfield Armory determined the tensile ductility of AISI 1060 steel heat treated to average hardness levels of R_C 48 and 55. The specimens were grit blasted prior to processing, and manganese or zinc phosphatized. Tension tests made at a crosshead speed of 0.081 in./min showed a definite decrease in ductility.

Aging and baking methods have been suggested for relieving hydrogen embrittlement. Zinc phosphatized specimens were aged for 54 hours at room temperature, or heated for 15 minutes at 200 F, while manganese phosphatized specimens were aged for 60 minutes at the same temperature. However, according to Bessey et al, these treatments did not provide a satisfactory increase in the tensile ductility at either of the two hardness levels mentioned above.

Wolff[14] of Rock Island Arsenal worked with two types of steel, AISI 1045 and 1095. Specimens were notched cylindrical tensile bars heat treated to a hardness level of R_C 50. Sustained load tests were performed on specimens stressed to 75 per cent of the untreated NTS. A life time of 200 hours was considered to be indicative of no damage. All runs were made with zinc phosphatized specimens. Fifty per cent were abrasive grit blasted prior to phosphatizing. An 8 hour baking time at 210 F was found inadequate for embrittlement relief of the 1095 steel, except where the surface had been abrasive grit blasted. For an unblasted 1045 steel surface, a baking time as long as 24 hours did not provide satisfactory embrittlement relief. However, a 48 hour bake at 210 F was effective. Air aging for 120 hours was not adequate for relief of the steels. Wolff considered that blasting pretreatment produced beneficial effects by introducing compressive stresses into the surface, and by increasing the surface area, which facilitates rapid release of the adsorbed hydrogen. The favorable results with the grit blasted surfaces confirm those obtained by Bessey et al.

Austin, Chek and Lurie[15] studied the hydrogen embrittlement problem in phosphatized AISI 4340 and 1095 steels heat treated to various strength levels. Notched tension specimens were loaded to 80 per cent of the NTS in stressing ring fixtures (Chapter 1). Bars with at least 1000 hours life time were considered to be unembrittled. A manganese phosphatizing bath (MIL-P-16232C) was used with the composition limits of 0.20 to 0.35% Fe and a free acid to total acid ratio of 1:53 to 1:60 as recommended by the phosphate coating manufacturers. Their results are portrayed in Figures 14.7, and 14.8.

Figure 14.7 shows that for the highest hardness levels of R_C 52-56, a 6 hour baking time is satisfactory. Fig. 14.8 shows that 128 hours of room temperature aging is sufficient for successfully relieving hydrogen embrittlement.

Austin et al. emphasized that specimens which were coated in baths maintained within the standard

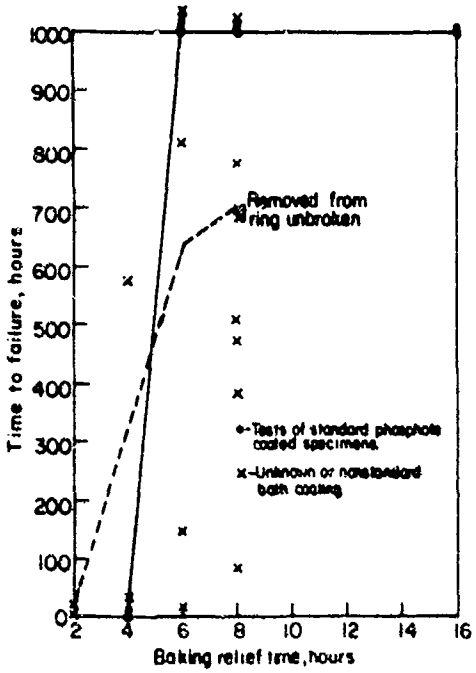

Fig. 14.7 – Effect of baking times at 210 F on relief of hydrogen embrittlement in phosphate coated (type MIL-P-16232) specimens. AISI 4340 steel notched specimens, R_C 52-56. Load sustained for 1000 hours indicates complete relief.

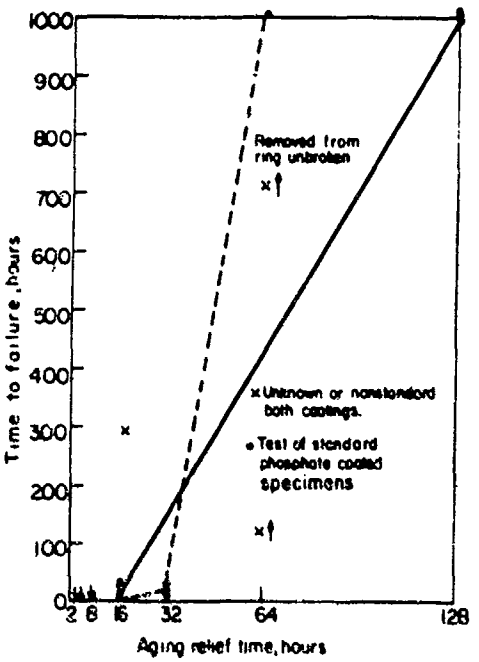

Fig. 14.8 – Effect of room temperature aging on hydrogen embrittlement of phosphatized (Type M, MIL-P-16232) steel. AISI 4340 notched specimens, R_C 52-56. Load sustained for 1000 hours indicates complete relief.

composition limits, recommended by coating manufacturers, could be consistently relieved of embrittlement by baking for 6 to 8 hours at 210 F.

Although 6 hours is the minimum baking time required to obtain satisfactory embrittlement relief, an 8 hour baking time is recommended for greater assurance. Specimens coated in baths which were not within the standard composition limits, exhibited variable stress rupture life results for both 6 and 8-hour baking relief treatments (compare Figs. 14.7 and 14.8). This fact might explain the discrepancy in the effectiveness of baking time and air aging, respectively, between the results obtained by Wolff and Austin.

Weinberg and Capello[16] performed sustained load notched tension tests on steel with a hardness of R_C 52-53 stressed to 90 per cent NTS. They concluded that zinc or manganese phosphatized test bars baked at 220 F for 60 minutes were completely relieved of embrittlement[17]. Apparently, more work is required for elucidation of the inconsistencies in the results of the embrittlement relief treatments.

REFERENCES

[1] C. A. Zapffe and M. E. Haslem, "Sensitivity of Different Steels to Pickling Brittleness", *Wire and Wire Products*, **23**, pp. 563-571 (1948).

[2] C. A. Zapffe and M. E. Haslem, "Acid Composition, Concentration, Temperature and Pickling Time as Factors in the Hydrogen Embrittlement of Mild Steel and Stainless Steel Wire", *Trans. ASM*, **39**, pp. 213-214 (1947).

[3] G. Sachs and W. Beck, "Survey of Low Alloy Aircraft Steels Heat Treated to High Strength Levels. Part 1, Hydrogen Embrittlement", WADC, Tech. Rept. 253/254 p. 19, Air Force Materials Lab. (WPAFB) Dayton, Ohio (1957).

[4] K. Sachs and M. Odgers, "Hydrogen Absorption and Ductility of Mild Steel after Pickling or Cathodic Treatment", *Metallurgia*, **69**, pp. 109-115 (1964).

[5] K. Sachs and M. Odgers, "Estimation of Hydrogen in Pickled Steel by Vacuum Extraction at 700 C", *J. Iron Steel Inst.* **190**, 406 ff (1960).

[6] T. P. Groenevelt, E. E. Fletcher, and A. L. Elsea, "Review of Literature On Hydrogen Embrittlement", NASA Contract NAS 8-20029, George C. Marshall Space Flight Center, Huntsville, Ala. pp. 27-38 (12 Jan 1966).

[7] R. L. Jones, "A New Approach to Bend Testing for the Determination of Hydrogen Embrittlement and Susceptibility of Sheet Materials", Rept. No. 235, Convair Astronautics, San Diego, Cal. (15 June 1961).

[8] S. J. Ketcham, "Chemical Milling of Alloy Steel", Report No. NAEC-AML-2418 Naval Air Development Center, Warminster, Pa. (Mar. 1966).

[9] E. J. Jankowsky, "The Effect of Cleaning and Paint Stripping Compounds on Stressed High Strength Steel", Report No. NAEC-AML-1983 Naval Air Development Center, Warminster, Pa. (July 1964).

[10] P. Fischer, W. Beck, "Evaluation of the Lawrence Hydrogen Detection Gage for the Prediction of Hydrogen Embrittlement", Report No. NADC-MA-7052, Naval Air Development Center, Warminster, Pa. (Oct. 1970).

[11] J. F. Andrew and E. S. Spencer – Timms, "Embrittlement of High Strength Steel by Pretreatment with Etching Primer Paints", *J. Iron Steel Inst.*, **204**, pp. 28-29 (1966).

[12] J. H. Maker, "Hydrogen Embrittlement in Springs", *Met. Progress*, **90** (1), pp. 73-75 (1966).

[13] R. E. Bessey and H. F. Hawthorne, "Hydrogen Embrittlement Relief of Phosphated Steel", Report SA-TR18-1067, Springfield Armory, Mass. (Feb. 1959).

[14] R. H. Wolff, "Hydrogen Embrittlement of Steel in Metal Finishing Process of Black Oxide and Zinc Phosphatizing, U. S. Army Weapons Command", Technical Report 66-2008, Rock Island Arsenal, Ill. (June 1966).

[15] P. H. Austing, S. V. Check, and W. Luric, "Investigation of the Effect of Hydrogen Embrittlement and its Relief, in Phosphate Coated AISI 4340 and 1095 Steels", Rept. 6509, NAVORD, Washington, D. C. (Aug. 1959).

[16] H. P. Weinberg and T. J. Capello, "Embrittlement of Phosphated Steel", *Met. Progress*, **71**, pp.78-81 (April 1957).

[17] E. Taylor, "Phosphate Coating, Cause of Fastener Failure", *Steel*, **163**, No. 25 p. 50, (Dec. 1968).

CHAPTER 15

PLATING EMBRITTLEMENT

In the preceeding chapters, reference was made quite frequently to plating embrittlement; however, a systematic discussion of hydrogen embrittlement, brought about by plating high strength steels with different metals and alloys, was not presented. This chapter was written to fill this gap. The problem of notch plating is also included, because of its importance with embrittlement and embrittlement testing.

15.1 PLATING EMBRITTLEMENT RESULTING FROM PLATING DIFFERENT METALS AND ALLOYS

15.1.1 PLATING CADMIUM FROM THE CYANIDE AND FLUOBORATE BATHS

The corrosion protection of low alloy steels used in aircraft construction is most efficiently accomplished with cadmium plating. Thin adherent coatings of cadmium provide excellent galvanic protection and are not susceptible to cracking, peeling or chipping. For these reasons, cadmium electrodeposits have become virtually indispensable in the aircraft industries. Cadmium plating from the alkaline cyanide bath has been and is the chief method of applying this metal electrolytically. The bath is easy to control, has excellent throwing power and produces bright uniform coatings over wide operating ranges. The plating efficiency is usually only slightly above 85 per cent, and as a result produces excessive hydrogen evolution at the surface of the part being plated. Whereas, the acid fluoborate bath operates at approximately 100 per cent plating efficiency with minimal production of hydrogen.

One of the first investigators who studied embrittlement of high strength steel brought about by cyanide plating was Zapffe[1], who performed bend tests on cadmium plated specimens by means of the test procedure described previously in Chapter 1. He found a high degree of embrittlement in specimens plated in three slightly different types of cyanide cadmium plating baths. His findings were in agreement with results published previously by Fischer and Barmann[2]. The strongly embrittling effect of cyanide cadmium plating is vividly depicted in Fig. 15.1 which shows the increased embrittlement susceptibility by prestressing as compared with that determined after plating on poststressed samples. These results demonstrate the necessity of relieving residual tensile stresses in high strength steel parts which are to be subjected to hydrogen producing processes.

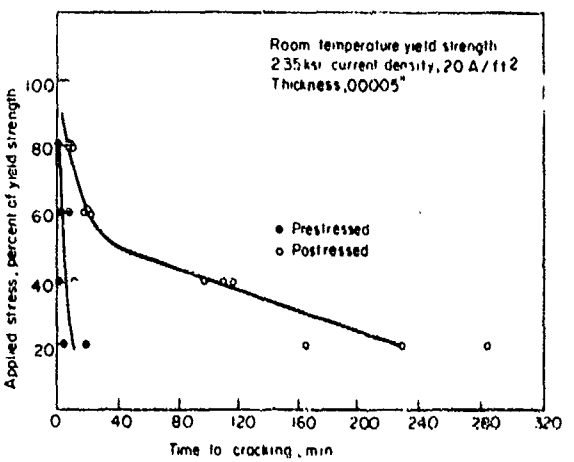

Fig. 15.1 – Effect of prestressing (30 min prior to plating) and poststressing (5 min after plating) of C-ring specimens (AISI 4340 steel, Y.S.-235 ksi) on time to cracking. Specimens plated from a cadmium cyanide bath.

Pertinent results of embrittlement measurements on cyanide and fluoborate plated high strength steel specimens will be presented in one of the following sections where comparisons will be made with chromium plating. The embrittlement behavior of high strength steels, plated from rather exotic cadmium baths formulated specifically to minimize embrittlement, will be discussed in the chapter dealing with modified cadmium plating baths.

15.1.2 ZINC AND COPPER PLATING

Results obtained by Zapffe and Fischer indicate that the acidic zinc and copper plating solutions are much less embrittling than those containing cyanide compounds[1-3]. Beck and Janowsky[4] found that the embrittling effect of pyrophosphate copper coating on steel is comparatively low.

15.1.3 NICKEL AND SILVER PLATING

Experimental work with notched high strength steel specimens (UTS 260 – 280 ksi) showed that plating nickel from the Watts bath produces only moderate embrittlement. The degree of embrittlement from plating is less than that from the Watts bath[4,5].

Data pertaining to hydrogen stress cracking induced by silver plating from the classical cyanide bath is of interest, since this type of plating is often used for bearing surfaces and parts which have application as electrical connectors. McDonnell Aircraft[6] and other investigators[2] performed delayed failure tests on silver plated notched AISI 4340 steel specimens.

The high degree of embrittlement by cyanide silver plating for steel substrates with strength levels from ~200-280 ksi is portrayed in Figure 15.2.

Intense baking of specimens with tensile strengths exceeding 200 ksi, does not restore the notched tensile strength of the unplated material completely. Despite the fact that this classical bath works with practically 100 per cent plating efficiency, the embrittlement by silver plating is essentially the same as that generated by plating any other metal from cyanide baths with lower efficiencies.

15.1.4 TIN PLATING

Tin is plated from the stannate bath at a temperature of about 140 F. Results obtained by Beck and Jankowsky [5] with prestressed C-ring specimens plated to an average thickness of 0.0005 in., showed that tin plating is strongly embrittling.

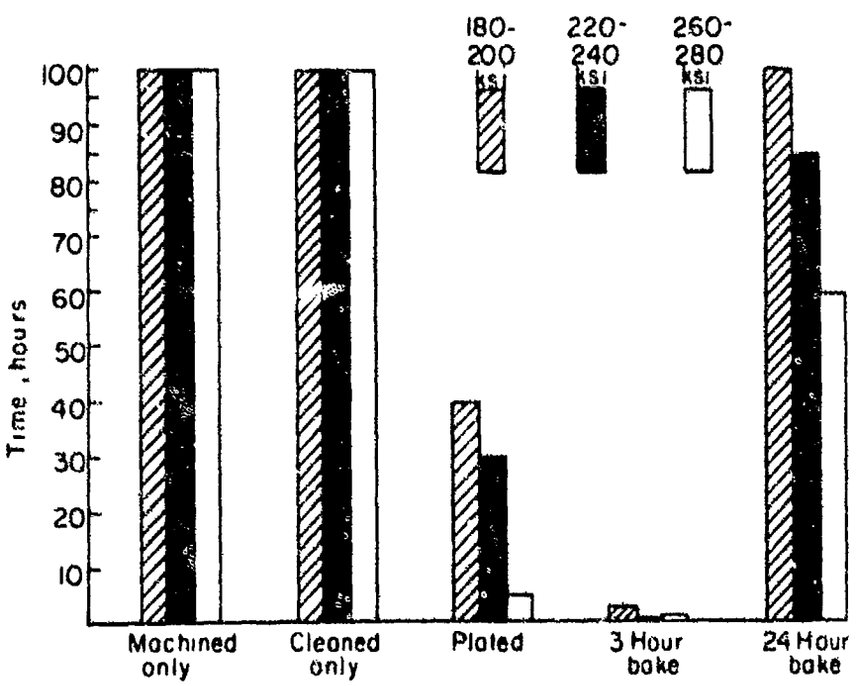

Fig. 15.2 – Delayed fracture times for unplated, plated and plated + baked AISI 4340 steel specimens (180-280 ksi). Specimens were plated with silver from the cyanide bath (thickness range 0.0006 to 0.0010 in.) and stressed to 75 per cent of NTS of the unplated tension bar. Baking temperature 375 F.

An instructive failure analysis, dealing with tin-plating, was performed by Lockheed[7]. The problem concerned cracking observed on turboprop engine mount attachment bolts after 6 1/4 hours of engine run-up and a flight time of only 3/4 hour. The bolts had been heat treated to the required strength level (180-210 ksi) and the material had perfect metallurgical integrity. The plating thickness on the head-to-shank-fillet was 0.001 in. which is much thicker than that normally plated. These bolts were baked for only 3 hours, which is definitely considered to be an insufficient time to completely restore them to their preplated ductility. Based on these facts the cracking shown in Fig's. 15.3 and 15.4 is considered to be related to hydrogen embrittlement.

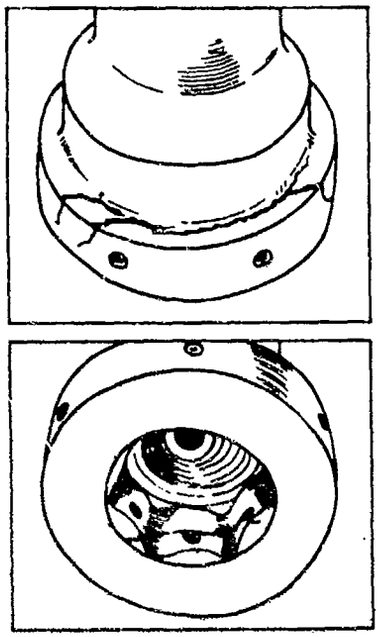

Fig. 15.3 – Close-up views of magnaflux indications, showing location and extent of brittle failure in the head of turboprop engine mount attachment bolt (210 ksi) which had been incompletely baked after having been tin plated to a thickness that was much greater than that normally used.

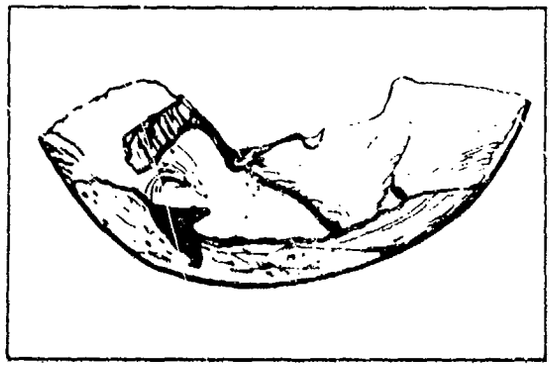

Fig. 15.4 – Enlarged view of fracture surface depicted in Fig. 15.3, indicating probability that failure originated in the fillet under the bolt head.

15.1.5 CHROMIUM PLATING

The excellent wear resistance and high hardness of chromium plating make it almost irreplaceable as a wear protective coating. It has been used extensively for aircraft parts, for gun barrels, gun parts, and many other applications in which wear is a problem. Generally speaking, steels with a hardness below R_c 40 can be plated with little danger, provided they are embrittlement relieved by proper baking after plating. For example, the barrel steel on the 20mm M39, with a hardness of R_c 32-36, would present no problem. When plating parts with a higher hardness, such as the breech face of the M39 (R_c 53-59), residual stresses in the parts combined with the high degree of embrittlement induced by chromium plating can cause cracking during the plating operation.

The low efficiency of the chromium plating bath in addition to the relatively long plating times, and the easy access of hydrogen to the metal substrate through the cracks in the chromium deposit may explain to a certain degree the marked embrittlement induced in the substrate. On the other hand, the cracks facilitate the removal of hydrogen from the substrate by baking.

The following figures show a comparison of delayed fracture behavior of notched steel specimens plated with chromium, cyanide cadmium, and fluoborate cadmium[8].

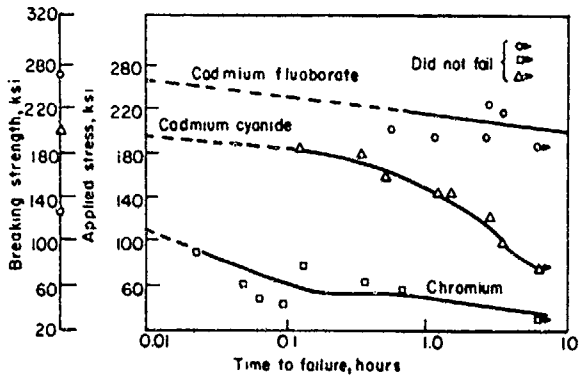

Fig. 15.5 – Breaking strength of unplated (320 ksi) and cadmium and chromium plated notched C-rings fabricated from AISI 4340 steel (260-280 ksi). Plot of applied stress versus time to failure.

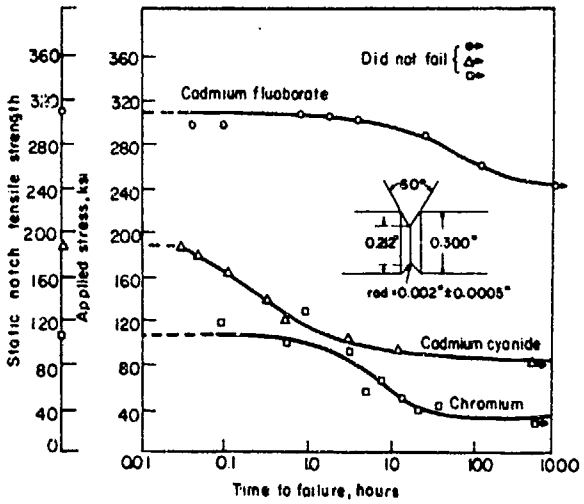

Fig. 15.6 – Notch tensile strength of unplated (360 ksi) and cadmium and chromium plated notched tension specimens fabricated from AISI 4340 steel (260-280 ksi). Plot of applied stress versus time to failure.

The curves show that, regardless of the geometry of the specimen, the fluoborate plated specimens are much less embrittled than those that were either chromium or cyanide cadmium plated. The embrittlement brought about by chromium plating is very severe and markedly exceeds that of strongly embrittling cyanide cadmium plating.

The laboratory results with chromium plating are in excellent agreement with a failure analysis of chromium plated main landing gear side strut bolts conducted by Lockheed [9]. The bolts failed after a very short service time and typical failure is illustrated in Fig. 15.7.

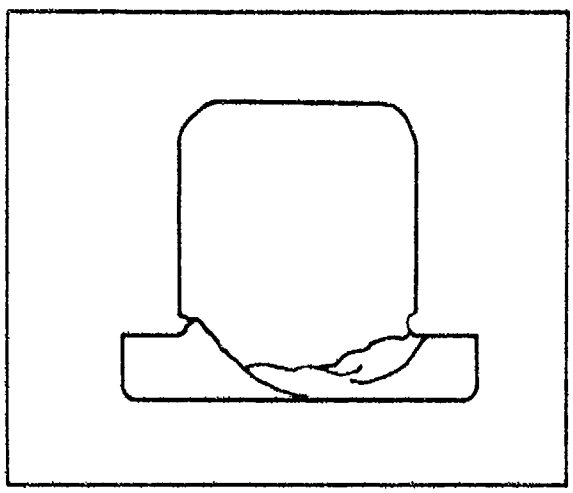

Fig. 15.7 – Sectional macrograph shows cracking in a main landing gear side strut bolt (220 ksi) plated with chromium. Failure after 13 hours of service on an airplane is probably induced by hydrogen.

The microstructure of the bolts was normal for quenched and tempered steel, with a hardness of approximately R_C 46, corresponding to a UTS of approximately 220 ksi. Failure of the bolts on standing under relatively low loads rather than during installation, the brittle nature of the fracture, the general appearance of the fracture surfaces, and the metallurgical integrity of the parts, strongly indicate that hydrogen embrittlement was primarily responsible for the failures.

15.1.6 ALLOY PLATING

Internal steel components of aircraft engines have been protected effectively against corrosion by tin-cadmium alloy coatings which were used extensively until a few years ago.

Brittle failures were reported to occur in tin-cadmium plated carburized and nitrided engine components. The possibility cannot be ruled out that these failures were initiated by hydrogen. The role played by tin-cadmium alloy plating in the generation of brittle cracks in high strength steels was studied by Beck and Jankowsky [10,11]. The alloy was produced by direct plating of its constituents from a complex fluoborate bath. Alloying was also attempted by thermal interdiffusion of the components, plated as two consecutive layers on the steel.

The results of delayed failure tests are pictured in Figs. 15.8 and 15.9. The figures clearly show that in the case of a specimen on which two metals have been consecutively deposited forming two layers, the induction periods are almost non-existent, and the lower critical stress is excessively low, whereas much higher values are obtained for direct alloy plating. Undesirable embrittling effects obtained with the duplex layer are similar to those resulting from tin stannate or cadmium cyanide plating (presented in the preceeding sections). The favorable effects found with fluoborate plating of the alloy, tin, or cadmium compare favorably with those reported by Cohen [12].

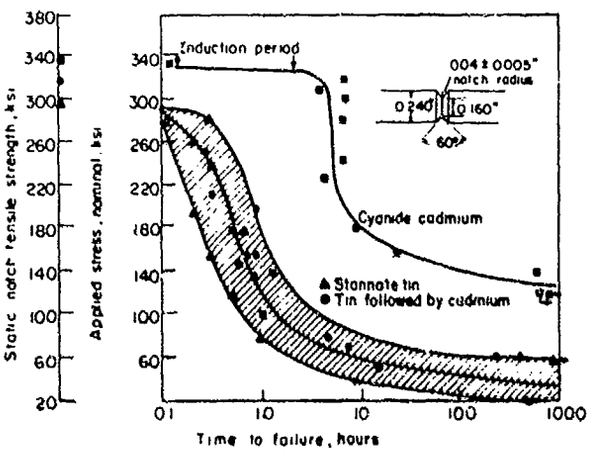

Fig. 15.8 – NTS of plated stressed specimens. Delayed failure times of steel test bars plated with stannate tin, cyanide cadmium and tin followed by cadmium. Tin-cadmium duplex coating contains approximately 50 per cent tin. Unplated specimens, UTS - 270 ksi, NTS - 380 ksi, K_t=4.2.

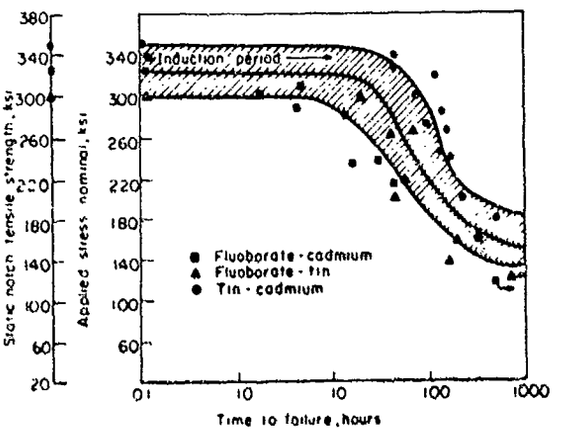

Fig. 15.9 – NTS of plated stressed specimens. Delayed failure times of steel test bars plated with fluoborate-cadmium, fluoborate-tin and tin-cadmium alloy (latter by codeposition of the metals from complex fluoborate bath) containing approximately 30 per cent tin. NTS of unplated specimen - 380 ksi.

Beck and Jankowsky demonstrated by metallographic analysis and electron-microscopy that the 30 minute heat treatment at 340 F (Fig. 15.8) is not sufficient to initiate metallic interdiffusion. Hence, only the simple duplex coating system prevails in which embrittlement is controlled by the most agressive plating component (stannate-tin). In addition, because of the barrier effectiveness of the plated double layer, the thermal treatment is not effective in removing the embrittling hydrogen.

15.2 THE PROBLEM OF NOTCH PLATING AS RELATED TO EMBRITTLEMENT AND EMBRITTLEMENT TESTING

Though this problem concerns embrittlement testing, it appears more appropriate to discuss it in the context of this chapter.

The delayed failure notch tension test is important for evaluation of the sensitivity of a steel to hydrogen stress cracking. It is known that a number of variables affect the reproductibility of this test, and therefore, it is highly desirable to reduce them whenever possible. One variable, the decrease in thickness of the coating with notch depth is frequently neglected and will be discussed in this section.

The complex conditions prevailing in sharp notches during cadmium plating were clearly demonstrated by Geyer et al.[13] who recorded the current, passing through the notch, independently of the total plating current carried by the test bar. They found that the notch current fell rapidly to a fraction of the total current, then decayed exponentially and finally approached a minimum value. A 50 per cent decrease of the total plating thickness was noted at the base of the notch, but no difference in plating efficiency was observed between gauge and notch current.

Wagner[14] calculated the current distribution in a narrow shallow rectangular slot, filled with electrolyte and subjected to cathodic polarization. He showed that with increasing distance from the surface, the current falls exponentially. This current drop may be the result of polarization processes or conductivity changes in the narrow space of the slot. However, to consider the above simple slot geometry a representative model of a sharp V notch has its limitations, because it does not seem permissible to ignore the effect of the radius of the notch on plating thickness. Sachs[15], working with notches having a depth of 0.04 in., did not succeed in obtaining a cadmium plating at the root, when the sharpness of the root was increased by reducing the notch radius to 0.001 in. However, for notches with low stress concentration factors, the notch may be completely covered with cadmium. Fig. 15.10 illustrates that despite the superb throwing power of the cyanide bath, the plating thickness decreases progressively with increasing notch depth, as explained by Wagner's calculations. The plating thickness at the notch base is 50 per cent less than on the gauge.

Besides the theoretical interest of the effect of notch acuity and depth on plating thickness distribution, it has an important implication in the domain of embrittlement testing. The rate of penetration of hydrogen atoms into the metal, and hence the rate of crack propagation, according to Troiano, depends on the number of hydrogen atoms, accumulating in the area of highest triaxiality. Therefore, the absence of the cadmium plating barrier at the notch root or a marked reduction in its thickness produces an exaggerated picture of hydrogen embrittlement of the steel when the sustained load test is used. To circumvent this problem, Hartgroves and Langstone[16] have suggested standardizing on a root radius between 0.003 and 0.005 in. for the delayed failure test, perhaps maintaining the most commonly used depth of 0.04 in.

In many cases, it will be desirable to ascertain that the notch root is at least covered by the electroplating. To simplify the rather time consuming metallographic sectioning, prior to metallographic examination, Strauss and Vlannes[17] have developed a colorimetric screening test for notch coverage by cadmium plating by using appropriate dyes. This test involves reactions in which: (a) a color is produced on the plate without affecting the substrate; (b) a color is produced on the substrate without affecting the plate; or (c) easily distinguishable contrasting colors are produced on both the plate and the substrate.

In general, the above problem of homogeneous notch plating applies exclusively to electrolytic plating[18].

Complete coverage should not be obtained on a notch root radius about 0.003 in. when a Ni-Cd duplex layer is electroplated. However, a diffusion heat treatment at 630 F, which slightly exceeds the eutectic temperature of the nickel cadmium system, is sufficient to level the coating in the notch root within a period of 30 minutes[19] as is seen in Fig. 15.11.

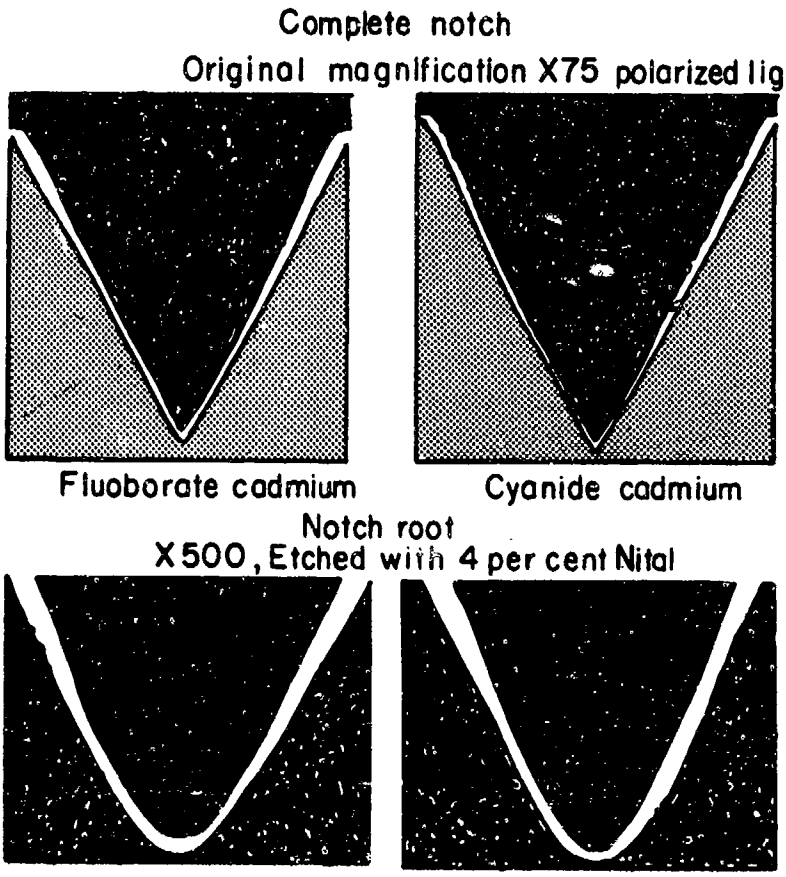

Fig. 15.10 – A comparison of the cadmium plated complete notch and notch root showing the plating thickness decreasing progressively with increasing depth of the notch (0.0005 in. on gauge, 0.0002 in. on notch root). Dimensions of notch; depth 0.040 in., angle 60°, radius 0.002 in. ± 0.0005 in.

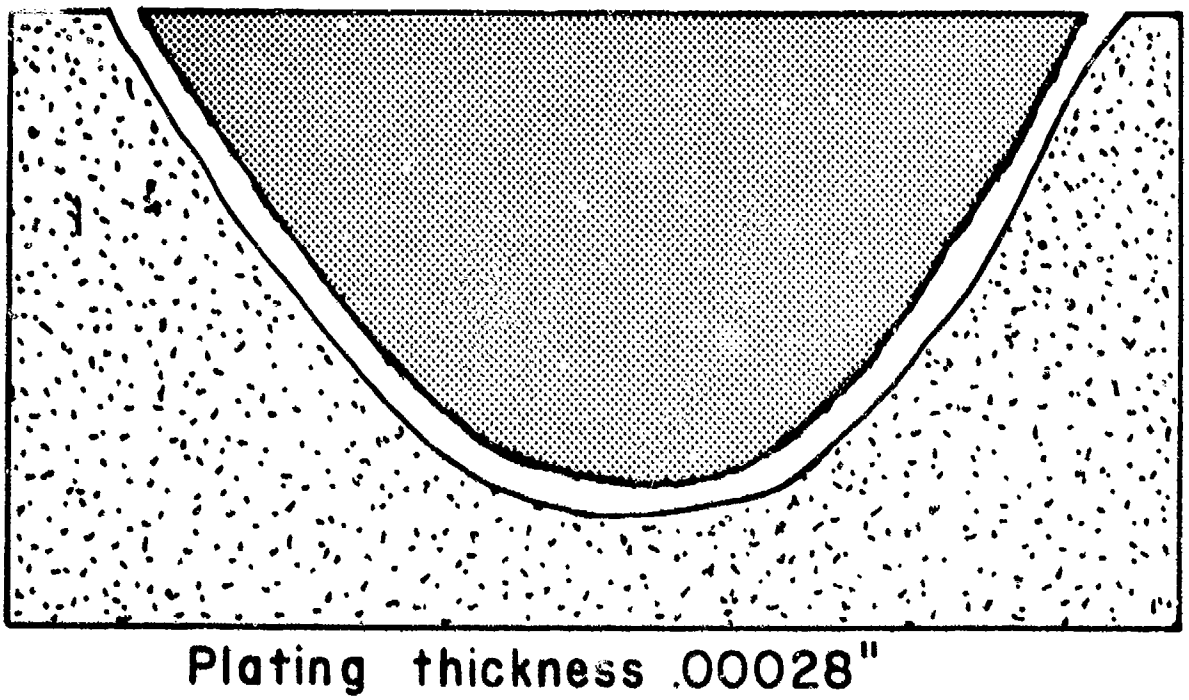

Fig. 15.11 – Ni-Cd duplex coating in notch root leveled by diffusion heat treatment for 30 min. at 630 F. Notch radius 0.003 in. Magnification - x 500. Etchant: 50 ml HCl, 25 ml HNO_3, 1g $CuCl_2$, 150 ml H_2O

REFERENCES

[1] C. A. Zapffe and M. E. Haslem, "Hydrogen Embrittlement in Cadmium and Zinc Electroplating", *Plating*, **37** (4), pp. 366-371 (1950).

[2] H. Fischer and H. Barmann, "The Problem of the Initiation of Hydrogen Embrittlement in Steel by Electrolytic Processes", *Korrosion und Metallschutz*, **16**, pp. 405-418 (1940)

[3] C. A. Zapffe and M. E. Haslem, "Hydrogen Embrittlement in Copper Electroplating", *Plating*, **36** (9), pp. 906-913 (1949).

[4] W. Beck and E. J. Jankowsky, "The Effectiveness of Metallic Undercoats in Minimizing Plating Embrittlement of Ultra High Strength Steel", *Proc. Am. Electroplaters' Soc.*, **47**, pp. 152-159 (1960).

[5] W. Beck and E. J. Jankowsky, "Effects of Plating High Tensile Strength Steel", *ibid.*, **44**, pp. 47-52 (1957).

[6] "Investigation of Hydrogen Embrittlement of Silver Plated 4340 Steel at Various Strength Levels", Report 9080, Ser. No. 20, McDonnel Aircraft Corp., St. Louis, Mo. (Feb. 1962).

[7] "Metallurgical Analysis of Failed Engine Mount Attachment Bolts", Report No. MCRM 1630, Lockheed Aircraft Co., Burbank, Cal. (June 1955).

[8] F. S. Williams, W. Beck, and E. J. Jankowsky, "A Notched Ring Specimen for Hydrogen Embrittlement Studies", *Proc. ASTM*, **60**, pp. 1192-1202 (1960).

[9] "Metallurgical Analysis of Failed Main Landing Gear Side Strut Bolts", Report No. LR-8591, Lockheed Aircraft Co., Burbank, Cal. (May 1952).

[10] W. Beck and E. J. Jankowsky, "Effect of Binary Alloy Plating on Delayed Brittle Failure of Ultra-High Strength Steel", *J. Electrochem. Soc.*, **109**, pp. 490-494 (1962).

[11] W. Beck and E. J. Jankowsky, "Effect of Tin-Cadmium Electrodeposits on Corrosion and Mechanical Behavior of Steel", *Proc. 2nd International Congress on Metallic Corrosion*, pp. 669-675 (1963).

[12] B. Cohen, "A Study of Cadmium-Tin and Zinc-Tin Alloy Electrodeposits", WADC Tech. Report 54-240 Air Force Materials Lab. (WPAFB), Dayton, Ohio (Sept. 1954).

[13] N. M. Geyer, G. W. Lawless and B. Cohen, "Progress Toward the Development of a Non-embrittling Cadmium Electroplating Process", *Proc. Am. Electroplaters' Soc.*, **47**, pp. 143-151 (1960).

[14] C. Wagner, "Calculation of the Current Distribution at Electrodes Involving Slots", *Plating*, **48**, pp. 999-1002 (Sept. 1961).

[15] E. P. Klier, B. B. Muvdi and G. Sachs, "The Response of High Strength Steels in the Range of 180-300 ksi to Hydrogen Embrittlement from Cadmium Plating", *Proc. ASTM*, **58**, 605 ff (1958).

[16] T. Hartgroves and P. F. Langstone, "Thickness of Electroplated Cadmium in Notches in High Strength Steel Sustained Load Test Specimens", *Corrosion Sci.*, **5**, p. 797 (1965).

[17] S. W. Strauss and P. N. Vlannes, "Progress Towards the Development of a Non-embrittling Cadmium Electroplating Process – IV – Use of Methanol as a Solvent in Cadmium Plating Solutions", *Plating*, **47**, 932 ff (1960).

[18] W. L. Cotton, "Hydrogen Embrittlement of High Strength Steels During Cadmium, Chromium and Electroless Nickel Plating", *ibid.*, **47**, pp. 169-175 (1960).

[19] "Static Fatigue Strength of Diffused Nickel-Cadmium Plated Vasco-max 250 and Vasco-max 300", Report A-733, Ser. No. 19, McDonnell Aircraft Corp., St. Louis, Mo. (June 1964).

CHAPTER 16

DIFFERENT CADMIUM PLATING BATH FORMULATIONS PROPOSED FOR REDUCTION OF EMBRITTLEMENT; SPECIAL PLATING PROCEDURES

A great deal of effort has been directed toward substituting other types (different chemical formulations) of plating baths with lower embrittling characteristics for the highly embrittling but widely used conventional cyanide bath. The efforts were made with the objectives of reducing hydrogen discharge with a minimum loss of the highly desirable plating characteristics of the cyanide bath. The composition and embrittlement characteristics of three different types of rather unorthodox cadmium plating baths will be summarized briefly. The baths are:

- The fluoborate bath
- The amino acid baths
- Nonaqueous baths

In addition to the above approaches a number of investigators with a less radical attitude toward changes in bath formulations kept the conventional cyanide bath, but made attempts to reduce embrittlement by using additives. Two additives commonly used are titanium and nitrate compounds. These types of plating baths will be briefly described and their embrittlement characteristics analyzed.

Other low or non-embrittling special plating procedures also included in this chapter are vacuum, spray, brush, gas plating, and mechanical or peen plating techniques.

16.1 PROPOSED CADMIUM PLATING BATHS FOR REDUCTION OF EMBRITTLEMENT

16.1.1 THE FLUOBORATE BATH

This bath[1] is an acid bath with a pH of about 3.8 which contains cadmium ammonium fluoborate and brighteners. The facts presented in the previous chapter dealing with plating embrittlement clearly indicated the superiority of this bath over the classical cyanide bath from the point of view of minimizing embrittlement[2]. Actually, the fluoborate plating process does not eliminate hydrogen embrittlement, but it does reduce it to an appreciable degree, (plating efficiency close to 100 per cent). Disadvantages are the poor throwing and covering power, the roughness, and the comparatively poor appearance of the fluoborate plating.

16.1.2 THE AMINO ACID BATHS

Formulations as well as results of experimental work in the development of a "non-embrittling" amino acid electroplating bath are given in detail in references[3-8]. It is generally agreed that more satisfactory electrodeposits are obtained from baths with the metal present largely as a complex rather than as a simple ion. It is also well known that the discharge of hydrogen ions in an electrode process depends strongly on their ionic concentration. From the point of view of diminishing hydrogen embrittlement, it is highly desirable to suppress hydrogen discharge and therefore, plate at a high pH. However, cadmium tends to precipitate as the hydroxide over a wide pH range (above 7), unless it is properly complexed. Thus, selection of a complexing agent is imperative, in order to obtain a good plate from an alkaline bath.

Vlannes[5] showed that the metal is deposited in preference to hydrogen at appropriate pH values from an ammoniacal plating bath, in which the cadmium is solubilized by an organic complexing agent. Based on polarographic measurements, this investigator suggested the use of an aqueous solution containing the ammonium salt of an aliphatic amino acid in an ammoniacal cadmium sulfate solution. He formulated a number of amino acid baths which were suitable for low embrittlement cadmium plating. The amino-n-butyric acid bath, selected from a number of other amino acid. The pH of the bath is about 9.5 and a current density of about 15 A/ft^2 is used in plating. Its superiority from the point of view of embrittlement reduction over the cyanide or fluoborate bath was shown in the histogram presented in Chapter 2 dealing with hydrogen determination.

It was established that the amino acid baths are capable of being adapted to barrel-plating conditions. Their throwing power in barrel plating is superior to that in tank plating. But the lack of brightness of the coatings and the difficulty in the maintenance of the baths, as found in the laboratory of the Naval Air Development Center, are still considerable drawbacks that have to be overcome before this procedure can be recommended for general use.

It should be noted that Vlannes et al. used a number of other nonembrittling amino acid baths with high cathode efficiency[6-8] for cadmium plating. For example, baths containing (1) triethanolamine, (2) methanol as a solvent and (3) pyridine as a complexing agent. The cathode current efficiency in all these baths approaches 100 per cent. Delayed failure tests did not indicate hydrogen stress cracking.

16.1.3 NON-AQUEOUS BATHS

Micillo of the Grumman Aerospace Engineering Corporation[9,10] used an entirely different approach. He excluded water completely from his bath formulation and plated cadmium from an all organic solution without codeposition of hydrogen. As a result of comprehensive studies, he selected n,n-dimethyl formamide (DMF) as solvent. This substance is polar having a rather high dielectric constant and a relatively good electrolytic conductivity. Cadmium iodide was used as the metal salt because of its solubility in DMF and its stability when cadmium is used as an anode in the electroplating bath. To obtain a fine crystalline cadmium deposit, it is necessary to reduce the high concentration of the free metal ions in DMF by binding the cadmium into a metal-chelate structure, with an aliphatic high molecular weight derivative of ethylenediamine.

Anodic as well as cathodic current efficiency of these baths is 100 per cent, when operated close to room temperature at a current density between 3 to 12 A/ft^2. According to Micillo, the adhesion of the plating and its capacity to protect against atmospheric corrosion compare favorably with the adhesion and protection of conventional cyanide cadmium deposits. Results of sustained load tests may be summarized as follows: At plating thicknesses from 0.0004 to 0.001 in., notched specimens (K_t=3) of AISI 4340 steel (260-280 ksi) could be stressed to 75 per cent of the unplated NTS up to 400 hours, and at 90 per cent NTS up to 360 hours without failure. The run was then discontinued. Although the stress rupture life is remarkably high, it should be emphasized that the plating bath has a number of serious drawbacks, such as being a fire hazard, toxic, hygroscopic, having a slow plating rate, and comparatively poor throwing power.

After these disadvantages have been eliminated or minimized, this plating method can be recommended for universal use without hesitation, because it is one of the few baths which "completely" eliminates hydrogen embrittlement. In addition it would eliminate the rather cumbersome procedure of baking. Moreover, it may be possible to adapt this method for plating chromium.

Arnold[11], who also made studies on non-aqueous electroplating, added dimethylsulfoxide or 1,2 ethanediol to the DMF solvent for his studies.

The electrodeposition of aluminum from non-aqueous solutions will be briefly covered. Aluminum is deposited from an ethereal solution of aluminum chloride, and a metal hydride, preferable lithium hydride[12,13]. The cathode current efficiency is close to 95 per cent, but the deposition rate is not very high. The effectiveness of lithium hydride is attributed to the formation of a complexion which promotes the deposition of aluminum. This ion is continually being replaced by the anodically dissolving aluminum and, therefore, assures a continuous deposition of this metal from a small quantity of the complex.

16.2 CONVENTIONAL CYANIDE CADMIUM BATH CONTAINING EMBRITTLEMENT REDUCING ADDITIVES

16.2.1 TITANIUM ADDITIVE

Workers at the Boeing Corporation approached the problem of suppressing the hydrogen evolution reaction differently[14]. They kept the conventional cyanide bath but added titanium by means of a propriety paste containing 15 per cent titanium. Addition of hydrogen peroxide is essential for proper functioning of the bath.

Jankowsky[15] has evaluated the embrittlement characteristics of this procedure by means of delayed failure tests. Hydrogen stress cracking was suppressed only to a limited extent in AISI 4340 steel (260-280 ksi).

A detailed procedure for titanium cadmium plating of high strength steel has been given recently by Weymuller[16]. He has reported successful titanium cadmium plating of the huge landing gears of the 280 ton Boeing 747 jet, which has four main landing gears under each wing and two under the fuselage. The gears are made of AISI 4340-M steel (silicon modified 4340) heat treated to a UTS exceeding 275 ksi. The apparent success of

titanium-cadmium process in the landing gear application is probably attributable to the lower embrittlement sensitivity of AISI 4340-M as compared to 4340. (See Chapter 5). A mechanism will be suggested in Chapter 18 dealing with mechanisms.

16.2.2 NITRATE ADDITIVE

Another approach for retarding the hydrogen evolution reaction was used by Hamilton and Levine[17], working at the Lockheed Aircraft Corporation. Their bath contains slightly higher concentrations of sodium cyanide, cadmium oxide, sodium hydroxide, and sodium carbonate than the conventional cyanide bath. Low concentrations of sodium nitrate and polyethylene glycol were used as additives.

Specimens were plated from this bath after being subjected to a nonembrittling pretreatment consisting of: (1) fine vapor honing to remove scale and rust, (2) anodic cleaning at 100 A/ft^2 for 5 min. in a commercial caustic cleaner, followed by a water rinse, (3) electro-honing at 100 A/ft^2 for 15 minutes in a sulfuric-phosphoric acid bath, followed by a water rinse. The favorable results of stress rupture tests on specimens plated from the modified bath are compiled in Table 16.1.

TABLE 16.1 – COMPARATIVE STRESS RUPTURE TESTS OF STEEL SPECIMENS PLATED FROM CONVENTIONAL AND NITRATE MODIFIED CADMIUM CYANIDE BATHS

Sample	Time to Failure (Hours)	Notch Radius (Inches)
Controls, nonprocessed	386, 500*, 369, 500*, 500* 500*, 500*, 167, 500*, 500*	0.005
Conventional Bath, 20 A/ft^2 unbaked 20 A/ft^2 baked (x) 60 A/ft^2 unbaked, 60 A/ft^2 baked	0.0, 0.3 0.7, 0.0 0.0, 0.0 20, 118	0.005
Modified Bath, 100 A/ft^2 unbaked 75 A/ft^2 unbaked 50 A/ft^2 unbaked	500*, 500*, 234 400, 109, 223 500*, 500* 500*	0.005
Controls, nonprocessed	600*, 600*, 600*	
Modified Bath, 75 A/ft^2 unbaked	600*, 600*, 600* 600*	0.025

*Indicates no failure at that period of time when test was terminated.
xBaking conditions unknown.

Specimens AISI 4340 steel (260-280 ksi) - Loaded to 75% of NTS
Coating thickness 0.0005 in.

However, Brittain[18], a former member of the research laboratories of Hawker Siddeley Aviation Ltd, obtained much less favorable results. He concluded from the data that the nitrate bath produces variable embrittlement of a sensitive steel, which is associated with hydrogen pick up. He also found that the addition agent is unstable. Pertinent results are compiled in Table 16.2. Note that poor embrittlement behavior was obtained in spite of a 2 hour bake at 200 C.

TABLE 16.2 – SUSTAINED LOAD NOTCHED TENSILE TESTS
AISI 4340 STEEL (240 ksi) PLATED FROM NITRATE MODIFIED CADMIUM CYANIDE BATH
(THICKNESS 0.0004 IN. ON BARREL)

Test/piece Number	Stress (ksi)	Hours to failure	Hydrogen* (ppm)
115	280	0.3	0.14 0.13
116	278	5.9	0.04
117	276	104.0	0.01 0.02
118	273	6.9	0.04
119	271	11.3	0.05
121	269	4.0	0.03
123	258	20.6	0.03
124	246	7.7	0.04
128	224	1000 (No failure)	0.00

Four unplated control specimens failed at 291, 334, 367 and 381 ksi respectively.

*Determined in sample taken from broken specimen by extraction at 350 C. Specimens baked at 200 C for 2 hours after plating.

16.3 SPECIAL PLATING PROCEDURES

16.3.1 GAS PLATING OF ALUMINUM

In the gas plating process a thermally unstable organic aluminum compound is used for the deposition of the metal. Plating is carried out at temperatures around 200 C and thermal decomposition occurs on the surface of the part to be coated. Decomposition gases are given off and pumped out of the decomposition chamber.

Jankowsky made delayed failure tests[19] on gas plated H-11 high strength steel three weeks after storage under normal atmospheric conditions. The fact that no indication of hydrogen stress cracking was found, is apparently due to the comparatively high decomposition reaction temperature counteracting the adsorption of the evolved hydrogen. Also, there is the possibility of the loss of hydrogen during storage.

16.3.2 BRUSH PLATING

In brush plating carbon is used as the anode (stylus). It is wrapped with absorbent cotton and saturated with the appropriate cleaning or plating solution. The part to be plated is made the cathode and plating is achieved by swabbing the metal surface with the cotton wrapped anode. This procedure has many practical applications, because it can be used in situ. A number of common applications is the plating of small sections of large assemblies that cannot conveniently be taken apart, the repair of scratches in a plated coating, the plating of small contact points on electrical components, stenciling, and the build up of mismachined or worn parts. Because of the high plating temperature (the solution often boils at the stylus contact points) and the continuous sweeping action, it would be expected that under these conditions there would be practically no hydrogen at the cathode surface. Thus embrittlement should be greatly reduced and even eliminated. Slow rate bend tests[20] performed by Beck and Jankowsky confirmed this expectation. However, the results of stress rupture tests[21] on notched high strength steel specimens were less favorable.

It should be noted that brush plating is not satisfactory for uniformly coating the root of a sharp notch or a thread, therefore, measurements on notched stress rupture specimens are hardly representative of the embrittlement behavior of brush plated parts under a variety of field conditions.

16.3.3 SPRAY METALLIZING AND VACUUM DEPOSITION

Spray metallizing and vacuum deposition have also been employed to avoid hydrogen embrittlement. In the first process, a metal wire is fed through an oxy-acetylene flame. The molten metal is forced through a nozzle by compressed air and sprayed out in the form of tiny droplets. Adhesion is determined by a keying mechanism. No hydrogen is formed by this procedure. In vacuum plating the coating is applied by vaporization of the metal in a vacuum chamber. As would be expected, hydrogen embrittlement tests on specimens metallized were negative also[22-24].

16.3.4 MECHANICAL (PEEN) PLATING

Another specialized plating procedure which is reported to produce little or no embrittlement is mechanical plating (peen plating). Satisfactory adhesion of the coating produced by this procedure can only be insured by a two step pretreatment, consisting of phosphatizing and then copper plating by immersion. The part is peen plated in a tumbling barrel, containing the powdered metal to be plated, glass beads and a proprietary compound, called the promotor. It must be strongly emphasized that the two step pretreatment is mandatory and is to be considered an integral part of the plating procedure.

Sustained load tests were performed immediately[25,26] after completing each of the two pretreatment steps. One group of specimens was phosphatized and the other copper plated. Results are given in Fig. 16.1. Due to technical reasons, embrittlement evaluations of peen plated notched tension specimen could not be started until 3 weeks after the specimens had been plated.

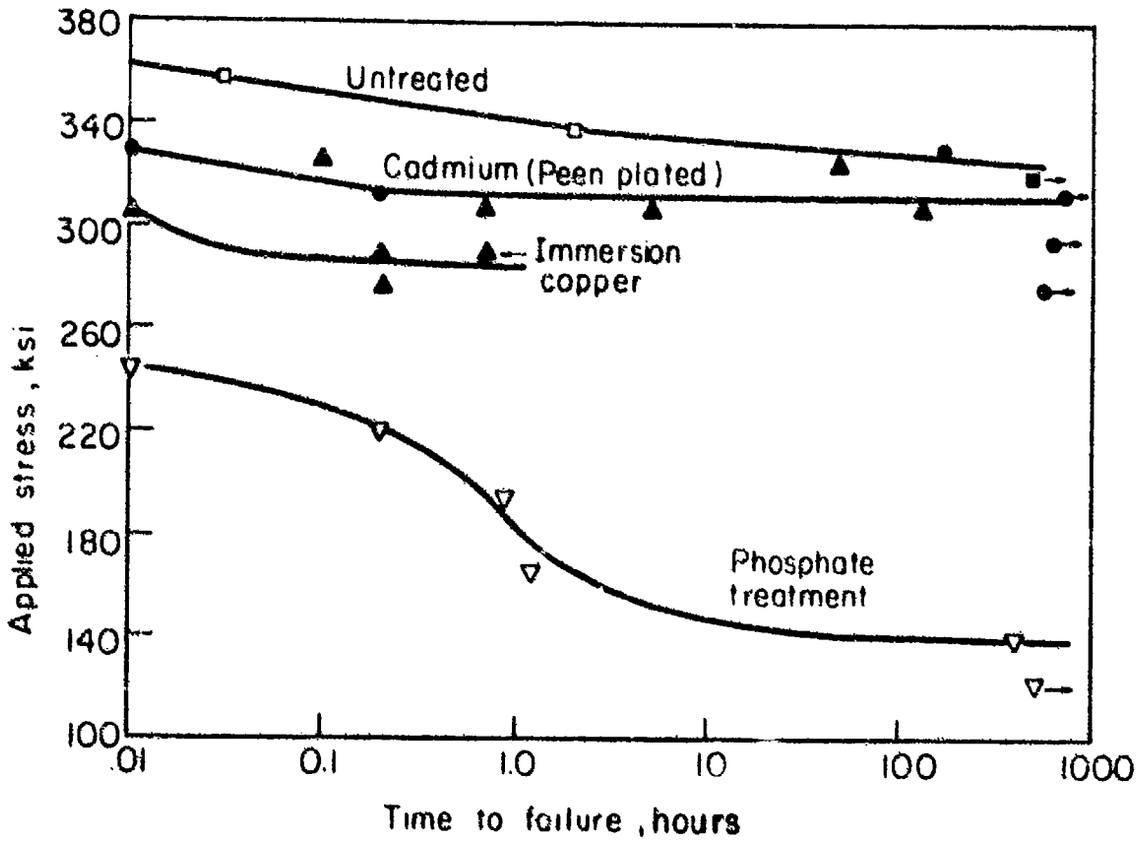

Fig. 16.1 – Stress rupture behavior of AISI 4340 steel specimens (260-280 ksi, K_t = 4.2) cadmium peen plated (tested after 3 week storage at ambient temperature). In addition data are presented for each of the two pretreatment procedures, phosphatizing and immersion copper plating (tested immediately after treatment).

As shown in the figure, the lower critical stress of the peen plated specimens is greatly improved and almost coincides with that of an unplated specimen. It is apparent from the results that the source of the embrittling hydrogen is primarily the phosphate treatment. These data are similar to those previously given under the discussion of the phosphatizing procedure in section 14.5. The comparatively low degree of embrittlement by phosphatizing, is easily removed by room temperature aging[27] as a result of the porosity of the peen-plated cadmium.

These findings are in good agreement with stress rupture tests performed in the laboratory of the Standard Pressed Steel Corporation.

REFERENCES

[1] F. A. Lowenheim, editor, *Modern Electroplating*, John Wiley and Sons, Inc., pp. 74-75, Second Edition 1963.

[2] "Testing of High Strength Steels for Hydrogen Embrittlement After Cadmium Plating by the Cyanide and the Fluoborate Plating Processes", Report 9083, Ser. No. 19, McDonnell Aircraft Corp., St. Louis, Mo. (Oct. 1962).

[3] P. N. Vlannes, S. W. Strauss and B. F. Brown, "Electroplating Baths for Ultra-High Strength Steels", Pt. I, NRL Report 4904 Naval Research Lab., Washington, D. C. (Mar. 1957).

[4] P. N. Vlannes, S. W. Strauss and B. F. Brown, "Progress in the Development of a Nonembrittling Cadmium Electroplating Process", *Plating*, **46**, pp. 467-468 (1959).

[5] P. N. Vlannes and S. W. Strauss", Part II – Use of Aliphatic Amino Acids as Complexing Agents in Aqueous Baths", *ibid.*, **46**, pp. 1046-1056 (1959).

[6] P. N. Vlannes, S. W. Strauss and B. F. Brown", Part III – The Use of Triethanolamine in Cadmium Plating Solutions", *ibid.*, pp. 1153-1157.

[7] S. W. Strauss and P. N. Vlannes", Part IV – Use of Methanol as a Solvent in Cadmium Plating Solutions", *Plating*, **47**, pp. 926-932 (1960).

[8] S. W. Strauss and P. N. Vlannes", Part V – The Use of Pyridine as a Complexing Agent in Cadmium Plating Solutions", *ibid.*, pp. 1037-1039.

[9] C. Micillo, "Embrittlement-Free Cadmium Electrodeposition on Ultra-High Strength Steels from Non-Aqueous Solutions", Report No. RDM-0100-809-1, Grumman Aircraft Eng'g. Corp., Beth Page (May 1961).

[10] C. Micillo, "Cadmium Plating Without Embrittlement", *Materials in Design Engineering*, **57**, No. 6, pp. 86-87 (1963).

[11] V. E. Arnold, "Non-Aqueous Electroplating to Eliminate Hydrogen Embrittlement", Report SC-RR-66-507, Sandia Corp., Albuquerque, N. Mexico (Sept. 1966).

[12] D. E. Couch and A. Brenner, "A Hydride Bath for the Electrodeposition of Aluminum", *J. Electrochem. Soc.*, **99**, pp. 234-44 (1952).

[13] G. B. Wood, "A Study of Embrittlement of High Strength Steel", *ibid.*, **110**, pp. 867-877 (1963).

[14] D. M. Erlwein and R. E. Short, "Cadmium-Titanium Plating: An Improved Process for Protecting High Strength Steels", *Metal Progress*, **87**, (2), pp. 93-96 (1965).

[15] E. Jankowsky, "Evaluation of the "Delta Cad" Plating Process", Report No. NAEC-AML-1875, (Feb. 1964); "Reevaluation of the "Delta Cad" Plating Process", Report No. NAEC-AML-2259, Naval Air Development Center, Warminster, Pa. (Sept. 1965).

[16] C. R. Weymuller, "Giant Landing Gears for the Giant Jet", *Metal Progress*, **95** (3), pp. 77-79 (1969).

[17] W. F. Hamilton and M. Levine, "Control of Hydrogen Embrittlement by Plating from Cadmium Cyanide Baths Containing Nitrate", *Proc. Am. Electroplaters' Soc.*, **47**, pp. 160-165 (1960).

[18] P. I. Brittain, "Protection of Very Strong Steels (Evaluation of the Lockheed Cadmium Plating Bath)", Hawker Siddeley Research Report No. R-240, p. 4, 63, England (Dec. 1963).

[19] E. Jankowsky, "Evaluation of Ethyl Corporation Aluminum Coating Process", Report No. NAEC-AML-1827, Naval Air Development Center, Warminster, Pa. (Dec. 1963).

[20] W. Beck and E. Jankowsky, "Investigation of the Dalic Brush Plating Process", Report No. NAMC-AML-AE-4187, Naval Air Development Center, Warminster, Pa. (July 1958).

[21] W. Beck and E. J. Jankowsky, "Evaluation of the Selectron High Speed Selective Plating Process", Report No. NAMC-AMI-1617, Naval Air Development Center, Warminster, Pa. (Feb. 1963).

[22] W. Beck and E. Jankowsky, "Effects of Coatings Other Than Chemical and Electrodeposits on the Properties of High Strength Steels", Report No. NAMC-AML-AE-4110, Part I, Naval Air Development Center, Warminster, Pa. (Aug. 1958).

[23] W. Beck and E. Jankowsky, "Evaluation of Vacuum Deposited Aluminum Coatings", Report No. NAMC-AML-1213, Naval Air Development Center, Warminster, Pa. (Aug. 1961).

[24] P. J. Clough, "Functional Surfaces by Vacuum Metallizing", *Metals Engineering Quarterly*, 1, pp. 7-14 (1961).

[25] E. Jankowsky, "Evaluation of the Minnesota Mining and Manufacturing Company's Mechanical Plating Process", Report No. NAEC-AML-1803, Naval Air Development Center, Warminster, Pa. (Nov. 1963).

[26] Tech. Report No. 737, "Mechanical Cadmium Plating on Nuts and Notched Tensile Specimens", Standard Pressed Steel, Jenkintown, Pa. (Dec. 1961).

(27) E. Taylor, "Phosphate Coating: Cause of Fastener Failure", *Steel*, p. 163 (25), 16 Dec. 1968.

CHAPTER 17

METHODS OF MINIMIZING HYDROGEN EMBRITTLEMENT

The most common method of minimizing hydrogen embrittlement is a thermal treatment called "baking." This method as well as less common procedures and their limitations will be discussed in this chapter.

17.1 REMOVAL OF SURFACE HYDROGEN

This method is only of theoretical interest and consists of removing the surface layers containing hydrogen (e.g., by grinding). Results obtained by Troiano et al.[1] are depicted in Fig. 17.1.

Grinding is performed immediately after four different aging times. Effective cooling conditions are strictly maintained during grinding to keep loss of hydrogen by sample heating to a minimum. With longer aging times, the quantity as well as the penetration depth of hydrogen diffusing into the bulk of the specimen increases and more of the metal has to be ground away to remove the embrittling hydrogen atoms. Finally, at the aging time of 600 hours hydrogen has penetrated to such a depth that the removal of a comparatively thin surface layer is insufficient for restoration of the initial ductility. Identical results were obtained by Toh and Baldwin[2] who removed the hydrogen carrying surface layers by electrochemical milling.

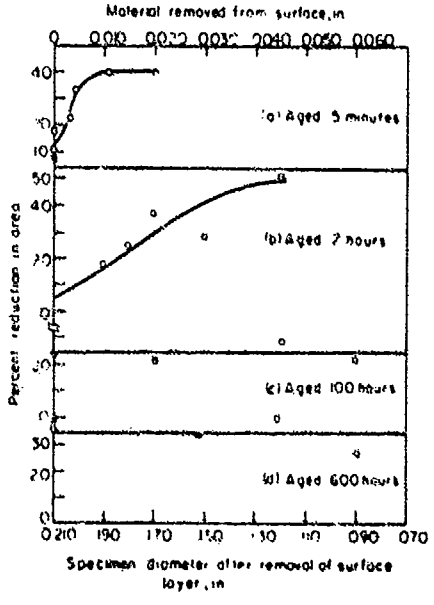

Fig. 17.1 – Plot showing effect of aging times and grinding off different thicknesses of hydrogen containing steel surface layers on embrittlement. AISI 4340 steel specimens (270 ksi) previously hydrogenated by cathodic charging.

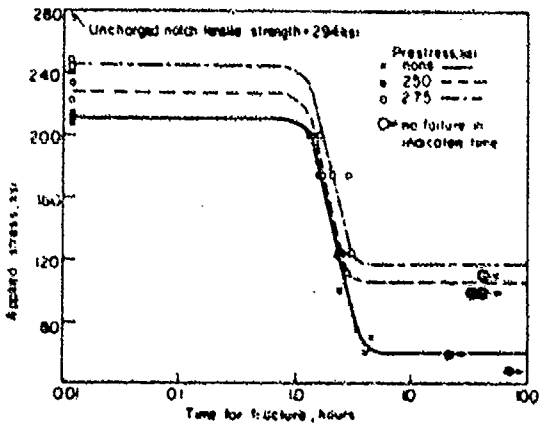

Fig. 17.2 – Delayed failure curves for sharply notched AISI 4340 steel specimens (240 ksi) prestressed to various strength levels, charged cathodically and aged for 5 minutes at ambient temperature.

17.2 PRESTRAINING

Troiano et al.[3,4] reduced susceptibility to hydrogen stress cracking by prestraining. Pertinent results are depicted in Fig. 17.2. The notch tensile strength, lower critical stress and to a limited degree time to fracture are improved by prestraining. The mechanism of this interesting phenomenon will be discussed in Chapter 18.

17.3 METALLIC UNDERCOATS

The high susceptibility of high strength steel to hydrogen embrittlement was demonstrated in preceeding chapters. Recent advances in the field of propellent-actuated devices have indicated a need for still higher strength steel components, many of which are spring loaded for extended periods. Since these items are protected against corrosion by electroplating, the aforementioned conditions are ideal for generating hydrogen embrittlement. For the plating of the above devices and munitions items, a duplex coating with the undercoat acting as a hydrogen diffusion barrier has definite advantages.

The procedure, suggested by Troiano and others[5-7], is based on the idea that cyanide cadmium plating is an effective hydrogen diffusion barrier and that the relatively small quantity of hydrogen introduced within the short time of electrodepositing a very thin coating can be easily driven out by baking. The undercoat may then be overplated by a thick or commercially used coating without generating embrittlement, making any further baking unnecessary. Fig. 17.3 shows, that with increasing thickness of the overplate (increasing plating time), the thickness of the undercoat (initial plate) must be increased to maintain the ductility of the unplated steel.

Dougherty[8] recommended the following duplex plating procedure for AISI 4340 steel:

First step - Plate to 0.125 mil from a cyanide cadmium bath, containing a brightener.*

Second step - Bake for two hours at 375 F.

Third step - Overplate to 0.5 mil to a bright fine-grained finish.

Sustained load tests with notched tensile specimens have shown this method to be unreliable[9,10]. Despite recovery of ductility obtained with thin plating after baking, subsequent replating with cyanide cadmium was found to embrittle high strength steel.

To conserve the useful properties of the cadmium plating, but decrease its embrittling effect, metallic undercoats other than cadmium have been tried. Desired properties of the undercoat are that it must be easily overplated with cadmium and produce only a negligible degree of embrittlement. Beck and Jankowsky[10] suggested the use of undercoatings of pyrophosphate copper or nickel (bright or sulfamate). A thin undercoat of either of the two metals embrittles only to a very slight degree, and is primarily the result of mechanical plating imperfections. Results obtained by these investigators are given in Fig. 17.4.

*Brightener is necessary, because there is no decrease in ductility while overplating a bright preplate. Dull coatings are more porous and, therefore, are poor diffusion barriers.

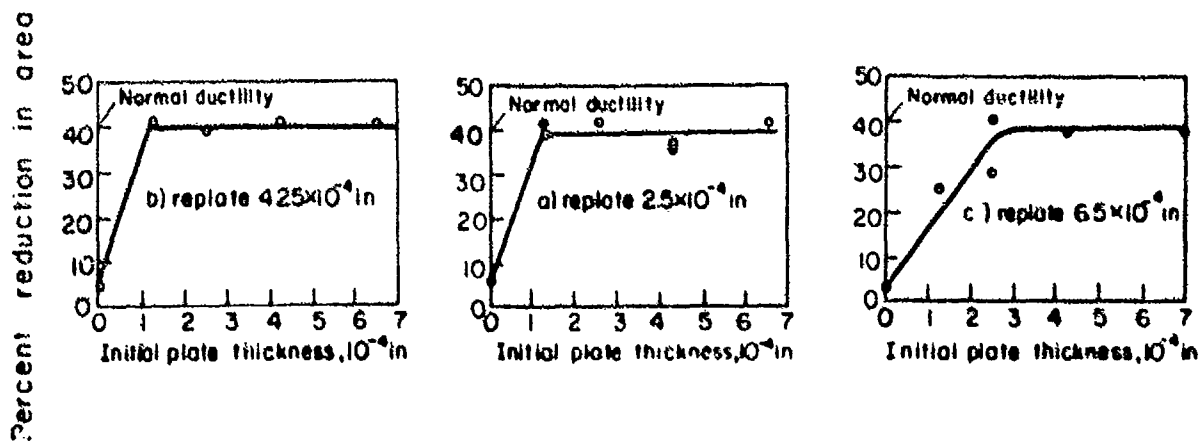

Fig. 17.3 – Plot showing that the undercoat thickness (initial plate) must be increased, when the thickness of the replate (overplate) is increased in order to maintain the ductility of the unplated steel. Cd over Cd plating on AISI 4340 steel (260 ksi).

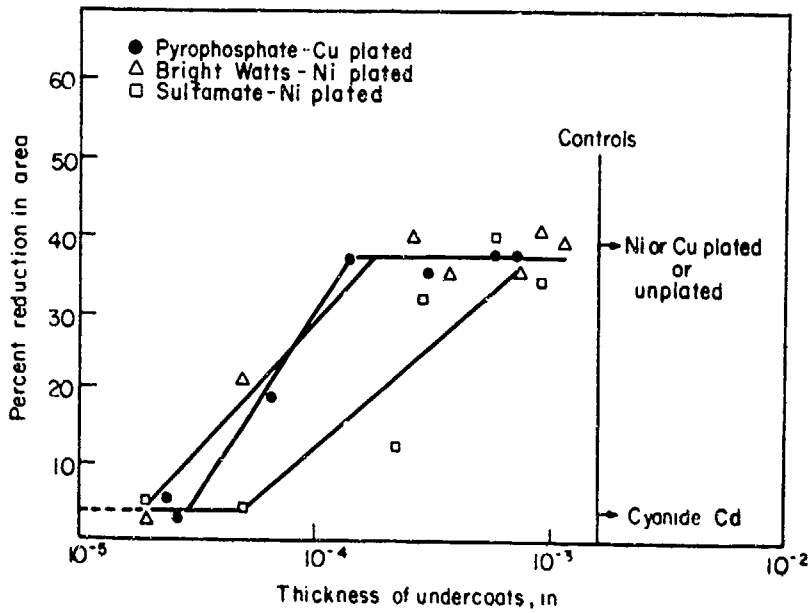

Fig. 17.4 – Relation of thickness of Ni and Cu undercoats to their effectiveness in reduction of embrittlement, when overplated with cyanide cadmium (10^{-4} in.). Substrate AISI 4340 steel (260 ksi). Rate of crosshead travel 0.1 in./min. Strain rate to yield maintained at 0.05 in./in./min.

The effectiveness of the undercoates as embrittlement reducers is clearly demonstrated. Dougherty[8], using the half ring bend test, also studied the effectiveness of nickel and copper undercoats. He found that neither type of preplate completely eliminated embrittlement, but both reduced that resulting from cadmium plating effectively. These findings are in agreement with those reported by Beck and Jankowsky[10]. However, it is Dougherty's considered opinion that due to their greater complexity undercoats other than cadmium offer no particular advantage over a duplex cadmium plating.

Freeman et al.[11] discovered that overplating a 2 mil copper layer, produced by immersion in a $CuSO_4$ solution with chromium from the standard chromic-sulfuric acid bath, did not produce hydrogen embrittlement. Similar results were obtained with an underlay of electroless gold, though the danger of marked galvanic action has to be taken into consideration. Nickel, when plated by an electroless process to a thickness of at least 1 mil, acted as an effective barrier when overplated with cadmium[12], which agrees well with the findings of Beck and Jankowsky[13]. According to Allread and Robinson electrolytically[14] plated zinc is also an effective hydrogen diffusion barrier.

17.4 NONMETALLIC COATINGS

The use of nonmetallic coatings for the protection of bolts on the thrust control valves for the Titan missile is a good example of their application for minimizing hydrogen stress cracking[15]. The bolts are made of 17-PH martensitic stainless steel (UTS 200 ksi, yield strength 180 ksi). Bolt failures were located in the vicinity of 7075-T6 aluminum alloy flanges and were associated with white chalky corrosion products on the flanges as well as rust spots (pits along the shank about 1/2 in. from the head). Hydrogen stress cracking had been induced by cathodically generated hydrogen. The current flow in the galvanic couple, stainless steel-aluminum, was effectively reduced by covering the bolts with a suspension of graphite in grease (Lox-Safe) or by chromic-acid anodizing of the aluminum, or by a combination of the two coatings.

17.5 AGING

Baking is the most commonly used procedure to remove embrittling hydrogen from steel parts, but some preliminary remarks about recovery of ductility of embrittled steel by the escape of hydrogen during room temperature storage (aging) may be helpful for a better understanding of the problems involved in the more complex procedure of baking. Fig. 17.5 shows[16] that with increasing aging time, increased quantities of hydrogen diffuse out of the specimen, as indicated by the improving elongation. The escape of hydrogen does not restore elongation to that of the uncharged specimens even after aging for as long as 7.6 days at 23 C.

Information about decrease of embrittlement in hydrogen steel castings by room temperature aging may be obtained[17] from the next figure. The data show that the decrease of embrittlement as well as loss of hydrogen after casting is very slow.

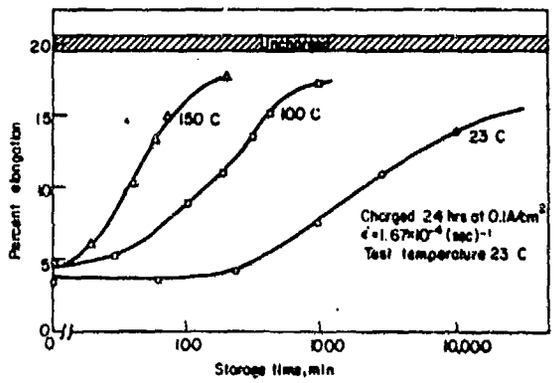

Fig. 17.5 – Limited recovery of tensile ductility of AISI 310 austenitic stainless steel after storage at different temperatures and times. Specimens charged cathodically in 1N H_2SO_4 + 250 mg of As at 100 mA/cm² for 24 hours.

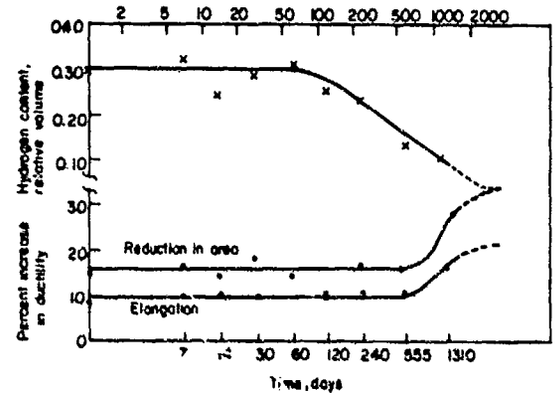

Fig. 17.6 – Plots showing very slow decrease in hydrogen content and embrittlement in steel test bars stored at ambient temperature immediately after casting.

No increase in ductility is observed until an aging time of about 550 days. Extrapolation of the curves in Fig. 17.6 indicates that it would require an aging time of about 5 years to lose all the hydrogen and to recover full ductility.

Fig. 17.7 shows in an impressive manner the increase[9] in fracture time with time of aging of cathodically cleaned and acid etched test bars. The examples given indicate that initial ductility is not always completely recovered after very long storage times at above ambient temperatures.

17.6 BAKING

If applicable, "baking" is and probably will be the procedure of prime importance for the removal of the embrittling hydrogen. There are two rather comprehensive publications dealing with baking, one by Groenevelt et al[18], published in 1966 as a part of a special report, and the other a monograph about hydrogen embrittlement by Sachs and Beck[19], published in 1954 as a part of a comprehensive survey of low alloy aircraft steels, heat treated to high strength levels. In the latter survey, instructive examples are presented, dealing with the effectiveness of baking treatments on plated high strength steel parts and laboratory specimens.

17.6.1 FACTORS AFFECTING BAKING EFFICIENCY

Valuable information[19] may be obtained from Fig. 17.8 which shows the relationship of the following three variables on the effectiveness of baking:

- Difference in hydrogen permeation through cadmium and chromium electrodeposits
- Baking temperature
- Strength level of the metal substrate

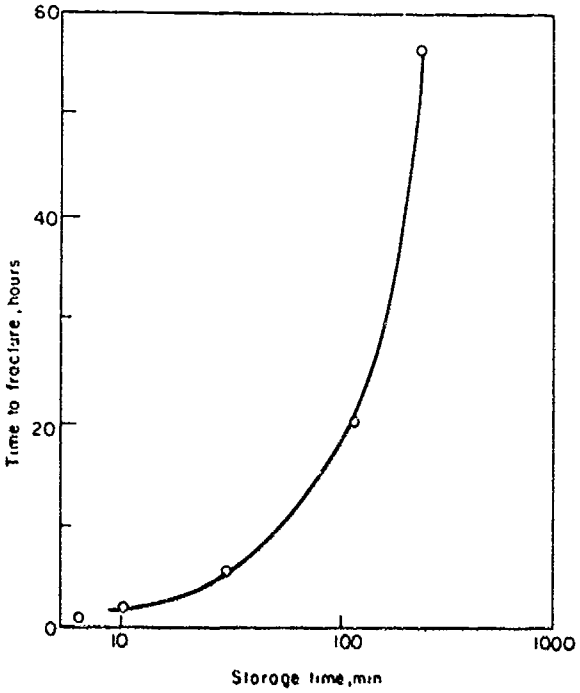

Fig. 17.7 – Increase in fracture time with aging time at ambient temperature. AISI 4340 steel (285 ksi) loaded at 50% NTS, cathodically cleaned and etched with HCl.

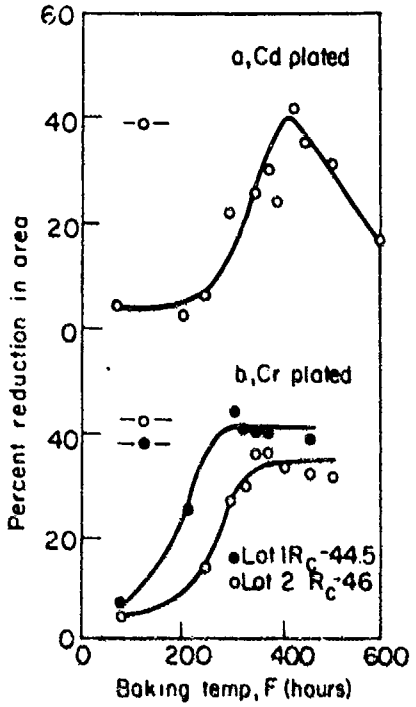

Fig. 17.8 – Curves depicting effect of baking temperature on ductility recovery of chromium and cadmium plated AISI 4340 steel. Average Plating Thickness, Cd 0.0005 in., Cr 0.003 in.

The plotted values confirm the fact that despite the greater thickness of the chromium plating, its tendency to form cracks makes it possible to recover ductility completely at about 350 F, whereas a temperature of about 450 F for the same baking time is needed for the specimens covered with the thinner cadmium plating. With increasing baking temperature, ductility is improved progressively. However, at temperatures of above 500 F ductility drops rapidly with increasing temperature, probably as a result of diffusion of embrittling cadmium atoms from the coating into the grain boundaries of the steel structure[20,21].

Another rate of recovery determining variable is baking time. Fig. 17.9 illustrates that a longer baking time is required to achieve immunity to cracking for a specimen with higher UTS than for one with a lower UTS. Delayed failure testing at 50 per cent NTS indicates that a sample, heat treated to a strength level of 225 ksi requires a baking time of about 25 hours to afford the steel immunity against fracturing, while about 45 hours is needed for a sample with a 280 ksi strength level.

Fig. 17.10 shows that the lower critical stress increases as an approximately linear function of the baking time.

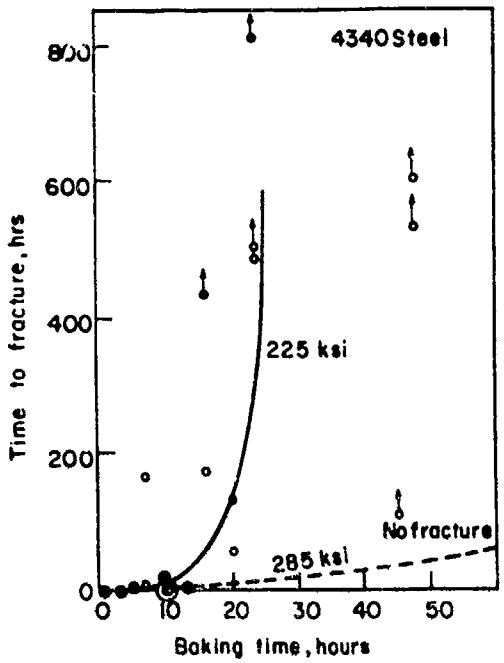

Fig. 17.9 – Effect of baking time (350 F) on time to fracture of cyanide-cadmium plated 4340 steel (5×10^{-4} in. on barrel). Both curves for 50% NTS.

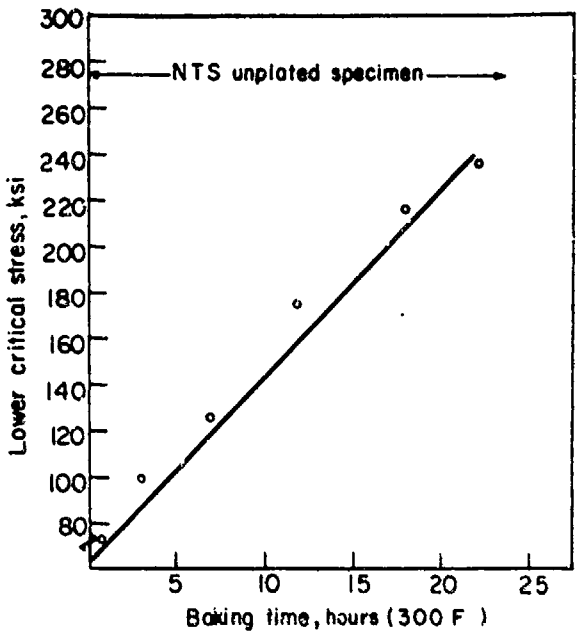

Fig. 17.10 – Plot indicating that the lower critical stress level increases almost linearly with baking time. AISI 4340 steel (280 ksi) sharp notched specimens plated with cyanide cadmium (thickness 0.0005 in. on barrel).

The next figure demonstrates[22] the increase in bend ductility with increasing baking time at different baking temperatures for two strength levels of spring steel strips plated with cadmium. Fig. 17.11 discloses that complete recovery of ductility was attained after about 2 hours of baking at 437 F for steel with a hardness of R_C 40.5. Decreasing the temperature to 392 F extended the required baking time to about 8 hours. At a hardness of R_C 56.5, almost complete recovery was attained after 2 hours at 527 F, while complete recovery was approached but not reached in 28 hours at 437 F. Baking temperatures of 212 F and 302 F resulted in very little recovery within the 28 hour baking time used.

As could be expected, there is a considerable effect of the size of a steel sample on the baking time necessary for recovery of ductility. It was established that baking a 1 in. square cast steel bar for 6 hours at 400 F restored normal ductility, whereas a 4 in. square bar required more than 100 hours at the same temperature to restore normal ductility at the center of the section. All bars retained residual hydrogen from casting. In the time-size relationship for a comparable level of hydrogen, there is some indication that with increasing size, the aging time required for recovery will increase directly with volume and inversely with surface area. For most compact shapes, recovery time according to Sims[23] increases as the 3/2 power of the diameter or thickness.

Another variable to be considered in the effectiveness of baking is the retardation of recovery by the hydrogen diffusion barrier action of the plating. Fig. 17.12 is concerned mainly with the role of the plating thickness and baking temperature on the baking time required for complete recovery of ductility[24,25]. It is evident in this graph, that increasing plating thickness makes a corresponding extension of the baking time necessary.

The S shape of the curves stems from the following facts: The effectiveness of the thin platings as hydrogen diffusion barriers is rather limited for thicknesses up to about 2×10^{-4} in. and complete recovery is accomplished by baking times less than 4 hours. However, the barrier effectiveness rapidly increases for a plate thickness greater than 2×10^{-4} in., requiring progressively longer baking times. For a plate thickness of 5×10^{-4} in. a baking time of about 20 hours at 300 F is required to bring about complete recovery. Increasing the plating thickness above this value does not increase the barrier effectiveness. Different strength levels of the steel substrate have practically no effect on baking time. Increasing baking temperature to 400 F has no influence on the shape of the recovery curve but shortens the baking time considerably.

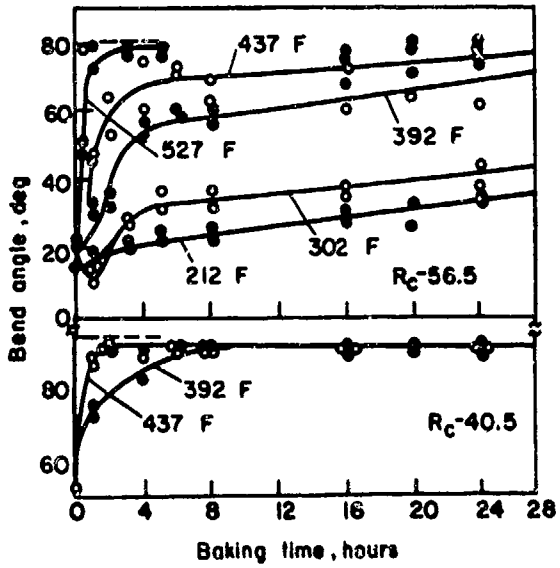

Fig. 17.11 – Effects of baking time and temperature on restoration of ductility of cyanide cadmium plated clock spring steel strips (Cd plate 0.0004 in.).

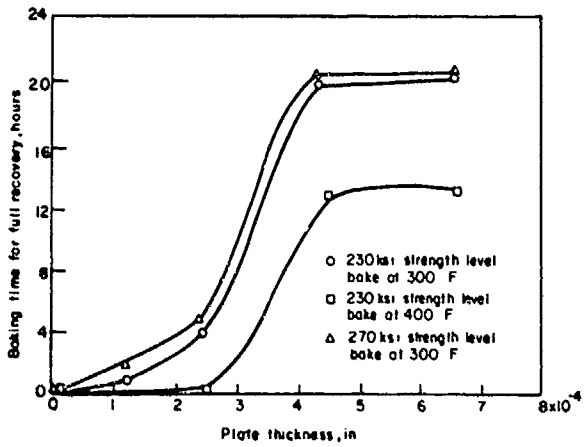

Fig. 17.12 – Plot showing relationship of plating thickness and baking temperature to baking time required to restore complete ductility. AISI 4340 steel substrate.

Additional experimental data are presented in Fig. 17.13 for three different cadmium plating thicknesses at a baking temperature of 400 F. Other metal platings behave similarly.

17.6.2 EXAMPLE OF FAILURE DUE TO INADEQUATE BAKING

An instructive case history of inadequate baking following cadmium plating deals with AISI 4140 steel nacelle eyebolts, heat treated to 180 to 200 ksi[26]. The bolts, which were baked under unknown conditions, showed no evidence of improper heat treatment or other metallurgical defficiencies. Tested in torsion, they failed at rather low loads. Cracks were located in the crest of the threads and secondary cracks in the area adjacent to the main fracture. Fracture surfaces showed very little evidence of ductility, but the root of the threads was free of defects. A typical thread failure is pictured in Fig. 17.14.

Rebaking the bolts at 375 F ± 10 F for 3 hours, materially improved the mechanical properties of the steel which clearly indicates the cause of the failure to be inadequate baking.

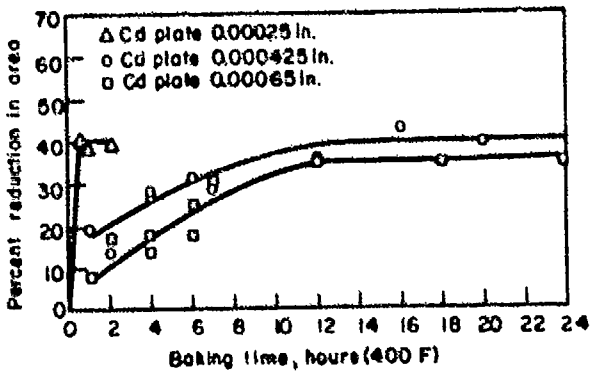

Fig. 17.13 – Plot of baking time and cadmium plate thickness versus rate of recovery of ductility of AISI 4340 steel substrate (230 ksi).

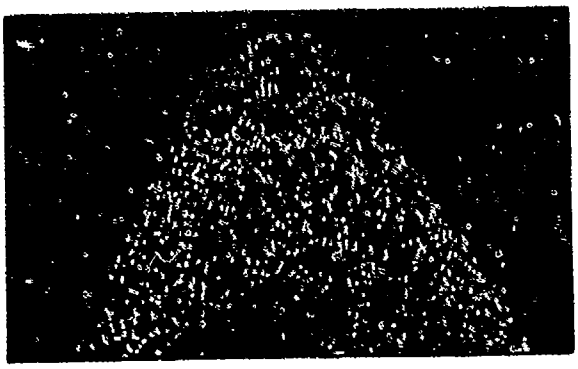

Fig. 17.14 – Example of a defect found in a cadmium plated steel. The defect in the crest of the thread of the nacelle eyebolt (AISI 4140 steel 180-200 ksi) extends to a maximum depth of 0.06 in. - 15% of the thread depth (x 200).

17.6.3 LIMITATIONS OF BAKING

The limitations of baking may be summarized as follows:

- Long baking times are impractical and expensive
- The presence of platings which drastically restrict hydrogen diffusivity, very large parts, and the use of temperatures in the range of blue brittleness of the steel substrate, render baking ineffective.
- Baking temperatures exceeding the tempering temperature of the steel substrate or approaching the melting point of the protective coating cannot be used because of the detrimental effects.

Because of the above limitations, procedures other than baking have to be used for minimizing hydrogen embrittlement.

17.7 INTRODUCTION OF COMPRESSIVE STRESSES

Shot peening has also been used to advantage[13] for reducing plating embrittlement. This method is only listed at this point, since a detailed discussion will be given in Chapter 18.

17.8 INHIBITING PICKLING EMBRITTLEMENT

17.8.1 ORGANIC ADDITIVES

This problem was discussed rather comprehensively in a report, issued by the Battelle Memorial Institute[18]. Until recently there was much doubt about the mechanism which controls inhibition of pickling embrittlement by low concentration additions of organic substances. A detailed analysis of a suggested mechanism will be given in Chapter 18.

17.8.2. OXIDIZING AGENTS

Beck et al.[27] found that addition of a small concentration of hydrogen peroxide to a sulfuric acid pickling bath, strongly retards the hydrogen evolution reaction and hydrogen embrittlement. More details about this reaction and the rate controlling variables will also be presented in the chapter dealing with mechanisms.

17.8.3 ULTRASONIC FIELD

Recently, investigators studied the effect of[28] ultrasonic vibration on the absorption of hydrogen by steel. Experimental results are presented in Fig. 17.5.

The data show that in certain intensity ranges of the ultrasonic field, the absorption of hydrogen shows a minimum (I=0.01 W/cm^2 and also I=1.3 to 2.4 W/cm^2). It follows that at these intensities, it should be possible to reduce drastically the introduction of hydrogen into steel. Mee[29] succeeded in inhibiting embrittlement by pickling or cadmium plating in an ultrasonic field. The electrochemical mechanism of embrittlement inhibition by this technique will be discussed in the chapter on mechanisms.

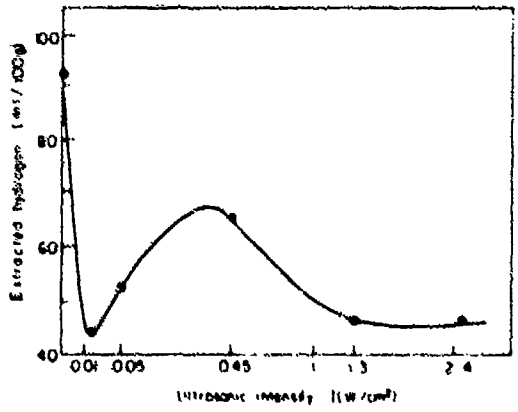

Fig. 17.15 – Effect of intensity of ultrasonic field on absorption of hydrogen in steel. Cathodically charged in 1N H_2SO_4 + As 10 mg/L at 75 mA/cm^2 for 5 min. Extraction time 60 min at 122 F.

REFERENCES

[1] R. D. Johnson, H. H. Johnson, W. Y. Barnett and A. R. Troiano, "Hydrogen Embrittlement and Static Fatigue in High Strength Steel", WADC Technical Note 55-404 Air Force Materials Lab. (WPAFB) Dayton, Ohio (1955).

[2] T. Toh and W. M Baldwin, Jr., "Ductility of Steel with Varying Concentrations of Hydrogen", *Symposium on Stress Corrosion Cracking and Embrittlement*, John Wiley and Sons, Inc. (1956).

[3] H. H. Johnson, J. G. Morlet and A. R. Troiano, "Hydrogen Crack Initiation and Delayed Failure in Steel", *Trans. AIME*, **212**, pp. 526-36 (1958).

[4] H. D. Johnson, H. H. Johnson, J. G. Morlet and A. R. Troiano, "Effects of Physical Variables On Delayed Failure in Steel", WADC Technical Report 56-220 Air Force Materials Lab. (WPAFB) Dayton, Ohio (1956).

[5] H. H. Johnson, E. G. Schneider and A. R. Troiano, "New Technique Rids Plated Steel of Hydrogen Embrittlement", *Iron Age*, **182**, pp. 47-50, (July 1958).

[6] D. Y. Cash and W. Scheuerman, "High Strength Steels can be Cadmium Plated without Embrittlement", *Metal Progress*, **75 (2)**, pp. 90-93 (1959).

[7] S. V. Check, H. P. Weinberg and W. E. McKenzie, "Effects of Cadmium Plating Thicknesses and Overlaying upon the Recovery from Hydrogen Embrittlement of AISI 4340 Steel", NAVORD. Rept. 6944, U. S. Naval Weapons Plant, Washington, D. C. (1959).

[8] E. E. Dougherty, "Methods of Minimizing Hydrogen Embrittlement in Electroplated High Strength Steel Alloys", *Plating*, **51**, pp. 415-422 (1964).

[9] B. F. Brown, "Effect of Baking on Delayed Fracture of Electroplated High-Strength Steel", NRL, Rept. 4839 Naval Research Lab., Washington, D.C. (1956).

[10] W. Beck and E. J. Jankowsky, "The Effectiveness of Metallic Undercoats in Minimizing Plating Embrittlement", *Proc. Am. Electroplaters' Soc.*, **47**, pp. 152-159 (1960).

[11] C. Freeman, W. Dingley and R. R. Rogers, "Preplating High Strength Steel with Copper to Prevent Embrittlement during Chromium Plating", *Electrochem. Technol.*, **6**, pp. 64-66 (1968).

[12] G. J. Biefer, "Environmental Cracking Susceptibility of High Strength Steels", *Mater. Protection*, **7**, pp. 23-26 (1968).

[13] W. Beck and E. J. Jankowsky, "Effects of Plating High Tensile Strength Steels", *Proc. Am. Electroplaters' Soc.*, **44**, pp. 47-52 (1957).

[14] W. O. Allread and G. H. Robinson, "A Simple Test for Hydrogen Embrittlement", *Metal Progress*, **86 (5)**, pp. 102-106 (Nov. 1964).

[15] L. Raymond and E. J. Kendall, "Why Titan's Bolts Failed", *ibid.*, **94**, pp. 103-106 (1968).

[16] M. B. Whiteman and A. R. Troiano, "Hydrogen Embrittlement of Austenitic Stainless Steel", *Corrosion*, **21**, pp. 53-56 (1965).

[17] C. E. Sims, "Hydrogen Elimination of Aging", *Trans. AIME*, **108**, 132 ff. (1950).

[18] T. P. Groeneveld, E. E. Fletcher and A. R. Elsea, "Review of Literature in Hydrogen Embrittlement", Battelle Memorial Institute Special report, 27/4 Columbus, Ohio (1966).

[19] George Sachs and W. Beck, "Survey of Low Alloy Aircraft Steels, Heat Treated to High Strength Levels, Pt. 1. Hydrogen Embrittlement WADC Techn. Report, 53/254, Air Force Materials Lab. (WPAFB) Dayton, Ohio (1954).

[20] D. N. Fager and W. F. Spurr, "Solid Cadmium Embrittlement: Steel Alloys", *Corrosion* **27**, pp. 72-76 (1971).

[21] E. M. Kennedy, "The Effect of Cadmium Plating on Aircraft Steels under Stress Concentration at Elevated Temperatures", WADC Technical Report 60/486 Air Force Materiasl Lab. (WPAFB), Dayton, Ohio (1961).

[22] C. T. Eakin and W. H. Lownie, "Reducing Embrittlement of Electroplating", *Iron Age*, **158**, pp. 69-72 (Nov. 1946).

[23] C. E. Sims, G. A. Moore and D. W. Williams, "The Effect of Hydrogen on the Ductility of Cast Steels", *Trans. AIME*, **176**, pp. 283-308, (1949).

[24] H. H. Johnson, E. J. Schneider and A. R. Troiano, "The Recovery of Embrittled, Cadmium Plated Steel", WADC, Technical Report 57/340 Air Force Materials Lab. (WPAFB) Dayton, Ohio (1957).

[25] A. R. Troiano, "Delayed Failure of High Strength Steel", *Corrosion*, **15**, pp. 207t-212t (1959).

[26] "Metallurgical Analysis of Failed Nacelle Eyebolts Model P2V", Report No. MCRM, 1472 Lockheed Aircraft Corp., Burbank, Calif. (1953).

[27] W. Beck and A. Aldum, "Oxidizing Agents as Embrittlement Inhibitors", unpublished results, (Syracuse University.

[28] L. Domnikov, "Effect of Ultrasonics on Hydrogen Absorption of Steel", *Metal Finishing*, **66 (9)**, pp. 59-61 (1968).

[29] J. W. Mee, "The Application of Ultrasonics to Electroplating with a View to Reducing Hydrogen Embrittlement", *Trans. Inst. of Metal Finishing*, pp. 39-40 (1962/1963).

CHAPTER 18

MECHANISMS SUGGESTED FOR THE EXPLANATION OF SOME HYDROGEN EMBRITTLEMENT PHENOMENA AND THERMODYNAMIC PARAMETERS USED IN RECENT INTERPRETATIONS

18.1 EARLY SUGGESTED MECHANISMS

Mechanisms have been advanced by numerous investigators but none of them covers all phases of this complex phenomenon. One of the earlier mechanisms, suggested by Zapffe, is the so called "planar pressure theory," another deals with the interaction of hydrogen with dislocations and dislocation locking. The latter mechanism would explain the effect of strain rate on hydrogen embrittlement. At comparatively slow strain rates, the Cottrell atmosphere would travel with the dislocations, thus having no appreciable effect on ductility but at higher strain rates, the dislocations would tend to break away from the atmosphere and ductility would be increased accordingly. Conversely, it was emphasized that hydrogen does not impede the movement of the dislocations, because of the fact that the stress-strain relationship is not affected by the embrittling hydrogen. The hydrogen induced delayed brittle failure phenomenon was analyzed by Troiano, as was mentioned in preceeding chapters.

A comprehensive survey of literature and analysis of proposed mechanisms of hydrogen embrittlement in steel and other metals was published by Cotterill[1] in 1961. In addition to the planar pressure throry, theories based on brittle fractures of the Griffith type, the interaction of hydrogen with dislocations, and the effect of hydrogen in interstitial solution proposed by various workers are discussed in detail.

18.2 AN INTERPRETATION OF SOME HYDROGEN EMBRITTLEMENT PHENOMENA EMPLOYING A THERMODYNAMIC APPROACH

Recently, an approach was advanced to interpret some phenomena such as the beneficial effects of compressive surface stresses and of a plastic prestrain on hydrogen embrittlement susceptibility and delayed brittle failure in the light of thermodynamic parameters such as the energy of interaction of hydrogen with the lattice, its partial molar entropy in it, and its binding energy with dislocations. It was found that these parameters can be calculated from the partial molar volume of hydrogen in steel and that this constant could be obtained from electrochemical hydrogen permeation measurements. Therefore, the determination of this value was of prime importance[2]. The calculations of the aforementioned parameters follow.

18.2.1 CALCULATION OF THE PARTIAL MOLAR VOLUME, V_H, IN α-IRON AND STEEL

There are two methods for calculating V_H, using the following relationships:

$$V_H = \left(\frac{\partial V}{\partial n_H}\right)_{T,P,n_{Fe}} \tag{18.1}$$

$$V_H = \left(\frac{\partial \mu_H}{\partial P}\right)_{T,n_{Fe},\eta_H} \tag{18.2}$$

where V is the volume of the system metal + hydrogen, μ_H the chemical potential of hydrogen in iron, T the temperature, P an applied hydrostatic stress and n_{Fe} and η_H the number of gram atoms of iron and hydrogen, respectively. Because of the low solubility of hydrogen in iron, the volume change equation 18.1 is too insignificant to be measurable with any degree of certainty, even by X-ray techniques. In order to utilize the second definition of V_H, equation 18.2, it became necessary to determine the change of μ_H with a hydrostatic stress, without changing the concentration of the interstitial solute hydrogen. Since hydrogen is highly mobile, it is practically impossible to comply with this requirement. Because of the relationship between μ_H and the low solubility of hydrogen(*) in iron and steel, equation 18.3 was derived which is equivalent to the right hand side of equation 18.2. It contains the hydrogen content in stressed as well as stress-free specimens[3,4]

*A stress induced change of hydrogen concentration can be neglected

$$\bar{V}_H = \left(\frac{\partial \mu_H}{\partial P}\right)_{T, n_{Fe}, \eta_H} = RT\left(\frac{\partial \ell n \left[\frac{C_{H,\sigma_h}}{C_{H,O}}\right]}{\partial \sigma_n}\right)_{T, n_{Fe}, \eta_H} \qquad (18.3)$$

Where C_{H,σ_h} signifies the hydrogen solubility in a stressed specimen, σ_h the hydrostatic component of an applied elastic stress, $C_{H,O}$ the hydrogen solubility in a stress-free specimen and η_H the overvoltage at which hydrogen is generated. Since stress does not affect the hydrogen diffusivity[2]. The hydrogen solubility is proportional to the hydrogen permeation current (J), which was measured electrochemically. The electrochemical method of measuring hydrogen permeation is extraordinarily sensitive to small changes in a hydrogen flux and therefore ideally suited for this type of work. Equation 18.3 may now be rewritten as

$$\bar{V}_H = RT\left(\frac{\partial \ell n \left[\frac{J_{\sigma_h}}{J_o}\right]}{\partial \sigma_h}\right)_{T, n_{Fe}, \eta_H} \qquad (18.4)$$

The ionization currents, corresponding to the hydrogen permeating through a thin iron membrane when stressed uniformly in tension and compression, are pictured in Figure 18.1. Irrespective of stress directionally, V_H is obtained from the slope of the lines, shown in this figure. In consideration of the proportionality between hydrogen solubility and μ_H, it is concluded that the reversible effect of stress on μ_H is thermodynamic in nature.

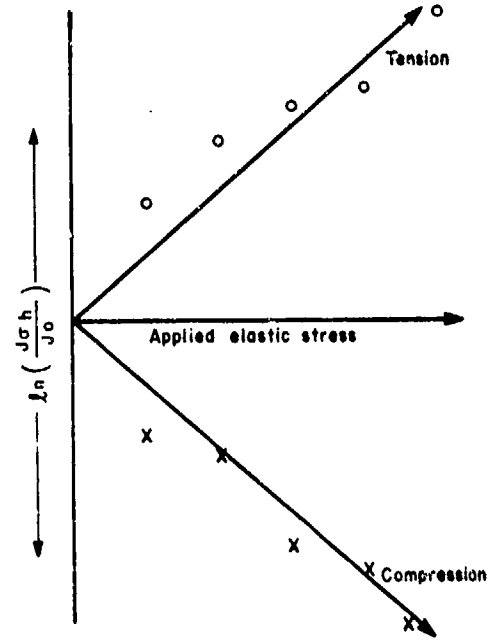

Fig. 18.1 – Effect of stress directionality on steady state currents permeating iron and steel membranes. Measurements made at ambient temperature.

At a constant external fugacity (or in electrochemical terms, overpotential), the hydrogen solubility decreases when the metal is stressed in compression but increases when stressed in tension[3,5].

The value of $\bar{V}_H$, which has a small temperature coefficient, has the attributes of a true material's constant which is demonstrated by the following example. The value of $\bar{V}_H$ in the ferritic ($\alpha \rightarrow$) Armco iron is 2.66 cc, whereas, in the hypoeutectic low alloy AISI 4340 steel (uts 150 ksi) it is 1.96 cc. All measurements were made at 27 C. Wriedt and Oriani[6], using a manometric method, obtained an approximate $\bar{V}_H$ value of 1.90 cc at 75 C for a 75 Pd + 25 Ag alloy (wt %).

18.2.2 THE ENERGY OF THE ELASTIC INTERACTION (U_H) OF HYDROGEN WITH THE STRESSED bcc LATTICE

The elastic interaction energy is calculated from

$$U_H = \int_0^{\epsilon} \frac{(\bar{V}_H)_\epsilon \, K d\epsilon}{N} \tag{18.5}$$

where K is the bulk modulus of iron, N the Avogadro number and $(\bar{V}_H)_\epsilon$ the increase in volume of the system, as a result of the addition of 1 gram atom of hydrogen, causing a lattice strain ϵ [3].

Supposing that all interstitial holes in a volume corresponding to 1 gram atom of iron (V_{Fe}) are filled with hydrogen atoms, the isotropic volume expension will be $3\bar{V}_H$, because there are 3N interstitial holes in 1 gram atom of bcc iron. Therefore, one obtains for ϵ.

$$\epsilon = \frac{3\bar{V}_H}{V_{Fe}} \tag{18.6}$$

Finally, by integration within the limits between O and ϵ, the elastic interaction energy for 1 gram atom of hydrogen, ($U'_H = NU_H$) is obtained

$$U'_H = 1.5K \frac{(\bar{V}_H)^2}{V_{Fe}} \tag{18.7}$$

where $K = 1.67 \times 10^{12}$ dynes/cm^2 and $V_{Fe} = 7.11$ cc. Under completely stress-free conditions for alpha iron (zero stress, externally and internally), $U'_{H,O}$ was found to be 59 kcal. For an externally applied stress field, the following relationship was established:

$$U'_{H,+\sigma_h} = (U'_{H,O} \mp a) = (59.0 \mp a) \text{ kcal/g atom of H} \tag{18.8}$$

where the numerical factor ia is

$$a = f(\sigma_h) \tag{18.8a}$$

An analysis of the values obtained for $U'_{H\pm\sigma_h}$, again reveals that the hydrogen solubility in the compressed lattice is smaller than that in the expanded lattice[3].

18.2.3 THE PARTIAL MOLAR ENTROPY, $\bar{S}_H$, OF HYDROGEN IN THE STRESSED bcc LATTICE

$\bar{S}_H$ is obtained from the differential effect of a constant stress, acting at different temperatures on the hydrogen solubility. The relationship between the partial molar free energy G of the two component system, Fe-H, and the solubility of hydrogen in gram atoms[3] can be expressed as follows:

$$\left(\frac{\partial G}{\partial n_H}\right)_{T,\sigma_h,n_{Fe}} = \left(\frac{RT \ln\left[\frac{C_{H,\sigma_h}}{C_{H,O}}\right]}{(C_{H,\sigma_h} - C_{H,O})\frac{1}{C_{H,\sigma_n}}}\right)_{T,\sigma_h,n_{Fe}} \tag{18.9}$$

$\bar{S}_H$ is obtained from the slope of a plot of the right hand side of equation 18.9 versus the temperature. Pertinent values for an uniaxial stress of $\pm$ 12 kg/mm^2, are

$$\bar{S}_{H,+\sigma_h} = 2.16 \text{ eu} \quad \text{and} \quad \bar{S}_{H,-\sigma_h} = 2.0 \text{ eu} \tag{18.10}$$

The entropy in the compressed lattice is decreasing.

18.2.4 THE AVERAGE HYDROGEN CONCENTRATION IN THE STRESS FIELD OF AN EDGE DISLOCATION

Rather involved calculations are based on equation 18.3,

$$C_{H,\sigma_h} = C_{H,O} \exp\left[\frac{\bar{V}_{H,\sigma_h}}{RT}\right] \tag{18.11}$$

which had to be integrated over the entire volume of the stress field around a dislocation, because σ_h depends on its position in this field. The hydrogen concentration, an exponential function of the binding energy, defined as $-\sigma_h \bar{V}_H$, varies with σ_h and increases in a region where this energy is positive. At the dislocation core, the interaction energy was calculated to be 53 kcal/gram atom, whereas in an unstrained lattice as given above, it is 59 kcal. Therefore, the value for the binding energy of hydrogen at the core is 6 kcal/gram atom.

Summarizing the above presented facts, it is strongly emphasized that the electrochemical permeation method made possible the precise calculation of the fundamental constant $\bar{V}_H$. This constant will be used for the determination of the thermodynamic parameters, which now will be applied to the interpretation of some cases of hydrogen embrittlement.

18.3 ANALYSIS OF SOME HYDROGEN EMBRITTLEMENT PHEMOMENA IN HIGH STRENGTH STEEL

Analyses of the following three embrittlement topics will be discussed in the light of the thermodynamic results presented above.

18.3.1 THE BENEFICIAL EFFECT OF COMPRESSIVE STRESSES

Slaughter et al[7] did not succeed in producing hydrogen embrittlement in a steel beam, which contained compressive bending stresses in the exposed surface. Corresponding results were obtained by Steigerwald et al[8]. Jankowsky[9] introduced compressive stresses into a steel surface by shot peening or bending, which rendered the high strength material resistant to plating embrittlement. McBreen[10] using the electrochemical permeation method with shot peened membranes obtained the results presented in Figure 18.2, which strongly support Jankowsky's findings. The graph indicates markedly reduced steady state permeation currents, recorded on the peened membrane, as compared with those on the unpeened surface. In addition, shot peening slows down build-up and decay of the hydrogen permeation transient. The decrease in hydrogen solubility, a result of the compressive stresses acting on the lattice, is indicated by a more positive interaction energy, and a decreasing entropy.

Generally speaking, the system under compression is in a less active energy state than a system under tension and thus hydrogen absorption and subsequent hydrogen embrittlement are minimized.

Finally, it is instructive to compare the above results on shot peened surfaces with those on cold rolled Armco iron, recently reported by Nanis, [11]. The data show good qualitative agreement as would be expected. The delay in build up and decay of the permeation transients is much more marked on the cold deformed specimens than on those with shot peened surfaces. It is inferred that the reason for the increased delay lies in the fact that the interaction energy of hydrogen becomes less positive and its entropy in the lattice more positive in a system subjected to severe plastic deformation than to shot peening.

18.3.2 THE BENEFICIAL EFFECT OF A PLASTIC PRESTRAIN

Figure 18.3 shows a steep increase in the lower critical stress[12] with increasing degree of prestraining. It is well known that cold deformation gives rise to an increase in the density of lattice imperfections and therefore, less restricting positions are provided for occupancy of hydrogen atoms[13]. Thus, when compared with unprestrained steel, the hydrogen solubility in the plastically deformed material is increased, the interaction energy becomes less positive, the entropy is increased (becomes more positive) and the susceptibility to hydrogen embrittlement is reduced accordingly.

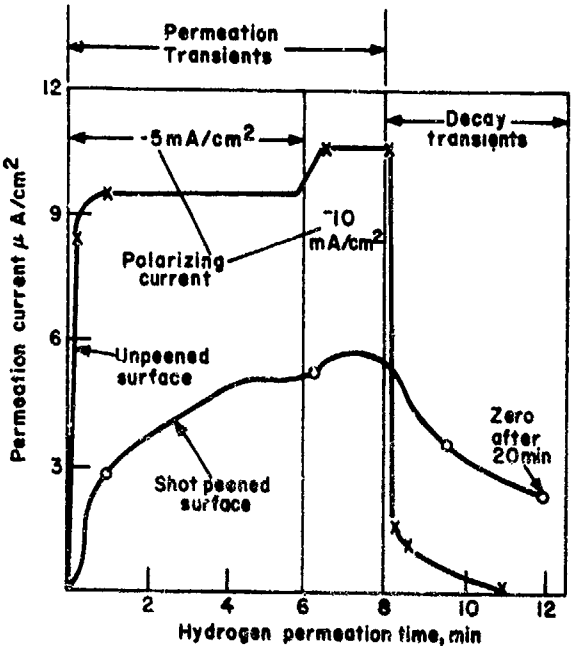

Fig. 18.2 – Effect of a compressive surface stress (shot peening) on hydrogen permeation currents. Armco iron (0.77 mm), surface shot peened to full coverage. Electrolyte 0.1N NaOH + 0.1N NaCN.

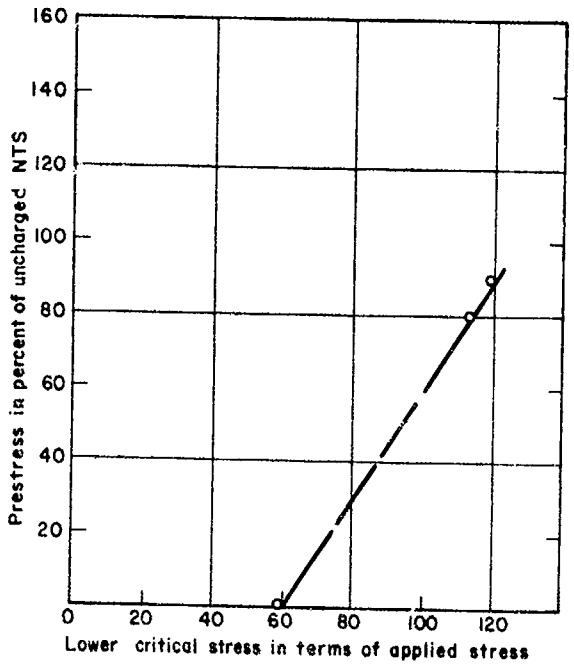

Fig. 18.3 – Effect of a plastic prestrain on lower critical stress of a sharply notched AISI 4340 steel tension specimen (UTS 240 ksi). After prestraining, charged in 1.5N H_2SO_4 at 3 mA/cm² for 5 min. Normalization of hydrogen distribution by 5 min. aging at ambient temperature.

The suitability of the thermodynamic theory for an explanation of the effect of rather complex mechanical processes on hydrogen embrittlement is demonstrated by recently published results. Uhlig et al[14] reported about the marked enhancement of the resistance to cracking of intensely cold deformed and hydrogen charged specimens, stressed parallel to the direction of rolling of low carbon martensitic iron alloys containing 10 to 19 per cent nickel.

The authors of this book explain this effect considering the same thermodynamic parameters, which were used above for the interpretation of the beneficial effect of a plastic prestrain. It is remarkable that the cracking time increased rapidly with increasing intensity of cold working, despite the progressively increasing hardness.

The rapidly increasing failure time, measured by Bates[15] on USS 18-2-2 stable austenitic steel between 10 and 20 per cent cold reduction, produced after a heat treatment of 1800 F, when discussed in view of a hydrogen induced failure, is explained also by the same mechanism. The initial decrease in fracture time indicates that the minimum degree of cold deformation must be greater than 10 per cent i.e., a minimum degree of lattice compression is required to make this mechanism applicable. The strongly acidic reaction near the crack tip and crack surface recently determined by various investigators[16-18] on stainless steel after testing in the conventional $MgCl_2$ solution under standard conditions of stressing, makes a hydrogen embrittlement mechanism entirely comprehensible. Bates used the same test for his studies.

18.3.3 HYDROGEN INDUCED DELAYED FAILURE

A hypothesis advanced by Troiano[19] explains to a remarkable degree complex delayed failure phenomena induced by hydrogen. The salient point in this hypothesis is the stress induced flux of hydrogen atoms into and their accumulation in areas of high stress concentrations. Unfortunately, there is a gap between the practical usefulness of this postulate and the fact that its mechanism is not well understood. However, the authors consider that this gap is narrowed by the thermodynamic results obtained in this study.

The driving force, brought about by the difference between the interaction energy of hydrogen in the unstrained lattice and that in a dislocation field, especially at the core of an edge type dislocation is sufficiently great

to initiate a diffusive flux of hydrogen atoms into the core[20]. In addition, a valuc of 6 kcal/gram atom represents a high binding energy of hydrogen atoms in the core of the dislocation. For dislocation densities of $10^9/cm^2$, which may be attained easily in areas of high triaxiality, it was computed that at the same fugacity, the average solubility of hydrogen is increased about 75 times above that in areas with dislocation densities much lower than given above[3]. The above presented results place Troiano's postulate of the inducement of delayed failure by hydrogen on a thermodynamically sound basis.

REFERENCES

[1] P. Cotterill, "The Hydrogen Embrittlement of Metals", *Progress in Mater. Science*, **9**, pp. 201-301 (1961).

[2] W. Beck, J. O'M. Bockris, J. McBreen and L. Nanis, "Hydrogen Permeation in Metals as a Function of Stress, Temperature and Dissolved Hydrogen Concentration", *Proc. Royal Society*, Vol. A290 pp. 220-235 (1966).

[3] J. O'M. Bockris, W. Beck, M. A. Genshaw, P. K. Subramanyan and F. S. Williams, "The Effect of Stress on Chemical Potential of Hydrogen in Iron and Steel", accepted for publication in Acta Met.

[4] J. O'M. Bockris and P. K. Subramanyan, "A Thermodynamic Analysis of Hydrogen in Metals in the Presence of an Applied Stress Field", accepted for publication in Acta Met.

[5] R. A. Oriani, "On the Partial Molar Volume of Hydrogen in α-Iron", *Trans. AIME* **236**, pp. 1368-1369 (1966).

[6] H. A. Wriedt and R. A. Oriani, "Effect of Tensile and Compressive Elastic Stress on Equilibrium Hydrogen Solubility in a Solid", *Acta Met.*, **18**, 753/760 (1970).

[7] E. R. Slaughter, F. F. Fletcher, A. R. Elsea and George K. Manning, "An Investigation of Effects of Hydrogen on the Brittle Failure of High Strength Steel", WADC Technical Rept. 56-83 Air Force Materials Lab. (WPAFB) Dayton, Ohio (1956).

[8] C. F. Barth, E. A. Steigerwald and A. R. Troiano, "Hydrogen Permeability and Delayed Failure of Polarized Martensitic Steels", *Corrosion* **25**, pp. 353-358 (1969).

[9] W. Beck and E. Jankowsky, "Effects of Plating High Tensile Strength Steels", *Proc. Am. Electroplaters' Soc.*, **44**, pp. 47-52 (1957).

[10] J. McBreen and W. Beck, unpublished work.

[11] L. Nanis and T. K. G. Namboodhiri, "Hydrogen in Iron", University of Pennsylvania, Technical Rept. UPH2-002 (NR 036-077) Dec., 1970.

[12] R. D. Johnson, H. H. Johnson, J. G. Morlet and A. R. Troiano, "Effects of Physical Variables on Delayed Failure in Steel", WADC Technical Report 56-220 Air Force Materials Lab. (WPAFB) Dayton, Ohio (1956).

[13] R. A. Oriani, "The Diffusion and Trapping of Hydrogen in Steel", *Acta. Met.*, **18**, pp. 147-157 (1970).

[14] J. A. Marquez, I. Matsushima and H. H. Uhlig, "Effect of Cold Rolling on Resistance of Ni-Fe_6 Alloys to Hydrogen Cracking", *Corrosion*, **26**, pp.215-222 (1970).

[15] J. F. Bates, "Thermomechanical Effects on Stress Corrosion Cracking of Austenitic Stainless Steels", *Mater. Protection*, **9**, pp. 27-32 (1970).

[16] M. Marek and R. F. Hochman, "Stress Corrosion Cracking of Austenitic Stainless Steel", *Corrosion*, **26**, pp. 5-6 (1970).

[17] H. R. Baker, M. C. Bloom, R. M. Bolster and C. R. Singleterry, "Film and pH Effects in the Stress Corrosion Cracking of Type 304 Stainless Steel", *ibid.*, pp. 420-426.

[18] A. M. Edwards, Discussion of E. H. Phelps and R. B. Mears, "Effect of Composition and Structure", *First International Congress on Metallic Corrosion London*, p.336 (1961).

[19] A. R. Troiano, "The Role of Hydrogen and other Interstitials in the Mechanical Behavior of Metals", *Trans. ASM*, **52**, pp. 54-80 (1960).

[20] R. A. Oriani, "Hydrogen in Metals", *Proc. of Conference on Fundamental Aspects of Stress Corrosion Cracking*, pp. 32-50 (1969).

CHAPTER 19

INTERPRETATION OF SOME HYDROGEN EMBRITTLEMENT INHIBITION CONTROLLING VARIABLES; ULTRASONIC FIELD, SURFACE ACTIVE AGENTS AND PEROXIDES

In this section an attempt is made to show that apparently totally unrelated topics, such as the inhibition of plating and pickling embrittlement in an ultrasonic field by certain surface active organic agents and hydrogen peroxide (H_2O_2) can be explained by the logical connection to inhibition controlling variables.

19.1 INHIBITON OF PICKLING AND PLATING EMBRITTLEMENT IN AN ULTRASONIC FIELD

Mee[1] showed that plating and pickling embrittlement are effectively retarded by ultrasonic vibrations. Pertinent results are pictured in the bar diagram, Figure 19.1. The beneficial effect is seen to be true in the severe case, where two embrittling procedures are performed sequentially, thus enhancing the conditions to induce embrittlement, for example, pickling followed by cadmium plating. As a result of this beneficial effect, an answer to the questions of the parameters, which control this type of embrittlement protection becomes important.

Useful information may be obtained from investigations conducted by Yeager[2] in the field of acousto-electrochemical effects in electrode systems. This investigator proved that ultrasonic vibrations decrease the hydrogen overvoltage when compared with measurements obtained when polarization is performed only with hydrogen gas stirring. The following modified Tafel plot, Figure 19.2, shows the decrease in hydrogen overvoltage on specimens polarized at different current densities.

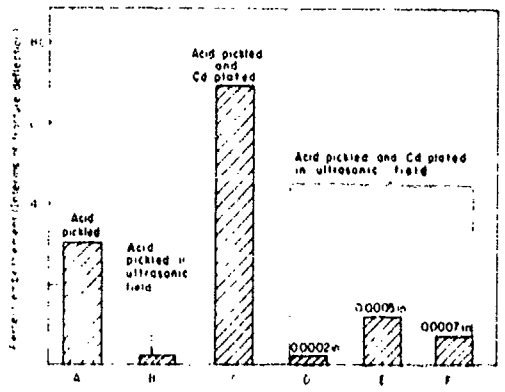

Fig. 19.1 – Effect of an ultrasonic field on acid pickling (5% HCl for 3 min) and on acid pickling followed by cyanide cadmium plating. UTS of steel substrate 130 tons/in² (291 ksi). Output of ultrasonic generator 60 watts, frequency 40 kc/sec.

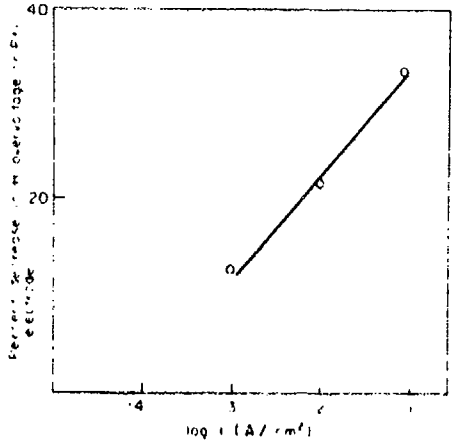

Fig. 19.2 – Modified Tafel plot showing decrease in overvoltage in an ultrasonic field. Electrolytic solution - IN H_2SO_4 at 25C. Acoustical intensity 1 watt/cm²; frequency 300 kc/sec.

The beneficial effect of the ultrasonic field may be interpreted in the light of the retardation of the diffusion rate of the embrittling hydrogen atoms into steel, as a result of the ultrasonically disturbed hydrogen coverage. Also, it has been shown that the acoustical intensity has a marked effect on hydrogen absorption[3,4].

Another plausible explanation of the beneficial effect of the ultrasonic vibrations may be based on the sonochemical formation of H_2O_2 by recombination of hydroxyl (OH) groups following[5] the dissociation of H_2O in cavitation bubbles. Though H_2O formation was observed predominantly in oxygen saturated water, it may be expected that small quantities of this substance are formed in water with the dissolved oxygen in equilibrium with the partial pressure of oxygen in the atmosphere. It will be shown in a following section, that peroxide concentration as low as 0.05 molar is sufficient to inhibit the formation of free hydrogen atoms. It is quite possible that the beneficial effect of the ultrasonic vibrations is brought about by a joint action of mechanical and chemical effects.

19.2 INHIBITION BY INCREASING THE HYDROGEN BARRIER EFFECTIVENESS OF THE PLATING BY GRAIN REFINEMENT

In addition to the electrochemical effect of the ultrasonic field, another factor must be taken in consideration. Devanathan, Beck and Stachurski[6] observed that during cyanide cadmium plating two time periods should be distinguished. The initial short period of plating when the number of hydrogen atoms introduced into a steel substrate is high. The following (second) period, when the number of hydrogen atoms which can diffuse into the basis metal is comparatively small, because of the increased barrier effectiveness of the thickening plating. If the embrittlement fate of the steel substrate is completely determined within the initial plating period; embrittlement inhibition would be controlled completely by the electrochemical mechanism. However, even when only a small number of hydrogen atoms diffuses into the steel substrate during the second period, they also become involved in the generation of embrittlement. In this case, the electrochemical mechanism may be supplemented as follows: It is well known that the refined grains, obtained by cadmium plating from a brightener containing bath, ensure a much higher barrier effectiveness than by plating from a bath free of brighteners (dull porous cadmium plating). The additional protection against embrittlement may then be explained by a further reinforcement of the cadmium barrier, caused by the grain refinement due to the electro deposition of the metal in the ultrasonic field[7].

19.3 INHIBITION OF PICKLING EMBRITTLEMENT BY SURFACE ACTIVE AGENTS

Acids, when used as pickling agents, may cause hydrogen embrittlement of high strength steels. Since pickling is an important operation, it is imperative that embrittlement be reduced as much as possible. Although Zapffe discovered that nonionic polymers such as polyethylene glycol and Carbowax markedly reduce pickling embrittlement, he did not propose a mechanism which controls this useful reaction[8].

An attempt will be made to disentangle the complex mechanism which controls inhibition of pickling embrittlement by these substances by an analysis of the effects of concentration and chain length. The results by Zapffe, plotted in Figure 19.3 indicate an exponential increase of the effectiveness of the addition agents with increasing concentration and molecular weight. The curves illustrate that adsorption is involved in the process of embrittlement inhibition. Because of the small quantity of molecules adsorbed, the total concentration of the adsorbate in solution is considered to have changed only very little after adsorption equilibrium has been attained. It is further assumed that a pickling time of 15 minutes at 77 C ensured a steady state of embrittlement and also indicated attainment of the adsorption equilibrium.

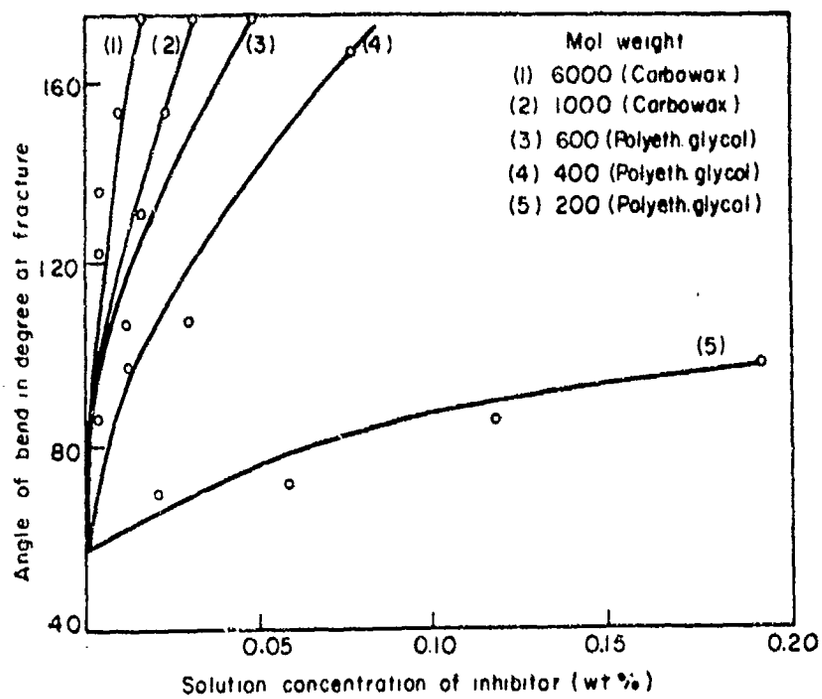

Fig. 19.3 -- Effect of non-ionic addition agents on pickling embrittlement of patented steel wire (SAE 1020 steel, UTS 182 ksi). Pickled in 1N H_2SO_4 for 15 min. at 77 C.

The log-log plot, Figure 19.4 depicts a linear relationship between increasing immunity to embrittlement and chain length. This relationship is considered to offer strong evidence that inhibition is controlled by adsorption of molecules of the organic addition agent on active sites. The very effective inhibition by Carbowax also supports the adsorption hypothesis, because the relatively high effectiveness of this substance, is attributed primarily to the presence of highly polar groupings in the hydrocarbon structure.

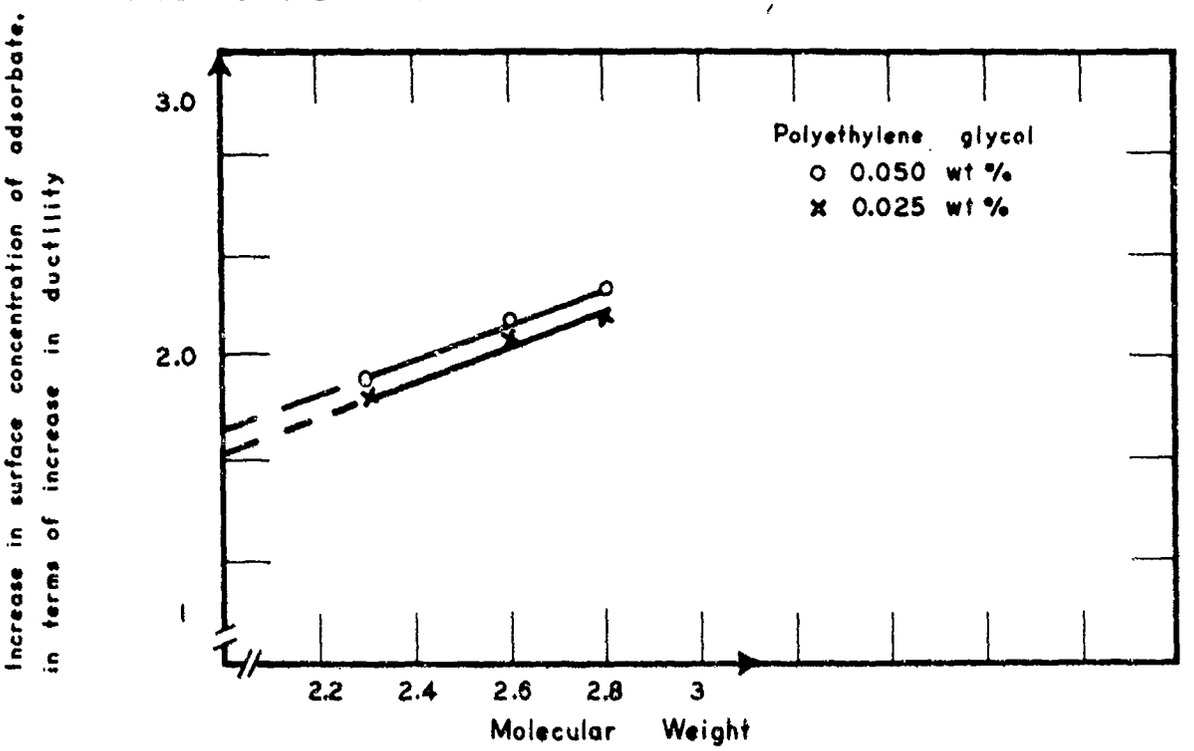

Fig. 19.4 – Effect of molecular weight (chain length) and solution concentration of polyethylenglycol on its surface concentration (log-log presentation) as related to reduction of hydrogen embrittlement. Patented steel wire (SAE 1020 steel, UTS 182 ksi). Pickled in 1N H_2SO_4 for 15 min. at 77 C.

The analysis of the process of inhibition of hydrogen embrittlement, performed so far was thermodynamic in nature, because it elucidated only the role of adsorption. As to the kinetic step in the group of reactions, it appears only logical to infer that it is related to the process of hydrogen generation. If the active sites are equated with the anodic areas, the hydrogen evolution reaction and hence hydrogen embrittlement are retarded as a result of preferential adsorption. This assumption is strongly supported by results recently published by Hudson and Riedy[9]. These investigators studied the retardation of hydrogen absorption in steel by addition of surface active agents such as acetylenic alcohols and -diols to dilute sulfuric acid. They showed, by extraction analysis, that in numerous cases decreased hydrogen absorption was associated with the degree of retardation of the iron dissolution rate.

Very recently, Cornet and Fuerstenau[10] found by corrosion current measurements an increase in inhibition of iron corrosion with increasing chain lengths of the surfactants in solution. Finally Beloglazo[11] presented important evidence that both embrittlement inhibition and rate of iron dissolution in sulfuric acid solutions containing aromatic amines, are determined by the strength of the chemical bond between adsorped amino groups and active sites, which is dependent on the electron density around the nitrogen atom. For corrosion inhibiting substances which promote hydrogen introduction into the steel, the above discussed relationship between hydrogen absorption and dissolution rate does not hold true[12].

19.4 INHIBITON OF HYDROGEN EMBRITTLEMENT BY HYDROGEN PEROXIDE (H_2O_2)

It was found at the Electrochemistry laboratory at the Naval Air Development center[13] that small amounts of hydrogen peroxide added to acid or cathodic pickling solutions effectively reduced embrittlement

effects in steels. To secure more information about the mechanism which controls this phenomenon polarization potential as well as bend ductility measurements were made on steel specimens which were charged cathodically in sulfuric acid containing hydrogen peroxide.

Pertinent results are plotted in Fig. 19.5. The strongly negative potential of the iron electrode immersed in the acid rapidly shifts in more positive direction with increasing concentration of added peroxide. This shift is accompanied by a progressive and drastic reduction in embrittlement.

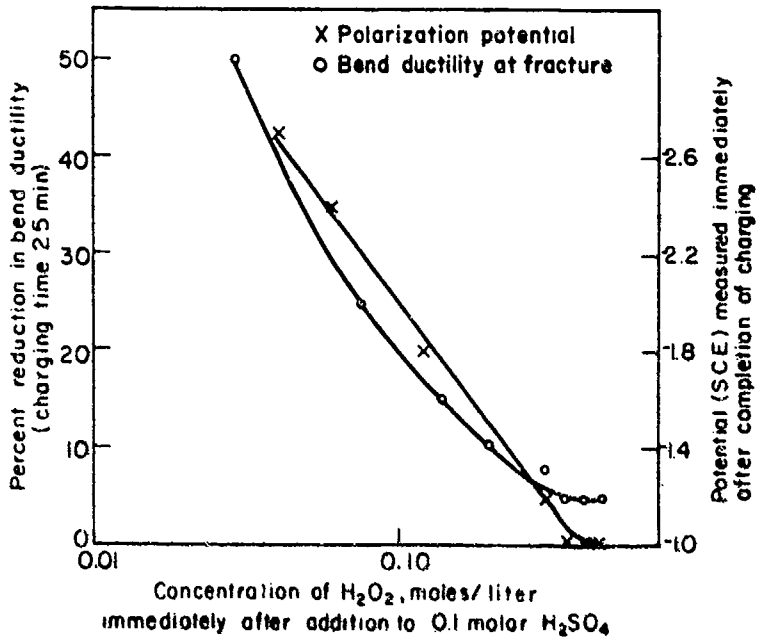

Fig. 19.5 – Effect of hydrogen peroxide additions on bend ductility and polarization potential. AISI 1070 steel, cathodically charged at 50 mA/cm^2. Rate of bending 0.020 cm/min.

The very small electrochemical effect of the species,

$$H_2O,\ H_3O^+,\ \text{and}\ O_2\ \text{(formed by catalytic decomposition of peroxide)}$$

present in the sulfuric acid containing peroxide, used for pickling, makes it possible to restrict the analysis to the effect of the peroxide on the hydrogen evolution kinetics[14]. The rapid positive shift of the potential, clearly indicates progressive retardation of the hydrogen evolution reaction. Finally, at potentials which are sufficiently more positive than the potential of the reversible normal hydrogen electrode, the hydrogen evolution reaction should be arrested. The disappearance of hydrogen embrittlement in the range of these potentials offers convincing evidence of the validity of the suggested electrochemical process. The high positive value (+ 1.77 volt vs. NHE) of the standard redox potential of the reaction*

$$H_2O_2 + 2e_0^- \rightarrow 2OH^- \qquad (19.1)$$

within the maximum possible value of the limiting diffusion current for the H_2O_2 species, explains the extinction of the hydrogen evolution reaction which is noted at about 0.5 moles/liter of peroxide[14].

It may be expected that not only pickling but also plating embrittlement is minimized by peroxide addition to the bath. A good example is the drop in embrittlement, achieved by addition of titanium compounds and hydrogen peroxide to the conventional cyanide cadmium bath[15], as mentioned in the section dealing with modified cadmium plating baths (Chapter 16). Jankowsky[16] discovered that the lower critical stress, on high

*Though the kinetic parameters necessary for complete description of the reduction mechanism of hydrogen peroxide on steel cathodes are not available as yet, the above suggested mechanism gives a good insight into the electrochemical variables which control the marked reduction in hydrogen embrittlement.

strength AISI 4340 steel plated from the conventional cyanide cadmium bath was about 30 per cent below that obtained in the titanium containing bath. One school of thought explains this beneficial effect is due to gettering action of the deposited titanium which results in a decrease of hydrogen pick-up by the substrate. Another proposed explanation infers that a portion of the hydrogen evolved on the cathode is used in the reduction of TiO_2, which is added or formed in the plating bath. The necessity of the continual addition of peroxide to the bath, in order to maintain a constant level of titanium concentration, makes it possible to replace the above mentioned thermodynamic but highly improbable hypothesis by the same peroxide mechanism discussed above.

In context with the peroxide reduction, the following observation is worthwhile mentioning[13]. The large hydrogen gas bubbles produced during steel pickling in a dilute sulfuric acid solution are immediately replaced by innumerable tiny bubbles after addition of a small concentration of peroxide. The evolution rate of these bubbles becomes so violent, that they form a turbid emulsion in the acid. Gas analysis, proved that the evolved gas is not hydrogen but primarily oxygen. Oxygen is not only generated in the catalytic decomposition of the peroxide[17] but probably also in side reactions associated with the reduction of the H_2O_2 molecule.

Favorable results with peroxide were obtained also with the cathodic pickling in a dilute NaOH solution[14]. In every type of pickling the commercial 33 per cent peroxide solution can be replaced to advantage by the more stable organic peroxides such as Lupersol 101 and di-t-butyl peroxide (produced by the Lucidol division of Wallace and Tiernan, Buffalo, N.Y.).

REFERENCES

[1] J. W. Mee, "The Application of Ultrasonics to Electroplating with a View of Reducing Hydrogen Embrittlement", *Trans. Inst. Metal Finishing*, **39/40**, pp. 242-248 (1962, 1963).

[2] E. Yeager, "Acousto-Electrochemical Effects in Electrode Systems", *Trans. of the Symposium on Electrode Processes*, Electrochemical Society (1959).

[3] L. Domnikov, "Effect of Ultrasonics on Hydrogen Absorption by Steel", *Metal Finishing*, **66**, pp. 59-61, 72 *(1968)*.

[4] B. A. Sheroi, K. S. Indira and R. Subramanian, "Ultrasonics in Metal Finishing II", *ibid.*, **68**, p. 60 (1970).

[5] M. Del Duca, E. Yeager, M. O. Davies and F. Havorka, "Isotopic Techniques in the Study of Sonochemical Formation of Hydrogen Peroxide", *J. Accoust. Soc. Am.*, **30 (4)**, pp. 301-307 (1958).

[6] M. A. Devanathan, R. Stachurski and W. Beck, "A Technique for the Evaluation of Hydrogen Embrittlement Characteristics of Electroplating Baths", *J. Electochem. Soc.*, **110**, pp. 886-890 (1963).

[7] J. F. Frawley and D. G. Childs, "Grain Refinement", *Trans AIME* **245**, pp. 2399-2404 (1969).

[8] C. A. Zapffe and M. E. Haslem, "Surface Active Agents and Pickling Embrittlement", *Wire and Wire Products*, **26**, pp. 127-133 (1951).

[9] R. M. Hudson and K. G. Riedy, "Limiting Hydrogen Adsorption and Dissolution of Steel during Pickling by Acetylene Alcohols and Diols", *Metal Finishing*, **62**, pp. 48-52 (1964).

[10] I. Cornet and P. N. Fuerstenau, "Interface Effects in Mass Transfer Controlled Corrosion Reactions", ONR Report No. M. S. E. 70-1 Contract No. N00014-67A-0114-0015 Office of Naval Research, Washington, D. C. (July 1970).

[11] S. M. Beloglazow, "Effect of Aromatic Amines on Diffusion of Hydrogen into Steel During the Cathodic Polarization in Acids", *Soviets Materials Science* **2 (6)**, pp. 628-654 (1966).

[12] R. M. Hudson, C. J. Warning, "Influence of Halide Mixtures with Organic Compounds on Dissolution of and Hydrogen Absorption by Low C-Steel in H_2SO_4", *Corrosion Sci.*, **10**, pp. 121-134 (1970).

[13] W. Beck and E. Taylor, unpublished work.

[14] W. Beck and A. R. Aidun, unpublished work.

[15] D. M. Erlwein and R. E. Short, "Cadmium Titanium Plating an Improved Process for Protecting High Strength Steels", *Metal Progress*, **87**, pp. 93-96 (1965).

[16] E. Jankowsky, "Re-evaluating the Delta Cadmium Plating Process", Report No. NAEC-AML-2265 Naval Air Development Center, Warminster, Pa., (Sept. 1965).

[17] D. Winkelmann, "Hydrogen Peroxide Reduction", *Z. F. Elektrochemie* **60**, 731 ff (1956).

CHAPTER 20

THE ROLE OF CN^- AND OTHER SURFACE ACTIVE ANIONIC GROUPS IN THE PROMOTION OF HYDROGEN EMBRITTLEMENT OF STEEL

It is evident that there is no hydrogen evolution reaction when plating from baths with 100 per cent efficiency, and hence hydrogen embrittlement is eliminated. Non-aqueous plating baths approaching this efficiency are described in Chapter 16. It might, therefore, be expected that by improving plating efficiency, hydrogen embrittlement would be minimized. A good example is the cadmium fluoborate bath having a plating efficiency greater than 95 per cent. Experimental results indicate that hydrogen embrittlement is reduced considerably, as compared with that of the cyanide bath with an efficiency of only about 85 per cent. Another instructive example is the favorable result when cadmium is plated from amino acid baths with efficiencies approaching 100 per cent. However, when silver is plated from the cyanide bath, a classical example of a bath working with an efficiency close to 100 per cent, high strength steel becomes badly embrittled (see chapter on plating embrittlement). In this context, it appears worthwhile mentioning that unpublished results obtained in this laboratory show that addition of KCN to the cadmium fluoborate bath, in low concentrations which did not decrease its high efficiency, markedly increases embrittlement of a high strength steel substrate. It is a general rule that hydrogen embrittlement, induced in steel by plating from a CN^- containing bath, regardless of the nature of the cation, markedly exceeds that produced by plating from a CN^- free-or an acidic bath. These examples show clearly that plating efficiency cannot be the only embrittlement controlling variable. Baths containing cyanide as the complexing agent are used extensively because of their superior plating properties, but production of embrittlement is a very serious handicap when high strength steels are plated.

Due to lack in knowledge about the mechanism which determines embrittlement stimulation by the CN^- group, different steps were taken to avoid this disadvantage. Suggestions were made to eliminate brighteners, to use unusual plating currents and addition agents or to reduce the concentration of cyanide below that necessary for the deposition of a good plating. All these recommendations were offered with the goal to improve plating efficiency. However, as was expected, minimization of embrittlement damage by plating from these modified baths, was only marginal. A breakthrough in this critical situation was made by Beck in collaboration with Glass and Taylor[1,2] and with Devanathan and Stachurski[3,4] who secured conclusive information about the complex processes which are involved in the promotion of embrittlement by CN^- action.

Beck and Glass determined the adsorbance of CN^- and other complexing groups which can be used in cadmium plating baths[2]. The inhomogenous nature of the steel surface along with the scarcity of experimental data, only made possible a rather preliminary analysis of the role of adsorption of certain species e.g., CN^- or an amino acid group in the hydrogen embrittlement of steel.

The main effort was directed toward establishing an adsorption isotherm. Also in these experiments, the steady state surface concentration of the respective species is extremely small as compared with the initial concentration of the respective adsorbates. Thus, the use of the initial concentrations for calculations introduces a negligible error. The quantity of the adsorbate, accumulated on the steel surface with and without cathodic polarization, or removed by desorption, was determined by appropriate radioactive counting techniques using C^{14}. Adsorption isotherms, recorded at different temperatures are presented in Fig. 20.1. As can be seen at the same concentration of the solute, the surface concentration of CN^- exceeds that of the amino acid group markedly. Adsorption equilibrium is approached at cyanide concentrations as low as 10^{-3} molar. In contrast the isotherm for the amino acid does not even approach a steady state at concentrations as high as 0.1 molar.

Beck et al[1] determined a much greater adsorption rate and differential heat of adsorption for $P-CN^-$ as compared with that for the d, l α-amino-n-butyric acid anionic group. The desorption rate of CN^- in sodium hydroxide solution was slow and desorption was incomplete. Whereas, the surface coverage for the amino acid group was incomplete and in no case did it approach a monolayer as with CN^-.

In summary, there can be no doubt that the CN^- as well as the $CH_3CH_2CH(NH_2)COO^-$ group prevailing in the strongly ammoniacal solution, are adsorbed on the steel surface during cathodic polarization. From their calculations[2], Beck et al concluded that the -CN- was directly attached to the active sites by a strong covalent bond, whereas the amino acid group was only weakly attached to a small portion of them either by

coordinate or hydrogen bonding. The marked adsorption of the CN^- stems partially from the extraordinarily high dipole moment associated with the -CN- grouping. The nature of the strong bond to the active sites on the iron surface and the high heat of adsorption, may be explained by the resonating structures, postulated for the ferrocyanide ions $[Fe(CN)_6]^{-4}$ by Pauling[5]. These complex, stable structures resonating with each other contain all of the CN groups, strongly attached to the central iron atoms by the same type of bond which is part ionic, in part a σ bond and a π bond. According to Pauling's theory of chemical bonding, because of the high heat of sublimation of iron, the strength of the Fe-H bond should even exceed that of the strong Ni-H bond.

Hydrogen permeation currents recorded in a number of solutions are reproduced in Figure 20.2. The order of magnitude of the steady state values of these currents[3], which indicate constant hydrogen coverage in CN^- and amino acid containing solutions, compare favorably with their degree of adsorption.

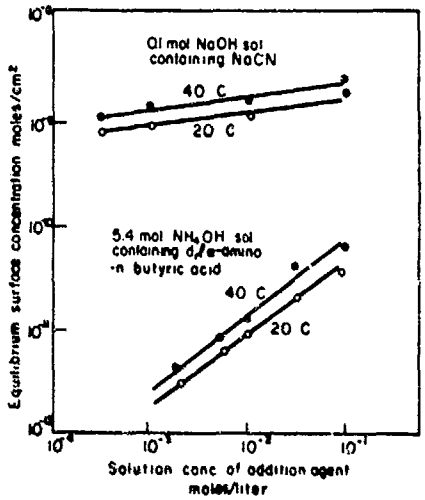

Fig. 20.1 – Log-log presentation of adsorption isotherms for NaCN and an amino acid on steel at different temperatures. Specimens polarized cathodically at 10mA/cm².

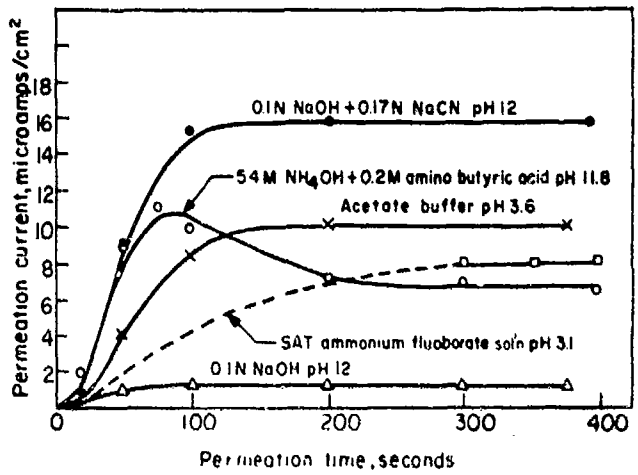

Fig. 20.2 – A comparison of steady state hydrogen permeation currents for different solutions (pH3.1 to 12.0). The permeation current is a function of the hydrogen coverage and the degree of adsorption of the solution consituents. Polarizing current density 8 mA/cm².

The relative high hydrogen coverage of the steel electrode in the cyanide solution[2] could be achieved by a retardation of the recombination rate of hydrogen ad atoms. If this is true, it should be indicated by an increased overpotential. Overpotential measurements would therefore be of great help in the establishment of the mechanism which controls the CN^- induced promotion of hydrogen embrittlement.

Results of direct overpotential measurements are reproduced in[1] Figure 20.3. Here, the difference between the steady state polarization potential in a NaOH solution and a NaOH solution containing an addition agent, NaCn, is considered to be a measure of the overpotential[6]. The curve indicates increasing hydrogen coverage with increasing solution activity of cyanide.

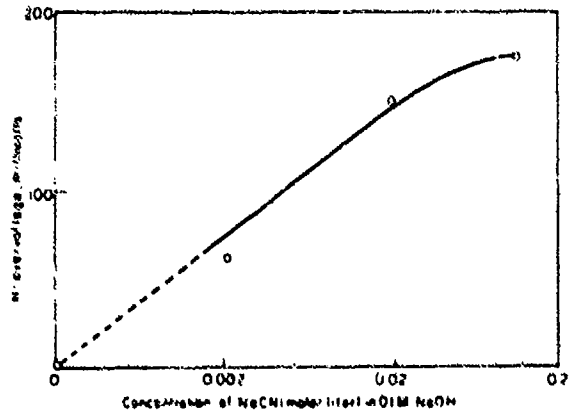

Fig. 20.3 – Effect of NaCN concentration on overvoltage.

The results of indirect overpotential measurements, pictured in Figure 20.4 agree well with those obtained by the direct method. The indirect method consists of making potential measurements in the solvent and the solvent containing the amino acid or NaCN at the end of a 10 minute polarization period (current density 10 mA/cm^2). Plotted are the corresponding fracture deflections[2]. The data demonstrate impressively the close relationship between hydrogen surface coverage as indicated by the overpotential and hydrogen embrittlement (see Chapter 2, is the difference between the potential of the solvent and amino acid or NaCN as clearly depicted in Fig. 20.4. Also plotted are the corresponding fracture deflections[2]. The data demonstrate impressively the close relationship between hydrogen surface coverage as indicated by the overpotential and hydrogen embrittlement (see Chapter 2, section 2.2.3).

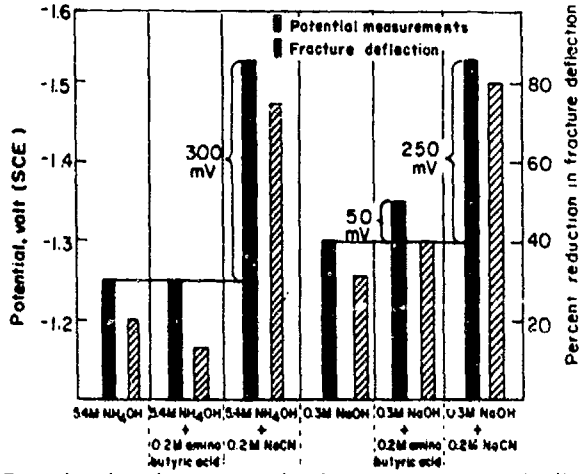

Fig. 20.4 – Data showing close connection between overpotential (indicating hydrogen surface coverage) and hydrogen embrittlement.

The mechanism which determines the generation of hydrogen atoms on cathodic surfaces, in presence of adsorbed surface active species[1] and the subsequent introduction of hydrogen atoms into the steel substrate, will now be discussed. Since strongly alkaline solutions have a negligible hydrogen activity, it is inferred that the first step in the reaction of generation of atomic hydrogen is the protonic discharge of water molecules:

$$2H_2O + 2e_0^- \rightarrow 2H + 2OH^- \qquad (20.1)$$

Under idealized conditions, the total area of the surface of the iron electrode, involved in the adsorption of hydrogen may be divided as follows:

$$Fe = \Sigma\, Fe^A + \Sigma\, Fe^B \qquad (20.2)$$

Fe^B sites are assumed to be in a highly active energy state as compared with Fe^A sites. Because of the comparatively low order of the hydrogen overvoltage on iron (Figures 20.3 and 20.4) it is further concluded that hydrogen evolution reaction (HER) is the result of a slow desorption step, coupled with a fast Tafel recombination. This reaction will proceed predominantly on the Fe^B sites, where the heat of hydrogen adsorption is high. The steps leading to HER, may then be designated as:

$$2\,Fe^B + 2H \rightarrow 2Fe^B - H \rightarrow 2Fe^B + H_2 \qquad (20.3)$$

When k signifies the rate constant for the recombination reaction in electrical units, $C_{H_{ads}}$ the surface concentration of the hydrogen adatoms and i_c the constant density of the polarizing current, the following relationship holds true:

$$i_c = kC^2_{H_{ads}} \qquad (20.4)$$

However, when CN is present and because of its strong preferential adsorption, the number of active sites still available for hydrogen adsorption is reduced drastically. The activation energy for hydrogen recombination is increased, and the rate of the recombination reaction retarded accordingly. At constant density of the polarizing current, i_c, the surface concentration of hydrogen adatoms, $C_{H_{ads}}$, must increase in order to compensate for the

decrease in the rate constant k. According to the diffusion laws, the quantity of hydrogen absorbed in the steel structure during unit time is proportional to $C_{H_{ads}}$. By increasing this concentration, the velocity of migration of the embrittling hydrogen atoms into the steel is increased and thus conditions are created which are most favorable for the promotion and production of hydrogen embrittlement.

Beck et al[1] interpreted the effect of adsorbed CN groups on hydrogen overvoltage and hydrogen recombination in the light of Frumkin's theory of the retarded hydrogen discharge. Specifically adsorbed anions render the ψ' potential more negative. This is the potential of the external Helmholtz layer, which corresponds to the mean value of a potential in the distance of one ionic radius from the electrode surface. Replacing equation 20.4 by equation 20.5, one obtains again for i_c the condition of generation of hydrogen atoms by protonic discharge:

$$i_c = Ka_{H_2O} \exp. \ (-\alpha F \ [\phi \cdot \psi']/RT) \tag{20.5}$$

where K is the rate constant for the hydrogen evolution reaction, a, the activity of the respective species, α, the ir electronic charge and ϕ, the electrochemical potential. One obtains the following expression for the overvoltage, η_H, on an electrode, partially covered with preferentially adsorbed CN

$$\eta_H = a_{CN^-} - \psi' - \frac{RT}{F} \ell n \, (OH^-) + \frac{RT}{\alpha F} \ell n i_c \tag{20.6}$$

and from this equation,

$$\left(\frac{d\eta}{d \ell n a_{CN^-}}\right) pH, i_c = - \left(\frac{d\psi'}{d \ell n a_{CN^-}}\right) pH, i_c \tag{20.7}$$

The value of η_H increases with increasing ψ' potential, which is caused by increasing adsorption of CN as a result of increased solution activity of this group. These facts explain the overvoltage results plotted in Figs. 20.3 and 20.4.

As can be concluded from equation 20.5, the rate of the hydrogen evolution reaction depends on the term $\phi - \psi'$ on which depends the activation energy for this reaction. Since this energy increases linearly with increasing $(\phi - \psi')$, it follows that as ψ' becomes more negative, the activation energy and retardation of the HER is increased accordingly. This is indicated by an increasing η_H.

The comparatively low steady state values of the hydrogen permeation currents in ammonium fluoborate and pure NaOH solutions (Fig. 20.2) are in good agreement with the low adsorption of the BF^- anion and particularly of the OH^- anion[7] and explain the low order of hydrogen embrittlement imparted to steel when cathodically charged in these solutions (Fig. 20.4).

The opposite is true for the $S^=$ anion which, on account of its very strong adsorption[8,9] is a powerful promotor of hydrogen embrittlement, as was demonstrated in the chapter dealing with sulfide corrosion hydrogen stress cracking. The same mechanism explains the effectiveness of other embrittlement promotors such as selenates, antimonates, arsenates and colloidal phosphorus[10] The high degree of embrittlement produced by plating tin from the alkaline stannate bath[11] again is explained by the strong adsorption of the stannate anion.

The hydrogen coverage hypothesis also explains the apparently paradoxical embrittlement behavior by organic polymers which protect against embrittlement as compared with CN^- and similarly acting anionic groups which promote this process. The effect on hydrogen embrittlement, of both types of species is related to adsorption on active areas. However, the adsorption of molecules of the nonionic polymers causes a decrease in hydrogen evolution and coverage (retardation of the dissolution rate of iron), whereas, with the adsorption of the anionic groups, (retardation of the recombination rate of hydrogen adatoms) there is an increase in hydrogen coverage. The reversal in the hydrogen embrittlement behavior is consistently explained by changes in the embrittlement controlling hydrogen evolution kinetics.

REFERENCES

[1] W. Beck, A. L. Glass and E. Taylor, "The Role of Adsorbed CN^- Groups in the Hydrogen Embrittlement of Steel", *J. Electrochem. Soc.*, **112**, pp. 53-59 (1965).

[2] W. Beck, A. L. Glass and E. Taylor, "Hydrogen Embrittlement and Adsorption of Complexing Agents on Cathodically Polarized Steel", *Plating*, **54**, pp. 732-734 (1968).

[3] M. A. V. Devanathan, R. Stachurski and W. Beck, "A Technique for the Evaluation of Hydrogen Embrittlement Characteristics of Electroplating Baths", *J. Electrochem. Soc.*, **110**, pp. 886-890 (1963).

[4] S. Venkatesan, R. Subramanian and M. A. V. Devanathan, "Co-deposition of Hydrogen in Zinc Electroplating", *Metal Finishing* **64**, pp. 50-53 (1966).

[5] L. Pauling, "The Nature of the Chemical Bond", pp. 336-337, Cornell University Press, New York, 1960.

[6] J. O. M. Bockris and B. E. Conway, "Hydrogen Overpotential and the Partial Inhibition of the Corrosion of Iron", *J. Phys. Chem.*, **53**, pp. 527-539 (1949).

[7] W. Beck and E. Jankowsky, "The Effectiveness of Metallic Undercoats in Minimizing Plating Embrittlement", *Proc. Am. Electroplaters' Soc.*, **47**, pp. 152-159 (1960).

[8] T. Erdey - Grusz and P. Szarwas, "About the Potentials of Mercury Electrodes in Electrolytic Solutions", *Z. Phys. Chemie*, **177 (A)**, pp. 277-291 (1937).

[9] D. C. Grahame, N. E. Coffin and J. D. Cummings, "Thermodynamic Properties of the Electric Double Layer", Research Contract - N 8-ONR 66903 Office of Naval Research, Washington, D.C. (Aug. 1950).

[10] T. P. Radnakrishnan and L. L. Shreir, "Permeation of Hydrogen through Steel of Electrochemical Transfer, Influence of Catalytic Poisons", *Electrochim. Acta.*, **11**, pp. 1007-1021 (1966).

[11] W. Beck and E. Jankowsky, "Effects of Plating High Tensile Strength Steels", *Proc. AM. Electroplaters' Soc.*, **44**, pp. 47-52 (1957).

APPENDIX

Abstracts are presented in this appendix of relevant papers, which were published after the manuscript had been prepared for publication. The abstracts are grouped under the following topics.

21.1 Effect of Composition on Delayed Failure and Mechanisms of Hydrogen Stress Cracking

21.2 Damage by Gaseous Hydrogen and Steam

21.3 Improvement of Resistance to Hydrogen Stress Cracking

21.4 Miscellaneous

21.1 EFFECT OF COMPOSITION ON DELAYED FAILURE AND MECHANISM OF HYDROGEN STRESS CRACKING

21.1.1 EFFECT OF NICKEL ON Cr-Ni STEELS ON THE CRITICAL POTENTIAL FOR STRESS CORROSION CRACKING

By H. H. Lee and H. H. Uhlig

J. of Electrochemical Soc., **117**, pp. 18-22 (1970)

Based on polarization and cracking velocity measurements, the authors are sceptical about the usability of any model of stress corrosion cracking, pertaining to a galvanic cell, the anode of which is located at the tip of the propagating crack. According to them, electrochemical parameters affect the corrosion potential, which in turn determines whether adsorption of Cl favor crack initiation and growth; but the mechanism is not one of metal dissolution at the crack tip.

21.1.2 EVALUATION OF HYDROGEN EMBRITTLEMENT MECHANISMS

C. F. Barth and E. A. Steigerwald

Metallurgical Transactions, **1**, pp. 3451-3455 (1971)

Tests were conducted with sharply notched hydrogenated 4340 steel specimens. The test procedure consisted of stressing almost to the end of the incubation period (commencement of crack nucleation) and then removing the stress. After aging for various times and at different temperatures, stress was reapplied and sustained. Aging times of 15 minutes at 75 F or 6 minutes at 252 F ensured no change in the length of the incubation period, which was considered to indicate that this parameter was truly reversible with respect to the applied stress. The kinetics involved to reproduce the incubation period could be directly related to the diffusion of hydrogen in the bcc lattice. Hydrogen stress cracking was also observed at the temperature of liquid nitrogen, where diffusion processes are excluded. The results dealing with the reversibility of the incubation period and the embrittlement experiments at low temperature, according to the authors, strongly support a hydrogen embrittlement theory based on the interaction of hydrogen atoms with the lattice.

21.1.3 HYDROGEN PERMEABILITY AND DELAYED FAILURE OF POLARIZED MARTENSITIC STEELS

C. F. Barth, E. A. Steigerwald and A. R. Troiano

Corrosion, **25**, pp. 353-358 (1970)

In this study, hydrogen permeability and delayed failure characteristics under conditions of cathodic and anodic polarization were directly correlated. It was discovered that with increasing anodic potentials in 3% NaCl solution, 9-4-45 steel displayed decreased times to failure, increased hydrogen permeability and surface pitting. These phenomena were observed on electrochemically preactivated surfaces, which exhibited a highly localized pitting type of attack after anodic polarization. It was necessary to activate both sides of the foil used for the permeation studies to obtain marked embrittlement. These experiments clearly demonstrate that it is possible to absorb hydrogen under conditions of anodic polarization, and that the hydrogen pick up is directly related to the delayed failure behavior. The argument that the decrease in failure time under anodic polarization rules out a generalized hydrogen embrittlement concept for stress corrosion cracking was concluded to be invalid.

21.1.4 MECHANISM OF CHLORIDE STRESS CORROSION CRACKING OF AUSTENITIC STAINLESS STEELS

F. R. Rhodes

Corrosion, **25**, pp. 463-472 (1970)

Electrochemical studies of the mechanism of chloride stress corrosion cracking of austenitic steels, (type 304) support a model requiring high rates of hydrogen evolution at the crack tip. The concept based on these studies

and consistent with published information deals with anodic reactions within corrosion pits and within the crack, leading to an intense hydrogen evolution reaction. The concomitant carthodic reduction of protons brings about hydrogen entry into the steel, affiliated with the initiation of formation of martensitic platelets and establishment of the path of crack extension. Above results indicate that the anodic reaction is the source for generating and maintaining the high aci lity, needed to sustain the high rates of the hydrogen evolution reaction near the crack tip.

21.1.5 HYDROGEN INDUCED CRACKING IN IRON: MORPHOLOGY AND CRACK PATH DEPENDENCE

I. M. Bernstein

Metallurgical Transactions, 1, pp. 3143-3149 (1970)

The main objective of this study was to determine the role of hydrogen in the production of crack nuclei and their growth into potential critical cracks. Specimens were hydrogen charged in poisoned sulfuric acid and transverse and longitudinal sections examined metallographically. Specimens were made mainly from Ferrovac, vacuum melted and zone refined iron.

The operative crack path can be varied systematically and reversibly from inter to transgranular, by suitable control of either prior thermal history or the concentration of interstitial solutes. In general, intergranular cracking is accelerated by high annealing temperature, moderately rapid cooling rates, a high oxygen to carbon ratio, or the absence of mobile interstitial solutes (carbon and nitrogen). Transgranular cracking in iron is heterogenous in nature with the density of nuclei increasing with decreasing purity.

21.1.6 THE HYDROGEN EMBRITTLEMENT OF Fe-Ni MARTENSITES

M. L. Wayman and G. C. Smith

Metallurgical Transactions, 1, pp. 1189-1193 (1970)

Hydrogen embrittlement in these materials is believed to be the result of high hydrogen contents in the vicinity of the prior austenite grain boundaries, combined with stress concentrations caused by boundary perturbations. During deformation, microcracks form and propagate in the prior austenite grain boundaries. This process, probably is assisted by internal hydrogen pressure and the lowering of crack-surface energy by hydrogen absorption.

21.1.7 EFFECTS OF STRESS ON ENTRY AND PERMEATION OF HYDROGEN IN IRON

H. E. Townsend, Jr.

Corrosion, 26, pp. 361-362 (1970)

Increase in hydrogen permeation, through thin membranes with tensile stresses applied, is attributed to an increase in hydrogen solubility due to an expansion of the stress lattice. Hydrogen reduction associated with the dissolution of iron in acid, is also accelerated by application of an elastic tensile stress. By combining these two phenomena, Townsend predicts an increase in hydrogen permeation rate with stress resulting from the accelerated rate of hydrogen reduction at constant potential.

Attempts are made to explain quantitatively the effect of stress on the permeation of hydrogen, in terms of a stress increased exchange current density for the hydrogen evolution reaction. The increased reduction of hydrogen by stress leads to an acceleration of the rate of entry of hydrogen into stainless steel also and is considered to be responsible for the intensification of stress cracking.

21.1.8 STRESS CORROSION CRACKING BEHAVIOR OF AN 18% NICKEL MARAGING STEEL

A. J. Stavros and H. W. Paxton

Metallurgical Transactions, 1, pp. 3049-3055 (1970)

Experiments were performed with six different structures of the maraging steel, obtained by appropriate heat treatments without changing the yield strength and hardness (R_c 52-53). A notched cantilever beam type of specimen was used.

Tests were conducted on stressed bars immersed in 3% NaCl solutions (pH of 1.7 and 6.3), 1N H_2SO_4 and distilled water.

Tests were also, performed in the NaCl solutions under conditions of anodic and cathodic polarization.

The threshold stress intensity was invariant with respect to heat treatment, composition of test solution, pH value and applied potential. Brown et al.* found that the pH in a NaCl solution at the crack tip was about 3.7 and the Fe^{++} concentration, in the "intracrackular" liquid was about 1 molar. Paxton assumes that similar conditions prevail in distilled water and concludes from an inspection of the Pourbaix diagram for the system iron-water that the thermodynamic requirements for hydrogen generation within the crack are satisfied. From this result he concludes further that the crack controlling mechanism is hydrogen embrittlement. In the light of these facts, it seems impossible to inhibit HSC by accumulation of alkaline, corrosion products on the steel surface (Bhatt and Phelps – Chapter 6, reference 4).

The fact that the fracture surface under all experimental conditions appears similar, further supports the assumption that the crack initiation and propagation were controlled by one and the same embrittlement mechanism. The marked effect of aging on fracture time was related to a change in hydrogen diffusivity in martensite, as a result of a change in the number and type of trapping sites.

21.1.9 ELECTROCHEMICAL CONDITIONS AT THE TIP OF AN ADVANCING STRESS CORROSION CRACK IN AISI 4340 STEEL

J. A. Smith, M. H. Peterson and B. F. Brown

Corrosion, **26**, pp. 539-542 (1970)

The electrochemical conditions at the crack tip were studied by pH and potential measurements using microelectrodes. The cracks were grown in the notched area of a 4340 steel specimen (YS 200 ksi) exposed to a NaCl solution (0.6 molar) with the pH varied between 2 to 10. Runs were conducted on specimens, which were not polarized by an external current and on those subjected to either anodic or cathodic polarization. The pH determined in the "intracrackular" liquid was between 3.5 and 3.9 and was invariant with respect to pH of the surrounding solution and conditions of polarization. From the Pourbaix diagram for iron, it was concluded that the low pH at the crack front and the appreciable negative potential, created favorable conditions for the evolution of hydrogen, as a result of the reaction of Fe^{++} with H_2O molecules.

It is the author's opinion that the qualitative inferences concerning the kinetics of the fracture mechanism support the thesis of the involvement of hydrogen in the cracking of the 4340 steel, under all conditions applied.

21.2 DAMAGE BY GASEOUS HYDROGEN AND STEAM

21.2.1 A STUDY OF GASEOUS HYDROGEN DAMAGE IN CERTAIN FCC METALS

R. M. Vennett and G. S. Ansell

Trans. ASM., **62**, pp. 1007-1013 (1969)

The stable austenitic stainless steel, 304 L SS, showed extensive cracking when subjected to 10 ksi hydrogen pressure. Transmission electron microscopy of the plastically deformed specimens produced evidence of strain induced martensite. It was concluded that martensite must be present and that plastic deformation in the presence of high pressure hydrogen is necessary for damage to occur in the steel.

*R. F. Brown, "Concept of the Occluded Corrosion Cell", *Corrosion*, **26**, pp. 249-250 (1970)
B. F. Brown, C. T. Fujii and E. P. Dahlberg, "Methods for Studying the Solution Chemistry within Corrosion Cracks", *J. Electrochem. Soc.*, **116**, pp. 218-219 (1969)
J. Sanduz, C. T. Fujii and B. F. Brown, "Solution Chemistry within Stress Corrosion Cracks", *Corrosion Science*, **10**, pp. 839-845 (1970)

21.2.2 EMBRITTLEMENT OF 4130 STEEL BY LOW PRESSURE GASEOUS HYDROGEN

D. P. Williams and H. G. Nelson

Metallurgical Transactions, **1**, pp. 63-68 (1970)

Slow crack growth rate was studied in fully hardened 4130 steel induced by low pressure hydrogen (<760 torr). In the temperature range between 80 to 25 C, the rate of crack propagation increases with decreasing temperature but between 0 and -80 C, it decreases with decreasing temperature. A surface reaction model was proposed and it was concluded that the rate controlling step in the crack growth induced by gaseous hydrogen or by hydrogen charging is activated surface adsorption of hydrogen. Hydrogen solubility and diffusivity in the control of crack propagation rate were considered to be of secondary importance, if they are at all involved. The authors emphasize the similarity of the surface reaction model suggested for control of hydrogen embrittlement with other ones of liquid metal embrittlement. This is in agreement with the conclusions made in chapter 7 about liquid metal embrittlement, where the similarity of these two phenomena was also stressed.

21.2.3 DISCUSSION OF EMBRITTLEMENT OF 4130 STEEL BY LOW PRESSURE GASEOUS HYDROGEN

A. R. Oriani

ibid., pp. 2346-2347

Oriani concludes from calculations, based on assumptions made by Williams et al. that the exponential dependency of the crack propagation rate on hydrogen pressure is not in agreement with the predictions by the proposed model of adsorption control. Thus, the idea that the kinetics of adsorption of hydrogen controls the crack growth rate cannot be accepted. However, Williams et al. in their reply (ibid., p. 2347) reject Oriani's arguments as being not relevant to their work.

21.2.4 HYDROGEN EMBRITTLEMENT FROM TEMPER BLUEING IN STEAM

J. C. Wright and S. E. Webster

J. IRSI, **208**, pp. 680-684 (1970)

It is a well known engineering practice, to blue-finish materials such as high strength bolts and screws, cutting tools, pins and particularly military items such as gun barrels, parts of revolvers, rifles and machine guns. These materials, when blue finished by tempering in steam, frequently fail in service in a brittle fashion. He found that there is a very significant loss in ductility and notched tensile strength of specimens after blue tempering in steam. It is his considered opinion that if the concentration of hydrogen inside the specimen is high, no additional hydrogen no additional hydrogen can be introduced, which was generated by decomposition of the H_2O molecules in the steam during blue tempering. However, if the initial hydrogen concentration in the specimen is low, an appreciable amount of embrittling hydrogen is introduced during blue tempering. After attainment of equilibrium, the concentration of absorbed hydrogen was high enough to ensure embrittlement. Hydrogen content in excess of 0.6 ml/cc (determined after tempering in steam) was severely embrittling.

21.3 IMPROVEMENT OF RESISTANCE TO HYDROGEN STRESS CRACKING

21.3.1 EFFECT OF COMPOSITION ON THE ENVIRONMENTALLY INDUCED DELAYED FAILURE OF PRECRACKED HIGH STRENGTH STEEL

E. A. Steigerwald and W. D. Benjamin

Metallurgical Transactions, **2**, pp. 606-608 (1970)

Data are presented to define the effect of composition on both the kinetic and steady-state parameters as measured in an environmentally-induced delayed failure test. Five quench and temper type martensitic high-strength

steels were used, all heat treated to the same strength level, 233 to 243 ksi. Center notched and precracked specimens were used in an environment of distilled water.

At a stress intensity of 75 ksi$\sqrt{in.}$ the time to cracking changed from approximately 90 minutes for low alloy 4340 steel to over 50,000 minutes for the higher alloyed H-11 and 9% Ni steels. The lower critical stress was not affected by alloy composition The difference in failure times was the result of an increase in time for the initiation of crack growth and a decrease in the rate of crack growth.

Their findings, of the improved resistance to delayed fracture of steels with increased nickel content and those of type H-11 as compared with 4340 steel were discussed in an earlier chapter.

21.3.2 A METHOD FOR IMPROVING HYDROGEN SULFIDE ACCELERATED CRACKING RESISTANCE OF LOW ALLOY STEELS

E. Snape, F. W. Schaller and R. M. Forbes-Jones
Corrosion, **25**, pp. 380-388 (1969)

A double temper was developed called "intercritical hardening" by which martensite was introduced into the microstructure of C-75, AISI 4140 and 4340 steels, and subsequently eliminated.

This was accomplished by heating above the lower critical A_c temperature, followed by tempering below this temperature. When specimens were subjected to this double heat treatment, their strength and resistance to sulfide corrosion hydrogen stress cracking were significantly improved. Very good results were obtained with a 4340 steel with a YS of 108 ksi.

21.3.3 COMPOSITION AND HYDROGEN STRESS CRACKING OF STEELS

John H. Hoke
Corrosion, **26**, pp. 396-397 (1970)

Experiments with 410 martensitic stainless steel established the fact that vacuum induction remelting greatly improves its resistance to hydrogen stress cracking. This improvement was not the result of structural changes. The high purity heat was immune to cracking in the various heat treated conditions. Crack propagation times were relatively long under severe conditions of heat treatment and stress level, indicating that these heats were much more resistant to cracking than commercial material, which was "not" vacuum refined.

These results are in excellent agreement with those of Beck et al. presented in the chapter, dealing with the effect of vacuum remelting on hydrogen stress cracking.

21.3.4 ON THE RESISTANCE OF TRIP STEEL TO HYDROGEN EMBRITTLEMENT

R. A. McCoy, W. W. Gerberich and V. F. Zackay
Metallurgical Transactions, **1**, pp. 2031-2034 (1970)

TRIP steels (transformation induced plasticity) recently developed by Zackay et al. are characterized by high strength, with high ductility and good fracture toughness. These metastable austenitic steels are relatively immune to hydrogen embrittlement at room temperature, whereas, after strain induced transformation to martensite, adverse hydrogen effects could be expected. These investigators used single edge fatigue precracked notched specimens, which were cathodically charged in phosphorus containing 4 percent by weight H_2SO_4 at various current densities, subsequently overplated with cadmium for 2 hours at 150 mA/in^2. Hydrogen homogenization was accomplished by baking at 300 F. The baking time was varied in order to adjust the hydrogen distribution. Specimens with a YS of 220 ksi were subjected to sustained load tests. In general, the test load was 80% of K_{Cr} (theoretical stress intensity factor) and the average value of this factor was 145 ksi in$^{1/2}$. It was concluded that crack growth was prevented by either the inability of absorbed hydrogen to diffuse from surrounding austenite (martensite was embrittled but the surrounding austenite was not) or, by the lack of sufficient hydrogen build up in any newly created martensite at the crack tip.

21.3.5 THE EFFECT OF PRIOR-AUSTENITE GRAIN SIZE ON THE STRESS-CORROSION CRACKING SUSCEPTIBILITY OF AISI 4340 STEEL

R. M. Proctor and H. W. Paxton
Trans. ASM, **62**, pp. 989-999 (1969)

A series of AISI 4340 steels was developed for this study having prior austenite grain sizes covering the range ASTM 7/12. The YS of these alloys after tempering at 205 C. was between 240 and 270 ksi. Fatigue precracked plane-strain cantilever beam specimens were used to investigate the stress corrosion susceptibility of these steels in a 3.5% NaCl solution. Results of fractographic investigations of the fracture surface indicated that it is feasible to increase YS quite markedly by grain refinement, accompanied by a decrease in the susceptibility to (hydrogen) stress cracking. An emperical relationship was derived between stress corrosion crack growth rate and applied plane-strain-stress intensity. (It is suggested that the authors should replace the terms SCC with HSC.)

21.3.6 FRACTOGRAPHIC OBSERVATION ON STRESS CORROSION CRACKING OF SOME AUSTENITIC STAINLESS STEELS IN $MgCl_2$ SOLUTIONS AT 154 C.

J. D. Harston and J. C. Scully
Corrosion, **26**, pp. 387-395 (1970)

The stress corrosion cracking of 304 austenitic stainless steels and steel alloys containing Cu, Co, Ni and Si, exposed to boiling $MgCl_2$, was examined fractographically by scanning electron microscopy. Tests were also performed on specimens under four point loading, which were semi-immersed in NaCl solutions (100 ppm Cl^-) at 270 C in autoclaves at 800 psi. Crack nucleation is retarded by additions of nickel (10 to 20%) and silicon (0.5 to 2%). The main reason for the favorable effect of nickel, is a chemical reaction proceeding on the freshly created surfaces at the propagating crack tip.

The acidic reaction found by analysis of the electrolyte contained inside of the crack should strongly support this hypothesis.

21.3.7 RESISTANCE OF 18Cr-18Ni-2Si STAINLESS STEEL TO STRESS CORROSION CRACK PROPAGATION IN BOILING MAGNESIUM CHLORIDE

J. A. Davis
Corrosion, **26**, pp. 95-98 (1970)

An interesting test specimen was developed by roll bonding together two sheets of 18-18-2 stainless steel. One sheet was the standard alloy while the other sheet was sensitized to stress corrosion cracking by the addition of phosphorus and molybdenum. Specimens were produced in the annealed, cold worked, and sensitized conditions. U-bend specimens were prepared so that half of them had the resistant (standard alloy) and the other half had the susceptible steel on the tension side. They were immersed in boiling $MgCl_2$ solution. When cracks appeared the specimens were kept in the solution for an additional 3 to 4 weeks to allow the cracks to propagate. No cracks were initiated in the standard 18-18-2 stainless steel, whereas cracks that were initiated in the susceptible steel propagated to the interface and stopped. (It is suggested that the author should replace the term SCC with HSC).

21.3.8 HYDROGEN EMANATION AND DISTRIBUTION IN METALS AND ALLOYS

S. M. Toy and A. Phillips
Corrosion, **26**, pp. 200-207 (1970)

Convincing evidence is presented that delayed fracture of 18 Ni maraging steel weldments in air is produced by cathodically generated hydrogen. Local stresses in conjunction with hydrogen action is necessary for initiation of transformation of the retained austenite along a perferential orientation, into the hydrogen embrittlement susceptible martensite.

To reduce cracking susceptibility, it was suggested to stabilize the austenite or to transform it completely during melting to martensite. This may be achieved by modifying the composition of the welding rod.

Neodymium was used to locate and estimate the quantity of hydrogen emanation. Detection is based on a chemical reaction. Neodymium or a similar rare earth metal reacts with the emanating hydrogen at a temperature

of 29 C or higher to form a metal hydride. In this test a thin neodymium film is evaporated on the polished and etched metal surface which is to be examined. This film is transparent except at the hydrogen reaction sites, where NdH_2 is formed. Therefore, the microstructural features of the metal surface are directly correlated to the H_2 emitting sites. The NdH_2 modules appear black when observed with an optical microscope. By measuring the size of the reaction sites and the thickness of the film, the quantity of hydrogen that has reacted with the Nd can be calculated. The sensitivity of this detection procedure can be further improved by resolving individual hydride modules with a scanning electron microscope.

21.3.9 STRESS CORROSION CHARACTERISTICS OF MARAGING STEEL WELDMENTS IN AIR AND PENTABORANE

S. M. Toy and A. Phillips
Welding J., Research Suppl. **49**, (11), pp. 497-504 (1970)

The applicability of the neodymium hydride method, described in the above paper is explained in greater detail.

21.4 MISCELLANEOUS TOPICS

21.4.1 NEW LOW-COST EQUIPMENT FOR HYDROGEN DETERMINATION IN METALS

Metallurgica, **82**, pp. 83-84 (1970)

A low cost hydrogen vacuum extraction device was designed by Daniel, Doncaster and Sons, Ltd., Sheffield, England. Hydrogen is extracted from the sample (steel, titanium and other metals) by a combination of heat and vacuum. The gas is determined by measuring pressure variations caused within the setup by the extracted hydrogen.

21.4.2 SULFIDE STRESS CRACKING OF STEELS

J. M. Dvoracek
Corrosion, **26**, pp. 177-189 (1970)

Tests were conducted to determine the cracking susceptibility of a number of steels used in the petroleum industry, which had been heat treated to moderately high strength levels. Notched tension and cantilever beam specimens, were exposed in stressed condition in closed containers, filled with NaCl solutions of various concentrations containing dissolved H_2S. The pH was kept constant.

Realistic critical nominal stresses and critical stress intensity factors for sulfide corrosion hydrogen stress cracking were obtained for the fatigue precracked cantilever beam specimens. Sodium chloride concentrations from 1 to 10 percent had no effect on cracking but decreasing the pH from 6 to 3 or increasing H_2S concentrations had a marked effect on crack growth by accelerating the kinetics of this process. Also surface notches and flaws with depths and lengths exceeding certain limits promoted crack formation. Conversely, cold working had a beneficial effect, see Chapter 18.

21.4.3 EFFECTS OF HYDROGEN GAS ON METALS AT AMBIENT TEMPERATURE

by J. E. Campbell
DMIC Report 5-31, Batelle Memorial Institute (1970)

This monograph contains chapters dealing with the effect of hydrogen on tensile properties and subcritical crack growth in low alloy steels, stainless steels and titanium alloys.

AUTHOR'S INDEX

D

E

F

G

S

T

U

SUBJECT INDEX

SUBJECT INDEX (Continued)

SUBJECT INDEX (Continued)

SUBJECT INDEX (Continued)

SUBJECT INDEX (Continued)

SUBJECT INDEX (Continued)

SUBJECT INDEX (Continued)